

***Cell and Receptor Tropism of
γ2-Herpesviruses***

Dissertation

for the award of the degree

“Doctor rerum naturalium”

of the Georg-August-Universität Göttingen

within the doctoral program

Emerging Infectious Diseases (EIDIS)

of the Georg-August University School of Science (GAUSS)

submitted by

Anna Katharina Großkopf

born in Fürth, Germany

Göttingen 2020

Thesis Committee

Dr. Alexander Hahn, Junior Research Group Herpesviruses, German Primate Center Göttingen

Prof. Dr. Lutz Walter, Primate Genetics Laboratory, German Primate Center Göttingen

Prof. Dr. Friedemann Weber, Institute of Virology, Faculty 10 - Veterinary Medicine, Biomedical Research Center Seltersberg (BFS), Justus Liebig University Giessen

Members of the Examination Board

Referee: Dr. Alexander Hahn, Junior Research Group Herpesviruses, German Primate Center Göttingen

2nd Referee: Prof. Dr. Uwe Groß, University Medical Center Göttingen, Institute for Medical Microbiology, Department of Medical Microbiology, Georg-August University Göttingen

Further members of the Examination Board

Prof. Dr. Lutz Walter, Primate Genetics Laboratory, German Primate Center Göttingen

Prof. Dr. Friedemann Weber, Institute of Virology, Faculty 10 - Veterinary Medicine of Justus Liebig University Giessen, Biomedical Research Center Seltersberg (BFS)

Prof. Dr. Stefan Pöhlmann, Infection Biology Unit, German Primate Center Göttingen

PD Dr. Christian Roos, Primate Genetics Laboratory, German Primate Center Göttingen

Date of oral examination: 23.03.2020

Table of contents

| | |
|--|-----|
| SUMMARY | 1 |
| ZUSAMMENFASSUNG | 2 |
| I INTRODUCTION | 3 |
| I.1 The pathogen KSHV - A historical view | 3 |
| I.2 KSHV tropism | 5 |
| I.2.1 Host tropism on an evolutionary scale | 5 |
| I.2.2 Cell and Tissue Tropism within the host | 6 |
| I.3 The KSHV life cycle | 8 |
| I.4 Virus - host interactions in KSHV entry | 11 |
| I.4.1 Part I – The viral glycoproteins | 11 |
| I.4.2 Part II – The cellular receptors | 12 |
| I.4.2.1. Spotlight - The Eph receptor tyrosine kinase family | 15 |
| I.5 Keeping it in the family - Simian model systems of KSHV | 17 |
| II AIMS | 19 |
| III RESULTS..... | 20 |
| III.1 Publication 1: A conserved Eph family receptor-binding motif on the gH/gL complex of Kaposi's sarcoma-associated herpesvirus and rhesus monkey rhadinovirus | 20 |
| III.2 Publication 2: EphA7 functions as receptor on BJAB cells for cell-to-cell transmission of the Kaposi's sarcoma-associated herpesvirus (KSHV) and for cell-free infection by the related rhesus monkey rhadinovirus (RRV) | 53 |
| III.3 Publication 3: Plxdc family members are novel receptors for the rhesus monkey rhadinovirus (RRV)..... | 68 |
| IV DISCUSSION and OUTLOOK..... | 97 |
| IV.1 Key findings..... | 97 |
| IV.2 Determinants of affinity and receptor usage..... | 98 |
| IV.3 Determinants of rhadinovirus tropism | 99 |
| IV.4 Animal models in rhadinovirus research and vaccine vector development | 100 |
| IV.5 Rhadinovirus mutants as probes for receptor-induced signaling | 102 |
| REFERENCES | 105 |
| APPENDIX | i |
| A1 Abbreviations..... | i |
| A2 Publications..... | iv |
| A3 Awards and Travel Grants..... | iv |
| A4 Conference contributions - Oral presentations | v |
| A5 Acknowledgements | vi |
| A6 Curriculum vitae..... | vii |

SUMMARY

Kaposi's sarcoma-associated herpesvirus (KSHV), the only rhadino- or γ 2-herpesvirus of humans, is associated with Kaposi's sarcoma (KS) and two B cell proliferative malignancies, primary effusion lymphoma (PEL) and a variant of multicentric Castleman's disease (MCD). As routes of primary infection, dissemination through the host, and development of virus-associated pathologies are at least partially shaped by viral cell and tissue tropism, it is crucial to understand the contribution of distinct viral glycoproteins and cellular receptor interactions to cell type-specific infection. In this context, the present thesis focuses on members of the Eph family of receptor tyrosine kinases, which were shown to play a role in KSHV infection of various adherent cell lines. While the KSHV gH/gL glycoprotein complex exhibits the highest affinity for EphA2, additional A-type Ephs have been described as interaction partners of KSHV. Even though the gH/gL-Eph interaction was subject of various studies, key questions regarding the role of Ephs in KSHV tropism and pathology remained unanswered. We therefore aimed to identify amino acid residues on the KSHV gH/gL complex that critically mediate the Eph interaction, create Eph detargeted virus recombinants mutated in the identified amino acid residues, and characterize the Eph usage on BJAB cells, as model for cell-to-cell transmission of KSHV into B cells. Similar to KSHV, the related rhesus monkey rhadinovirus (RRV) interacts with Eph receptors while exhibiting differing affinities for individual Eph family members. Comparison of the two viruses allowed us to identify conserved amino acid residues in the N-terminal domain of gH which are critical for the gH/gL-Eph interaction. Mutation of these amino acids in KSHV and RRV recombinants abrogated the viral interaction with Eph receptors and allowed us to analyze the cell type-specific contribution of the Eph family to KSHV and RRV infection. This system was also employed in our second study which identified two additional A-type Ephs as functional KSHV and RRV receptors on BJAB cells. The role of EphA5 and EphA7 in KSHV cell-to-cell transmission and RRV cell-free infection was demonstrated using CRISPR/Cas9-mediated knockout. We furthermore addressed the question whether additional cellular, Eph-independent interaction partners of the gH/gL complex shape the rhadinoviral infection of different cell types. We identified the Plexin domain containing proteins 1 and 2 (Plxdc1/2) as specific interactors for RRV, but not KSHV, and characterized a crucial Plxdc-interaction motif in close proximity to the identified Eph-interacting residues on RRV gH. Receptor function of Plxdcs was demonstrated by lentiviral overexpression of Plxdc1 and 2 in target cells and a Plxdc-detargeted RRV deletion mutant. Collectively, the present studies identify additional A-type Eph members as functional receptors for KSHV and RRV, characterize the role of a novel family of gH/gL-interacting proteins for RRV infection, and underline the importance of the N-terminal domain of the rhadinoviral gH as conserved receptor-binding domain, which mediates the interaction of KSHV and RRV with Eph receptors and the independent interaction of RRV with Plxdc family members.

ZUSAMMENFASSUNG

Das Kaposi-Sarkom-Herpesvirus (KSHV), das einzige Rhadino- oder $\gamma 2$ -Herpesvirus im Menschen, ist mit dem Kaposi Sarkom (KS) und zwei B-Zell-Lymphomen, dem primären Effusionslymphom und der multizentrischen Castleman-Erkrankung, assoziiert. Da der Mechanismus der Primärinfektion, die Ausbreitung im Wirt und die Entstehung Virus-assoziiierter Erkrankungen zumindest teilweise durch den viralen Zell- und Gewebetropismus bestimmt werden, ist es entscheidend den Beitrag spezifischer Interaktionen zwischen viralen Glykoproteinen und zellulären Rezeptoren zur Infektion unterschiedlicher Zelltypen zu verstehen. Der Fokus dieser Arbeit liegt hierbei auf der Familie der Eph Rezeptortyrosinkinasen, die an der Infektion diverser adhärenter Zelllinien beteiligt sind. Indes der KSHV gH/gL Glykoproteinkomplex die höchste Affinität für EphA2 aufweist, wurden weitere Eph Rezeptoren des A-Typs als Bindepartner von KSHV beschrieben. Obwohl die gH/gL-Eph Interaktion Gegenstand verschiedener Studien war, gibt es weiterhin unbeantwortete Fragen bezüglich der Rolle von Eph Rezeptoren für den KSHV Tropismus und KSHV-assoziierte Pathologien. Unsere Zielsetzung lag demnach in der Identifikation von Aminosäuren in KSHV gH/gL, welche essentiell für die Eph-Interaktion sind, in der Konstruktion von rekombinanten Viren mit Mutationen in den identifizierten Aminosäuren, sowie in der Charakterisierung der Eph Rezeptor Nutzung auf BJAB Zellen, einem Modell für die Zell-assoziierte KSHV Infektion von B-Zellen. Analog zu KSHV interagiert das verwandte Rhesusaffen Rhadinovirus (RRV) mit Eph Rezeptoren, zeigt hierbei jedoch abweichende Affinitäten für einzelne Mitglieder der Eph Familie. Durch Vergleiche zwischen beiden Viren konnten wir konservierte Aminosäuren in der N-terminalen Region von gH identifizieren, welche essentiell für die gH/gL-Eph Interaktion sind. Mutation dieser Aminosäuren in KSHV und RRV verhinderte die Interaktion mit Eph Rezeptoren und ermöglichte uns die Analyse des Zelltyp-spezifischen Beitrags von Eph Rezeptoren zur KSHV und RRV Infektion. Dieses System kam außerdem in unserer Studie zum Einsatz, die zwei weitere Eph Rezeptoren des A-Typs als funktionelle KSHV und RRV Rezeptoren auf BJAB Zellen charakterisierte. Die Funktion von EphA5 und EphA7 in der KSHV Zell-Zell Übertragung, sowie in der zellfreien RRV Infektion wurde durch Knockout mit Hilfe der CRISPR/Cas9 Methode nachgewiesen. Ferner beschäftigten wir uns mit der Frage, ob weitere, Eph-unabhängige Interaktionspartner des gH/gL Komplexes die Infektion verschiedener Zelltypen durch Rhadinoviren beeinflussen. Wir identifizierten die *Plexin domain containing* Proteine 1 und 2 (Plxdc1/2) als spezifische Interaktionspartner von RRV im Gegensatz zu KSHV und beschrieben ein essentielles Plxdc-Interaktionsmotiv nahe dem Eph-Interaktionsmotiv in RRV gH. Die Plxdc-Rezeptorfunktion wurde mittels lentiviraler Überexpression sowie mit Hilfe von zur Plxdc-Bindung unfähigen RRV Deletionsmutanten nachgewiesen. Zusammengefasst beschreiben die vorliegenden Studien weitere Eph Rezeptoren vom A-Typ als funktionelle Rezeptoren für KSHV und RRV, charakterisieren die Funktion einer neuen Rezeptorfamilie für die RRV Infektion und verdeutlichen die Bedeutung der N-terminalen Region des rhadinoviralen gHs als konservierte Rezeptorbindedomäne, welche die Interaktion von KSHV und RRV mit Eph Rezeptoren und die Interaktion von RRV mit Plxdc Rezeptoren vermittelt.

I INTRODUCTION

I.1 The pathogen KSHV - A historical view

The Kaposi's sarcoma-associated herpesvirus (KSHV) or human γ -herpesvirus 8 (HHV-8) is one of the seven human oncogenic viruses (i.e. Epstein-Barr Virus (EBV), Hepatitis B and C Virus (HBV/HCV), Human Papillomavirus (HPV), Human T-lymphotropic virus (HTLV), KSHV, and Merkel cell polyomavirus (McPyV)) characterized today¹. Dating back only 26 years, the identification of KSHV was a recent event in the history of infectious diseases. Nevertheless, cases of KSHV-associated diseases, namely the Kaposi's sarcoma (KS) in elderly men, were reported as early as 1872 by the Hungarian physician Moritz Kaposi (Figure 1) as "idiopathic multiple pigmented sarcoma of the skin"². In addition to the initially described KS variant, classified today as classic or sporadic KS³, case reports in the late 1940s started to document a distinct form of KS which is prevalent in Sub-Saharan Africa and most commonly occurs in young males⁴⁻⁶. In children, this form, now generally referred to as endemic KS³, often presents with lymphadenopathy involving multiple nodes and an aggressive clinical course in addition to typical skin lesions⁷. However, KS did not gain a broader attention until the onset of the human immunodeficiency virus and acquired immune deficiency syndrome (HIV/AIDS) epidemic, and associated reports of a highly aggressive KS form in HIV⁺ men who have sex with men in 1981⁸, which is classified today as AIDS-related KS or epidemic KS³. While the link between immunosuppression and development of KS is well established by now, the first



Figure 1 Cover of the February 2018 Lancet Oncology edition depicting Moritz Kaposi, who first described the skin tumor today referred to as Kaposi's sarcoma. Cover art by Daniël Roozendaal (www.danielroozendaal.com).

AIDS-KS cases occurred before the connection between AIDS-related immunodeficiency and KSHV as opportunistic infection was established. Today, iatrogenic KS, the fourth form of KS in recipients of solid-organ allografts, is recognized to correlate with the level of immunosuppression after transplantation⁹, and both the classic as well as the endemic form of KS are suggested to rely on impaired immune function either due to an aging immune system and related “immune senescence”¹⁰ or due to chronic infections and malnutrition¹¹. Nevertheless, KS was reported to occur significantly more frequent in patients with AIDS than in other immunosuppressed patient groups^{12–14} which could hint to a possible role for HIV co-infection that exceeds the described immunosuppression. The marked dependence of KS development on HIV co-infection was further underlined by the introduction of combination antiretroviral therapy (cART) for the treatment of HIV infection in 1996, which – without further treatment of the KSHV infection – dramatically decreased the incidence of AIDS-KS¹⁵.

In 1994, led by epidemiological studies which suggested an infectious agent independent of HIV as cause for KS, directed attempts to detect and analyze pathogen DNA in KS lesions resulted in the identification of KSHV, a novel human herpesvirus in the γ 2- or rhadinovirus lineage¹⁶. Soon after, KSHV infection was additionally associated with two lymphoproliferative disorders, the primary effusion lymphoma (PEL)¹⁷ and one form of multicentric Castleman disease (MCD)¹⁸.

Like KS, KSHV-associated MCD (KSHV-MCD) can occur in the context of HIV co-infection but is not restricted to HIV⁺ patients, whereby HIV-independent MCD is most prominently seen in KSHV-endemic regions^{19,20}. Classical symptoms of KSHV-MCD include enlarged lymph nodes and systemic symptoms, such as fever, spleno- and hepatomegaly and effusions²¹. Patients with KSHV-MCD commonly present with KS as well. Additionally, in some cases progression of MCD to aggressive diffuse large B cell lymphoma has been reported²².

PEL, formerly called “body cavity lymphoma”, presents with malignant effusions in e.g. abdominal, pericardial or pleural cavities without solid tumor mass in most cases, even though extra-cavitary lesions have been described^{23,24}. Similar to other KSHV-associated malignancies, PEL most commonly occurs in the context of immunosuppression and EBV co-infection has been detected in the majority of cases^{17,25}. Even though treatment of PEL patients with cART led to complete remission in some cases^{26–28} (as seen for KS), prognosis is extremely poor as PEL is generally resistant to chemotherapy and prospective clinical trials are difficult due to the low case numbers²⁹.

In recent years, the KSHV inflammatory syndrome (KICS) was described as a fourth KSHV-associated disease. While the clinical symptoms, including elevated levels of viral and human interleukin-6 and interleukin-10 leading to a systemic inflammation, resemble KSHV-MCD, KICS presents without generalized lymphadenopathy or clinical evidence of MCD in lymph nodes³⁰.

I.2 KSHV tropism

I.2.1 Host tropism on an evolutionary scale

While the host range of individual members of the order *Herpesvirales* is highly restricted, the over 200 herpesviruses described to date were identified in a broad spectrum of host organisms, including not only vertebrates (ranging from fish to primates^{31,32}) but also invertebrates (such as oysters³³). The members of the family *Herpesviridae* fall in three taxonomically divided subfamilies, α -, β - and γ -herpesviruses. While assignment to subfamilies was initially based on distinct biological properties and tissue tropism, advances in genomics led a more precise classification based on sequence homology³⁴.

Phylogenetic analysis of 48 virus species indicated co-speciation and co-evolution of herpesviruses with their respective host for lineages from all subfamilies based on branching patterns in phylogenetic trees of mammalian hosts and their respective herpesviruses^{35–37}. While the diversification time point for α -, β - and γ -herpesvirinae was approx. 200 million years ago, the emergence of major *genera* within the subfamily dates back to at least the mammalian radiation 60–80 million years ago^{36,38}. Consequently, human pathogenic members of the three subfamilies and even within the γ -herpesvirus subfamily (e.g. EBV and KSHV) are genetically more divergent than members of the same *genus* – in case of KSHV *rhadinovirinae* – from different species (Figure 2). The *genus rhadinovirinae* can be further sub-divided into two lineages, the rhadinoviruses 1 (RV1), which contains KSHV and rhadinoviruses 2 (RV2), without a described human pathogenic member. The RV1 lineage of Old World monkeys comprises the *macaca* (*M.*) retroperitoneal fibromatosis–associated herpesviruses (RFVHs) identified in *M. mulatta* and *M. nemestrina*³⁹, as well as the recently isolated colobine γ -herpesvirus 1 (CbGHV1)⁴⁰ and rhadinovirus sequences obtained from different African green monkey (*Chlorocebus aethiops*) species (namely RV1caa [*Chlorocebus aethiops aethiops*], RV1cap [*Chlorocebus aethiops pygerythrus*], RV1cas [*Chlorocebus aethiops sabaeus*])⁴¹. The RV2 lineage includes RV2mac strains from rhesus macaques (rhesus macaque rhadinovirus [RRV, RV2mmu^{42,43}], *M. mulatta*), Japanese macaques (Japanese macaque rhadinovirus⁴⁴, *M. fuscata*), Crab-eating macaques (RV2mfa^{45,46}, *M. fascicularis*) and southern pig-tailed macaques (RV2mne⁴⁶, *M. nemestrina*) as well as viruses of the *Chlorocebus aethiops* species described above (RV2caa, RV2cap, RV2cas⁴¹). While non-human primate rhadinoviruses of the RV1 lineage are genetically closer related to KSHV than members of the RV2 lineage, most studies in non-human primates focused on the *M. mulatta* - RRV analogue model system as detailed below.

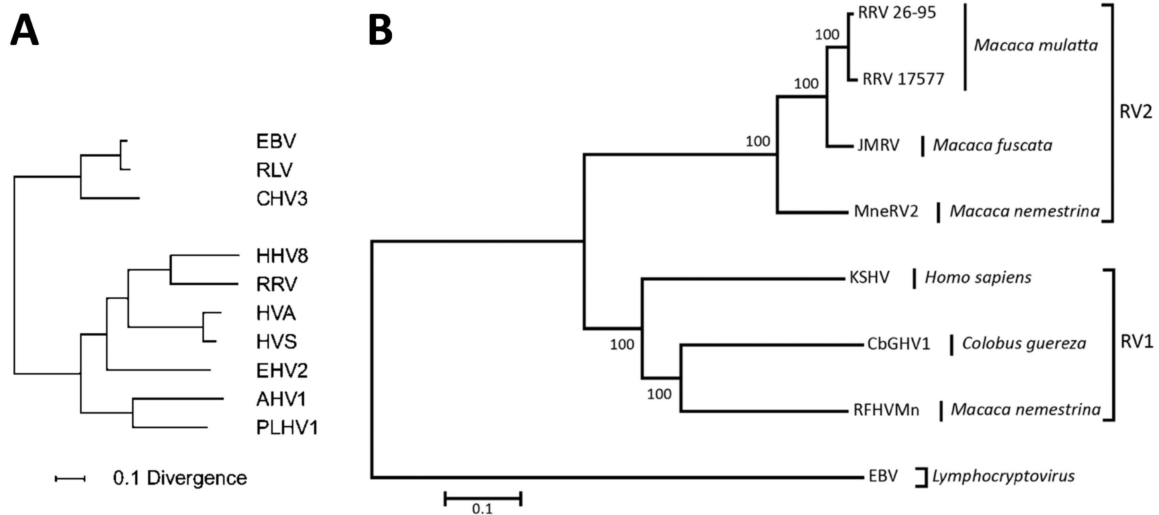


Figure 2 Phylogenetic trees of γ -herpesviruses. **A)** Amino acid sequence-based phylogenetic analysis of eight genes from ten γ -herpesviruses demonstrates the phylogenetic relationship of the γ 1-herpesviruses/lymphocryptoviruses (EBV, RLV, CHV3) and the γ 2-herpesviruses/ rhadinoviruses (HHV8/ KSHV, RRV, HVA, HVS, EHV2, AHV1, PLHV1) of different mammalian species. The analyzed genes have sufficiently conserved orthologues in all sequenced genomes of mammalian and avian α -, β - and γ -herpesviruses^{36,38}. **B)** Nucleotide sequence-based phylogenetic analysis of the genomes of seven non-human primate γ 2-herpesviruses and EBV as outgroup depicts the two lineages (RV1/ RV2) of γ 2-herpesviruses. Modified figures from McGeoch et al., 2005³⁷ (A) and Dhingra et al., 2019⁴⁰ (B). Abbreviations: EBV: Epstein-Barr virus, RLV: rhesus lymphocryptovirus, CHV3: Callitrichine herpesvirus 3, HHV8/ KSHV: Human γ -herpesvirus 8/ Kaposi's sarcoma-associated herpesvirus, RRV: rhesus monkey rhadinovirus, HVA: Herpesvirus ateles, HVS: Herpesvirus saimiri, EHV2: Equid herpesvirus 2, AHV1: Alcelaphine herpesvirus 1, PLHV1: Porcine lymphotropic herpesvirus 1, JMRV: Japanese macaque rhadinovirus, MneRV2: *Macaca nemestrina* rhadinovirus 2, CbGHV1: colobine γ -herpesvirus 1, RFHVMn: retroperitoneal fibromatosis-associated herpesviruses of *Macaca nemestrina*.

1.2.2 Cell and tissue tropism within the host

Reminiscent of the wide range of host species of the family *Herpesviridae*, individual members exhibit a broad cell and tissue tropism, both *in vivo* and *in vitro*. As understanding the viral life cycle, spread through the host organism, and associated diseases relies on detailed knowledge of this tropism, we need to identify molecular factors and interactions that determine and shape these preferences. While KSHV can infect numerous cell types *in vitro*^{47,48}, KSHV transmission *in vivo* is believed to occur mainly through saliva, and subsequent infection of the oral mucosa⁴⁸. Epidemiological studies and molecular evidence support this mode of transmission for early childhood infections in endemic regions^{49–52}, while sexual transmission of KSHV, particularly in men who have sex with men, plays a more substantial role in non-endemic areas^{53–56}. Nevertheless, the initial target cell types infected by KSHV, the cellular origin of KSHV-associated diseases, and potential intermediate target cells that could influence KSHV spread and dissemination throughout

the host are not well characterized. Potential initial target cells for the transmission through the salivary-mucosal route include cells of the local oral epithelium and submucosa, e.g. keratinocytes, monocytes, macrophages, B lymphocytes and endothelial cells⁵⁷⁻⁶². For instance, it has been demonstrated that primary tonsillar B cells can be productively infected by KSHV, leading to proliferation and plasmablast differentiation^{58,63}. B cells are widely recognized as the most likely reservoir of KSHV lifelong persistence in the host, even though primary B cells and established B cell lines are largely refractory to cell-free KSHV infection *in vitro*. Notably, this refractoriness can be overcome in cell-to-cell transmission systems⁶⁴, raising questions about a potential role of cell-associated virus in host colonization *in vivo*. Additionally, primary keratinocytes are susceptible to KSHV infection *in vitro* and various reports demonstrated the presence of KSHV in skin keratinocytes^{65,66} and the oral epithelium *in vivo*^{52,67,68}. Interestingly, terminal differentiation of KSHV infected basal keratinocytes was shown to induce lytic replication^{57,61} providing a possible rationale for oral KSHV shedding as well as a putative additional reservoir of latent KSHV in the host.

Similar to initial target cells, the cellular origin of KSHV-associated diseases, in particular KS is still under discussion. While spindle cells, the primary cell type found in KS, were initially thought to be of polyclonal endothelial origin^{69,70}, subsequent studies demonstrated that in addition to lineage markers of blood and lymphatic endothelial cells, spindle cells can express markers of macrophages, dendritic cells, and smooth muscle cells⁷¹⁻⁷⁷. Additionally, a recent study suggested oral mesenchymal stem cells as origin of AIDS-KS spindle cells based on the expression of neuroectodermal stem cell marker Nestin and oral mesenchymal stem cell marker CD29 in spindle cells and induction of mesenchymal-to-endothelial transition after KSHV infection of mesenchymal stem cells⁷⁸.

As the terminology indicates, the cell type giving rise to KSHV-associated B cell malignancies is less controversial. However, various studies involving different B cell lines as well as primary B cells, including tonsillar B cells and activated peripheral blood cells^{79,80}, could not decisively answer the question which type of B cells, B cell progenitors or stages of B cell development are susceptible to KSHV. Even though in KSHV-MCD, infected lymphocytes most closely resemble the plasmablast stage, both regarding specific transcription factors as well as expression of cell surface markers, they do not harbor somatic mutations in the rearranged Ig genes, which suggests naïve, pre germinal-center (GC) B cells⁸¹ or possibly IgM memory B cells⁶³, as cellular origin. KSHV-infected B cells from PEL on the other hand do exhibit somatic hypermutations and Ig class-switching, compatible with GC maturation, at least in the context of EBV co-infection^{82,83}. A study by Hassman et al.⁶³ suggested the infection of IgM λ tonsillar B cells as common initial target population for both malignancies, followed by KSHV-driven differentiation of infected B cells, which would also be compatible with the phenotype displayed for example by EBV-negative PEL cell lines, BC-3 and BCBL-1^{63,82}. According to this model, naïve, polyclonal B cells – of a until now not specified phenotype – could form the latent

KSHV reservoir and develop distinct lymphoproliferative diseases depending on co-factors, such as HIV or EBV co-infection, immune deficiency or aging. Studies concerning the cellular origin of KSHV-associated B cell malignancies are hampered by the general refractoriness of B cells to cell-free KSHV infection *in vitro* as well as the broad potential range of target B cell types and developmental stages *in vivo*. Interestingly, a recent publication identified a human B cell line, MC116 cells, which could be infected with cell-free KSHV at high virus concentrations⁸⁴ and may therefore serve as model for cell-free KSHV infection of human B lymphocytes in future studies.

1.3 The KSHV life cycle

Herpesviruses are enveloped viruses, carrying a large double-stranded (ds) DNA genome, which encodes for up to 200 genes, encapsulated in an electron-dense icosahedral capsid which in turn is surrounded by a proteinaceous tegument layer, and a lipid bilayer harboring diverse glycoproteins that mediate the initial virus-host interactions³². Specifically, the 165 to 170kb KSHV genome encodes for over 90 identified proteins, many of which are conserved within the herpesvirus family. Open reading frames (ORFs) uniquely found in KSHV and simian Old World rhadinoviruses are denoted “K” genes⁴⁸. Additionally, in recent years, an increasing number of small non-coding RNAs, microRNAs and a polyadenylated nuclear RNA have been identified in the KSHV genome (Figure 3)⁴⁸.

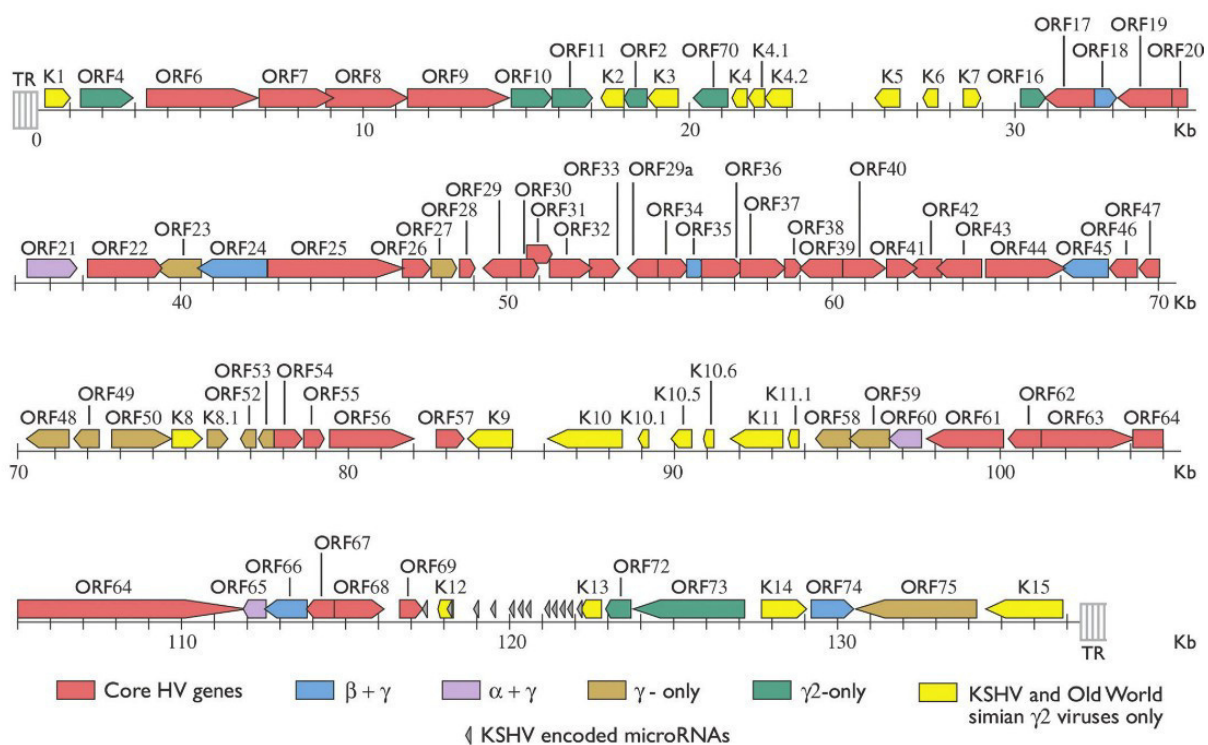


Figure 3 Genome map of the Kaposi's sarcoma-associated herpesvirus. Open reading frames are indicated by arrows. Conservation of genes in related α-, β- or γ-herpesviruses is indicated by color. Figure taken from Field's Virology (Damania, B. and Cesarman, E. Kaposi's Sarcoma-Associated Herpesvirus)⁴⁸.

Prototypic for herpesviruses, the KSHV life cycle (Figure 4) can be divided into two distinct phases, latent infection and lytic reactivation. In general, latency is the default mode upon primary infection *in vitro* and *in vivo* with sporadic bursts of lytic reactivation provoked by various triggers. KSHV enters target cells in a sequential, multistep process, which consists of, most likely, cell type-independent attachment to target cells followed by the interaction of viral glycoproteins with specific cellular receptors⁴⁸. Upon binding to the respective cell-surface molecules, signaling cascades and subsequent entry pathways are triggered to induce the uptake of KSHV virions into the cell⁸⁵. While multiple KSHV receptors have been described, as detailed below, inhibition of individual glycoprotein-receptor interactions is not sufficient to completely abrogate KSHV infection^{86–88}, indicating an at least partially redundant role of different entry receptors and pathways.

Upon entry of viral capsids into target cells, most likely by macropinocytotic or clathrin-mediated endocytotic uptake and fusion of the viral envelope with endosomal membranes under low pH conditions^{85,89–92}, capsids are shuttled to the nucleus via directed transport along the microtubule cytoskeleton^{48,93}. Subsequently, the capsid is disassembled and the viral genome is released into the nucleus, where it is circularized, chromatinized and maintained in an episomal state during latency⁹⁴. Latency is characterized by the production of a limited subset of viral gene products (e.g. the latency associated nuclear antigen (LANA, ORF73), viral (v)Cyclin (ORF72), vFLIP (ORF71) and kaposins A, B, and C) as well as the 12 viral pre-microRNAs^{95–97} and maintenance of a limited genome copy number, evenly distributed to daughter cells during division^{98,99}. Various physiological stimuli, such as hypoxia and oxidative stress^{100–102} can trigger sporadic lytic reactivation leading to a temporally regulated gene expression cascade of immediate early, early and late genes^{103–107}. In KSHV infection, expression of the replication and transcription transactivator (RTA)/ORF50, the “lytic switch” protein, is both indispensable and sufficient to initiate the lytic replication cycle and activates various cellular and viral promoters^{108,109}. After expression of all lytic gene classes, viral progeny are assembled by packaging of replicated genomes into newly synthesized capsids, engulfment of DNA-containing capsids in viral tegument proteins and subsequent incorporation in a host-derived membranous envelope containing KSHV glycoproteins. In analogy to other herpesviruses the mature envelope is most likely acquired through the use of physiological vesicular transport systems, such as the trans-Golgi network (HSV)^{110–112} or recycling endosomes (HCMV)¹¹³. Subsequently, mature virions are released by fusion of vesicle membranes with the plasma membrane.

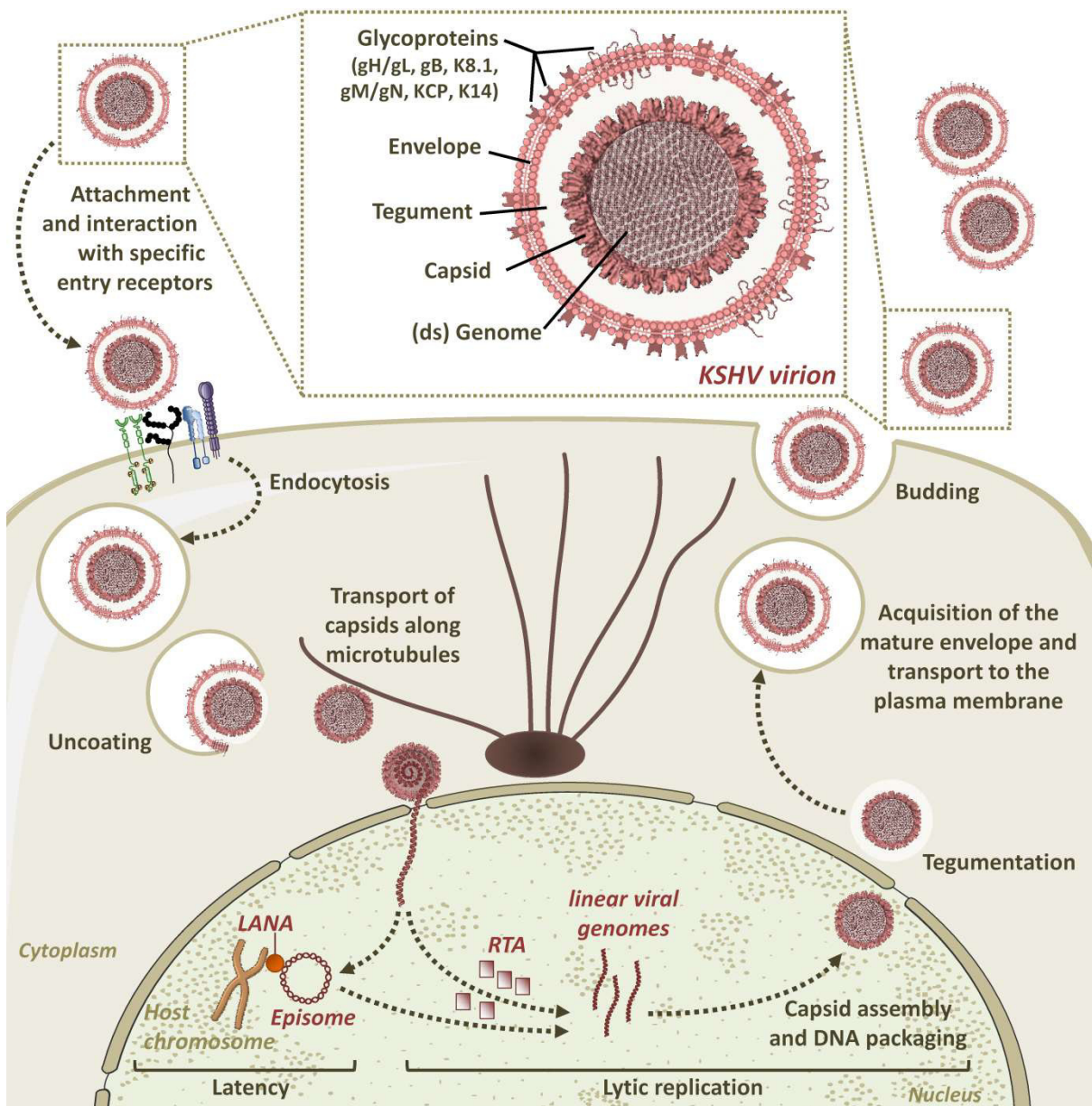


Figure 4 KSHV virion structure and life cycle. The different components of the KSHV virion are indicated. Upon interaction of viral glycoproteins with cellular attachment factors and entry receptors, viral particles enter target cells via clathrin-mediated endocytosis or macropinocytosis. Viral capsids are released in the cytoplasm after pH-dependent fusion of the viral envelope with endosomal membranes and transported to the nucleus. Latency, characterized by episomal genomes tethered to host chromosomes via LANA and expression of a limited number of KSHV gene products is the default outcome after release of the viral genome into the nucleus in most, if not all experimental setups. Upon RTA-dependent initiation of the lytic cycle, viral DNA and proteins are synthesized and genomes are packaged in newly assembled capsids. Mature virions containing the viral envelope, tegument and glycoproteins are formed and transported (most likely in host-derived compartments) to the plasma membrane where they are released. Abbreviations: ds: double-stranded, LANA: latency-associated nuclear antigen, RTA: replication and transcription transactivator.

I.4 Virus - host interactions in KSHV entry

I.4.1 Part I – The viral glycoproteins

At least seven KSHV glycoproteins, namely ORF8/glycoprotein B (gB), ORF22/gH, ORF39/gM, ORF47/gL, ORF53/gN, ORF4/KCP, K14/vOx2 and K8.1^{48,114–116} are associated with the KSHV envelope. Similar to other herpesviruses, these glycoproteins can be divided into two categories, proteins specific for KSHV and Old World simian rhadinoviruses and ones that share homology with glycoproteins of other members of the α -, β - and γ -herpesvirinae.

Common to all herpesviruses is the core fusion machinery, consisting of the gH/gL glycoprotein complex as fusion activator and interactor with cellular receptors and the driver of membrane fusion gB^{117–119}. These glycoproteins consequently represent the best characterized contributors to KSHV cell entry, partially derived from homology studies of other herpesviruses. gB is synthesized as a 110kDa precursor protein, which is subsequently cleaved at a consensus furin protease cleavage site and modified by N-linked and O-linked glycosylation giving rise to two disulfide-linked subunits of 59kDa and 75kDa¹²⁰. The KSHV gH/gL heterodimeric complex consist of the approx. 80kDa gH and the approx. 16kDa gL, which depends on the expression of gH for efficient expression, processing and incorporation into the virion¹²¹. By similarity, receptor-glycoprotein complexes formed by gH/gL and the respective cellular receptors interact with the KSHV fusion executer gB and trigger structural changes in the metastable prefusion state which ultimately lead to fusion of the viral and cellular membranes leaving gB in a stable postfusion state¹²². Even though the basic components of this core fusion machinery are conserved between all herpesviruses, the recruitment of additional non-conserved viral proteins or cellular receptors shapes the differences and virus-specific cell tropism exhibited within the herpesvirus family^{117,123}.

The KSHV complement control protein (KCP/ORF4) shares homology with herpesviral and cellular regulators of complement activation. All three proposed KCP isoforms inhibit the complement pathway at the C3-convertase step and are able to interact with heparan sulfate^{115,124,125}. Functional characterization of glycoproteins M and N, named according to their homologs found in other herpesviruses and proposed to have a conserved function as fusion inhibitors¹²⁶, is still rather sparse.

K8.1 and K14 on the other hand do not have described homologs in α - and β -herpesviruses. However, K14 is a homolog of the mammalian CD200/OX2 and its suggested functions encompass a similar role in immunomodulation in addition to potential roles in cell adhesion¹¹⁶. K8.1A, one of two alternatively spliced reading frames encoded by the K8.1 gene¹²⁷, is the most abundant glycoprotein incorporated into the viral envelope^{128,114,129} and highly immunogenic in the host^{130,131}. While a recent

study suggested a critical role of K8.1A for the B cell tropism of KSHV¹³², it appears to be dispensable for infection of endothelial cells and 293 cells^{133,134} and a B cell specific receptor is still lacking. While ORF68 was initially classified as glycoprotein in the viral envelope¹¹⁴ subsequent studies demonstrated its role as a DNA binding protein, involved in KSHV genome encapsidation¹³⁵, making a function in KSHV entry unlikely.

1.4.2 Part II – The cellular receptors

An increasing number of cellular interaction partners of KSHV glycoproteins have been identified that potentially contribute to the cell and tissue tropism of KSHV (Figure 3).

Members of the Heparan sulfate proteoglycan (HSPG) family were the first cellular factors shown to be involved in the binding of KSHV to target cells^{133,136}. While the role of HSPGs in KSHV attachment was initially attributed to the interaction with KSHV glycoproteins K8.1A¹³³ and gB¹³⁶, further viral glycoproteins, namely the gH/gL glycoprotein complex¹²¹ and ORF4/KCP^{115,125} have subsequently been described as interaction partners of HSPGs. The redundancy of the KSHV-HSPG interaction reflects the importance of proteoglycans for the attachment of KSHV to target cells. Using HSPGs for initial attachment is comprehensible considering its promiscuous expression on the majority of cell types – with the exception of e.g. B cells⁷⁹. The rather unselective virus adhesion and potential concentration on the cell surface is then followed by the – most likely – cell type-dependent interaction of viral glycoproteins with specific cellular receptors.

Similar to HSPGs, integrins – the second class of KSHV interacting cellular receptors – are widely expressed on a range of cell types and are implicated in the attachment or entry process of several enveloped as well as non-enveloped viruses¹³⁷. Initially, integrin $\alpha_3\beta_1$ was shown to mediate KSHV infection of Chinese hamster ovary cells via interaction with a classical Arg-Gly-Asp (RGD) binding motif in the N-terminal ectodomain region of KSHV gB^{88,138}. However, while integrin $\alpha_3\beta_1$ belongs to the laminin-binding, RGD-independent integrin (group II) subfamily¹³⁹, the RGD motif in KSHV gB suggested the involvement of RGD-specific (group I) integrins in the gB-mediated cell adhesion. Indeed, $\alpha_v\beta_3$, a group I integrin receptor, was identified as direct interaction partner of the RGD motif on KSHV gB, whereas this study did not observe interaction of KSHV gB with integrin $\alpha_3\beta_1$ ¹⁴⁰. Subsequently, the presence of an additional group I integrin ($\alpha_v\beta_5$) in a multimolecular complex was demonstrated upon KSHV infection¹⁴¹.

In contrast to the binding to HSPGs, this gB-integrin interaction may exceed a mere role in attachment and is thought to trigger cellular signaling cascades that ultimately lead to the internalization of the viral particle (detailed in Figure 5). While the importance of integrins for KSHV infection has been demonstrated for various cell types (reviewed in ¹⁴²), a recent study suggested an

infection mechanism which is independent of integrin $\alpha_3\beta_1$, $\alpha_v\beta_3$ and $\alpha_v\beta_5$ but relies on HSPG (for attachment) and on the interaction with another cellular receptor family, the erythropoietin-producing human hepatocellular (Eph) receptors¹⁴³. One member of this family, EphA2, was already identified as receptor for the KSHV gH/gL glycoprotein complex by Hahn et al. in 2012⁸⁶. Subsequently, the importance of the gH/gL-EphA2 interaction was verified in several studies that characterized cell type-specific effects, activation of signaling pathways and induction of uptake mechanisms^{86,143–149}. While within the Eph family KSHV gH/gL exhibits the highest affinity for EphA2, recent reports demonstrated that other A-type members of the Eph family, e.g. EphA4 and EphA5, can functionally substitute for EphA2 upon overexpression in certain settings^{143,150}. In general, the ability of KSHV gH/gL to bind a broad range of Eph receptors may indicate a redundant function of the Eph family in KSHV infection conveying specificity at least partially through absolute expression levels as well as the ratio of expression between different Eph members.

Interestingly, HSPG as well as EphA2 are not expressed on most B cell lines, which correlates with poor susceptibility of these cell lines *in vitro*. However, while stimulation of HSPG expression on BJAB cells, a widely used B cell line, enhanced binding of KSHV to the cell surface it did not allow for efficient infection⁷⁹ which indicates the need of additional cellular factors crucial for the cell-free infection of B cells *in vitro*. In accordance with these observations, a recent publication identified K8.1A as critical for infection of MC116 cells (a B cell line marginally permissive for infection with cell-free KSHV) and tonsillar B cells and determined this function to be independent of the K8.1A-HSPG binding¹³². One cellular receptor described to mediate KSHV infection of activated B cells, dendritic cells, macrophages, and monocytes is the Dendritic Cell-Specific Intercellular adhesion molecule-3-Grabbing Non-integrin (DC-SIGN)^{80,87}, a C-type lectin receptor mainly expressed on dendritic cells and certain types of macrophages^{151–153}. DC-SIGN recognizes viral glycoproteins modified with high mannose sugars, such as KSHV gB, via a carbohydrate recognition domain (CRD)^{153–155} which also facilitates the interaction with its physiological ligands, the intracellular adhesion molecules (ICAMs)¹⁵⁶. Interestingly, DC-SIGN has already been described to play a role in the infection of human dendritic cells by flaviviruses^{157–159} and to facilitate the infection of HIV-1 permissive cells *in trans* by “transporting” attached virus to CD4⁺ T cells, the intended target cells, during physiological dendritic cell migration^{160,161}. As DC-SIGN expression on dendritic cells also mediates dendritic rolling on endothelial cells¹⁵¹, one of the KSHV target cell types *in vivo*, the interaction of gB with DC-SIGN might play a similar role in KSHV infection, enabling the “shuttling” and spread of KSHV throughout the host to the intended reservoir cell types.

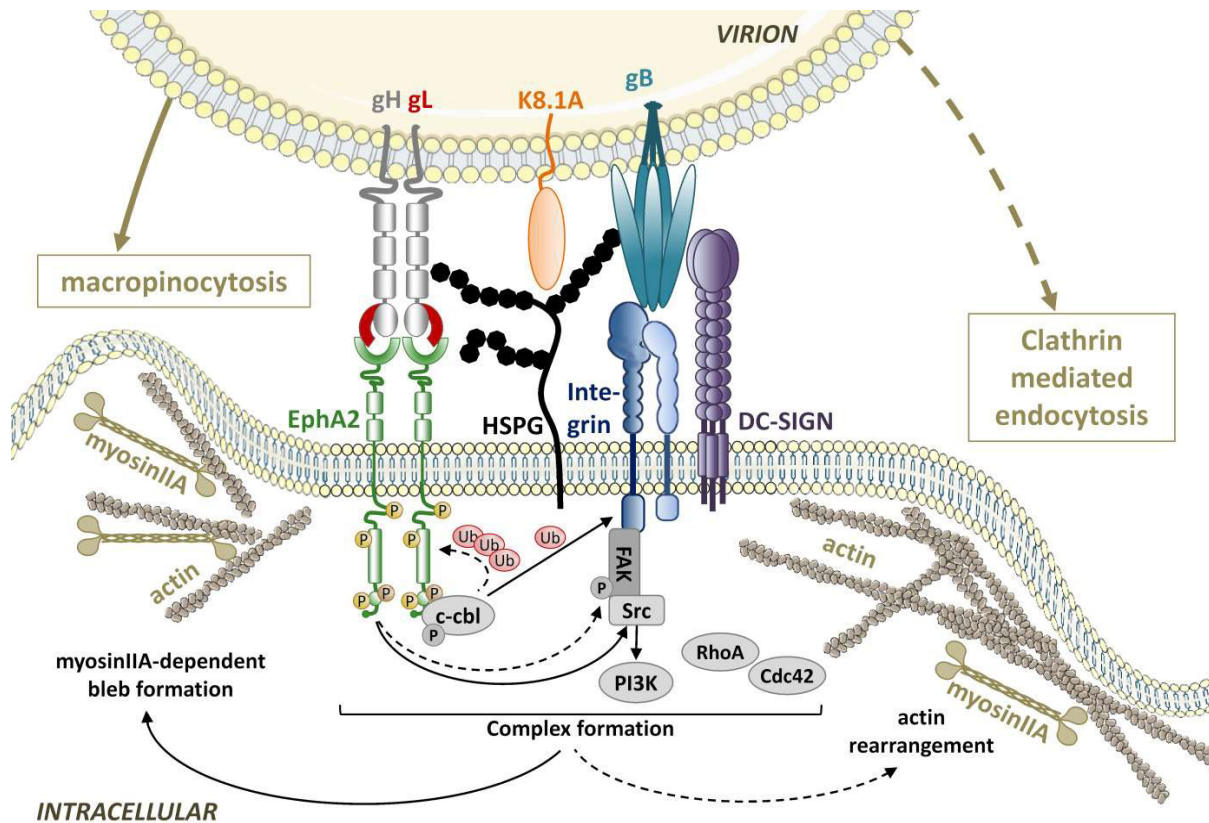


Figure 5 Receptor interactions and signaling events leading to KSHV entry as characterized on human foreskin fibroblasts (HFF) and human dermal microvascular endothelial cells (HMVEC-d). Processes shown in HFF are indicated by dashed lines, processes shown in HMVEC-d are indicated by solid lines. On HFF, interaction of gB with integrin $\alpha_3\beta_1$ via a classical RGD motif was reported to induce phosphorylation of focal adhesion kinase (FAK) which led to the activation of Src and Phosphoinositide-3-kinase (PI3K) and subsequent actin cytoskeleton rearrangement via RhoA and Cdc42 Rho GTPases^{162,163}. Activation of EphA2 was suggested to enhance pre-existing FAK/Src/PI3K phosphorylation, resulting in recruitment and activation of various signaling adaptors such as c-cbl and myosinIIA, c-cbl-dependent polyubiquitination of EphA2 and subsequent clathrin-mediated endocytosis¹⁴⁴. In HMVEC-d, analog, gB-integrin and EphA2-dependent signaling cascades were described to initiate translocation of multimolecular signaling complexes to lipid rafts. Here, EphA2 knockout was shown to have no effect on FAK phosphorylation¹⁴⁵. Lipid raft localization and induction of macropinocytosis was determined to rely on c-cbl-mediated monoubiquitination of integrins and interaction with myosinIIA^{164,165}. Disruption of macropinocytosis resulted in clathrin-mediated endocytosis, which led to non-productive infection in HMVEC-d. Additional proposed co-regulatory factors and adaptors, such as CIB1, Crk, p130Cas, Hrs, AP-2 and Eps-15^{144,146,147,165} are not shown for clarity. Of note, other studies did not detect a role of $\alpha_3\beta_1$ in KSHV infection but demonstrated the relevance of the specific interaction of $\alpha_v\beta_3$ with the gB RDG motif for KSHV infection of epithelial cells^{47,140,166,167} and a recent study described integrin $\alpha_3\beta_1$ $\alpha_v\beta_3$ and $\alpha_v\beta_5$ independent infection of two cancer cell lines (SLK/Caki-1 and HeLa)¹⁴³. How these – potentially cell type-specific – mechanistic differences are regulated remains to be determined.

Another cellular host factor described to be involved in KSHV entry is the glutamate/cysteine exchange transporter xCT¹⁶⁸, one of the variable light chains composing the heteromeric CD98/xCT complex. CD98, the common heavy chain, regulates amino acid transport¹⁶⁹ and is involved in

integrin activation and signaling^{170–172}. Correspondingly, the presence of xCT/CD98 has been demonstrated in multimolecular complexes with integrins during KSHV infection^{141,173}. However, a viral interaction partner for the xCT/CD98 complex has yet to be identified.

1.4.2.1. Spotlight - The Eph receptor tyrosine kinase family

With 14 members, Eph receptors comprise the largest known family of receptor tyrosine kinases in the human proteome. The family is subdivided in nine A-type and five B-type Ephs, which preferentially interact with the five glycosylphosphatidylinositol (GPI)-anchored ephrin A-ligands or the three transmembrane ephrin B-ligands, respectively, at sites of cell-cell contact^{174,175}. Eph-ephrin complexes are unique in their bidirectional signaling capacity, in which Eph kinase activity induces signaling cascades in the receptor-expressing cells^{176,177}, while reverse signaling in the ligand-expressing cells depends on non-receptor tyrosine kinases¹⁷⁸. Rearrangement of the actin cytoskeleton as well as activation of integrins and intracellular adhesion molecules induced by Eph signaling are implicated in a wide range of cellular processes, including cell morphology, adhesion, migration and invasion^{177,179}. Furthermore, Eph-ephrin signaling is involved in many aspects of embryogenesis, such as segmentation, neural crest cell migration, angiogenesis, and axon guidance^{180–182}.

Additionally, cumulative evidence links Eph expression to cancer development and progression. For instance, EphA1, the first described Eph receptor was identified in a screen for new oncogenic tyrosine kinases¹⁸³. Similarly, EphA2, the high-affinity receptor for the KSHV gH/gL complex was initially identified in a cDNA library of a cervical cancer cell line¹⁸⁴. Since then, EphA2 overexpression was reported in a wide range of solid tumors including cancers of the reproductive system (e.g. breast, ovary, cervical, prostate cancers), the gastrointestinal system (e.g. esophageal, gastric, colorectal cancers) and cancers in additional organs (e.g. lung, pancreas and renal cancer, glioblastoma, melanoma and neck squamous cell carcinomas)^{185–191}. High expression of EphA2 is generally correlated with more aggressive cancer phenotypes and poor prognosis^{192–196} and was found to promote metastasis, angiogenesis, and resistance development to therapeutical approaches directed against e.g. the ErbB tyrosine kinase^{197–204}. However, in recent years the dogma of EphA2 as mere oncogene was challenged. The current literature supports a role of the canonical ephrin-dependent activation of EphA2 tyrosine kinase activity in tumor suppression, while the non-canonical EphA2 tyrosine kinase-independent phosphorylation on Ser897, mediated by Akt kinase, activated by several growth factors (e.g. epidermal growth factor (EGF), basic fibroblast growth factor (bFGF), hepatocyte growth factor/scatter factor (HGF/SF), and platelet-derived growth factor (PDGF)) has pro-oncogenic functions^{205–209}.

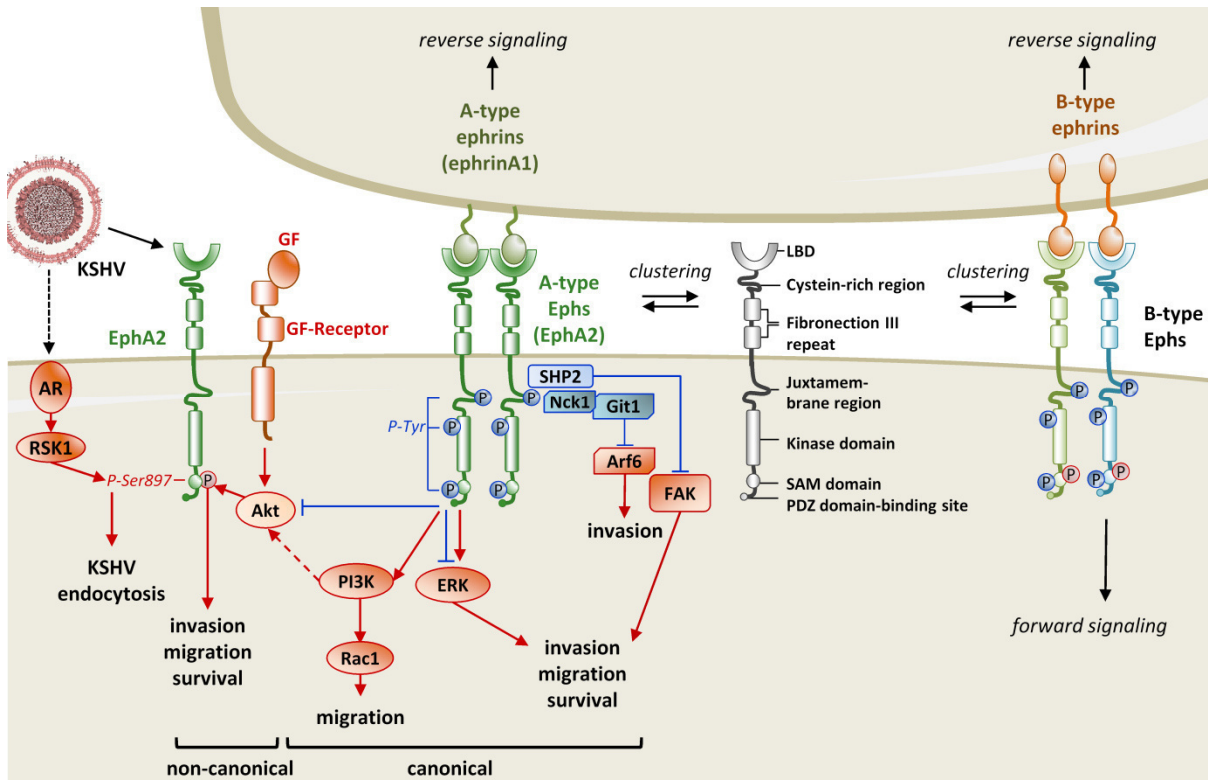


Figure 6 Eph receptor domain structure, canonical and non-canonical signaling pathways. Ligand-induced Eph receptor forward signaling is characterized by autophosphorylation of tyrosine residues (blue P), clustering into hetero- or homomeric complexes and recruitment of adaptor and effector proteins. Receptor binding induces reverse signaling events through non-receptor tyrosine kinases in GPI-anchored A-type ephrin and transmembrane B-type ephrin expressing cells^{175–177}. **The canonical pathway of ephrinA1-ligand dependent EphA2 tyrosine phosphorylation and activation** confers tumor suppressor activity of EphA2 by 1) inhibition of the PI3K/Akt pathway^{205,210,211}, 2) reduction of Integrin- or Growth Factor (GF) Receptor-dependent phosphorylation of focal adhesion kinase (FAK) through the Src homology region 2 domain-containing phosphatase 2 (SHP2) which leads to an inhibition of the FAK/Src pathway^{212–214} and 3) suppression of the ADP-ribosylation factor 6 (Arf6) through interaction with the adaptor protein Nck1 and the G protein-coupled receptor kinase-interacting protein 1 (Git1)²¹⁵. EphrinA1-dependent tyrosine phosphorylation and activation of EphA2 has been shown to both inhibit²¹⁶ or stimulate²¹⁷ the MAP/ERK kinase signaling cascade leading to anti- or pro-oncogenic cellular responses. One study proposes a pro-oncogenic role of ephrinA1-EphA2 interaction through activation of Phosphoinositide-3-kinase (PI3K) and Ras-related C3 botulinum toxin substrate 1 (Rac1)²⁰⁷. In general, discrepancies between ephrinA1-EphA2 induced signaling observed in various studies could e.g. be due to cell type-specific signaling, effects of the interaction of ephrinA1 with additional A-type Eph receptors or as recently proposed due to differences in the spatial organization of EphA2 receptor and ephrinA1 ligands^{218,219}. **The non-canonical, ligand-independent pathway** relies on phosphorylation of serine 897 (Ser897, red P) through the Akt kinase upon induction of growth factor (GF) receptor signaling^{205–209}. Upon KSHV infection, androgen receptor-mediated activation of the p90 ribosomal S6 kinase1 (RSK1) and subsequent EphA2 phosphorylation at Ser897 was shown to regulate efficient KSHV endocytosis¹⁴⁸. Pathways/components involved in tumor suppression are depicted in shades of blue; Pathways/components involved in tumor promotion or depicted in shades of orange.

Supporting this notion, the ephrinA1-dependent activation of EphA2 can inhibit migration and proliferation in vascular endothelial cells²²⁰ and attenuate growth factor-induced activation of the Ras/ERK cascade to reduce migration, invasion, proliferation and survival of cancer cells^{206,216}. Furthermore, the ephrin-dependent inactivation/inhibition of e.g. the focal adhesion kinase (FAK) and Akt pathways regulate motility, viability, and proliferation of cancer cells^{205,210,212,213}. In solid tumors, such as breast cancer, glioblastoma and hepatocellular carcinoma overexpression of EphA2 and ephrinA1 was shown to be mutually exclusive in many cases^{206,221–225}, which further supports a role of the canonical signaling pathway in tumor suppression (detailed in Figure 6).

Notably, the pathological functions of EphA2 are not restricted to oncology. In addition to KSHV, EphA2 has been described as host factors for a wide range of pathogen species, including viruses (i.e. EBV^{226,227}, hepatitis C virus²²⁸), bacteria (i.e. *Chlamydia trachomatis*²²⁹), fungal pathogens (*Cryptococcus neoformans*²³⁰), and parasites (i.e. *plasmodium*²³¹). However, the reasons for the apparent preference of different pathogens for EphA2 as a host factor remain to be elucidated.

I.5 Keeping it in the family - Simian model systems of KSHV

Analyses of the complete KSHV life cycle as well as KSHV propagation and dissemination in the host organism are limited by the lack of traditional permissive lytic systems that allow us to study a full herpesviral life cycle, and established permissive animal models, which support a systemic KSHV infection. While one study demonstrated the experimental infection of common marmosets (*Callithrix jacchus*) with KSHV²³², follow-up studies refining this model system are still lacking. Therefore, studying simian homologs of KSHV and their associated malignancies in non-human primate models provides important approaches for understanding KSHV biology as well as the role of γ -herpesviruses in tumorigenesis in general.

Several studies have addressed the suitability of RRV infection in rhesus macaques as model for the development of AIDS-related KS after experimental co-infection with simian immunodeficiency virus (SIV). Up to date, two cloned RRV isolates, namely RRV 26-95²³³ and RRV 17577²³⁴, that represent the two major RRV sequence groups based on glycoprotein primary sequence²³⁵, are available. Analogous to KSHV-associated lymphoproliferative disorders, RRV infection was correlated with lymphomagenesis in models of simian (human) immunodeficiency virus (SIV/SHIV) infected rhesus macaques^{236,237}. Similarly, co-infection with SIV led to B cell lymphoma development in animals experimentally infected with RRV 17577^{238,239}. Even though there is no clear association of RRV with solid malignancies, RRV, in addition to retroperitoneal fibromatosis herpesvirus (RFHV), has been identified in retroperitoneal fibromatosis tissue^{237,239,240}. Since the first use of RRV as model for AIDS-associated KSHV-malignancies in SIV co-infected rhesus macaques^{238,241},

RRV has found applications not only in studies to unravel rhadinovirus disease development in the context of HIV/SIV infection^{237,239}, but has also shown promise as vaccine vector for HIV/SIV^{242–245} and as viral vector for e.g. antibody delivery²⁴⁶.

Studying parallels and differences between KSHV and its non-human primate homologs in cell culture settings can help decipher the complex entry process of KSHV by e.g. highlighting fundamental, conserved mechanisms and host factors. Up to date, all obtained RRV glycoprotein sequences can be classified in one of two distinct sequence clades that are characterized by stark differences in the extracellular domain of gH as well as gL, while other glycoproteins, including gM and gN show only minor variation²³⁵. Despite of these differences in the primary sequences, interaction of the gH/gL complex with members of the Eph family – which parallels the KSHV gH/gL- Eph interaction – is conserved between RRV 26-95 and RRV 17577 as the prototypic members of both clades. However, differences do exist between both RRV isolates as well as between RRV and KSHV regarding the affinities for different Eph receptors, most notably seen in the preference of KSHV for A-type and of RRV for B-type Ephs²⁴⁷. Nevertheless, this separation is not stringent as KSHV gH/gL also co-immunoprecipitated EphB1 in mass spectrometry experiments and both RRV isolates were shown to interact with EphA4, EphA5 and EphA7 in the same setting²⁴⁷. Two of the RRV-interacting A-type Ephs, namely EphA4 and EphA5 were described as functional KSHV receptors in overexpression systems^{143,150,247} hinting to a possibly congruent role for Eph receptors in RRV and KSHV – and in extension rhadinovirus – entry. Interestingly, while established B cell lines are generally refractory to KSHV cell-free infection, certain B cell lines, such as BJAB cells support cell-free RRV infection. Analyzing parallels and differences in the infection of these model cell lines could help to direct studies regarding the mechanism of KSHV B cell infection *in vitro*.

II AIMS

In spite of advances in unraveling the rhadinoviral entry process, the complex mechanism is still not completely understood. While Eph receptors were identified as key players in KSHV and RRV infection, and the interaction domain on the cellular Eph receptor has been described¹⁴⁹, the distinct viral sequence motif or domain that mediates this interaction has not yet been identified. The generation of targeted intervention strategies and virus mutants, e.g. as attenuated vaccine vectors, relies on detailed information on the structural and amino acid level. The identification of these viral interaction motifs therefore not only furthers basic research on rhadinoviral entry but could also provide starting points for the development of KSHV prevention and treatment strategies.

Furthermore, even though the role of Eph receptors in the KSHV entry of adherent cell lines has been the focus of several studies, reports on the usage of specific Eph receptors for the infection of B cells are still sparse. As B cells represent the major reservoir for latent KSHV and RRV infection *in vivo* and give rise to two KSHV-associated malignancies, elucidating the process of B cell infection is important for the understanding of KSHV biology and pathogenesis.

In general, blocking of one individual receptor interaction (e.g. the gH/gL-Eph interaction) does not completely abrogate the infection of KSHV and RRV on the majority of analyzed cell types which implies the usage of alternative, redundant entry receptors for rhadinoviral infection. A recent report demonstrated the strict necessity of gH for KSHV infection of fibroblasts, epithelial and endothelial cells²⁴⁸ which could suggest the existence of at least one additional gH-interacting host factor. Therefore, the aims of this study were as follows:

Aim1: Characterize the Eph interaction motif on the rhadinoviral gH/gL complex and evaluate the cell type-specific contribution of the Eph interaction to KSHV/ RRV infection

Aim2: Identify Eph receptors that play a role in the infection of B cells, using the BJAB model cell line

Aim3: Identify and characterize putative additional rhadinoviral receptors that interact with gH or the gH/gL complex

III RESULTS

III.1 Publication 1: A conserved Eph family receptor-binding motif on the gH/gL complex of Kaposi's sarcoma-associated herpesvirus and rhesus monkey rhadinovirus

Plos Pathogens, Published: February 12, 2018

Author Contributions

Conceptualization: **Anna K. Großkopf**, Ronald C. Desrosiers, Alexander S. Hahn
Formal analysis: **Anna K. Großkopf**, Alexander S. Hahn
*Data analysis of all Figures was performed by **Anna K. Großkopf** and reviewed by **Alexander S. Hahn**.*
Funding acquisition: Alexander S. Hahn
Investigation: **Anna K. Großkopf**, Frank Neipel, Doris Jungnickl, Sarah Schlagowski, Alexander S. Hahn
***Anna K. Großkopf:** designed and performed the experiments which led to the results in Fig 1C, Fig 2A and B, Fig 3, Fig4, Fig 5, Fig 6, Fig 7, Supplementary Fig 1A – C and Supplementary Fig 2; **Frank Neipel:** provided data on a KSHV gL deletion mutant, which not reactivate to produce virus; **Doris Jungnickl:** performed the Illumina-based next-generation sequencing of virus stocks; **Sarah Schlagowski:** prepared part of the viral stocks and performed repeat experiments for Fig 2B and C and Supplementary Fig 1A – C; **Alexander S. Hahn:** designed and performed the experiments which led to the results in Fig 1A and B, Fig 2C and performed the experiments which led to the results in Supplementary Fig 1D and E.*
Methodology: **Anna K. Großkopf**, Armin Ensser, Alexander S. Hahn
***Anna K. Großkopf:** designed experiments which led to the results in all Figures expect Fig 1A and B, Fig 2C; **Armin Ensser:** designed and analyzed the Illumina-based next-generation sequencing of virus stocks; **Alexander S. Hahn:** designed constructs and experiments which led to the results in Fig 1A and B, Fig 2B and C.*
Project administration: Alexander S. Hahn
Resources: Armin Ensser, Ronald C. Desrosiers
Supervision: Alexander S. Hahn
Validation: Armin Ensser
Visualization: **Anna K. Großkopf**
Writing - original draft: **Anna K. Großkopf**

As detailed above, different aspects of the rhadinoviral interaction with members of the Eph receptor family still warrant further analysis. Therefore, the first part of my thesis addressed the questions:

- 1) Whether an essential sequence motif on gH/gL confers KSHV/ RRV interaction with Eph family receptors

- 2) Whether the functional conservation of the gH/gL-Eph interaction displayed by KSHV and RRV relies on a similar conservation on primary sequence or structural level
- 3) Whether the Eph interaction is essential for infectivity or tropism on distinct cell types, which can be determined by mutation of the Eph-interacting region on gH/gL

To identify regions in KSHV gH/gL that specifically mediate the interaction with the high-affinity KSHV receptor EphA2, we performed co-immunoprecipitation experiments of a series of KSHV/ RRV glycoprotein H and L chimeras with full-length EphA2. This approach indicated the N-terminal regions of gH as well as gL as crucial for the interaction with EphA2. Further analyses demonstrated that mutation of two amino acids in a five amino acid motif in domain I of KSHV and RRV gH to alanine (Glu-Leu-Glu-Phe-Asn [ELEFN → ELAAN]) is sufficient to abrogate the KSHV gH/gL-EphA2 and the RRV gH/gL-EphB3 interaction, respectively. Interestingly, although KSHV and the two RRV isolates 26-95 and 17577 display distinct, divergent affinities for members of the Eph receptor family, this motif is fully conserved between all three virus isolates.

In depth analysis of KSHV and RRV 26-95 virus strains mutated in the described ELEFN motif (KSHV gH-ELAAN, RRV gH-AELAAN) confirmed the essential nature of this motif for Eph-interaction using soluble decoy receptors and ligands in inhibition experiments and demonstrated the versatility of this mutant virus system for the analysis of Eph receptor contribution to rhadinovirus entry. In contrast to the single cycle KSHV stock production, RRV stock production requires multi-step lytic replication. We therefore included an additional mutation in RRV gH which further disrupts the gH/gL-Eph interaction to avoid functional reversion. An RRV control mutant, negative for gL, which is equally essential for the Eph-interaction as gH confirmed findings obtained with RRV gH-AELAAN.

Analysis of virus attachment as well as specific infectivity on different adherent cell types showed, that while KSHV and RRV attachment was not significantly altered by mutation of the Eph-interaction motif or deletion of RRV gL, the specific infectivity of Eph de-targeted mutants was reduced on all analyzed cell types when compared to wild-type virus infection normalized to viral particles. For both viruses, the effects ranged from approx. 5-fold to at least 9-fold, or even 20-fold (for RRV on endothelial cells). However, a consistent cell type-specific effect could only be observed for RRV.

RESEARCH ARTICLE

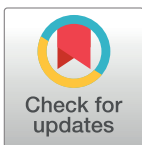
A conserved Eph family receptor-binding motif on the gH/gL complex of Kaposi's sarcoma-associated herpesvirus and rhesus monkey rhadinovirus

Anna K. Großkopf¹, Armin Ensser², Frank Neipel², Doris Jungnickl², Sarah Schlagowski¹, Ronald C. Desrosiers³, Alexander S. Hahn^{1*}

1 German Primate Center - Leibniz Institute for Primate Research, Göttingen, Germany,

2 Universitätsklinikum Erlangen, Institute for Clinical and Molecular Virology, Erlangen, Germany, **3** Miller School of Medicine, University of Miami, Miami, United States of America

* ahahn@dpz.eu



OPEN ACCESS

Citation: Großkopf AK, Ensser A, Neipel F, Jungnickl D, Schlagowski S, Desrosiers RC, et al. (2018) A conserved Eph family receptor-binding motif on the gH/gL complex of Kaposi's sarcoma-associated herpesvirus and rhesus monkey rhadinovirus. *PLoS Pathog* 14(2): e1006912. <https://doi.org/10.1371/journal.ppat.1006912>

Editor: Lindsey Hutt-Fletcher, Louisiana State University Health Sciences Center, UNITED STATES

Received: October 27, 2017

Accepted: January 30, 2018

Published: February 12, 2018

Copyright: © 2018 Großkopf et al. This is an open access article distributed under the terms of the [Creative Commons Attribution License](https://creativecommons.org/licenses/by/4.0/), which permits unrestricted use, distribution, and reproduction in any medium, provided the original author and source are credited.

Data Availability Statement: All relevant data are within the paper and its Supporting Information files.

Funding: This work was supported by the German Research foundation, grants CRC 796, TP B1 (to AE), NE 740/2-1 (to FN), HA 6013/1-1 and HA 6013/2-1 (to ASH), by the Wilhelm Sander foundation 2013.105.1 (to AE), by the Interdisciplinary Center for Clinical Research

Abstract

Kaposi's sarcoma-associated herpesvirus (KSHV) is a human oncogenic virus associated with Kaposi's sarcoma and two B-cell malignancies. The rhesus monkey rhadinovirus (RRV) is a virus of nonhuman primates that is closely related to KSHV. Eph family receptor tyrosine kinases (Ephs) are cellular receptors for the gH/gL glycoprotein complexes of both KSHV and RRV. Through sequence analysis and mutational screens, we identified conserved residues in the N-terminal domain of KSHV and RRV glycoprotein H that are critical for Eph-binding *in vitro*. Homology-based structural predictions of the KSHV and RRV gH/gL complexes based on the Epstein-Barr-Virus gH/gL crystal structure located these amino acids in a beta-hairpin on gH, which is likely stabilized by gL and is optimally positioned for protein-protein interactions. Guided by these predictions, we generated recombinant RRV and KSHV strains mutated in the conserved motif as well as an RRV gL null mutant. Inhibition experiments using these mutants confirmed that disruption of the identified Eph-interaction motif or of gL expression resulted in complete detargeting from Ephs. However, all mutants were infectious on all cell types tested, exhibiting normal attachment but a reduction in infectivity of up to one log order of magnitude. While Eph-binding-negative RRV mutants were replication-competent on fibroblasts, their infectivity was comparatively more reduced on endothelial cells with a substantial subpopulation of endothelial cells remaining resistant to infection. Together, this provides evidence for a cell type-specific use of Ephs by RRV. Furthermore, our results demonstrate that gL is dispensable for infection by RRV. Its deletion caused a reduction in infectivity similar to that observed after mutation of Eph-binding residues in gH. Our findings would be compatible with an ability of KSHV and RRV to use other, less efficient entry mediators in lieu of Ephs, although these host factors may not be uniformly expressed by all cells.

Erlangen (IZKF), grants J44 (to ASH) and A66 (to AE), by the NIH grant 5R37AI063928 (to RCD) and by intramural funding of the German Primate Center - Leibniz Institute for Primate Research (to ASH). The funders had no role in study design, data collection and analysis, decision to publish, or preparation of the manuscript.

Competing interests: The authors have declared that no competing interests exist.

Author summary

In immunocompromised individuals in general and in the context of HIV infection in particular, KSHV is a major cause of cancer and B-cell proliferative malignancies. We identified and mutated conserved residues in the N-terminal domain of the gH/gL glycoprotein complex of KSHV and the related monkey virus RRV that are critical for the interaction with cellular receptors from the Eph family. These findings provide important insight into the function of the γ -herpesviral entry machinery. Using recombinant KSHV and RRV carrying these mutations, we demonstrated that while not strictly essential, gH/gL-Eph interactions are important for efficient infection—for RRV also in a cell-specific manner—but not for attachment of KSHV and RRV. The Eph-detargeted virus mutants described in this study can be used to further dissect the requirements for KSHV and RRV entry and to identify potential alternative entry mediators. Domains and residues on the viral glycoproteins with critical roles in receptor recognition, such as the Eph-binding motif described in this paper, can be informative for the design of inhibitory monoclonal antibodies.

Introduction

Kaposi's sarcoma-associated herpesvirus (KSHV), the etiological agent of Kaposi's Sarcoma [1], is also closely associated with two B-cell malignancies, namely the primary effusion lymphoma [2] and the plasmablastic variant of multicentric Castleman's disease [3] (reviewed in [4]). Together with the rhesus monkey rhadinovirus (RRV), a closely related herpesvirus of rhesus macaques, KSHV belongs to the rhadinovirus, or $\gamma 2$, genus of herpesvirus [5]. Two RRV isolates, RRV isolate 26–95 [6] and RRV isolate 17577 [7], representing different subtypes have been characterized. RRV shares many biological features with KSHV and is therefore regarded as an *in vivo* model system for many aspects of $\gamma 2$ -herpesvirus biology [8–10] (reviewed in [11]). With regard to entry into target cells, some differences but also strong similarities exist between KSHV and RRV. A prominent difference is the interaction with integrins, which is shared by most herpesviruses (reviewed in [12]). In the case of KSHV, interaction with integrins is mediated through glycoprotein B (gB) [13], the conserved herpesviral fusion executor. Detectable interaction of RRV with integrins has not been observed, at least not via the same glycoprotein or mechanism [14]. On the other hand, the interaction of the respective gH/gL glycoprotein complex of KSHV and RRV with members of the Ephrin receptor tyrosine kinase (RTK) family of proteins (Ephs) is a conserved feature in the entry process of both rhadinoviruses. Whether the interaction of rhadinoviral gH/gL with Ephs also promotes fusion is so far unclear. In contrast, contribution to virus endocytosis, trafficking, and establishment of infection has been described by several reports [15–19]. KSHV binds EphA2 with high affinity and only exhibits very weak interactions with other A-type Ephs [15,16]. Despite very divergent primary sequences of gH and gL of RRV 26–95 and 17577, both isolates were found to interact with a broad spectrum of A- and B-type Eph receptors and to bind EphB3 with the highest avidity [16]. In addition, both KSHV and RRV require the presence of gH as well as gL in the gH/gL complex for Eph-interaction.

While we recently have shown that the binding site for the KSHV gH/gL complex on EphA2 is similar to that of natural ephrin ligands [20], the corresponding interaction site on the gH/gL complex has remained elusive until now. Recent structure-function analyses of other herpesviruses suggested different domains of the herpesviral gH as determinants for entry into target cells. For instance, the N-terminal tip of domain (D)I of the varicella-zoster

virus (VZV) homolog was shown to play a role in virus entry and fusion, as well as VZV skin tropism [21]. Similarly, in Epstein-Barr-Virus (EBV) infection, DI of gH was described as a determinant of membrane fusion activity and gB interaction [22]. Additionally, the monoclonal anti-gH/gL antibody E1D1 which inhibits EBV membrane fusion with epithelial cells was shown to bind to the tip of the gH/gL DI through interaction with gL residues [23]. Other studies suggested a role of residues in DII of EBV gH in gB-mediated membrane fusion, which is mediated by an integrin-binding 'KGD' motif located in the central region of the gH/gL complex [24]. Therefore, the site of the Eph interaction cannot easily be inferred from similar receptor interactions by other viruses. A detailed analysis of the evolutionarily conserved interaction with Eph family receptors and the regions on the gH/gL complex involved in this interaction would further our general understanding of the herpesviral gH/gL glycoprotein complex.

The actual contribution of the Eph receptor interaction to infection of different cell types by KSHV and RRV also deserves further analysis. Inhibition of KSHV infection by blocking of the Eph interaction ranged from almost complete to around twofold in previous studies depending on experimental setup and cell type [16,18]. These findings raised the question whether the interaction with Eph family receptors by KSHV and RRV is obligatory, obligatory only on certain cell types, or simply has a very strong enhancing effect on infection. Such a strong enhancing effect, depending on the setting, may still make this interaction obligatory to achieve detectable infection. Studying entry of KSHV and RRV is complicated by the fact that the Eph family comprises 14 homologous members in both humans and rhesus monkeys, by the complexity of the Eph-ephrin signaling network, and by the physiological importance of this RTK family. Various members of the Eph family were shown to play prominent roles in a wide range of physiological and pathological events, including the regulation of developmental processes, angiogenesis, cancer, and inflammation (reviewed in [25–27]). Blocking or ablating expression of Ephs may have strong effects on some cell types, exemplified by the dependence of several tumor cell lines on EphA2 expression for ongoing growth *in vitro* [28,29]. Furthermore, RRV binds very promiscuously to many of the 14 A- and B-type Ephs, impeding clean knockout experiments of distinct Ephs by compensatory effects of other members of the family. Even for KSHV, which binds EphA2 very selectively with high affinity, weak interactions with other A-type Ephs were detectable [16] and may confound results. Targeting the viral side of the gH/gL-Eph interaction would overcome this limitation.

Therefore, the aim of this study was first to address the question of whether the conserved interaction with Ephs is based on an equally conserved viral binding motif on gH/gL and to map this interaction site on the gH/gL complex of KSHV and RRV. Second, we sought to use this information to generate mutant KSHV and RRV strains that are unable to interact with Eph family receptors and to evaluate the relative importance of this interaction for infection of different cell types.

Results

An evolutionarily conserved motif in domain I of gH is critical for Eph receptor interaction

Based on the known structures of the herpes simplex virus type 2 and EBV gH/gL complex [22,30] and the conserved nature of this glycoprotein complex, it can be assumed that gH of KSHV comprises domain I (D I) to domain IV (D IV), a transmembrane domain (TM) and a short C-terminal intravirion domain (IVD). To identify the region of gH/gL critical for Eph receptor interaction, we constructed chimeras composed of different regions derived from either the KSHV or RRV gH primary sequence. Transfected chimeric gH constructs were co-

expressed with KSHV gL to form stable gH/gL complexes. Using co-immunoprecipitation assays, we tested the complexes of KSHV/RRV chimeric gH and KSHV gL for their ability to bind EphA2, which is the high affinity Eph family receptor for KSHV gH/gL and exhibits only marginal or no interaction with RRV gH/gL (Fig 1A). Out of the seven tested constructs, three were detected in Western blot analysis (Fig 1A, lane 2, 4, 8). Due to the relatively high sequence diversity of rhadinovirus gH proteins, molecular mass and glycosylation vary slightly between KSHV and RRV derived regions leading to visible shifts in apparent migration of gH chimeras when compared to KSHV gH. All of the chimeras that were expressed, even if only comprising the N-terminal and so-called shoulder region of KSHV gH (Fig 1A, lane 8), were found to complex with KSHV gL and to bind EphA2. In contrast, while full-length RRV gH did form a complex with KSHV gL, this complex did not interact with EphA2 (Fig 1A, lane 9). Likewise, N-terminal KSHV/RRV chimeras of gL or full-length RRV gL did not support binding to EphA2 when co-expressed with full-length KSHV gH in the gH/gL complex (Fig 1B). Additionally, KSHV gH/gL Δ 135–164, consisting of full-length KSHV gH and a C-terminal gL truncation mutant, precipitated EphA2 to wild-type levels (Fig 1C). This indicates that the N-terminal domains of KSHV gH and of KSHV gL in the gH/gL complex are essential for the interaction with EphA2. The natural ligands of Ephs, the eight ephrins, interact with their respective receptors through a structurally conserved G-H loop that also exhibits substantial conservation on the amino acid level [31]. We therefore aimed to identify an equally conserved Eph interaction motif on the rhadinoviral gH. First, we performed comparative sequence analysis of the gH proteins of KSHV and the two RRV isolates 17577 and 26–95, comparing the three rhadinoviral gH sequences to that of EBV gH (Fig 2A). Interestingly, we found a highly conserved motif present in all three gH sequences listed here as well as in all RRV and KSHV sequences currently listed in the NCBI database that consists of the five amino acids Glu(E)-Leu(L)-Glu(E)-Phe(F)-Asn(N) (Fig 2A, black rectangle) and is not perfectly conserved in EBV. To investigate the relevance of this E-L-E-F-N motif for the interaction with Eph receptors, a mutational scan of the N-terminal regions of KSHV and RRV gH was performed by substituting single amino acids with alanine. First, we tested the influence of these amino acid substitutions on the stability of the gH/gL heterodimer by immunoprecipitation assays (S1A and S1B Fig). The mutant KSHV and RRV gH/gL complexes were immunoprecipitated via the V5-tagged gH in the absence of recombinant Eph receptors and complexation with gL was assayed by Western blot after normalization for differences in expression levels. Mutations L47A and I49A (KSHV) and W64A (RRV) resulted in a strongly decreased interaction with gL. RRV gH E52A and L53A exhibited a reduced expression and slightly aberrant glycosylation pattern, and L53A also incorporated fully glycosylated gL less efficiently (S1B Fig). The ability of mutant gH/gL complexes to interact with either myc-tagged full-length EphA2 for KSHV gH/gL (Fig 2B), or myc-tagged full-length EphB3 for RRV gH/gL (Fig 2C) was analogously analyzed by immunoprecipitation via the V5-tagged gH and Western blot. This approach identified several point mutations that resulted in a loss of EphA2 or EphB3 interaction, respectively. Among those, the described mutations that lead to a reduced gL interaction represent one group. As loss of gL in the gH/gL complex in itself is sufficient to abolish Eph interaction (Fig 2B and 2C, first lane), the reduced interaction of these gH point mutants with Eph receptors can most likely be attributed to a loss of the gL interaction. We therefore aimed to identify gH point mutants that exhibited a normal expression level and glycosylation pattern and incorporated gL to wt levels. Notably, we identified two amino acids in the conserved E-L-E-F-N motif (Glu52 and Phe53 for KSHV, Glu54 and Phe55 for RRV) whose side chains are essential for Eph receptor interaction but at the same time dispensable for gL binding (Fig 2B and 2C, indicated by black lines). Single point mutations of other amino acids adjacent to

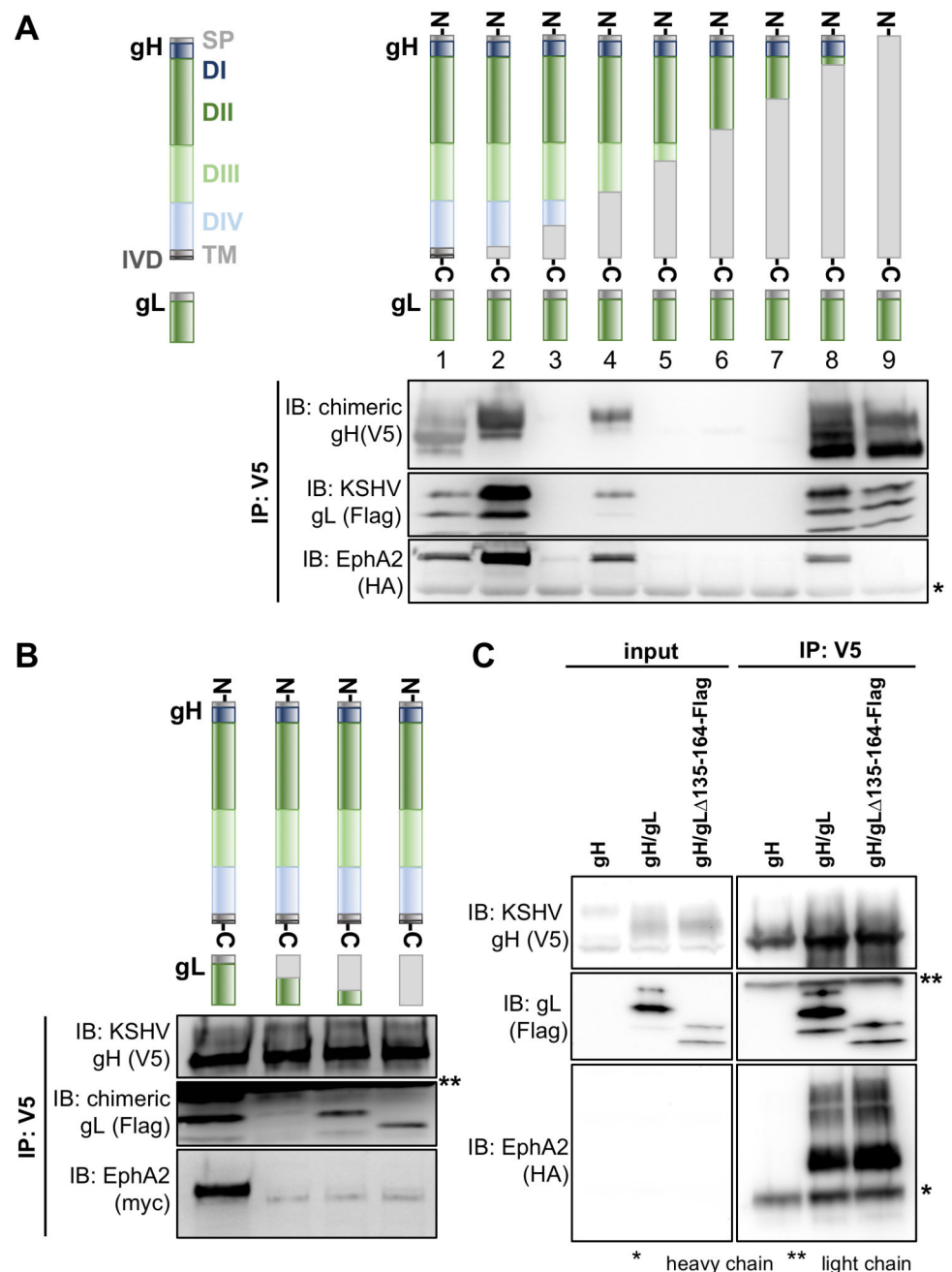


Fig 1. The Eph RTK interaction maps to the N-terminal region of KSHV gH. **A** Co-Immunoprecipitation of depicted V5-tagged RRV/KSHV gH chimeras in complex with KSHV gL-Flag identifies KSHV gH domains necessary for binding of EphA2. Monoclonal antibody to the V5-tag was used for precipitation of complexes. Equal amounts of HA epitope-tagged EphA2 ectodomain was added to each reaction. EphA2, gH, gL were detected using their respective tag. RRV-derived parts of the chimeric constructs are displayed in light grey; lane 1: KSHV gH, lane 9: RRV gH. Four gH chimeras (lanes 3 and 5–7) were not expressed to detectable levels. All chimeras harboring domain I of KSHV gH (lanes 2, 4, 8) were still able to interact with EphA2. **B** Co-Immunoprecipitation of V5-tagged KSHV gH in complex with Flag-tagged RRV/KSHV gL chimeras identifies KSHV gL domains necessary for binding of EphA2. gH-V5/gL-Flag complexes were immunoprecipitated in the presence of full-length EphA2-myc using monoclonal antibody to the V5-tag and precipitates were analyzed by Western blot as in A. RRV-derived parts of the chimeric constructs are displayed in light grey; first lane: KSHV gL, fourth lane: RRV gL. **C** Co-Immunoprecipitation of V5-tagged KSHV gH in complex with a Flag-tagged C-terminally truncated KSHV gL mutant (gLΔ135–164). gH-V5/gL-Flag complexes were immunoprecipitated in the presence of EphA2-HA (ectodomain) using monoclonal antibody to the V5-tag and

precipitates were analyzed by Western blot as in A. Full-length KSHV gH/gL serves as a positive control, KSHV gH alone serves as a negative control. Asterisks indicate non-specific bands. Abbreviations: D: domain, TM: transmembrane domain, SP: signal peptide, IVD: intravirion domain, IP: immunoprecipitation, IB: immunoblotting.

<https://doi.org/10.1371/journal.ppat.1006912.g001>

the described E-L-E-F-N motif, specifically V51A, R59A and Y60A (RRV) as well as L60A and W62A (KSHV) also abrogated binding of Eph receptors while apparently causing only a minor decrease in gL association. This might indicate additional, direct interaction with EphB3 or EphA2, respectively, at those positions.

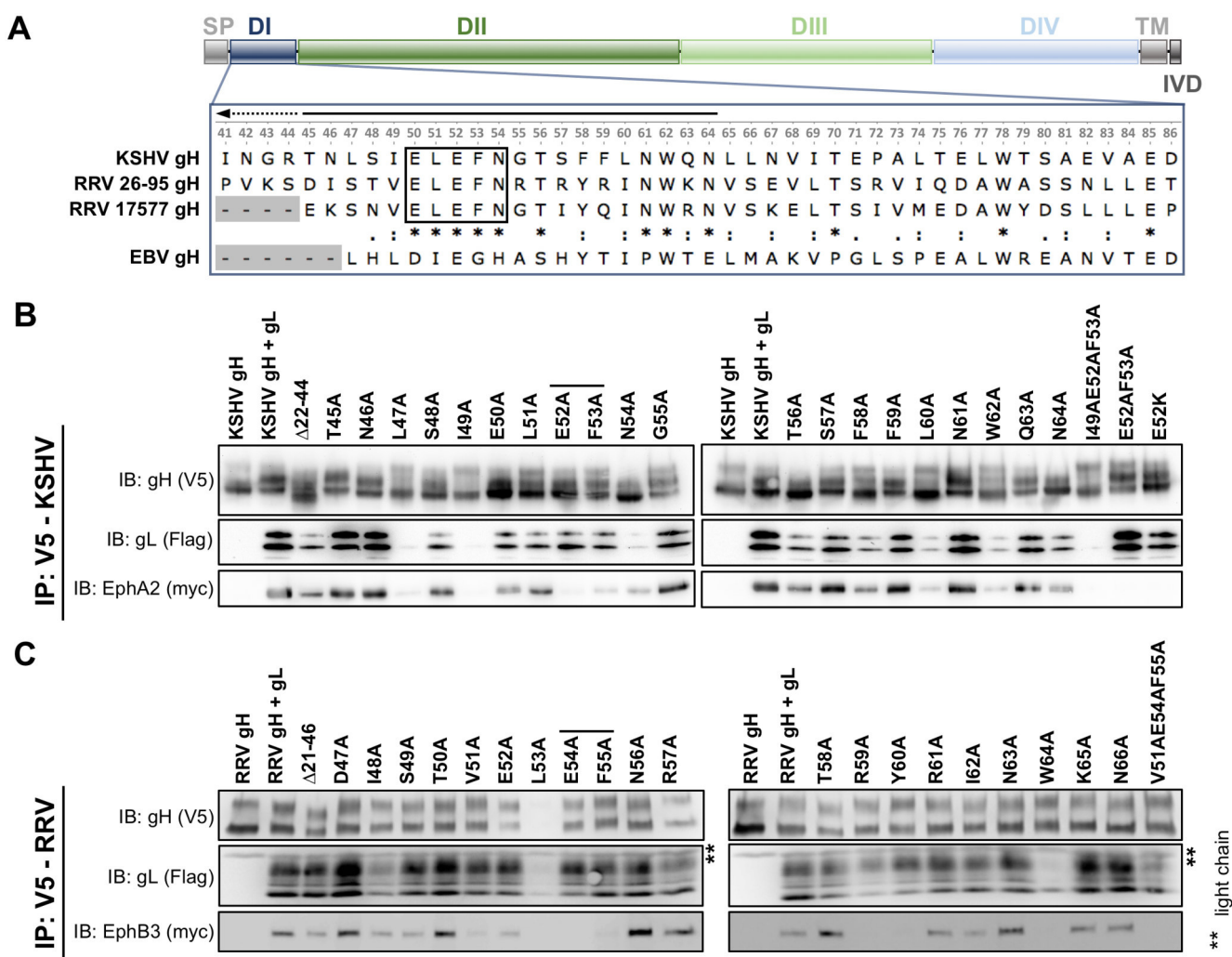


Fig 2. Two amino acids of a conserved E-L-E-F-N motif in the N-terminal region of KSHV and RRV gH are essential for Eph interaction. A Domain structure of KSHV and RRV gH. Multiple sequence alignment of domain I of gH of KSHV and the two RRV isolates 26–95 and 17577 (enlarged inset, numbers corresponding to KSHV gH). The EBV gH sequence is included as a reference. B Mutational scan of the N-terminal region of KSHV gH identifies EphA2-interacting residues. V5-tagged KSHV gH mutants were co-expressed with Flag-tagged KSHV gL. gH-V5/gL-Flag complexes were immunoprecipitated in the presence of full-length EphA2-myc using monoclonal antibody to the V5-tag and precipitates were analyzed by Western blot. KSHV gH alone serves as negative control. C Mutational scan of the N-terminal region of RRV gH identifies EphB3-interacting residues. V5-tagged gH mutants were co-expressed with Flag-tagged RRV gL. gH-V5/gL-Flag complexes were immunoprecipitated in the presence of full-length EphB3-myc using monoclonal antibody to the V5-tag and precipitates were analyzed by Western blot. RRV gH alone serves as negative control. Residues in the conserved E-L-E-F-N motif that are critical for Eph interaction are indicated by black lines. Asterisks indicate non-specific bands. Abbreviations: D: domain, TM: transmembrane domain, SP: signal peptide, IVD: intravirion domain, IP: immunoprecipitation, IB: immunoblotting.

<https://doi.org/10.1371/journal.ppat.1006912.g002>

Combination of mutations E52A and F53A of KSHV gH completely abrogated EphA2 binding without affecting gL association or expression ([Fig 2B](#), second lane from the right, [S1C Fig](#)). Likewise, a V51A-E54A-F55A triple mutant of RRV gH was negative for EphB3 interaction, while maintaining the capacity to bind RRV gL and a normal expression level ([Fig 2C](#), rightmost lane, [S1C Fig](#)). Finally, introducing a charge reversal by mutating glutamic acid at position 52 of KSHV gH to lysine (E52K) also abrogated EphA2 binding ([Fig 2B](#), rightmost lane), implicating a critical role of this negative charge in the interaction.

The importance of the E-L-E-F-N motif and its surrounding region for binding of KSHV and RRV gH/gL to their respective high-affinity binding partners from the Eph family was additionally supported by a structural prediction of the KSHV and RRV gH/gL complex based on the crystal structure of the Epstein-Barr-Virus gH/gL complex [22]. In this prediction, the residues of gH crucial for Eph interaction *in vitro*, E52/F53 (KSHV) and E54/F55 (RRV), form the turn region residues of a putative beta-hairpin in an optimal array for protein-protein interaction ([Fig 3](#)). The spatial layout of gH and gL in this region suggests a possible stabilizing effect of the N-terminal domain of gL on the parallel beta-sheet structure. Formation of such a putative receptor-binding sub-domain of gH/gL fits with the observation that the N-terminal domain of gL is crucial for Eph interaction as well, as shown by co-immunoprecipitation of KSHV and RRV chimeras ([Fig 1B](#)).

Viruses bearing mutations in the E-L-E-F-N motif are detargeted from Eph family receptors

Based on the results of our alanine scan and the structural predictions, we constructed mutant KSHV Bac16 and RRV-YFP 26–95, in which amino acids E52/F53 or E54/F55, respectively, are mutated to alanine (termed KSHV gH-ELAAN and RRV gH-AELAAN) ([Fig 4A and 4B](#)). For RRV we additionally mutated the valine at position 51 (V51) to alanine to avoid reversion as production of RRV stocks requires several rounds of lytic replication, which will select for revertants if these have a growth advantage. KSHV, on the other hand, is produced by induction of one lytic cycle after expansion of latently infected producer cells making emergence of revertants less likely. As an additional Eph-binding-deficient control we included a RRV-YFP 26–95 gL deletion mutant (RRV ΔgL) ([Fig 4A and 4B](#)). Western Blot analysis of KSHV and RRV wt and mutant virus particles verified that KSHV gH-ELAAN ([S1D Fig](#)) and RRV gH-AELAAN ([S1E Fig](#)) incorporate gH to wt levels and confirmed the complete deletion of gL on protein level for RRV ΔgL and the efficient incorporation of gL by RRV gH-AELAAN ([S1E Fig](#)). All gH mutants that were introduced into KSHV and RRV also reached expression levels comparable to wt when expressed alone or together with gL in transfected cells ([S1C Fig](#)). Analysis of KSHV gL in virus particles was precluded by our inability to generate antibodies to KSHV gL despite several attempts. All mutants were viable and infectious *in vitro* as assayed by the expression of green fluorescent protein (GFP) for KSHV or yellow fluorescent protein (YFP) for RRV under the control of a constitutively active promoter ([Fig 4C](#)).

To evaluate the receptor usage of the described KSHV and RRV mutants we conducted blocking experiments by either pre-incubation of viral inocula with soluble Eph decoy receptor fused to the Fc part of IgG (EphA2-Fc/EphB3-Fc) ([Fig 5A and 5B](#)) or ligand competition on target cells to block access to Eph receptors ([Fig 5C and 5D](#)). For ligand-dependent blocking experiments of KSHV infection, we used recombinant ephrinA4 (ephrinA4-Fc) as a high affinity ligand [16,20], which blocks EphA2 on target cells. As RRV was shown to interact with both A- and B-type Ephs, a mix of all described recombinant ligands of Ephs (ephrinA1, ephrinA2, ephrinA3, ephrinA4, ephrinA5, ephrinB1, ephrinB2 and ephrinB3, each fused to Fc

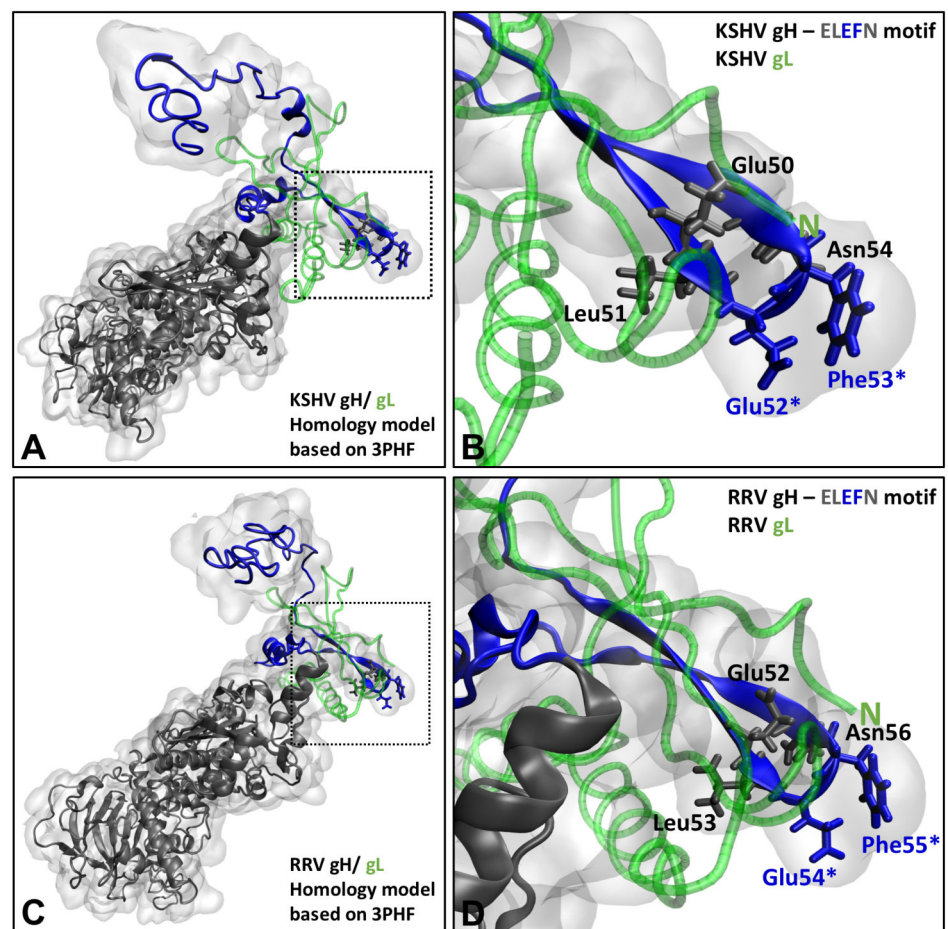


Fig 3. The E-L-E-F-N motif is located in a putative beta-hairpin at the KSHV and RRV gH/gL interaction site. Homology-based structure prediction of the KSHV gH/gL and RRV gH/gL complexes based on the crystal structure of the EBV gH/gL complex (PDB number 3PHF) using the Iterative Threading ASSEMBLY Refinement (I-TASSER) server and the CO-THreader algorithms for protein-protein complex structure and multi-chain protein threading. **A** KSHV gH/gL complex. Domain I is colored in blue. gL is colored in green. **B** Enlarged view of the inset indicated in **A** by dotted lines, showing the E-L-E-F-N motif in a putative beta-hairpin. Amino acids Glu52 and Phe53 that are critical for Eph binding are highlighted by asterisks. **C** RRV gH/gL complex. Domain I is colored in blue. gL is colored in green. **D** Enlarged view of the inset indicated in **C** by dotted lines, showing the E-L-E-F-N motif in a putative beta-hairpin. Amino acids Glu54 and Phe55 that are critical for Eph binding are highlighted by asterisks.

<https://doi.org/10.1371/journal.ppat.1006912.g003>

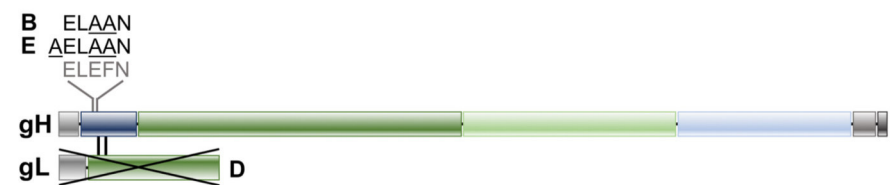
at the end of the extracellular part of the protein) was used in ligand competition experiments. For both viruses, wt and Eph-binding-negative mutants were titrated and normalized to achieve comparable infections in the absence of inhibitor.

In blocking experiments targeting viral particles, pre-incubation of the virus with soluble Fc alone as a control did not appreciably influence KSHV or RRV infection while soluble Eph decoy receptors led to a dose-dependent inhibition of KSHV infection of up to 90% (Fig 5A) and RRV infection of approximately 80% (Fig 5B) on SLK cells, as described before [15,16]. Contrarily, we observed no influence of saturating concentrations of EphA2-Fc/EphB3-Fc on the infection with Eph-binding-negative mutants KSHV gH-ELAAN, RRV gH-AELAAN or RRV ΔgL when compared to infection with untreated or soluble Fc treated viral inocula (Fig 5A and 5B). Correspondingly, soluble ephrinA4-Fc significantly reduced KSHV infection of

A

| | Name | Mutation site | Eph binding capacity |
|---|---------------|----------------------------------|----------------------|
| A | KSHV Bac16 | wt | + |
| B | KSHV gH-ELAAN | gH Glu52 and Phe53 to Ala | - |
| C | RRV 26-95 | wt | + |
| D | RRV ΔgL | gL deletion | - |
| E | RRV gH-AELAAN | gH Val51, Glu54 and Phe55 to Ala | - |

B



C

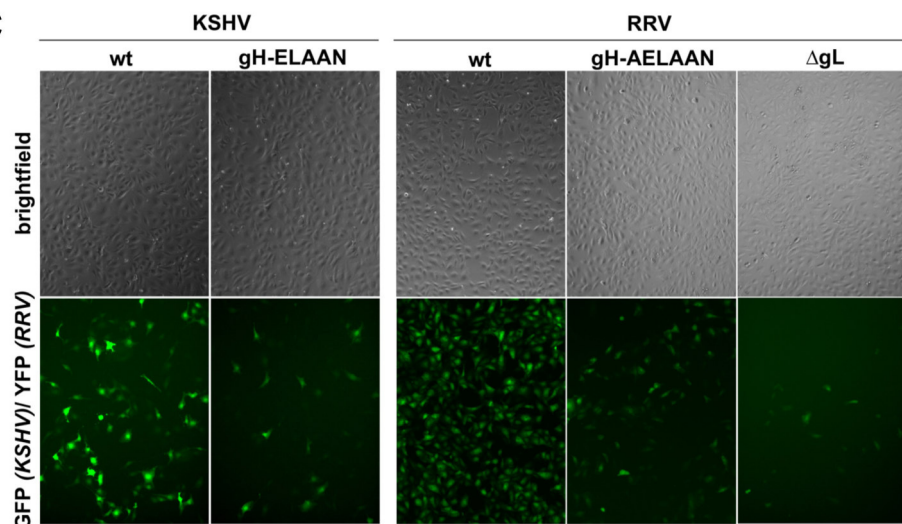


Fig 4. KSHV and RRV mutants. A List of bacmid-derived recombinant viruses generated for this study. B Schematic representation of mutations introduced into gH/gL. C SLK cells infected with wt or mutant KSHV or RRV.

<https://doi.org/10.1371/journal.ppat.1006912.g004>

SLK, human umbilical vein endothelial cells (HUVEC), lymphatic endothelial cells (LEC), and human foreskin fibroblasts (HFF) in a range from approximately 35% to 70% depending on the cell type (Fig 5C). Ligand competition using the recombinant ephrin-Fc mix resulted in similar, significant blocking of RRV infection of SLK, HUVEC, LEC, and rhesus monkey fibroblasts (RF) (Fig 5D). Pre-treatment of target cells with soluble ephrins did not influence infection with Eph receptor-detargeted virus mutants (Fig 5C and 5D), comparable to soluble decoy receptor pre-incubation.

In summary, using either soluble Eph decoy receptors or recombinant ephrins as blocking agents we observed a robust inhibition of infection with wt KSHV and RRV, while infection with Eph-detargeted mutants remained unaffected.

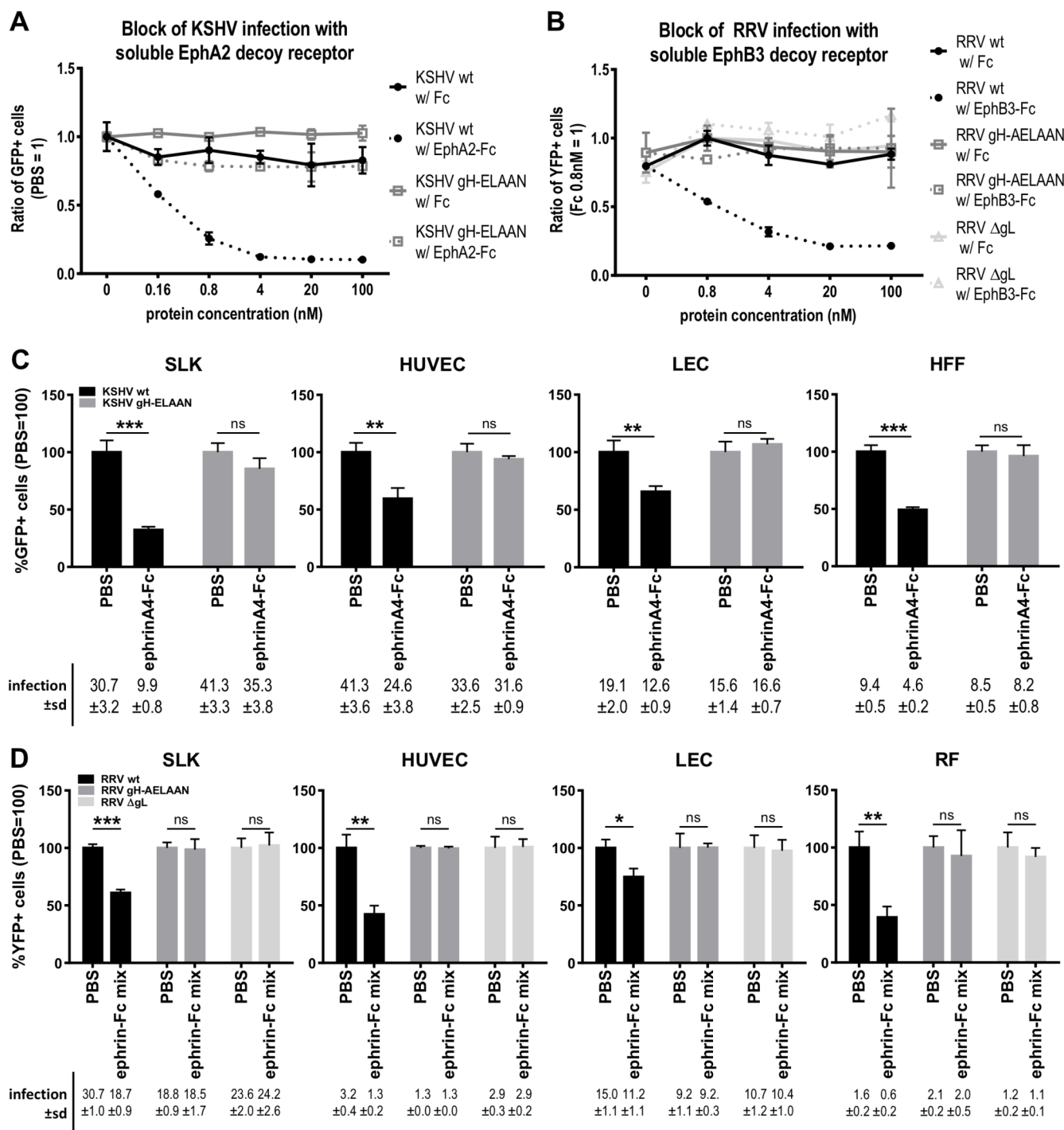


Fig 5. Mutation of the E-L-E-F-N motif is sufficient for Eph receptor detargeting. A Dose-dependent inhibition of KSHV infection by soluble EphA2-Fc on SLK cells. KSHV wt or gH-ELAAN were pre-incubated with EphA2-Fc. Fc alone and PBS were used as controls. GFP expression as indicator of infection was measured by flow cytometry. Infection without protein (PBS control) was set to 1 (duplicates, error bars represent range). B Dose-dependent inhibition of RRV infection by soluble EphB3-Fc on SLK cells. RRV 26–95 wt, ΔgL or gH-AELAAN were pre-incubated with EphB3-Fc. Fc alone and PBS were used as controls. YFP expression as indicator of infection was measured by flow cytometry. Infection with Fc 0.8nM was set to 1 (duplicates, error bars represent range). C Target cells were pre-incubated with a soluble ephrinA4-Fc fusion protein at 2μg/ml for 30min prior to infection with KSHV wt or gH-ELAAN. Infection was measured as in A. Infection without protein (PBS control) was set to 100% (triplicates, error bars represent sd). Non-normalized infection (%GFP+ cells) ±sd is listed below the

respective bars. **D** Target cells were pre-incubated with a soluble ephrin-Fc fusion protein mix (ephrinA1, ephrinA2, ephrinA3, ephrinA4, ephrinA5, ephrinB1, ephrinB2, ephrinB3) at 2 µg/ml each for 30 min prior to infection with RRV 26–95 wt, ΔgL or gH-AELAAN. Infection was measured as in B. Infection without protein (PBS control) was set to 100% (triplicates, error bars represent sd). Non-normalized infection (%YFP+ cells) ± sd is listed below the respective bars. ns: not significant, *: p-value < 0.05, **: p-value < 0.01, ***: p-value < 0.001.

<https://doi.org/10.1371/journal.ppat.1006912.g005>

Disruption of the Eph-binding motif does not affect virus attachment but results in reduced infectivity

To analyze the importance of the Eph interaction for cellular attachment and infectivity of KSHV and RRV particles, we normalized infectious dose to genome copies per cell. First the capacity of wt and mutant virus to bind target cells was analyzed. A comparison of the ratio of input genome copy numbers and bound genome copy numbers at 4°C revealed no differences in the attachment of KSHV wt and KSHV gH-ELAAN (Fig 6A) or RRV wt and RRV gH-AELAAN and RRV ΔgL (Fig 6B). We observed attachment comparable to wt of both Eph-binding-negative KSHV and RRV mutants over a range of 3 logs of input virus per cell (Fig 6A and 6B).

In contrast, KSHV gH-ELAAN and RRV gH-AELAAN/ΔgL exhibited a reduced specific infectivity on cells of epithelial (S2A and S2B Fig) and endothelial origin, as well as fibroblasts when compared to their corresponding wt virus. For both viruses, a representative experiment and averaged, fitted curves from repeat experiments are shown (Fig 6C and 6D, upper panels). The effect of the introduced mutations on specific infectivity was determined by the ratio of the rate constant K of fitted curves for wt and mutant viruses. K_{wt}/K_{mutant} describes the shift of fitted curves of Eph-binding-negative viruses to the right indicating the fold increase in input virus required to achieve wt infection levels. The impairment of specific infectivity of KSHV gH-ELAAN ranged from a factor of 4.4 on LEC to a factor of 9 on HUVEC. Eph-binding-negative RRV mutants exhibited a reduction in specific infectivity from 5-fold for RRV gH-AELAAN on RF to approx. 20-fold for RRV gH-AELAAN and RRV ΔgL on HUVEC and LEC, respectively. Similarly, when comparing infection with an identical number of viral input genomes for wt and mutant KSHV and RRV, we observed a robust reduction in the percentage of infected cells with Eph-binding-negative viruses. For example, infection with KSHV was reduced approx. 5-fold to 10-fold on HFF and 5-fold to 25-fold on HUVEC or LEC when identical input genome numbers for KSHV wt and KSHV gH-ELAAN were compared in a range of 500 to 25000 genomes/cell (Fig 6C, bar graphs). Similarly, for RRV the reduction in the percentage of infected cells ranged from approx. 2.5-fold to 8.5-fold on RF and 2.6-fold to 10-fold on LEC to approx. 5-fold to 82-fold on HUVEC when comparing identical input genome numbers of wt and mutant viruses in a range of 500 to 5000 genomes/cell (Fig 6D, bar graphs). Results using the mean fluorescence intensity (MFI) of the reporter gene instead of percentage of infected cells as a readout corroborated the same conclusions (S2C and S2D Fig). Notably, RRV gH-AELAAN and RRV ΔgL performed highly similar in these assays.

Contribution of the gH/gL-Eph interaction to RRV infection *in vitro* is cell type-specific. As mentioned above, the extent of impairment of infection with RRV Eph-binding-negative viruses differed notably between analyzed cell types (Fig 6D). To explore this finding in more detail, we directly compared KSHV and RRV infection of wild type and mutant viruses on fibroblasts of human or rhesus monkey origin to primary human endothelial cells, plotting infection of fibroblasts against infection of endothelial cells for identical viral inocula.

Comparing KSHV and the Eph-binding-negative KSHV gH-ELAAN mutant on HFF and on LEC or HUVEC (S3 Fig), high variability was observed, which may be caused by fluctuating expression levels of e.g. Ephs or other factors in these primary cells as described before for HUVEC [15] and precludes a conclusion regarding the cell type-specific importance of Eph

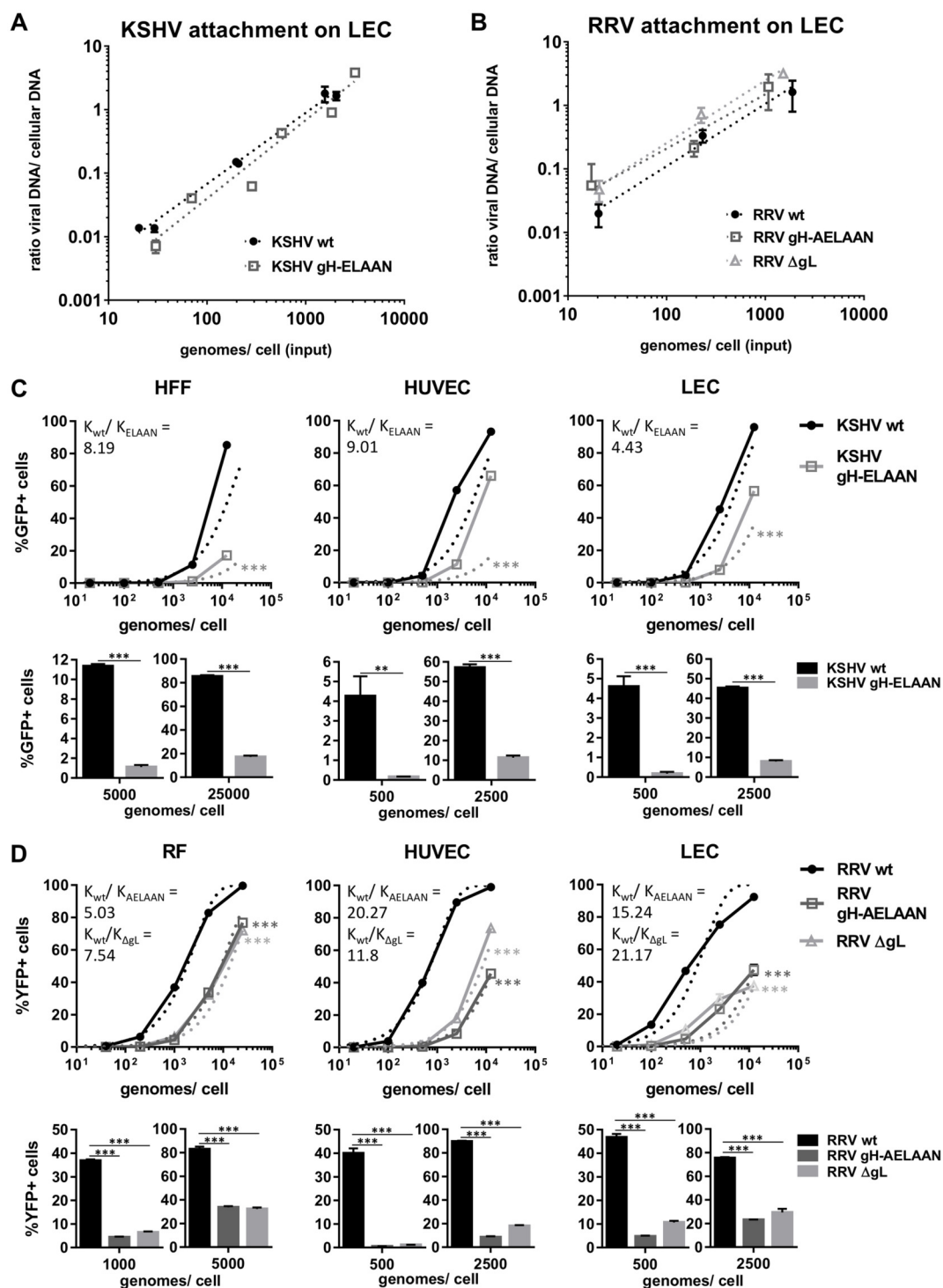


Fig 6. Eph-binding-negative RRV and KSHV mutants exhibit normal attachment and reduced specific infectivity. A Attachment of KSHV on LECs is not affected by mutational ablation of the Eph interaction. Cells were incubated with cold virus at the indicated concentrations at 4°C for 30min followed by genomic DNA isolation. The ratio of viral to cellular DNA as a measurement for attached virus was calculated based on ΔCt values of a genomic (CCR5) and a viral locus (ORF59, KSHV or ORF73, RRV) as determined by qPCR and plotted against input viral genome number. B Attachment of RRV on LECs is not affected by mutational ablation of the Eph interaction. Attachment was determined as in A. C-D Eph-binding-negative RRV and

KSHV mutants exhibit a reduced specific infection. Target cells were infected with KSHV wt and gH-ELAAN (C) or RRV wt, gH-AELAAN and ΔgL (D) at the indicated virus concentrations. GFP (KSHV) or YFP (RRV) expression as indicator of infection was measured by flow cytometry. Solid lines represent one representative experiment (triplicates, error bars indicate sd). Dotted lines represent non-linear fitting of combined representative experiments of three independent pairs (KSHV) or two independent triplets (RRV) of virus stocks. The ratio K_{wt}/K_{mutant} of the rate constant K of fitted curves for wt (K_{wt}) and mutant viruses (K_{ELAAN} , K_{AELAAN} , $K_{ΔgL}$) represents the effect of introduced mutations on specific infectivity. Bar graphs represent infections achieved by two specific input virus concentrations normalized to genome copies for one representative experiment per cell type. *: p-value < 0.05, **: p-value < 0.01, ***: p-value < 0.001.

<https://doi.org/10.1371/journal.ppat.1006912.g006>

receptor usage for KSHV infection. Even though differences between some cell populations seem to exist, these were not consistently observed for KSHV.

For RRV on the other hand, the results followed a clear pattern. In all experiments (three out of three for all mutants on LEC, five out of five for RRV ΔgL on HUVEC, and four out of four for RRV gH-AELAAN on HUVEC each compared to RF) the Eph-binding-negative RRV mutants exhibited a stronger impairment on endothelial cells compared to fibroblasts (Fig 7). In a representative experiment, the same RRV wt inoculum that resulted in infection of approximately 10% on RF resulted in approx. 60% infection on LEC, whereas inocula of RRV gH-AELAAN and RRV ΔgL that resulted in approx. 10% infection on RF, yielded only around 25% infection on LEC (Fig 7A). Additionally, while from the second highest to the highest concentration, representing a twofold increase in input virus, infection of RF with RRV gH-AELAAN doubled, infection of LEC increased only marginally from approx. 35% to approx. 40% infected cells. Similarly, although to a lesser degree, we observed this phenotype when analyzing HUVECs as an alternative endothelial cell model (Fig 7B).

Using the MFI of the virally encoded reporter genes as a readout for infection paralleled results using the percentage of GFP+/YFP+ cells as a readout for infection with both KSHV and RRV (Fig 7D and 7E and S3 Fig). For RRV, using the MFI, the cell type-specific differences in infectivity amounted to about one log order of magnitude with regard to reporter gene intensity. Notably, results with RRV gH-AELAAN and RRV ΔgL vs RRV wt were again practically indistinguishable. As opposed to KSHV, this pattern was stably observed for different virus stocks as wells as different cell passages and batches of primary cells. Taken together, these results confirm that use of Eph family receptors plays a larger role for infection of endothelial cells than for infection of fibroblasts by RRV.

Discussion

Eph family receptors, and specifically EphA2, have been described as host factors for a wide range of pathogens besides KSHV and RRV [15,16], including hepatitis C virus [32], Chlamydia trachomatis [33], Cryptococcus neoformans [34], malaria parasites [35], and as very recently reported EBV [36,37]. While it has been shown that KSHV interacts specifically with the ligand-binding domain of EphA2 in a manner that competes with the natural ephrin ligands [20], little was known until now about the specific interaction sites or motifs on the surface proteins of the respective pathogens. In this study, we present evidence for a conserved, distinctive binding site on DI of the gH/gL complex of the rhadinoviruses KSHV and RRV that is crucial for interaction with members of the Eph family of receptor tyrosine kinases.

Using a combination of comparative sequence and structural analysis together with *in vitro* mutational screens, we were able to map the Eph interaction site to the central amino acids of a conserved five amino acid motif Glu(E)-Leu(L)-Glu(E)-Phe(F)-Asn(N) on KSHV and RRV gH. Even though the amino acid sequence of gH is relatively variable within the herpesvirus family, and even so between KSHV and the RRV isolates 26–95 and 17577 (Fig 2A) as well as

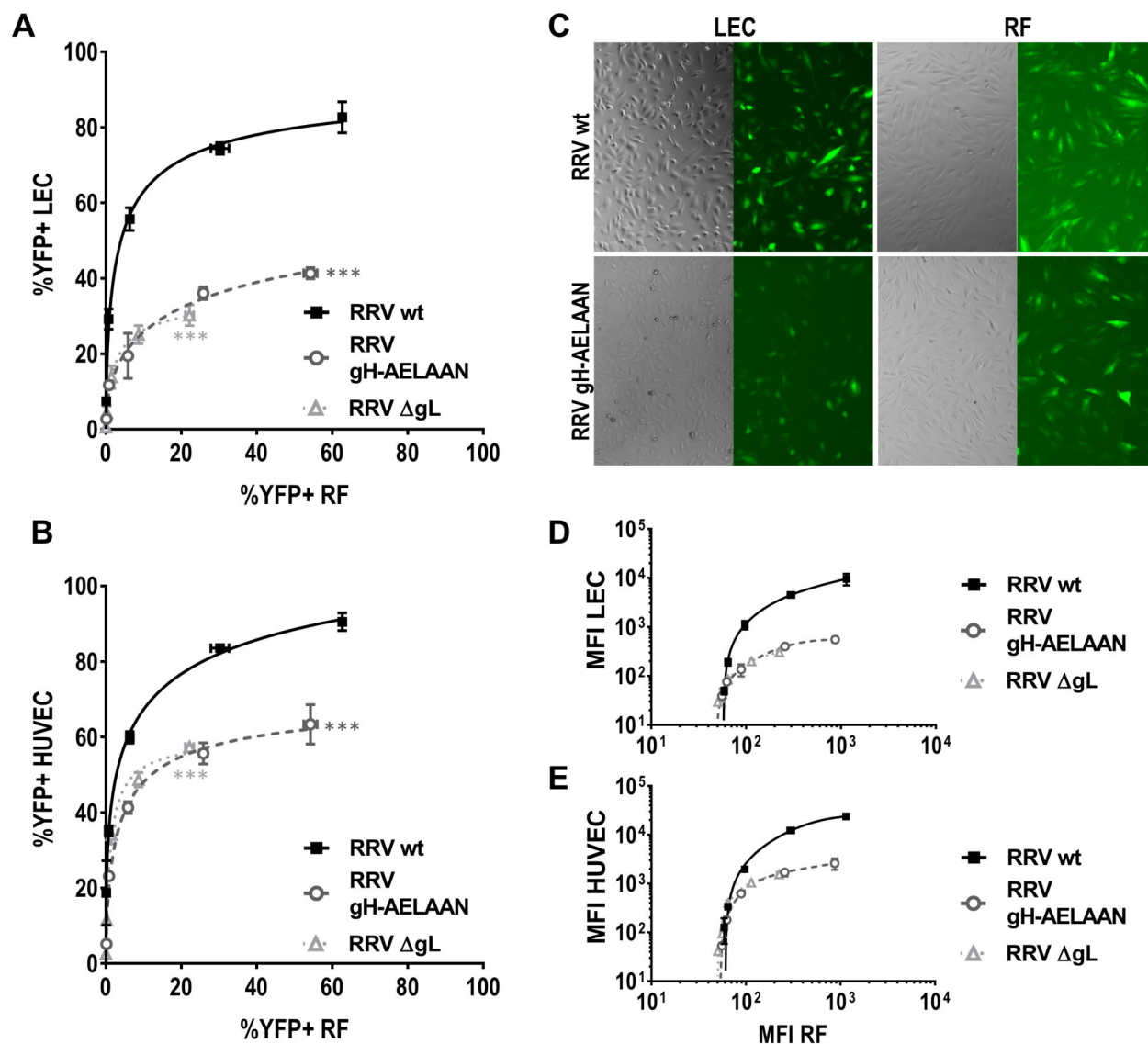


Fig 7. Contribution of the gH/gL-Eph interaction to RRV infection is cell type-specific. A–B Comparative infection on LEC (A) or HUVEC (B) and RF by RRV wt, RRV gH-AELAAN, and RRV ΔgL. RF and LEC or HUVEC were infected with the same inocula of the respective virus stock, and the percentage of reporter gene-positive cells as determined by flow cytometry for each dilution was plotted. C Micrograph of RF and LEC infected with the same respective inocula of wt and Eph-binding-negative RRV gH-AELAAN. D–E Comparative infection on LEC (D) or HUVEC (E) and RF by RRV wt, RRV gH-AELAAN, and RRV ΔgL as in A based on mean fluorescence intensity (MFI) as determined by flow cytometry. ***: p-value < 0.001.

<https://doi.org/10.1371/journal.ppat.1006912.g007>

within a large number of RRV gH sequences isolated by Shin et al [38], the described E-L-E-F-N motif is strictly conserved in all KSHV and RRV gH sequences.

Direct evidence for the functional role of the conserved rhadinoviral Eph receptor interaction motif, and in particular of residues E52/F53 (KSHV) and E54/F55 (RRV) of gH, for Eph targeting was provided by the construction of KSHV gH-ELAAN and RRV gH-AELAAN virus mutants and subsequent inhibition experiments using either soluble decoy receptors (Fig 5A and 5B) or soluble ephrins (Fig 5C and 5D).

Interestingly, the conserved asparagine of the E-L-E-F-N motif is also a conserved N-glycosylation site, and its mutation leads to a visible shift in molecular weight (Fig 2B and 2C).

While the asparagine itself does not seem to contribute to Eph binding, glycosylation could potentially play a role in steric shielding of this region from antibodies, as described for example for human immunodeficiency virus type 1 (HIV-1) gp120 [39], Ebola Virus (EBV) glycoprotein [40] and influenza virus hemagglutinin [41], as well as from MHC presentation [42].

High conservation on the amino acid sequence level also translates into an equally conserved structural prediction of the gH/gL complex of KSHV and RRV 26–95 (Fig 3), when modeled using the crystal structure of the EBV gH/gL complex [22]. In these computational models the amino acid residues E52/F53 of KSHV gH and E54/F55 of RRV gH that are crucial for Eph interaction are located in a predicted outward-angled beta-hairpin. Several reports indicate that the interaction of both A- and B-type ephrins with different Eph receptors is structurally conserved and mediated by insertion of the so-called G-H loop of ephrins into a conserved hydrophobic groove on the Eph receptors [31,43–45]. KSHV gH/gL interacts with the ephrin binding region of EphA2, which suggests that binding of rhadinoviral gH/gL complexes to Ephs may occur in a fashion that structurally mimics the binding of ephrins to their receptors. The importance of this structural motif is further supported by the effect of gH point mutants R59A, Y60A (RRV) and L60A, W62A (KSHV) on binding of Eph receptors but not on gH/gL complexation. In our model, these residues are located in the base region of the anti-parallel beta-sheets that form the beta-hairpin. Disruption of the base region may lead to a destabilization of the beta-hairpin structure and therefore loss of Eph receptor interaction on gH while binding to gL is maintained. Alternatively, these residues might directly contact Eph receptors and help determine the specificity of the interaction for e.g. EphA2 or EphB3.

According to our model, the putative beta-hairpin makes considerable contact with the N-terminal region of gL, suggesting that proper folding of the Eph interacting sub-domain may be gL-dependent. The importance of the N-terminal region of gL is also supported by our co-expression and immunoprecipitation experiments, in which the N-terminal regions of both gH and gL were necessary for Eph binding (Fig 1A and 1B). Furthermore, mutation of several amino acids adjacent to the E-L-E-F-N motif which led to a reduced gL interaction also led to reduced binding to EphA2 or EphB3, respectively, most likely due to an instability or a lack of gL in the gH/gL complex (Fig 2B and 2C). Our results are in good agreement with several reports on the functional importance of the N-terminal domain of the gH/gL complex for the entry process of EBV and VZV [21–23,46,47]. Our approach, however, does not exclude the existence of additional Eph interaction sites on gH/gL, which might determine the specificity of KSHV and RRV for individual Eph receptors. While this manuscript was in revision, EBV was reported to also interact with EphA2 not only through gH/gL, but additionally also through gB [36]. Whether the mechanism by which EBV and KSHV interact with EphA2 is conserved remains to be determined. Likely, differences do exist as EBV fuses directly with the membrane of epithelial cells, whereas KSHV enters through endocytosis. To validate our model and to fully elucidate structural aspects of the role of the rhadinoviral gH/gL, as well as of potential additional interaction sites, for receptor binding and entry into target cells, crystal structures of rhadinoviral gH/gL complexes are needed, preferably in complex with the respective high affinity receptor from the Eph family.

Surprisingly, the deletion of *orf47*, which encodes gL, from the RRV genome did not abrogate the production of infectious virus particles. Similar attempts at deleting gL of KSHV were so far unsuccessful as recombinant bacmids harboring the corresponding deletion did not yield infectious virus. One explanation for this might be the function of recently described spliced genes enclosing the *orf47-orf46-orf45* locus during reactivation from latency [48]. RRV, however, replicates lytically on RFs and rarely enters latency, which could mask defects in reactivation and make potential homologous RRV transcripts dispensable for RRV growth in culture. Accordingly, in our experiments RRV ΔgL performed practically indistinguishable from

RRV gH-AELAAN. Interestingly, an essential role for infectivity was described for gL of herpes simplex virus type 1 [49] and both human and rhesus cytomegalovirus [50], whereas gL was described as non-essential for infectivity and cell-to-cell spread of the murine gamma-herpesvirus MHV-68 [51]. Similarly, pseudorabiesvirus gL null mutants remain infectious, although exhibiting impaired entry and cell-to-cell spread [52–54]. Thus, whether gL is essential for infectivity *in vitro* or not seems to vary within the herpesviruses.

The question of the quantitative contribution of Eph receptors to rhadinovirus infection could not be answered satisfactorily until now, due to the intrinsic limitations of blocking assays, such as concentration and amount of blocking agent, and possible confounders of knockout experiments, such as potential use of alternative Eph receptors or detrimental effect of the knockout on the cell in general. The dramatic inhibition of KSHV and RRV wt infection demonstrated by specifically targeting the Eph interaction or after EphA2 knockdown or knockout [15,16,18,55] is similar in extent to what we observed using a soluble decoy receptor block (Fig 5A and 5B). This is also in very good agreement with our experiments analyzing the specific infectivity of our mutants where the percentage of infected cells with Eph-binding-deficient mutant virus was reduced 2.5-fold to 82-fold when compared to wt virus using equal input genome numbers. Similarly, approx. 4 to 20 times more Eph-binding-deficient mutant virus was needed to achieve infection levels comparable to those of wt virus (Fig 6C and 6D). Our results now quite unequivocally demonstrate that the interaction of gH/gL with Ephs is not essential for KSHV and RRV infection but contributes significantly to infectivity.

The interaction of gH with different viral or cellular proteins is thought to be a determinant of cell tropism in a wide range of herpesviruses [56–58,21]. In previous studies, we observed differences in the amount of inhibition of KSHV and RRV infection achieved by blocking the Eph interaction [15,16] depending on the cell type. While for KSHV, the cell type-specific defect in infectivity of KSHV gH-ELAAN varied significantly between different batches of fibroblasts and endothelial cells and did not allow for a clear conclusion, for RRV the cell type-specific differences were consistently observed. On LEC and HUVEC, both RRV gH-AELAAN and RRV ΔgL exhibited a defect in infectivity that was more pronounced than that observed on primary RF. These results confirm our previous findings that Eph receptors play a minor role in the infection of fibroblasts compared to infection of endothelial cells by RRV [16], as also exemplified by the ability of RRV gH-AELAAN and RRV ΔgL to replicate to high titers on RF.

The observation that ablation of the Eph interaction does not fully abrogate infectivity and has cell type-specific effects for RRV suggests the contribution of yet to be identified additional host factors for RRV and potentially also KSHV; for RRV in particular as integrins do not seem to play a major role for RRV [14]. This becomes most apparent for the infection of lymphatic endothelial cells with Eph-binding-deficient RRV mutants. Despite increasing amounts of input virus the infection appeared to be approaching a plateau at around 50% infected cells (Figs 6D and 7A), which is in good agreement with previous observations where RRV failed to infect a sizable subpopulation of endothelial cells despite increasing amounts of input virus when the Eph interaction was blocked [16]. In our opinion, the most likely explanation would be that the cell population that is refractory to Eph-independent infection lacks a host factor that can functionally substitute for the Ephs.

The critical sub-domain on the gH/gL glycoprotein complex identified in our study may serve as a target for inhibition by monoclonal antibodies. We identified several critical amino acid residues that most likely mediate direct interaction with Eph receptors. Even if the gH/gL-Eph interaction is not strictly essential, strong inhibition of KSHV infection can be achieved by targeting this region. Blocking this highly conserved region with an antibody might afford inhibition similar to that achieved by soluble EphA2-Fc decoy receptor (Fig 5A),

which presumably binds in a manner that should be very similar to antibodies targeting the E-L-E-F-N motif.

The Eph-ephrin system is a complicated signaling network that may play a role beyond simple receptor interaction in the viral infection and that interacts with a surprising number of pathogens. With the construction of Eph-binding-negative rhadinovirus mutants described in this paper we not only present direct evidence for a conserved Eph interaction motif of KSHV and RRV, but also provide a useful toolkit for the future analysis of EphA2-specific signaling in the case of KSHV and signaling of a broader range of both A-type and B-type Ephs for RRV.

Materials and methods

Cells

A549 [59] (laboratory of Stefan Pöhlmann, German Primate Center—Leibniz Institute for Primate Research, Göttingen, Germany), Human embryonic kidney (HEK) 293T cells [60,61] (laboratory of Stefan Pöhlmann), human foreskin fibroblasts (HFF) (laboratory of Klaus Korn, Universitätsklinikum Erlangen, Institute for Clinical and Molecular Virology, Erlangen, Germany), SLK cells [62,63] (NIH AIDS Research and Reference Reagent program) and rhesus monkey fibroblasts (RF) (laboratory of Prof. Rüdiger Beer, German Primate Center—Leibniz Institute for Primate Research, Göttingen, Germany) were cultured in Dulbecco's Modified Eagle Medium (DMEM), high glucose, GlutaMAX, 25mM HEPES (Thermo Fisher Scientific) supplemented with 10% fetal calf serum (FCS) (Thermo Fisher Scientific), and 50μg/ml gentamycin (PAN Biotech). iSLK cells [64] (laboratory of Don Ganem, Novartis Institutes for Bio-Medical Research, Emeryville, CA, USA) were maintained in DMEM supplemented with 10% FCS, 50μg/ml gentamycin, 2.5μg/ml puromycin (InvivoGen) and 250μg/ml G418 (Carl Roth). Human vascular endothelial cells (HUVEC) (PromoCell) were maintained in standard Endothelial Cell Growth Medium 2 (PromoCell). Human lymphatic endothelial cells (LEC) from juvenile donors (a kind gift from Anja Boos, Universitätsklinikum Erlangen, Department of Plastic and Hand Surgery, Erlangen, Germany) were maintained in Endothelial Cell Growth Medium MV 2 (PromoCell).

BAC mutagenesis, virus production, viral nucleic acid isolation and analysis

Eph-interaction-negative KSHV (KSHV gH-ELAAN) and RRV (RRV gH-AELAAN, RRV ΔgL) recombinants were generated using a two-step, markerless λ-red-mediated BAC recombination strategy as described by Tischer et al. [65]. KSHV gH-ELAAN and RRV gH-AELAAN harbor amino acid substitutions E52A and F53A (KSHV) or V51A, E54A and F55A respectively. The deletion in RRV ΔgL encompasses 128 nucleotides from position 78 to position 205 (amino acids 27 through 68), resulting in a frameshift after amino acid 26 and a stop codon after 37 amino acids. Deletion in this region was chosen in order not to destroy known and potential overlapping genes that may so far not have been charted, and because we identified sequences reminiscent of regulatory elements in the region directly surrounding the start codon. Bacmid clones BAC16 (KSHV) [66] and BAC35-8 (RRV) were used, respectively. In short, recombination cassettes were generated from the pEPKanS template by polymerase chain reaction (PCR) with Phusion High Fidelity DNA polymerase (Thermo Fisher Scientific) using long oligonucleotides (Ultramers; purchased from Integrated DNA Technologies (IDT)) (see S1 Table for a complete list of primers). Recombination cassettes were transformed into BAC16-carrying *Escherichia coli* strain GS1783 or RRV-YFP-carrying GS1783 respectively,

followed by kanamycin selection, and subsequent second recombination under 1% L(+)-arabinose (Sigma-Aldrich)-induced I-SceI expression. Colonies were verified by PCR of the mutated region followed by sequence analysis (Macrogen), pulsed-field gel electrophoresis and restriction fragment length polymorphism. For this purpose, bacmid DNA was isolated by standard alkaline lysis from 5ml liquid cultures. Subsequently, the integrity of bacmid DNA was analyzed by digestion with restriction enzyme *Xho*I and separation in 0.8% PFGE agarose (Bio-Rad) gels and 0.5×TBE buffer by pulsed-field gel electrophoresis at 6 V/cm, 120-degree field angle, switch time linearly ramped from 1s to 5s over 16 h (CHEF DR III, Bio-Rad). Infectious KSHV recombinants were generated by transfection of purified bacmid DNA (NucleoBond Xtra Midi (Macherey-Nagel)) into iSLK cells using GenJet Ver. II (Signagen) according to manufacturer's instructions. After visible GFP expression, selection was performed using 200µg/ml hygromycin B (InvivoGen) until only GFP positive cells remained. Lytic replication of KSHV-BAC16 was induced in DMEM supplemented with 10% fetal calf serum (FCS) and 50µg/ml gentamycin by addition of 2.5mM sodium-butyrate and 1µg/ml doxycycline. Supernatant was harvested after the cell monolayer was destroyed.

For RRV, infectious recombinants were generated by transfection of purified bacmid DNA (NucleoBond Xtra Midi) into 293T cells with GenJet Ver. II (Signagen) according to manufacturer's instructions. After 2 days, BAC-transfected 293T cells were transferred onto a confluent rhesus monkey fibroblasts monolayer and co-cultivated until a visible cytopathic effect (CPE) was observed. Virus stocks were prepared by inoculating fresh primary rhesus monkey fibroblasts with virus containing supernatant of 293T/rhesus monkey fibroblast co-cultures at a very low multiplicity of infection (MOI; about 1 infected cell in 1000 cells) and letting the virus replicate until the cell monolayer was destroyed. Virus-containing cell supernatant from iSLKs and rhesus monkey fibroblasts was clarified by centrifugation (4750g, 10 minutes), concentrated by overnight centrifugation (4200rpm, 4°C) and careful aspiration of approximately 95% of the supernatant. The pellet was resuspended overnight in the remaining liquid. Stocks of wt and recombinant viruses were aliquoted and stored at -80°C. The integrity of the L-DNA part of virus recombinants was confirmed by Illumina-based next-generation sequencing. For isolation of viral DNA, concentrated virus stocks were incubated with DNaseI (40 units/ml) for 1h at 37°C. Addition of EDTA to a final concentration of 15mM was followed by a second incubation step (70°C, 10min). After a third incubation step with ProteinaseK (1mg/ml) and SDS (0.5%) (60°C, 2h) standard phenol chloroform extraction was performed. Sample preparation was performed using the Nextera DNA Sample Preparation system, dual indexing, and sequencing using the MiSeq Reagent Kit, 600 Cycles on the Illumina MiSeq system. Demultiplexed paired 300 nt sequence reads were analyzed by Genomics Workbench 10 (Qiagen Bioinformatics, Aarhus, DK).

Plasmids

pcDNA4 vectors containing full-length EphA2 (ref[NM_004431], pcDNA4-EphA2-myc), the soluble ectodomain of EphA2 (amino acids 1–534) (ref[NM_004431], pcDNA4-EphA2-HA), a soluble EphA2-Fc fusion construct comprising amino acids 25–534 of human EphA2 in the pAB61 Fc-fusion backbone vector (pEphA2-Fc) [15] and EphB3 (ref[BC052968], pcDNA-EphB3-myc) [15,16] were described elsewhere. KSHV/RRV chimeric gH constructs were generated based on pcDNA6aV5His/pcDNA3.1 backbone vectors containing RRV/KSHV gH and gL coding sequences (ref[GQ994935.1], pcDNA6aV5-KSHV-gH, pcDNA3.1-KSHV-gL-Flag; ref[AF210726.1], pcDNA6aV5-RRV-gH, pcDNA3.1-RRV-gL-Flag) [15,16] by PCR based restriction enzyme cloning. The KSHV gLΔ135-164-Flag construct (pcDNA3.1-KSHV-gLΔ135-164-Flag) was generated by a PCR-based mutagenesis using phosphorylated primers

followed by blunt end ligation of the PCR product (see [S1 Table](#) for a complete list of primers and constructs). Plasmids harboring point mutations in domain I of RRV/KSHV gH used in the alanine scan were purchased from GenScript based on pcDNA6aV5-KSHV-gH and pcDNA6aV5-RRV-gH.

Recombinant proteins

Recombinant, soluble EphA2 Fc/Strep-fusion protein was purified under native conditions by Strep-Tactin chromatography from 293T cell culture supernatant. 293T cells were transfected by Polyethylenimine "Max" (PEI) (Polysciences) [67] transfection with pEphA2-Fc. The protein-containing cell culture supernatant was filtered through 0.22µm PES membranes (Millipore) and passed over 0.5ml of a Strep-Tactin Superflow (IBA Lifesciences) matrix in a gravity flow Omniprep column (BioRad). Bound protein was washed with approximately 50ml phosphate buffered saline pH 7.4 (PBS) and eluted in 1ml fractions with 3mM desthiobiotin (Sigma-Aldrich) in PBS. Protein-containing fractions were pooled and buffer exchange to PBS via VivaSpin columns (Sartorius) was performed. Protein concentration was determined by absorbance at 280nm. Aliquots were frozen and stored at -80°C. Recombinant, human, soluble EphB3-Fc (5667-B3-050) and soluble ephrin ligands, as either human (rh) or mouse (rm) Fc-fusion proteins (rm-ephrinA1, rm-ephrinA2, rh-ephrinA3, rh-ephrinA4, rh-ephrinA5, rm-ephrinB1, rm-ephrinB2 and rh-ephrinB3 Fc) (SMPK3) were purchased from R&D Systems.

Quantitative realtime-PCR-based viral genome copy number analysis and virus attachment assay

Concentrated virus samples were treated with DNaseI (0.1 units/µl) to remove any non-encapsidated DNA (37°C, overnight). Subsequently, DNaseI was deactivated and viral capsids were disrupted by heating the samples to 95°C for 30 minutes. Realtime-PCR (qPCR) was performed on a StepOne Plus cycloer (Thermo Fisher Scientific) in 20µl reactions using the SensiFAST Probe Hi-ROX Kit (Bioline) (cycling conditions: 3min initial denaturation at 95°C, 40 cycles 95°C for 10s and 60°C for 35s). All primer-probe sets were purchased from IDT as complete PrimeTime qPCR Assays (primer:probe ratio = 4:1). Samples were analyzed in technical triplicates. A series of six 10-fold dilutions of bacmid DNA was used as standard for absolute quantification of viral genome copies based on qPCR of ORF59 for KSHV and ORF73 for RRV (see [S1 Table](#) for a complete list of primers). For virus attachment assays LEC were plated at 50 000 cells/cm². Target cells were incubated with ice-cold virus dilutions at the indicated concentrations, normalized to genomes per cell, at 4°C for 30min. After three washes with ice-cold PBS genomic DNA was isolated using the ISOLATE II Genomic DNA Kit (Bioline) according to manufacturer's instructions. The ratio of viral DNA to cellular DNA as a measurement of attached virus was determined by qPCR as described above. Relative values of bound viral genomes to cellular DNA were calculated on the basis of ΔCt values for viral genomic loci (ORF59 for KSHV, ORF73 for RRV) and a cellular genomic locus (CCR5).

Infection assays and flow cytometry

For infection assays cells were plated at 50 000 cells/cm² (SLK, HUVEC, LEC) or 25 000 cells/cm² (RF, HFF) respectively. One day after plating, cells were infected with the indicated amounts of virus. 24h or 48h post infection cells were harvested by brief trypsinization, followed by addition of 5% FCS in PBS to inhibit trypsin activity, spun down (1200rpm, 10min), washed once with PBS, re-pelleted and fixed in PBS supplemented with 2% formaldehyde (Carl Roth). A minimum of 10 000 cells was analyzed per sample for GFP or YFP expression on a LSRII flow cytometer (BD Biosciences). Data was analyzed using Flowing Software

(Version 2.5). For block with soluble ephrins, cells were pre-incubated with the indicated ephrin-Fc fusion proteins at a final concentration of 2 μ g/ml for 30min at room temperature followed by infection with KSHV or RRV. Block of KSHV/RRV infection with soluble decoy receptor was assayed by infection with virus inocula that were pre-incubated with the indicated concentrations of soluble EphA2-Fc, EphB3-Fc or Fc alone at room temperature for 30min.

Immunoprecipitation and Western blot analysis

293T cells were transfected using PEI [67] or Lipofectamine with Plus reagent (Thermo Fisher Scientific) as per the manufacturer's instructions. Recombinant gH-V5/gL-Flag complexes were precipitated from the lysates of 293T cells transfected with the respective expression constructs. Lysates were prepared in NP40 lysis buffer (1% Nonidet P40 Substitute (Sigma-Aldrich), 150mM NaCl (Sigma-Aldrich), 50mM HEPES (VWR), 1mM EDTA (Amresco) with freshly added Protease Inhibitor Cocktail, General Use (Amresco)) and subsequently incubated with agitation with 0.5 μ g V5-tag antibody (Serotec or Bio-Rad) and ProteinG sepharose (GenScript or GE Healthcare) for 2h or overnight at 4°C. Amount of input gH/gL between mutants was normalized by diluting lysates with cell lysate from non-transfected 293T cells prior to immunoprecipitation according to Western blot analysis of lysates and evaluation of the gH/gL content for each construct. After one wash, pre-coupled complexes were incubated overnight at 4°C with agitation with equal amounts of lysate of full-length EphA2-myc or full-length EphB3-myc expression plasmid transfected 293T cells (for KSHV gH/gL or RRV gH/gL binding analysis, respectively) or with supernatant of 293T cells transfected with an expression plasmid for HA-tagged EphA2 ectodomain (for KSHV gH/gL binding analysis). ProteinG beads were collected by brief centrifugation and washed 3 times in NP40 lysis buffer. Precipitates were heated in SDS sample buffer and analyzed by polyacrylamide gel electrophoresis (PAGE) using 8–16% tris-glycine gradient gels (Thermo Fisher Scientific) and Western blot (100mA, max 30V, 1h in Towbin buffer (25mM Tris, 192mM glycine)). For Western blot analysis of virus particles, a 5% OptiPrep (Sigma-Aldrich) in PBS cushion was overlaid with 1ml concentrated virus stock and centrifuged for 2h at 20 000g. Approx. 95% of the supernatant was discarded and the virus pellet was washed once with 1ml PBS and spun down (20 000g, 1h). The virus pellet was resuspended in 30 μ l PBS, dissolved overnight and subsequently heated after the addition of 50 μ l SDS sample buffer (99°C, 15min). Western Blot analysis was performed as described above.

Structure prediction and analysis

Homology based structure prediction was performed using the Iterative Threading ASSEMBLY Refinement (I-TASSER) server on standard settings for structure prediction of KSHV or RRV gH based on the crystal structure of the EBV gH/gL complex (3PHF). Modeling of the KSHV or RRV gH/gL complexes was additionally performed using both the SPRING and CO-THreader algorithms for protein-protein complex structure and multi-chain protein threading with no differences between determined structures. Resulting CO-THreader and I-TASSER structures were aligned with the VMD 1.9.3 OpenGL RMSD Trajectory Tool based on the overlapping region of gH domain I predicted in both models (KSHV amino acids 43 to 87, RRV amino acids 45 to 88) at an RMSD of 0.589Å for KSHV and 0.616Å for RRV. All further analyses and visualizations were performed using VMD 1.9.3 OpenGL.

Mathematical and statistical analysis

Curve fitting of specific infectivity normalized to genome copies/cell was performed using the built-in exponential equation for one phase association of GraphPad Prism version 6 for Windows (GraphPad Software, La Jolla California USA) based on the poisson distribution [68]. The span was set from 0 to 100, representing 0% or 100% infected cells, respectively, resulting in the simplified function $f(x) = 100 * (1 - e^{-K * x})$, with x representing input genome number and K representing the specific infectivity per input genome. The ratio between K_{wt} and K_{mutant} was used to calculate the differences in infectivity between wt and mutant viruses. Statistical difference between fitted curves was determined by the extra sum-of-squares F test with confidence intervals corrected for multiple comparisons using the Bonferroni correction. Statistical analysis of multiple groups was performed using regular two-way analysis of variance (ANOVA) followed by Sidak's multiple comparison test. Statistical difference between two groups was determined by unpaired Student's t-tests followed by correction for multiple comparison using the Holm-Sidak method when necessary. All Statistical analyses were performed with GraphPad Prism version 6. For all statistics, *: p-value < 0.05, **: p-value < 0.01, ***: p-value < 0.001.

Primers

See [S1 Table](#) for a complete list of primers.

Antibodies

See [S1 Table](#) for a complete list of antibodies.

Supporting information

S1 Fig. Effect of single point mutations in the N-terminal domain of gH on gH/gL stability and complexation as well as gH and gL incorporation in the virus particles. **A** Effects of point mutations on the stability of KSHV gH/gL complexes in the absence of recombinant Eph receptors. V5-tagged KSHV gH mutants were co-expressed with Flag-tagged KSHV gL. gH-V5/gL-Flag complexes were immunoprecipitated using monoclonal antibody to the V5-tag and precipitates were analyzed by Western blot. KSHV gH/RRV gL and KSHV gH alone serve as negative control. **B** Effects of point mutations on the stability of RRV gH/gL complexes in the absence of recombinant Eph receptors. V5-tagged RRV gH mutants were co-expressed with Flag-tagged RRV gL. gH-V5/gL-Flag complexes were immunoprecipitated and analyzed as in A. KSHV gH/RRV gL and RRV gH alone serve as negative control. **C** Point mutations in the E-L-E-F-N motif of KSHV and RRV gH do not influence stability of gH alone or of the gH/gL complex. V5-tagged KSHV gH wt, gH E52AF53A (gH-ELAAN), RRV gH wt and gH V51AE54AF55A (gH-AELAAN) were either expressed alone or co-expressed with Flag-tagged KSHV/RRV gL. gH-V5 and gH-V5/gL-Flag complexes were immunoprecipitated and analyzed as in A. **D** Double mutation E52AF53A in KSHV gH does not influence the incorporation of gH into the virus particle. KSHV wt, and gH-ELAAN virus preparations were analyzed by Western Blot. K8.1 was used as loading control. K8.1 runs in a diffuse molecular weight pattern due to its complex O-glycosylation. **E** Triple mutation V51AE54AF55A in RRV gH (gH-AELAAN) does not influence the incorporation of gH and gL into the virus particle. RRV wt, gH-AELAAN and RRV ΔgL virus preparations were analyzed by Western Blot. gB was used as loading control. Abbreviations: IP: immunoprecipitation, IB: immunoblotting. (TIF)

S2 Fig. Specific infectivity of Eph-binding-negative RRV and KSHV mutants. **A-B** Eph-binding-negative RRV and KSHV mutants exhibit a reduced specific infection on epithelial cells. Target cells were infected with KSHV wt and gH-ELAAN (**A**) or RRV wt, gH-AELAAN and ΔgL (**B**) at the indicated virus concentrations. GFP (KSHV) or YFP (RRV) expression as indicator of infection was measured by flow cytometry (triplicates, error bars indicate sd). **C-D** Eph-binding-negative RRV and KSHV mutants exhibit a reduced specific infection assayed by mean fluorescence intensity (MFI) of the respective reporter gene. Target cells were infected with KSHV wt and gH-ELAAN (**C**) or RRV wt, gH-AELAAN and ΔgL (**D**) at the indicated virus concentrations. GFP (KSHV) or YFP (RRV) MFI as indicator of infection was measured by flow cytometry (triplicates, error bars indicate sd). (TIF)

S3 Fig. Contribution of the gH/gL-Eph interaction to KSHV infection of endothelial cells and fibroblasts. **A-B** Comparison of KSHV wt with KSHV gH-ELAAN infection based on GFP reporter gene-positive cells on LEC (**A**) or HUVEC (**B**) and HFF. HFF and LEC or HUVEC were infected with the same inocula of the respective virus stock, and the percentage of reporter gene-positive cells as determined by flow cytometry for each dilution was plotted. **C** Micrograph of HFF and LEC infected with the same inocula of wt and Eph-binding-negative KSHV. **D-E** Comparison of KSHV wt and KSHV gH-ELAAN infection based on MFI on LEC (**D**) or HUVEC (**E**) and HFF performed as in (A-B). (TIF)

S1 Table. List of accession numbers, primers, and antibodies used in this study. (XLSX)

Acknowledgments

We thank Jan Willem Robering and Dr. Anja Boos for providing Lymphatic Endothelial Cells (LEC), Prof. Rüdiger Beer for providing rhesus monkey fibroblasts (RF), Prof. Scott Wong for providing anti RRV gB antibody 3H8.1 and Dr. Effi Wies, Robert Becker and Candice D'Costa for critical reading of the manuscript.

Author Contributions

Conceptualization: Anna K. Großkopf, Ronald C. Desrosiers, Alexander S. Hahn.

Formal analysis: Anna K. Großkopf, Alexander S. Hahn.

Funding acquisition: Alexander S. Hahn.

Investigation: Anna K. Großkopf, Frank Neipel, Doris Jungnickl, Sarah Schlagowski, Alexander S. Hahn.

Methodology: Anna K. Großkopf, Armin Ensser, Alexander S. Hahn.

Project administration: Alexander S. Hahn.

Resources: Armin Ensser, Ronald C. Desrosiers.

Supervision: Alexander S. Hahn.

Validation: Armin Ensser.

Visualization: Anna K. Großkopf.

Writing – original draft: Anna K. Großkopf.

Writing – review & editing: Anna K. Großkopf, Armin Ensser, Ronald C. Desrosiers, Alexander S. Hahn.

References

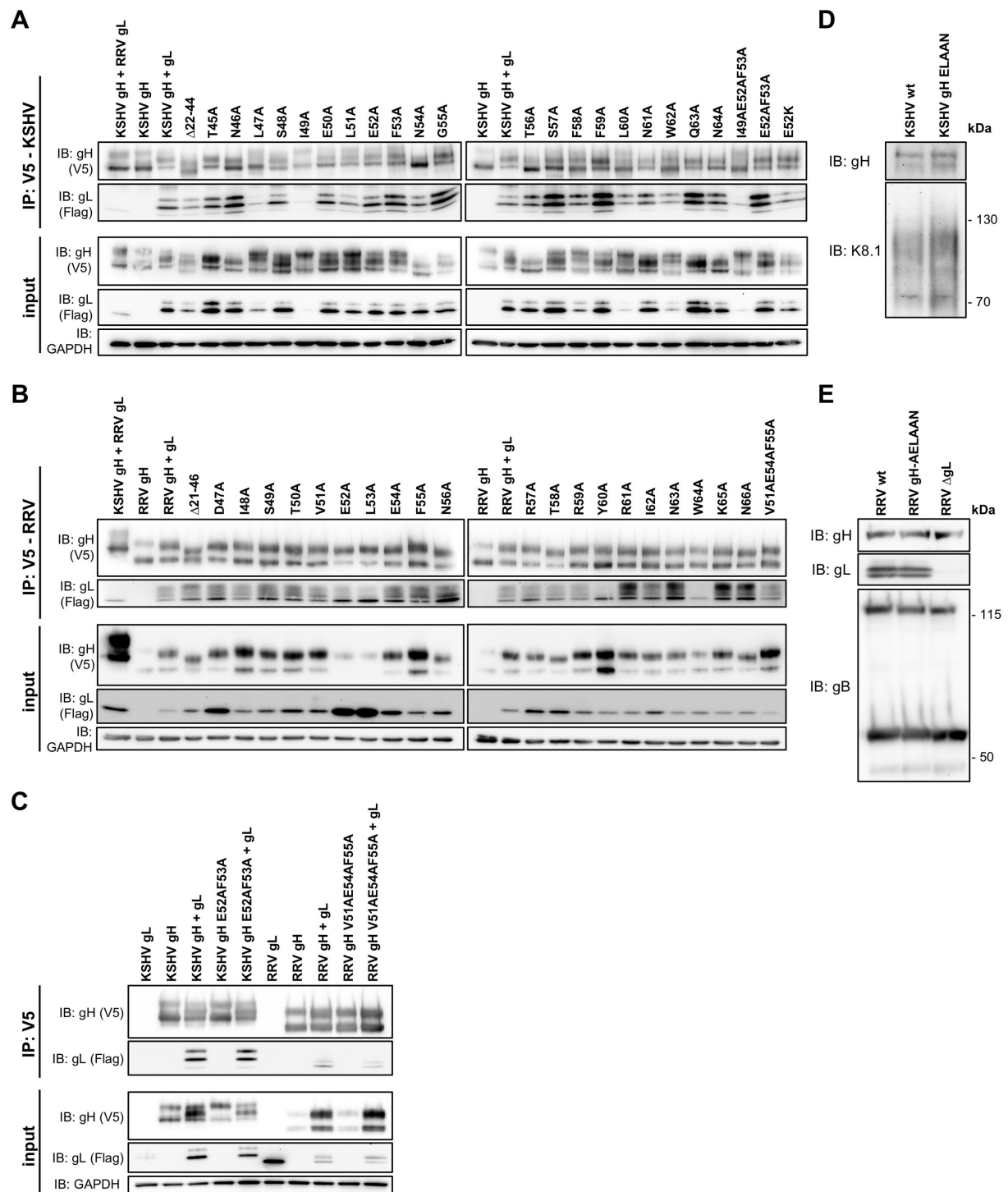
1. Chang Y, Cesarman E, Pessin MS, Lee F, Culpepper J, Knowles DM, et al. Identification of herpesvirus-like DNA sequences in AIDS-associated Kaposi's sarcoma. *Science*. 1994; 266: 1865–1869. PMID: [7997879](#)
2. Cesarman E, Chang Y, Moore PS, Said JW, Knowles DM. Kaposi's sarcoma-associated herpesvirus-like DNA sequences in AIDS-related body-cavity-based lymphomas. *N Engl J Med*. 1995; 332: 1186–1191. <https://doi.org/10.1056/NEJM199505043321802> PMID: [7700311](#)
3. Soulier J, Grollet L, Oksenhendler E, Cacoub P, Cazals-Hatem D, Babinet P, et al. Kaposi's sarcoma-associated herpesvirus-like DNA sequences in multicentric Castelman's disease. *Blood*. 1995; 86: 1276–1280. PMID: [7632932](#)
4. Wen KW, Damania B. Kaposi sarcoma-associated herpesvirus (KSHV): Molecular biology and oncogenesis. *Cancer Lett*. 2010; 289: 140–150. <https://doi.org/10.1016/j.canlet.2009.07.004> PMID: [19651473](#)
5. Damania B, Desrosiers RC. Simian homologues of human herpesvirus 8. *Philos Trans R Soc B Biol Sci*. 2001; 356: 535–543. <https://doi.org/10.1098/rstb.2000.0782> PMID: [11313010](#)
6. Desrosiers RC, Sasseville VG, Czajak SC, Zhang X, Mansfield KG, Kaur A, et al. A herpesvirus of rhesus monkeys related to the human Kaposi's sarcoma-associated herpesvirus. *J Virol*. 1997; 71: 9764–9769. PMID: [9371642](#)
7. Searles RP, Bergquam EP, Axthelm MK, Wong SW. Sequence and genomic analysis of a Rhesus macaque rhadinovirus with similarity to Kaposi's sarcoma-associated herpesvirus/human herpesvirus 8. *J Virol*. 1999; 73: 3040–3053. PMID: [10074154](#)
8. Mansfield KG, Westmoreland SV, DeBakker CD, Czajak S, Lackner AA, Desrosiers RC. Experimental infection of rhesus and pig-tailed macaques with macaque rhadinoviruses. *J Virol*. 1999; 73: 10320–10328. PMID: [10559350](#)
9. Wong SW, Bergquam EP, Swanson RM, Lee FW, Shiigi SM, Avery NA, et al. Induction of B cell hyperplasia in simian immunodeficiency virus-infected rhesus macaques with the simian homologue of Kaposi's sarcoma-associated herpesvirus. *J Exp Med*. 1999; 190: 827–840. PMID: [10499921](#)
10. Gilardi KV, Spinner A, Canfield DR, Valverde CR, Hatcher S, Larkin E, et al. T-cell lymphoproliferative disorder in an aged rhesus macaque. *J Am Vet Med Assoc*. 2000; 217: 384–387, 341. PMID: [10935045](#)
11. O'Connor CM, Kedes DH. Rhesus monkey rhadinovirus: a model for the study of KSHV. *Curr Top Microbiol Immunol*. 2007; 312: 43–69. PMID: [17089793](#)
12. Campadelli-Fiume G, Collins-McMillen D, Gianni T, Yurochko AD. Integrins as Herpesvirus Receptors and Mediators of the Host Signalosome. *Annu Rev Virol*. 2016; 3: 215–236. <https://doi.org/10.1146/annurev-virology-110615-035618> PMID: [27501260](#)
13. Akula SM, Pramod NP, Wang FZ, Chandran B. Integrin alpha3beta1 (CD 49c/29) is a cellular receptor for Kaposi's sarcoma-associated herpesvirus (KSHV/HHV-8) entry into the target cells. *Cell*. 2002; 108: 407–419. PMID: [11853674](#)
14. Garrigues HJ, Rubinchikova YE, DiPersio CM, Rose TM. Integrin {alpha}V 3 Binds to the RGD Motif of Glycoprotein B of Kaposi's Sarcoma-Associated Herpesvirus and Functions as an RGD-Dependent Entry Receptor. *J Virol*. 2008; 82: 1570–1580. <https://doi.org/10.1128/JVI.01673-07> PMID: [18045938](#)
15. Hahn AS, Kaufmann JK, Wies E, Naschberger E, Panteleev-Ivlev J, Schmidt K, et al. The ephrin receptor tyrosine kinase A2 is a cellular receptor for Kaposi's sarcoma-associated herpesvirus. *Nat Med*. 2012; 18: 961–966. <https://doi.org/10.1038/nm.2805> PMID: [22635007](#)
16. Hahn AS, Desrosiers RC. Rhesus Monkey Rhadinovirus Uses Eph Family Receptors for Entry into B Cells and Endothelial Cells but Not Fibroblasts. Gao S-J, editor. *PLoS Pathog*. 2013; 9: e1003360. <https://doi.org/10.1371/journal.ppat.1003360> PMID: [23696734](#)
17. Chakraborty S, Veettil MV, Bottero V, Chandran B. Kaposi's sarcoma-associated herpesvirus interacts with EphrinA2 receptor to amplify signaling essential for productive infection. *Proc Natl Acad Sci*. 2012; 109: E1163–E1172. <https://doi.org/10.1073/pnas.1119592109> PMID: [22509030](#)
18. Dutta D, Chakraborty S, Bandyopadhyay C, Valiya Veettil M, Ansari MA, Singh VV, et al. EphrinA2 regulates clathrin mediated KSHV endocytosis in fibroblast cells by coordinating integrin-associated signaling and c-Cbl directed polyubiquitination. *PLoS Pathog*. 2013; 9: e1003510. <https://doi.org/10.1371/journal.ppat.1003510> PMID: [23874206](#)
19. Wang X, Zou Z, Deng Z, Liang D, Zhou X, Sun R, et al. Male hormones activate EphA2 to facilitate Kaposi's sarcoma-associated herpesvirus infection: Implications for gender disparity in Kaposi's

- sarcoma. *PLOS Pathog.* 2017; 13: e1006580. <https://doi.org/10.1371/journal.ppat.1006580> PMID: 28957431
20. Hahn AS, Desrosiers RC. Binding of the Kaposi's sarcoma-associated herpesvirus to the ephrin binding surface of the EphA2 receptor and its inhibition by a small molecule. *J Virol.* 2014; 88: 8724–8734. <https://doi.org/10.1128/JVI.01392-14> PMID: 24899181
21. Vleck SE, Oliver SL, Brady JJ, Blau HM, Rajamani J, Sommer MH, et al. Structure-function analysis of varicella-zoster virus glycoprotein H identifies domain-specific roles for fusion and skin tropism. *Proc Natl Acad Sci.* 2011; 108: 18412–18417. <https://doi.org/10.1073/pnas.1111333108> PMID: 22025718
22. Matsuura H, Kirschner AN, Longnecker R, Jardetzky TS. Crystal structure of the Epstein-Barr virus (EBV) glycoprotein H/glycoprotein L (gH/gL) complex. *Proc Natl Acad Sci.* 2010; 107: 22641–22646. <https://doi.org/10.1073/pnas.1011806108> PMID: 21149717
23. Sathiyamoorthy K, Hu YX, Möhl BS, Chen J, Longnecker R, Jardetzky TS. Structural basis for Epstein-Barr virus host cell tropism mediated by gp42 and gHgL entry glycoproteins. *Nat Commun.* 2016; 7: 13557. <https://doi.org/10.1038/ncomms13557> PMID: 27929061
24. Chesnokova LS, Nishimura SL, Hutt-Fletcher LM. Fusion of epithelial cells by Epstein-Barr virus proteins is triggered by binding of viral glycoproteins gHgL to integrins $\alpha v \beta 6$ or $\alpha v \beta 8$. *Proc Natl Acad Sci.* 2009; 106: 20464–20469. <https://doi.org/10.1073/pnas.0907508106> PMID: 19920174
25. Kania A, Klein R. Mechanisms of ephrin-Eph signalling in development, physiology and disease. *Nat Rev Mol Cell Biol.* 2016; 17: 240–256. <https://doi.org/10.1038/nrm.2015.16> PMID: 26790531
26. Chen J. Regulation of tumor initiation and metastatic progression by Eph receptor tyrosine kinases. *Adv Cancer Res.* 2012; 114: 1–20. <https://doi.org/10.1016/B978-0-12-386503-8.00001-6> PMID: 22588054
27. Coulthard MG, Morgan M, Woodruff TM, Arumugam TV, Taylor SM, Carpenter TC, et al. Eph/Ephrin signaling in injury and inflammation. *Am J Pathol.* 2012; 181: 1493–1503. <https://doi.org/10.1016/j.ajpath.2012.06.043> PMID: 23021982
28. Binda E, Visioli A, Giani F, Lamorte G, Copetti M, Pitter KL, et al. The EphA2 receptor drives self-renewal and tumorigenicity in stem-like tumor-propagating cells from human glioblastomas. *Cancer Cell.* 2012; 22: 765–780. <https://doi.org/10.1016/j.ccr.2012.11.005> PMID: 23238013
29. Udayakumar D, Zhang G, Ji Z, Njauw C-N, Mroz P, Tsao H. EphA2 is a critical oncogene in melanoma. *Oncogene.* 2011; 30: 4921–4929. <https://doi.org/10.1038/ncr.2011.210> PMID: 21666714
30. Chowdary TK, Cairns TM, Atanasiu D, Cohen GH, Eisenberg RJ, Heldwein EE. Crystal structure of the conserved herpesvirus fusion regulator complex gH–gL. *Nat Struct Mol Biol.* 2010; 17: 882–888. <https://doi.org/10.1038/nsmb.1837> PMID: 20601960
31. Himanen JP, Goldgur Y, Miao H, Myshkin E, Guo H, Buck M, et al. Ligand recognition by A-class Eph receptors: crystal structures of the EphA2 ligand-binding domain and the EphA2/ephrin-A1 complex. *EMBO Rep.* 2009; 10: 722–728. <https://doi.org/10.1038/embor.2009.91> PMID: 19525919
32. Lupberger J, Zeisel MB, Xiao F, Thumann C, Fofana I, Zona L, et al. EGFR and EphA2 are host factors for hepatitis C virus entry and possible targets for antiviral therapy. *Nat Med.* 2011; 17: 589–595. <https://doi.org/10.1038/nm.2341> PMID: 21516087
33. Subbarayal P, Karunakaran K, Winkler A-C, Rother M, Gonzalez E, Meyer TF, et al. EphrinA2 Receptor (EphA2) Is an Invasion and Intracellular Signaling Receptor for Chlamydia trachomatis. Luo Z-Q, editor. *PLOS Pathog.* 2015; 11: e1004846. <https://doi.org/10.1371/journal.ppat.1004846> PMID: 25906164
34. Aaron PA, Jamklang M, Uhrig JP, Gelli A. The Human Blood-Brain Barrier Internalizes Cryptococcus neoformans via the EphA2-Tyrosine Kinase Receptor. *Cell Microbiol.* 2017; <https://doi.org/10.1111/cmi.12811> PMID: 29197141
35. Kaushansky A, Douglass AN, Arang N, Vigdorovich V, Dambrauskas N, Kain HS, et al. Malaria parasites target the hepatocyte receptor EphA2 for successful host infection. *Science.* 2015; 350: 1089–1092. <https://doi.org/10.1126/science.aad3318> PMID: 26612952
36. Zhang H, Li Y, Wang H-B, Zhang A, Chen M-L, Fang Z-X, et al. Ephrin receptor A2 is an epithelial cell receptor for Epstein-Barr virus entry. *Nat Microbiol.* 2018; <https://doi.org/10.1038/s41564-017-0080-8> PMID: 29292383
37. Chen J, Sathiyamoorthy K, Zhang X, Schaller S, Perez White BE, Jardetzky TS, et al. Ephrin receptor A2 is a functional entry receptor for Epstein-Barr virus. *Nat Microbiol.* 2018; <https://doi.org/10.1038/s41564-017-0081-7> PMID: 29292384
38. Shin YC, Jones LR, Manrique J, Lauer W, Carville A, Mansfield KG, et al. Glycoprotein gene sequence variation in rhesus monkey rhadinovirus. *Virology.* 2010; 400: 175–186. <https://doi.org/10.1016/j.virol.2010.01.030> PMID: 20172576
39. Back NKT, Smit L, De Jong J-J, Keulen W, Schutten M, Goudsmit J, et al. An N-Glycan within the Human Immunodeficiency Virus Type 1 gp120 V3 Loop Affects Virus Neutralization. *Virology.* 1994; 199: 431–438. <https://doi.org/10.1006/viro.1994.1141> PMID: 8122371

40. Francica JR, Varela-Rohena A, Medvec A, Plesa G, Riley JL, Bates P. Steric Shielding of Surface Epitopes and Impaired Immune Recognition Induced by the Ebola Virus Glycoprotein. Basler CF, editor. *PLoS Pathog.* 2010; 6: e1001098. <https://doi.org/10.1371/journal.ppat.1001098> PMID: 20844579
41. Ekiert DC, Bhabha G, Elsliger M-A, Friesen RHE, Jongeneelen M, Throsby M, et al. Antibody Recognition of a Highly Conserved Influenza Virus Epitope. *Science.* 2009; 324: 246–251. <https://doi.org/10.1126/science.1171491> PMID: 19251591
42. Rouas N, Christophe S, Housseau F, Bellet D, Guillet JG, Bidart JM. Influence of protein-quaternary structure on antigen processing. *J Immunol Baltim Md 1950.* 1993; 150: 782–792.
43. Himanen J-P, Chumley MJ, Lackmann M, Li C, Barton WA, Jeffrey PD, et al. Repelling class discrimination: ephrin-A5 binds to and activates EphB2 receptor signaling. *Nat Neurosci.* 2004; 7: 501–509. <https://doi.org/10.1038/nn1237> PMID: 15107857
44. Himanen J-P, Rajashankar KR, Lackmann M, Cowan CA, Henkemeyer M, Nikolov DB. Crystal structure of an Eph receptor–ephrin complex. *Nature.* 2001; 414: 933–938. <https://doi.org/10.1038/414933a> PMID: 11780069
45. Chrencik JE, Brooun A, Recht MI, Kraus ML, Koolpe M, Kolatkar AR, et al. Structure and Thermodynamic Characterization of the EphB4/Ephrin-B2 Antagonist Peptide Complex Reveals the Determinants for Receptor Specificity. *Structure.* 2006; 14: 321–330. <https://doi.org/10.1016/j.str.2005.11.011> PMID: 16472751
46. Omerović J, Lev L, Longnecker R. The amino terminus of Epstein-Barr virus glycoprotein gH is important for fusion with epithelial and B cells. *J Virol.* 2005; 79: 12408–12415. <https://doi.org/10.1128/JVI.79.19.12408-12415.2005> PMID: 16160168
47. Plate AE, Smajlovic J, Jardetzky TS, Longnecker R. Functional Analysis of Glycoprotein L (gL) from Rhesus Lymphocryptovirus in Epstein-Barr Virus-Mediated Cell Fusion Indicates a Direct Role of gL in gB-Induced Membrane Fusion. *J Virol.* 2009; 83: 7678–7689. <https://doi.org/10.1128/JVI.00457-09> PMID: 19457993
48. Chang P-J, Hung C-H, Wang S-S, Tsai P-H, Shih Y-J, Chen L-Y, et al. Identification and characterization of two novel spliced genes located in the orf47-orf46-orf45 gene locus of Kaposi's sarcoma-associated herpesvirus. *J Virol.* 2014; 88: 10092–10109. <https://doi.org/10.1128/JVI.01445-14> PMID: 24965448
49. Roop C, Hutchinson L, Johnson DC. A mutant herpes simplex virus type 1 unable to express glycoprotein L cannot enter cells, and its particles lack glycoprotein H. *J Virol.* 1993; 67: 2285–2297. PMID: 8383241
50. Bowman JJ, Lacayo JC, Burbelo P, Fischer ER, Cohen JI. Rhesus and Human Cytomegalovirus Glycoprotein L Are Required for Infection and Cell-to-Cell Spread of Virus but Cannot Complement Each Other. *J Virol.* 2011; 85: 2089–2099. <https://doi.org/10.1128/JVI.01970-10> PMID: 21191007
51. Gillet L, May JS, Colaco S, Stevenson PG. Glycoprotein L disruption reveals two functional forms of the murine gammaherpesvirus 68 glycoprotein H. *J Virol.* 2007; 81: 280–291. <https://doi.org/10.1128/JVI.01616-06> PMID: 17050601
52. Flamand A, Bennardo T, Babic N, Klupp BG, Mettenleiter TC. The Absence of Glycoprotein gL, but Not gC or gK, Severely Impairs Pseudorabies Virus Neuroinvasiveness. *J Virol.* 2001; 75: 11137–11145. <https://doi.org/10.1128/JVI.75.22.11137-11145.2001> PMID: 11602753
53. Klupp BG, Fuchs W, Weiland E, Mettenleiter TC. Pseudorabies virus glycoprotein L is necessary for virus infectivity but dispensable for virion localization of glycoprotein H. *J Virol.* 1997; 71: 7687–7695. PMID: 9311852
54. Klupp BG, Mettenleiter TC. Glycoprotein gL-independent infectivity of pseudorabies virus is mediated by a gD-gH fusion protein. *J Virol.* 1999; 73: 3014–3022. PMID: 10074151
55. Chakraborty S, Veettil MV, Bottero V, Chandran B. Kaposi's sarcoma-associated herpesvirus interacts with EphrinA2 receptor to amplify signaling essential for productive infection. *Proc Natl Acad Sci U S A.* 2012; 109: E1163–1172. <https://doi.org/10.1073/pnas.1119592109> PMID: 22509030
56. Wang X, Kenyon WJ, Li Q, Müllberg J, Hutt-Fletcher LM. Epstein-Barr virus uses different complexes of glycoproteins gH and gL to infect B lymphocytes and epithelial cells. *J Virol.* 1998; 72: 5552–5558. PMID: 9621012
57. Mori Y, Akkapaiboon P, Yonemoto S, Koike M, Takemoto M, Sadaoka T, et al. Discovery of a Second Form of Tripartite Complex Containing gH-gL of Human Herpesvirus 6 and Observations on CD46. *J Virol.* 2004; 78: 4609–4616. <https://doi.org/10.1128/JVI.78.9.4609-4616.2004> PMID: 15078943
58. Wang D, Shenk T. Human cytomegalovirus virion protein complex required for epithelial and endothelial cell tropism. *Proc Natl Acad Sci.* 2005; 102: 18153–18158. <https://doi.org/10.1073/pnas.0509201102> PMID: 16319222

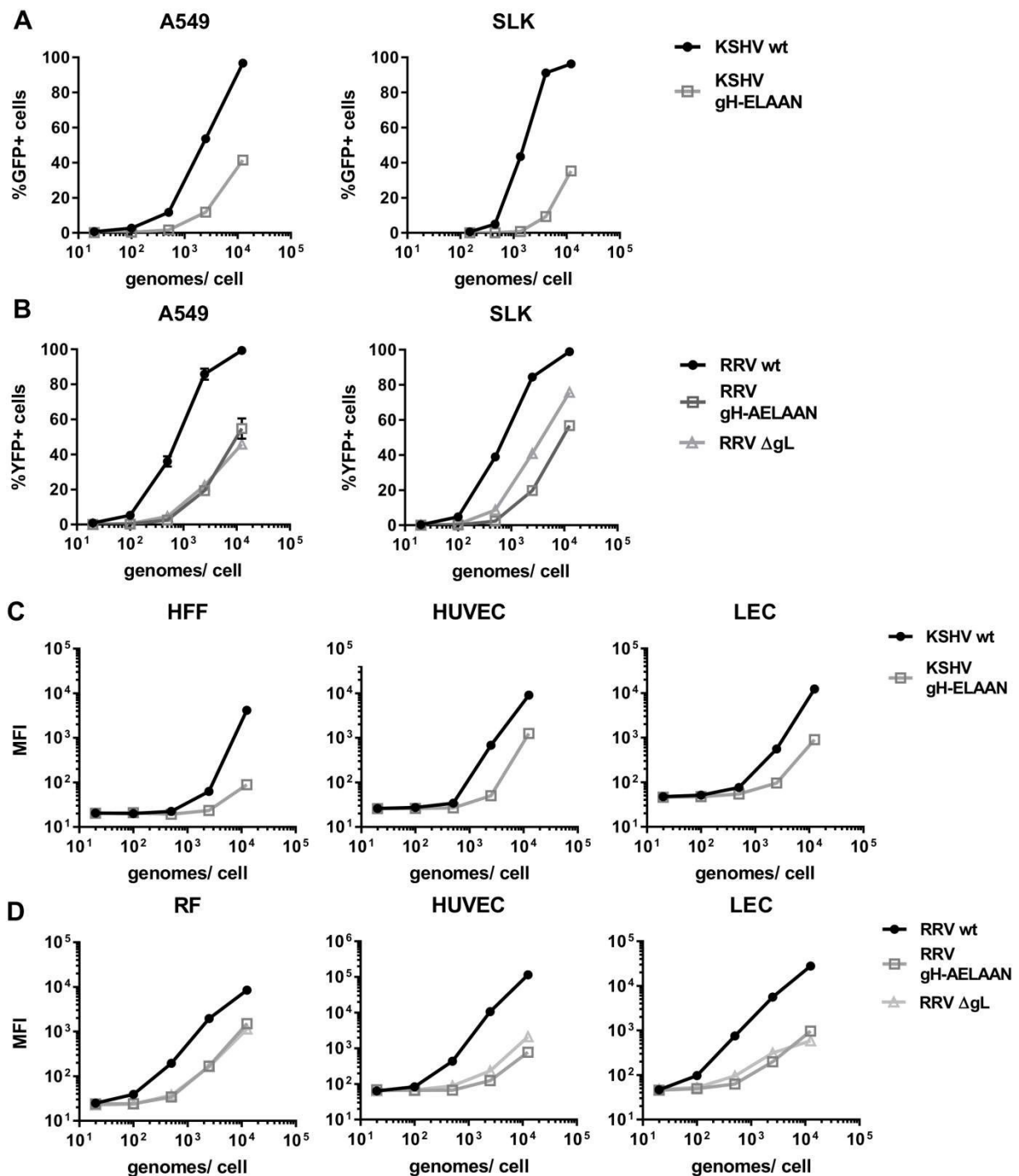
59. Giard DJ, Aaronson SA, Todaro GJ, Arnstein P, Kersey JH, Dosik H, et al. In vitro cultivation of human tumors: establishment of cell lines derived from a series of solid tumors. *J Natl Cancer Inst.* 1973; 51: 1417–1423. PMID: [4357758](#)
60. DuBridge RB, Tang P, Hsia HC, Leong PM, Miller JH, Calos MP. Analysis of mutation in human cells by using an Epstein-Barr virus shuttle system. *Mol Cell Biol.* 1987; 7: 379–387. PMID: [3031469](#)
61. Pear WS, Nolan GP, Scott ML, Baltimore D. Production of high-titer helper-free retroviruses by transient transfection. *Proc Natl Acad Sci U S A.* 1993; 90: 8392–8396. PMID: [7690960](#)
62. Herndier BG, Werner A, Arnstein P, Abbey NW, Demartis F, Cohen RL, et al. Characterization of a human Kaposi's sarcoma cell line that induces angiogenic tumors in animals. *AIDS Lond Engl.* 1994; 8: 575–581.
63. Stürzl M, Gaus D, Dirks WG, Ganem D, Jochmann R. Kaposi's sarcoma-derived cell line SLK is not of endothelial origin, but is a contaminant from a known renal carcinoma cell line. *Int J Cancer.* 2013; 132: 1954–1958. <https://doi.org/10.1002/ijc.27849> PMID: [22987579](#)
64. Myoung J, Ganem D. Generation of a doxycycline-inducible KSHV producer cell line of endothelial origin: Maintenance of tight latency with efficient reactivation upon induction. *J Virol Methods.* 2011; 174: 12–21. <https://doi.org/10.1016/j.jviromet.2011.03.012> PMID: [21419799](#)
65. Tischer BK, von Einem J, Kaufer B, Osterrieder N. Two-step red-mediated recombination for versatile high-efficiency markerless DNA manipulation in *Escherichia coli*. *BioTechniques.* 2006; 40: 191–197. PMID: [16526409](#)
66. Brulois KF, Chang H, Lee AS-Y, Ensser A, Wong L-Y, Toth Z, et al. Construction and Manipulation of a New Kaposi's Sarcoma-Associated Herpesvirus Bacterial Artificial Chromosome Clone. *J Virol.* 2012; 86: 9708–9720. <https://doi.org/10.1128/JVI.01019-12> PMID: [22740391](#)
67. Longo PA, Kavran JM, Kim M-S, Leahy DJ. Transient Mammalian Cell Transfection with Polyethylenimine (PEI). *Methods in Enzymology.* Elsevier; 2013. pp. 227–240. <https://doi.org/10.1016/B978-0-12-418687-3.00018-5>
68. Knipe D, Howley P. *Fields virology.* 6th ed. Philadelphia: Wolters Kluwer/Lippincott Williams & Wilkins Health; 2013. pp. 42–50.

Supplemental Data

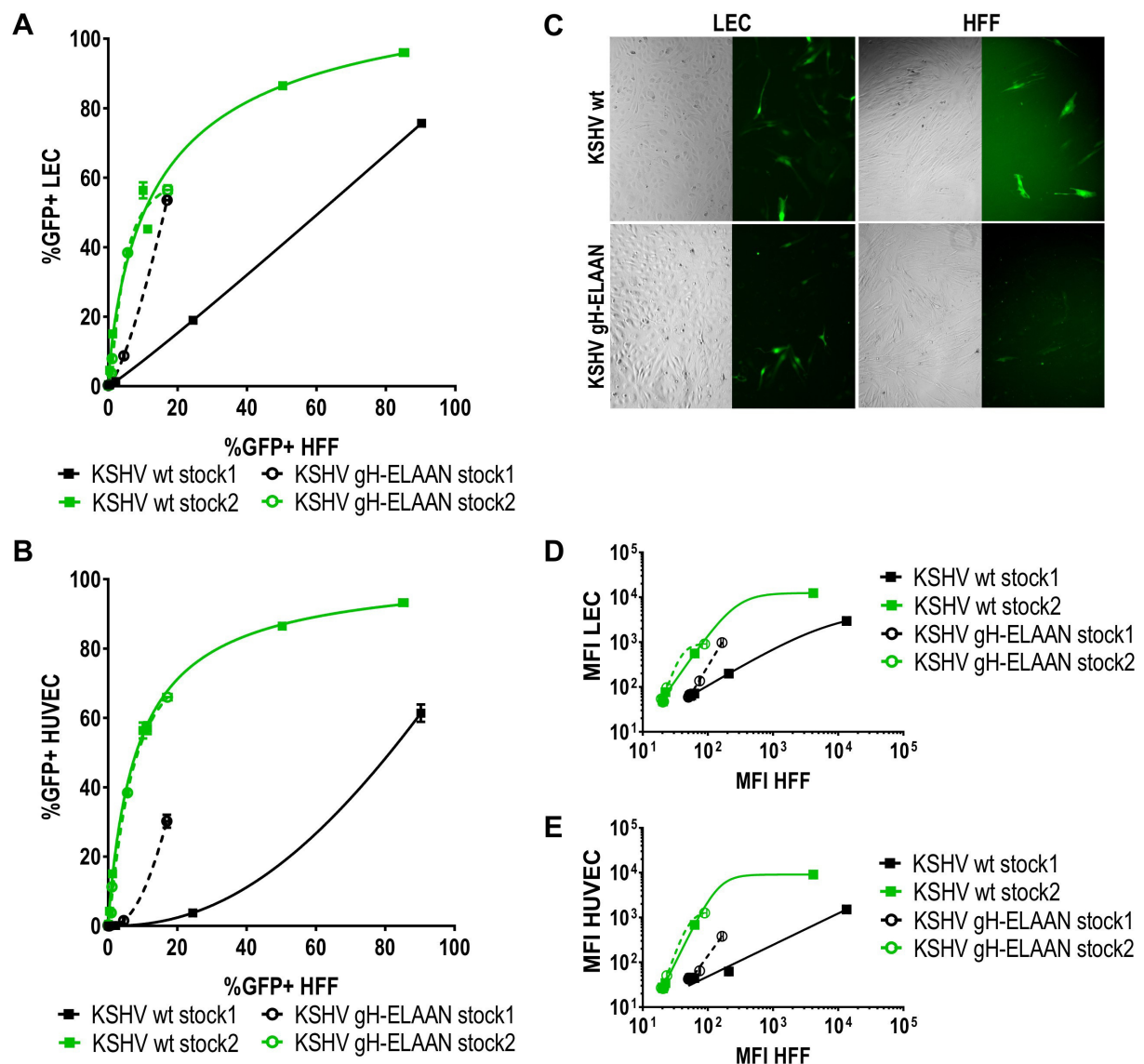


S1 Fig. Effect of single point mutations in the N-terminal domain of gH on gH/gL stability and complexation as well as gH and gL incorporation in the virus particles. A Effects of point mutations on the stability of KSHV gH/gL complexes in the absence of recombinant Eph receptors. V5-tagged KSHV gH mutants were co-expressed with Flag-tagged KSHV gL. gH-V5/gL-Flag complexes were immunoprecipitated using monoclonal antibody to the V5-tag and precipitates were analyzed by Western blot. KSHV gH/RRV gL and KSHV gH alone serve as negative control. **B** Effects of point mutations on the stability of RRV gH/gL complexes in the absence of recombinant Eph receptors. V5-tagged RRV gH mutants were co-expressed with Flag-tagged RRV gL. gH-V5/gL-Flag complexes were immunoprecipitated and analyzed as in A. KSHV gH/RRV gL and RRV gH alone serve as negative control. **C** Point mutations in

the E-L-E-F-N motif of KSHV and RRV gH do not influence stability of gH alone or of the gH/gL complex. V5-tagged KSHV gH wt, gH E52AF53A (gH-ELAAN), RRV gH wt and gH V51AE54AF55A (gH-AELAAN) were either expressed alone or co-expressed with Flag-tagged KSHV/RRV gL. gH-V5 and gH-V5/gL-Flag complexes were immunoprecipitated and analyzed as in A. **D** Double mutation E52AF53A in KSHV gH does not influence the incorporation of gH into the virus particle. KSHV wt, and gH-ELAAN virus preparations were analyzed by Western Blot. K8.1 was used as loading control. K8.1 runs in a diffuse molecular weight pattern due to its complex O-glycosylation. **E** Triple mutation V51AE54AF55A in RRV gH (gH-AELAAN) does not influence the incorporation of gH and gL into the virus particle. RRV wt, gH-AELAAN and RRV Δ gL virus preparations were analyzed by Western Blot. gB was used as loading control. Abbreviations: IP: immunoprecipitation, IB: immunoblotting.



S2 Fig. Specific infectivity of Eph-binding-negative RRV and KSHV mutants. A-B Eph-binding-negative RRV and KSHV mutants exhibit a reduced specific infection on epithelial cells. Target cells were infected with KSHV wt and gH-ELAAN (A) or RRV wt, gH-AELAAN and Δ gL (B) at the indicated virus concentrations. GFP (KSHV) or YFP (RRV) expression as indicator of infection was measured by flow cytometry (triplicates, error bars indicate sd). C-D Eph-binding-negative RRV and KSHV mutants exhibit a reduced specific infection assayed by mean fluorescence intensity (MFI) of the respective reporter gene. Target cells were infected with KSHV wt and gH-ELAAN (C) or RRV wt, gH-AELAAN and Δ gL (D) at the indicated virus concentrations. GFP (KSHV) or YFP (RRV) MFI as indicator of infection was measured by flow cytometry (triplicates, error bars indicate sd).



S3 Fig. Contribution of the gH/gL-Eph interaction to KSHV infection of endothelial cells and fibroblasts. A-B Comparison of KSHV wt with KSHV gH-ELAAN infection based on GFP reporter gene-positive cells on LEC (A) or HUVEC (B) and HFF. HFF and LEC or HUVEC were infected with the same inocula of the respective virus stock, and the percentage of reporter gene-positive cells as determined by flow cytometry for each dilution was plotted. C Micrograph of HFF and LEC infected with the same inocula of wt and Eph-binding-negative KSHV. D-E Comparison of KSHV wt and KSHV gH-ELAAN infection based on MFI on LEC (D) or HUVEC (E) and HFF performed as in (A-B).

S4 Table List of accession numbers, primers, and antibodies used in this study.

A) NCBI database sequence accession numbers

| | Gene | accession number |
|-------|--------------|------------------|
| human | EphA2 | NM_004431 |
| | EphB3 | BC052968 |
| viral | KSHV gH | GQ994935.1 |
| | KSHV gL | GQ994935.1 |
| | RRV 26-95 gH | AF210726.1 |
| | RRV 26-95 gL | AF210726.1 |

B) Oligos

| | name | sequence | |
|-----------------|------------------------------|--|--|
| BAC mutagenesis | KSHV gH-ELAAN forward | 5'-GCTCCGCCACGCAGCTCATCAATGGGAGAACCACTCTCCATAGAACTGGCAGCCAACGGCACTAGTTTTTTCTAGGATGACGACGATAAGTAGGG-3' | |
| | KSHV gH-ELAAN reverse | 5'-CACATTCACAGATTTTGCCAATTTAGAAAAAACTAGTGCCGTTGGCTGCCAGTTCTATGGAGAGGTTGCAACCAATTAACCAATTCTGATTAG-3' | |
| | RRV gH-AELAAN forward | 5'-GCCACAACAACACCAAGTTAAAAGCGATATATCAACTGCGGAACCTGGCAGCTAATAGAACACGGTAAGGATGACGACGATAAGTAGGG-3' | |
| | RRV gH-AELAAN reverse | 5'-ACTCACATTTTTCCAATTAATACGATACCGTGTCTATTAGCTGCCAGTTCCGCAAGTTGATATATCAACCAATTAACCAATTCTGATTAG-3' | |
| | RRV ΔgI forward | 5'-AACGCCCTAAGGTGAAAACCATTCACACATAACTCTGTAGTAACATGGATTGGAATTAACCACCAAGAGTAGCCAATATAGGATGACGACGATAAGTAGGG-3' | |
| | RRV ΔgI reverse | 5'-TATGTATACATTAAGTTTTTTACAATTTATTTTATACTATATATTGGCTACTCTGGTGGTTTAATTCCAAATCCATGTTCAACCAATTAACCAATTCTGATTAG-3' | |
| Sequencing PCR | KSHV gH-ELAANseq forward | 5'-GCCTGGCACACAAGGAGGAA-3' | |
| | KSHV gH-ELAANseq reverse | 5'-TCGGCACCTCGCACGTATAG-3' | |
| | RRV gH-AELAANseq forward | 5'-TCCAGATTGACTCATCGGTTTC-3' | |
| | RRV gH-AELAANseq reverse | 5'-TCCAATCGGCTGTCAATAATACC-3' | |
| qPCR | KSHV ORF59 | primer1 | 5'-GCCACACCTTCCACTTCTAATA-3' |
| | | primer2 | 5'-GGTTAGCCTGGAGTCCTTAATC-3' |
| | | probe | 5'-/56-FAM/CACTGTGTAA/ZEN/AGTCCCGGTTGGTT/3IABkFQ/-3' |
| | RRV ORF73 | primer1 | 5'-AAAGATGACTCCGTGACACC-3' |
| | | primer2 | 5'-GCGATACCCATTCCCATAC-3' |
| | | probe | 5'-/56-FAM/CCCAAGAAA/ZEN/TACCGCCACAGAGAA/3IABkFQ/-3' |
| | genomic CCR5 (human/ rhesus) | primer1 | 5'-CCCAGTGGGACTTTGGAAATA-3' |
| | | primer2 | 5'-CGATTGTCAGGAGGATGATGAA-3' |
| | | probe | 5'-/56-FAM/TGTGTCAAC/ZEN/TCCTGACAGGGCTCT/3IABkFQ/-3' |

C) gH and gL constructs and primers

| | KSHV | amino acids | RRV | amino acids |
|------------------------|---|-------------|---|-------------|
| <i>chimera1</i> | DI-DIV | 1-700 | TM | 698-end |
| <i>chimera2</i> | DI-DIV | 1-601 | DIV-TM | 599-end |
| <i>chimera3</i> | DI-DIII | 1-504 | DIII-TM | 502-end |
| <i>chimera4</i> | DI-DIII | 1-400 | DIII-TM | 401-end |
| <i>chimera5</i> | DI-DII | 1-301 | DII-TM | 301-end |
| <i>chimera6</i> | DI-DII | 1-199 | DII-TM | 199-end |
| <i>chimera7</i> | DI-DII | 1-94 | DII-TM | 99-end |
| <i>chimera1-7</i> | KSHV fragment forward | | RRV fragment reverse | |
| | 5'-AAGGATCCACCATGCAGGTCTAGCCTCTTG-3' | | 5'-CTAGAAGGCACAGTCGAGGC-3' | |
| <i>chimera1</i> | KSHV fragment reverse | | RRV fragment forward | |
| | 5'-CAGGGCATGTCTTCTATACATGCCCTTATCTC-3' | | 5'-GTATAGAAGACATGCCCTGTCACTATCGC-3' | |
| <i>chimera2</i> | 5'-GACACAACATTGCACTCTTGAGGAAGATCTCC-3' | | 5'-CTCAAGAGTGCAATGTTTGTCTGTCAG-3' | |
| <i>chimera3</i> | 5'-GCAGGCTTAGAAAGCAGGGGAGAATG-3' | | 5'-CATCTCCCCCTGCTTCTGAGCCTGC-3' | |
| <i>chimera4</i> | 5'-GGCAAGTTTGACCATGGCCAGCACTGTTTCC-3' | | 5'-GGCCATGGTCAAACCTGCCAATAATAACAATGTTG-3' | |
| <i>chimera5</i> | 5'-GGTTTTGGCAGGCGCGCTGCGCTC-3' | | 5'-CCAGGCGCGCTGCCCCAACCAAGTG-3' | |
| <i>chimera6</i> | 5'-GAGAATCCAATCATCTCCGACACCACTCCATAG-3' | | 5'-GTGTCGGAAGATGATTGGATTCTCGTCTCCATC-3' | |
| <i>chimera7</i> | 5'-GACTTCTCTTTTTCAGAGTTACCTGAG-3' | | 5'-CTCTGAAAAAGAGAAAGTCAATCTGAAAC-3' | |
| <i>KSHV gLΔ135-164</i> | forward | | reverse | |
| | 5'-AGGGAAAAGACTACAAGGACGACGATG-3' | | 5'-TTATTATAATTATGTTTACGTTGTG-3' | |

D) Antibodies

| Western Blot | Target | Clone/ Number | Species | concentration | Manufacturer |
|-----------------------------------|---------------------|---------------|---------|---------------|--|
| primary antibodies | V5 tag/ PK tag | SV5-Pk1 | mouse | 1:1000 | Bio-Rad |
| | c-myc | 9E10 | mouse | 1:1000 | Santa Cruz Bio |
| | c-myc | C3956 | rabbit | 1:1000 | Sigma-Aldrich |
| | DYKDDDDK tag (Flag) | 6F7 | rat | 1:1000 | Serotec |
| | DYKDDDDK tag (Flag) | D6W58 | rabbit | 1:1000 | Cell Signaling Technology |
| | HA tag | HA-7 | mouse | 1:1000 | Sigma-Aldrich |
| | RRV gH-2 | custom | rabbit | 1:500 | GenScript |
| | RRV gL-1 | custom | rabbit | 1:500 | GenScript |
| | RRV gB | 3H8.1 | mouse | 1:1000 | Scott W. Wong (Vaccine and Gene Therapy Institute, Oregon Health & Science University) |
| | KSHV gH-1 | custom | rabbit | 1:500 | GenScript |
| | KSHV K8.1 | Bs555 | mouse | 1:1000 | Lang et al., J Clin Microbiol. 2002 |
| secondary antibodies (HRP) | mouse | | donkey | 1:20 000 | Jackson ImmunoResearch |
| | rat | | chicken | 1:10 000 | Santa Cruz Bio |
| | rabbit | | donkey | 1:20 000 | Jackson ImmunoResearch |
| | rabbit | | goat | 1:10 000 | Thermo Fisher Scientific |

Correction of RRV-YFP-ΔgL sequence

Posted by ahahn101 on 10 Oct 2019 at 17:44 GMT

As a result of a sequencing oversight that we recently noticed after depositing our sequences in GenBank, the RRV-YFP-ΔgL virus described in our publication that is negative for gL expression in virus particles contains not only the indicated 128 base pair deletion from position 80 to 207 of the coding sequence but also a single base pair deletion at position 66. The corrected sequence of RRV-YFP-ΔgL has been deposited under accession number MN488838. The conclusions of our publication are not affected.

III.2 Publication 2: EphA7 functions as Receptor on BJAB Cells for Cell-to-Cell Transmission of the Kaposi's Sarcoma-Associated Herpesvirus (KSHV) and for Cell-Free Infection by the Related Rhesus Monkey Rhadinovirus (RRV)

Journal of Virology, Published: July 17, 2019

Author Contributions

Conceptualization: **Anna K. Großkopf**, Alexander S. Hahn

Formal analysis: **Anna K. Großkopf**, Alexander S. Hahn

*Data analysis of all Figures was performed by **Anna K. Großkopf** and reviewed by **Alexander S. Hahn**.*

Funding acquisition: Alexander S. Hahn

Investigation: **Anna K. Großkopf**, Sarah Schlagowski, Bojan F. Hörnich, Thomas Fricke, Alexander S. Hahn

***Anna K. Großkopf**: designed and performed the experiments which led to the results in Fig 1D, Fig 2E and F, part of Fig 2D, Fig 3B and E and Fig 4; **Sarah Schlagowski**: performed the experiments which led to the results in Fig 2A – E, Fig 3A, C and D and prepared RRV stocks; **Bojan F. Hörnich**: performed repeat experiments for Fig 1D; **Thomas Fricke**: contributed to large scale cell culture; **Alexander S. Hahn**: designed and performed experiments which led to the results in Fig 1A and B and analyzed pre-existing data which led to Fig 1C.*

Methodology: **Anna K. Großkopf**, Alexander S. Hahn

***Anna K. Großkopf**: designed experiments which led to the results in all Figures except Fig 1A and B and Fig 2A and B; **Alexander S. Hahn**: designed experiments which led to the results in Fig 1A and B and designed Eph-targeting sgRNAs used in this study.*

Project administration: Alexander S. Hahn

Resources: Ronald C. Desrosiers

Supervision: Alexander S. Hahn

Visualization: **Anna K. Großkopf**

Writing - original draft: **Anna K. Großkopf**

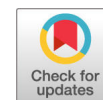
A longstanding problem in the KSHV field lies in the inability of KSHV to infect B cell cultures as cell-free virus *in vitro*. Even though this refractoriness to cell-free infection can be partially overcome by a co-culture infection approach⁶⁴, data on the receptor usage of KSHV for B cell infection is still sparse. We therefore aimed to analyze:

- 1) Which Eph receptors mediate rhadinovirus entry into B cells, using BJAB cells as a model cell line
- 2) The contribution of identified Eph receptors to cell-to-cell transmission of KSHV and cell-free infection of RRV on BJAB B cells
- 3) If Eph receptor expression in BJAB cells is paralleled in KSHV-associated malignancies, using KSHV-PEL cell lines as a model system

To identify Eph family members that could mediate KSHV and RRV infection of BJAB cells, LC-MS/MS had been performed after precipitation of BJAB cell lysate with the gH/gL complexes of KSHV, RRV 26-95 and RRV 17577 by Alexander Hahn in the laboratory of Ron Desrosiers. The identified interaction of RRV and KSHV with EphA7 as well as of KSHV with EphA5 fitted well with published Eph mRNA expression profiles in BJAB cells and was verified by further immunoprecipitation experiments. In CRISPR/Cas9 knockout experiments, abrogation of the EphA7 expression in BJAB cells led to an approx. 75% reduction of KSHV cell-to-cell transmission and 95% reduction of RRV cell-free infection, respectively. Similarly, knockdown of EphA5 reduced KSHV infection by approx. 60% and RRV infection by approx. 40%.

Rescue of KSHV and RRV infection upon lentiviral reconstitution of EphA7 expression in monoclonal EphA7 knockout cells confirmed the dependence of both viruses on EphA7 for entry into BJAB cells and excluded a contribution of CRISPR/Cas9 off-target effects.

Interestingly, one of three analyzed PEL cell lines expressed EphA7 to similar levels as BJAB cells in our experimental setup, while the remaining two PEL cell lines expressed high levels of EphA2 but were negative for EphA7. This could hint to a role of KSHV-interacting Eph receptors in the development or maintenance of PEL and in extension KSHV-associated B cell malignancies in general.



EphA7 Functions as Receptor on BJAB Cells for Cell-to-Cell Transmission of the Kaposi's Sarcoma-Associated Herpesvirus and for Cell-Free Infection by the Related Rhesus Monkey Rhadinovirus

Anna K. Großkopf,^a Sarah Schlagowski,^a Bojan F. Hörnich,^a Thomas Fricke,^a  Ronald C. Desrosiers,^b  Alexander S. Hahn^a

^aJunior Research Group Herpesviruses, German Primate Center–Leibniz Institute for Primate Research, Göttingen, Germany

^bDepartment of Pathology, Miller School of Medicine, University of Miami, Miami, Florida, USA

ABSTRACT Kaposi's sarcoma-associated herpesvirus (KSHV) is the causative agent of Kaposi's sarcoma and is associated with two B cell malignancies, primary effusion lymphoma (PEL) and the plasmablastic variant of multicentric Castleman's disease. On several adherent cell types, EphA2 functions as a cellular receptor for the gH/gL glycoprotein complex of KSHV. KSHV gH/gL also has previously been found to interact weakly with other members of the Eph family of receptor tyrosine kinases (Ephs), and other A-type Ephs have been shown to be able to compensate for the absence of EphA2 using overexpression systems. However, whether these interactions are of functional consequence at endogenous protein levels has remained unclear so far. Here, we demonstrate for the first time that endogenously expressed EphA7 in BJAB B cells is critical for the cell-to-cell transmission of KSHV from producer iSLK cells to BJAB target cells. The BJAB lymphoblastoid cell line often serves as a model for B cell infection and expresses only low levels of all Eph family receptors other than EphA7. Endogenous EphA7 could be precipitated from the cellular lysate of BJAB cells using recombinant gH/gL, and knockout of EphA7 significantly reduced transmission of KSHV into BJAB target cells. Knockout of EphA5, the second most expressed A-type Eph in BJAB cells, had a similar, although less pronounced, effect on KSHV infection. Receptor function of EphA7 was conserved for cell-free infection by the related rhesus monkey rhadinovirus (RRV), which is relatively even more dependent on EphA7 for infection of BJAB cells.

IMPORTANCE Infection of B cells is relevant for two KSHV-associated malignancies, the plasmablastic variant of multicentric Castleman's disease and PEL. Therefore, elucidating the process of B cell infection is important for the understanding of KSHV pathogenesis. While the high-affinity receptor for the gH/gL glycoprotein complex, EphA2, has been shown to function as an entry receptor for various types of adherent cells, the gH/gL complex can also interact with other Eph receptor tyrosine kinases with lower avidity. We analyzed the Eph interactions required for infection of BJAB cells, a model for B cell infection by KSHV. We identified EphA7 as the principal Eph receptor for infection of BJAB cells by KSHV and the related rhesus monkey rhadinovirus. While two analyzed PEL cell lines exhibited high EphA2 and low EphA7 expression, a third PEL cell line, BCBL-1, showed high EphA7 and low EphA2 expression, indicating a possible relevance for KSHV pathology.

KEYWORDS B cell, EPH receptors, Kaposi's sarcoma-associated herpesvirus, receptors, virus entry

In addition to Kaposi's sarcoma, Kaposi's sarcoma-associated herpesvirus (KSHV) is associated with a variant of multicentric Castleman's disease (MCD) and with primary effusion lymphoma (PEL) (1). Several publications demonstrate the importance of the

Citation Großkopf AK, Schlagowski S, Hörnich BF, Fricke T, Desrosiers RC, Hahn AS. 2019. EphA7 functions as receptor on BJAB cells for cell-to-cell transmission of the Kaposi's sarcoma-associated herpesvirus and for cell-free infection by the related rhesus monkey rhadinovirus. *J Virol* 93:e00064-19. <https://doi.org/10.1128/JVI.00064-19>.

Editor Jae U. Jung, University of Southern California

Copyright © 2019 American Society for Microbiology. All Rights Reserved.

Address correspondence to Alexander S. Hahn, ahahn@dpz.eu.

Received 15 January 2019

Accepted 15 May 2019

Accepted manuscript posted online 22 May 2019

Published 17 July 2019

cellular receptor EphA2 for KSHV entry into various adherent target cells (2–5). While the KSHV gH/gL complex exhibits the highest avidity for EphA2, it can also interact with other members of the Eph family of receptor tyrosine kinases (Ephs), similar to the gH/gL complex of the related rhesus monkey rhadinovirus (RRV) (6). However, it remains unclear to what extent these interactions may be of functional relevance for KSHV infection at endogenous protein levels. Interestingly, although B cells are likely the major KSHV reservoir during lifelong persistence, infection of established B cell lines by cell-free KSHV is extremely inefficient (7–10). While cell-free infection with KSHV, using high levels of input virus and achieving approximately 20% infected cells maximum, was reported for one B cell line (11), coculture of KSHV-producing cells with target cells leads to robust infection of various B cell lines (12). BJAB cells, an Epstein-Barr virus-negative lymphoblastoid B cell line (13), have been used as a model for B cell infection by KSHV (9, 12) and B cell biology in general (14). While BJAB cells, like other established B cell lines, are generally refractory to cell-free KSHV infection (7, 8), KSHV can establish latency in BJAB cells under continuous antibiotic selection after cell-to-cell transmission, free virus infection, or electroporation of viral DNA (12, 15, 16). Our previous work had already demonstrated that cell-to-cell transmission of KSHV into BJAB cells is susceptible to inhibition of the interaction with receptors from the Eph family (6). However, which member of the Eph family of receptor tyrosine kinases is the principal receptor for infection of these cells has remained an open question. Additionally, to further characterize the significance of RRV as an animal model virus for KSHV, we investigated the receptor requirements for BJAB infection by this closely related gamma2 herpesvirus of rhesus macaques (17).

(This article was submitted to an online preprint archive [18].)

RESULTS

Identification of endogenous EphA7 as interaction partner of the gH/gL complexes of KSHV and RRV in BJAB cells. We performed a two-step pulldown from the lysate of BJAB cells using Strep-tagged Fc fusion proteins of soluble versions of the gH proteins (3, 6, 19) of KSHV, RRV 26-95, and RRV 17577 (20) in complex with the respective gL proteins as bait to identify cellular interaction partners (Fig. 1A). In this experiment, we used two gH/gL complexes from two RRV isolates, 26-95 and 17577 (20), as representatives of the two discrete phylogenetic groups of RRV gH and gL sequences described by Shin et al. (21) to identify possible differences in receptor interactions between the isolates. Mass spectrometry analysis identified EphA7 as a prey in all three binding reactions (Fig. 1B). In pulldowns with either of the RRV gH/gL complexes, EphA7 was the only membrane protein identified in excised bands in the 100- to 130-kDa molecular weight range. In the KSHV pulldown, we additionally found several peptides derived from EphA5. A comparison of the mRNA expression profiles of the 14 human Eph family receptors in a data set (22) deposited in the Gene Expression Omnibus database revealed that BJAB cells predominantly express EphA7 (Fig. 1C). We therefore focused our analysis on this member of the Eph receptor family. To confirm our mass spectrometry results, we repeated the pulldown with a similar experimental protocol and tested the precipitate for the presence of EphA7 by Western blot analysis. Using soluble gH/gL complexes of KSHV and RRV 26-95, we pulled down a protein from BJAB lysate, but not from 293T lysate, that reacted with an antibody to EphA7, confirming the mass spectrometry data (Fig. 1D). In contrast, EphA2 was precipitated by KSHV gH/gL from 293T lysate but not from BJAB lysate, which mirrors expression of the two receptors in BJAB or 293T cells, respectively.

EphA7 as a functional receptor for infection of BJAB cells by KSHV and RRV. To test the functional relevance of the gH/gL-EphA7 interaction, we generated EPHA7 knockout (KO) cell pools by transducing BJAB cells with lentiCRISPRv2-based constructs targeting EPHA7. All four tested single guide RNAs (sgRNAs) abrogated EphA7 expression compared to two nontargeting guide RNAs or two guide RNAs targeting EPHA2, as assayed by Western blotting (Fig. 2A). EphA2, the described KSHV receptor for adherent cells, is not expressed to reliably detectable levels in BJAB cells, which is in

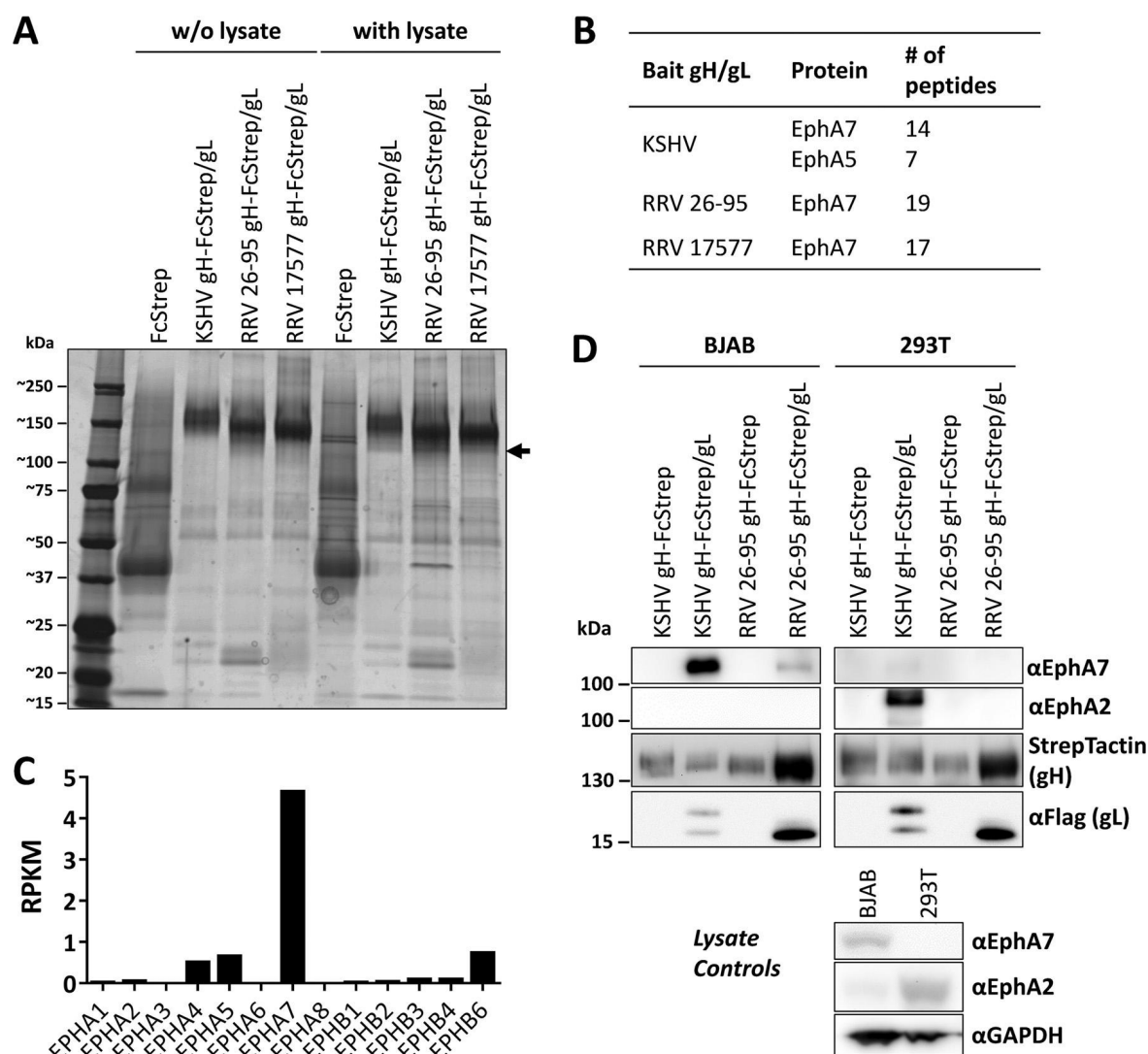


FIG 1 Identification of EphA7 as a gH/gL-interacting protein in BJAB cells. (A) Pulldown from BJAB cells with recombinant soluble gH-FcStrep/gL complexes. The precipitates were analyzed by PAGE and silver stained, and bands at the indicated molecular weights (arrow) were excised and analyzed by mass spectrometry. w/o, without. (B) Proteins and number of peptides per protein identified in the excised bands of each sample. (C) RNA sequencing, in reads per kilobase million (RPKM), of the 14 EPH receptor genes as found in GEO data set series [GSE82184](#) (BJAB control, accession no. GSM2185732). (D) Pulldown from BJAB and 293T lysate using recombinant soluble KSHV or RRV 26-95 gH/gL complexes as bait. Input amounts were normalized to wet cell pellet. Precipitates were analyzed by Western blotting with the indicated antibodies. For KSHV gL, two bands, representing differentially glycosylated forms, were detected. The same lysates used for the pulldown were analyzed by Western blotting as expression controls.

accordance with mRNA expression profiles in databases and the absence of EphA2 in our initial pulldown experiment (Fig. 1). After confirmation of the CRISPR/Cas9 knockout efficiency (Fig. 2A), we used the knockout cell pools to analyze receptor function of EphA7 for infection of BJAB cells (Fig. 2B and C). As BJAB cells are not readily amenable to infection with cell-free KSHV, we resorted to the previously described coculture cell-to-cell transmission system (12). This method allows for efficient infection of BJAB cells by overlaying chemically induced iSLK cells containing recombinant BAC16 KSHV with BJAB cells and resolution of the two populations by flow cytometry after staining for expression of CD13 (as an iSLK cell marker) and CD20 (as a B cell marker) as described by Myoung and Ganem (12). As a control for Eph-independent infection, we included iSLK cells harboring our previously described Eph-detargeted gH-ELAAN mutant (23) in BJAB coculture experiments. To quantify the impact of EPHA7^{KO} on KSHV transmission to BJAB cells, we averaged the percentage of green fluorescent protein-positive (GFP⁺) cells in the CD13⁺ CD20⁺ population individually obtained with all

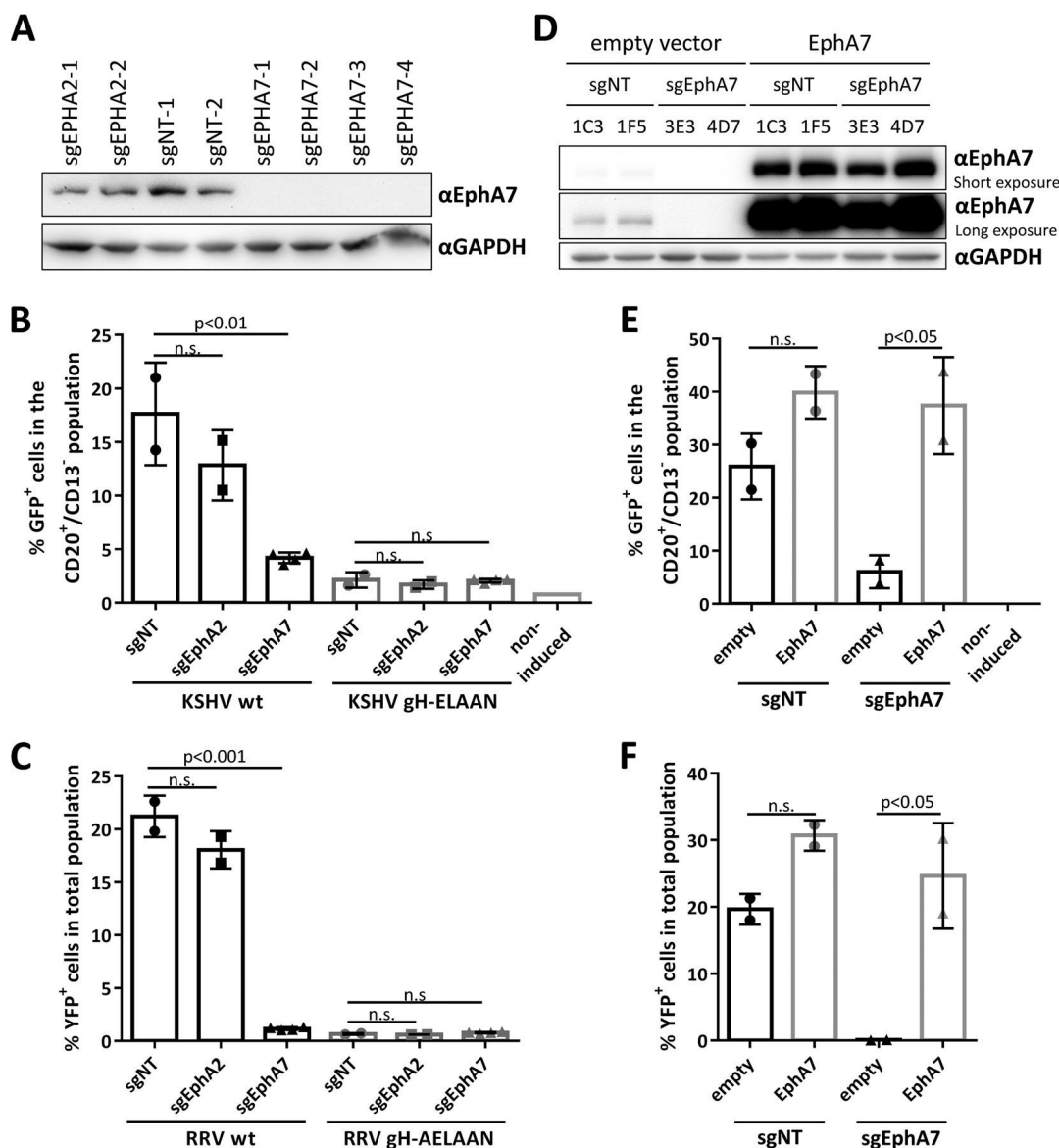


FIG 2 Knockout of EPHA7 reduces infection by KSHV and RRV. (A) Knockout of EPHA7 in BJAB cells. BJAB cells were transduced with the indicated lentiCRISPRv2-based constructs and briefly selected, and cell pools were analyzed by Western blotting. GAPDH, glyceraldehyde-3-phosphate dehydrogenase. (B) BJAB cells transduced with the lentiCRISPRv2-based constructs targeting the indicated genes were cocultured with iSLK cells harboring either BAC16 KSHV wt or BAC16 KSHV gH-ELAAN. GFP reporter gene expression in the CD13⁻ C20⁺ population, as an indicator of BJAB cell infection, was analyzed by flow cytometry. The means across groups of sgRNAs ($n = 3$ infections per sgRNA) targeting EPHA2 (two sgRNAs), EPHA7 (four sgRNAs), or nontargeting (sgNT; two sgRNAs) are indicated by columns. The standard deviations from the means are indicated by the error bars. The means from the individual triplicate infections for each sgRNA BJAB population within a group are given as symbols within the respective columns. Statistical significance was determined by pairwise comparison to the sgNT control group using one-way analysis of variance (ANOVA) with Bonferroni correction for multiple comparisons. n.s., not significant. (C) The same BJAB cell pools as those in panel B were infected with cell-free RRV-YFP wt or RRV-YFP gH-AELAAN. YFP reporter gene expression, as an indicator of infection, was analyzed by flow cytometry. Statistical analysis was performed as described for panel B. (D) Reconstitution of EphA7 expression in monoclonal sgNT or sgEPhA7 cell lines. Monoclonal cells were transduced with a lentivirus carrying an EphA7 expression cassette or an empty vector control and briefly selected, and cell pools were analyzed by Western blotting. Designation of each clone indicates the respective parental sgRNA and clone number. (E) Monoclonal BJAB cell lines stably overexpressing EphA7 were cocultured with iSLK cells harboring BAC16 KSHV wt and analyzed as described for panel B. The means across two clonal cell lines per target gene ($n = 6$ infections per clonal cell line and lentiviral vector in two repeated independent experiments) are indicated by columns. The standard deviations from the means are indicated by the error bars. The means from two independent experiments for each BJAB population within a group (sgRNA, reconstitution) are given as symbols within the respective columns. The indicated individual comparisons were made using two-way ANOVA with Bonferroni correction for multiple comparisons. (F) The same reconstituted, monoclonal cells as those used for panel E were infected with cell-free RRV-YFP wt. YFP reporter gene expression, as an indicator of infection, was analyzed by flow cytometry. Statistical analysis was performed as described for panel E.

different sgRNA constructs targeting one specific gene (four sgRNAs for EPHA7 or two sgRNAs for EPHA2) and compared them to the averaged percentage of infected cells obtained with the two nontargeting control sgRNAs (Fig. 2B). Knockout of EPHA7 resulted in a 76% reduction of infection with wild-type (wt) KSHV, whereas targeting EPHA2, which is not expressed at detectable levels as assayed by Western blotting, resulted in a 27% reduction of wt KSHV infection, which was not significant. Analysis of all BJAB cell pools treated with sgRNAs targeting either EPHA2 or EPHA7 compared to cell pools treated with nontargeting sgRNAs in infection experiments with KSHV gH-ELAAN did not indicate significant changes between any of the groups. RRV 26-95, as opposed to KSHV, readily infects BJAB cells as free virus (6). Therefore, we infected the same set of BJAB knockout cell pools with cell-free wt RRV-yellow fluorescent protein (YFP) and with RRV-YFP gH-AELAAN, an Eph-detargeted RRV mutant (23), analogous to KSHV gH-ELAAN (Fig. 2C). While the results obtained with RRV essentially paralleled those with KSHV, ablating EphA7 expression resulted in an even more pronounced and significant reduction in infection for all EPHA7-targeting constructs compared to the nontargeting controls. The average level of RRV-YFP infection of all BJAB EPHA7^{KO} cell pools was reduced by 95% compared to averaged infection of nontargeting sgRNA controls. Infection levels of RRV-YFP gH-AELAAN equaled RRV wt infection with matched genome copy numbers on BJAB EPHA7^{KO} cells, with no significant differences between cell pools treated with control sgRNAs and sgRNAs targeting EPHA2 or EPHA7. To exclude the contribution of off-target effects to the observed reduction in KSHV and RRV infection, we overexpressed EphA7 by lentiviral gene transduction in monoclonal EphA7^{KO} cells and monoclonal nontargeting control cells (Fig. 2D). EphA7 reconstitution in EphA7^{KO} cells restored KSHV cell-to-cell transmission (Fig. 2E) and cell-free RRV infection (Fig. 2F) to infection levels obtained on nontargeting control cells transduced with an empty vector control when averaged over two single-cell clones per target. On nontargeting controls, EphA7 overexpression had a slightly enhancing, albeit nonsignificant, effect on KSHV and RRV infection compared to that of the empty vector control.

Impact of additional Eph receptors on the infection of BJAB cells by KSHV and RRV. As we observed slight differences in the transmission of KSHV wt and the Eph-detargeted KSHV mutant to EPHA7^{KO} BJAB cells, we wanted to address the question of whether other members of the Eph family of receptor tyrosine kinases play a role in infection of BJAB cells by KSHV. To test this hypothesis, we performed ligand-dependent blocking experiments of KSHV infection, using recombinant ephrinA4, a soluble Fc-fusion protein of a natural Eph ligand, which targets A-type Ephs and blocks infection of adherent cells by cell-free KSHV (3). We treated a reduced set of knockout cell pools with either phosphate-buffered saline (PBS) (control) or ephrinA4 in PBS during the coculture experiment (Fig. 3A). While ephrinA4 treatment significantly inhibited infection of both EPHA2^{KO} BJAB cells and nontargeting control BJAB cells compared to PBS by over 85%, infection of EPHA7^{KO} BJAB cells was reduced by only 20% in the presence of ephrinA4, a level which did not reach significance. It should be noted that knockout of EPHA2 also led to a small (approximately 35%) but significant reduction in infection in this experiment using a reduced set of sgRNA constructs.

As we had detected peptides of EphA5 in the initial pulldown using the KSHV gH/gL complex (Fig. 1A and B), we proceeded to analyze the role of EphA5 in KSHV transmission to BJAB cells. Pulldown experiments with KSHV and RRV 26-95 gH/gL complexes followed by Western blot analysis of precipitates confirmed the binding of KSHV gH/gL but not RRV 26-95 gH/gL to endogenous EphA5 in BJAB lysate. Similar to EphA7, EphA5 was not detected in 293T lysate precipitated with either KSHV gH/gL or RRV gH/gL. EphA2 binding to KSHV gH/gL in 293T lysate was used as a control (Fig. 3B). Stable EPHA5^{KO} cell pools were generated using the lentiviral CRISPR/Cas9 system, and knockout was verified by Western blotting (Fig. 3C). Analogous to experiments with EphA7^{KO} cells, cell pools with confirmed EPHA5 knockout (sgEPHA5-1 and sgEPHA5-2) were tested for cell-to-cell transmission of KSHV in coculture experiments (Fig. 3D) as well as for cell-free infection with RRV (Fig. 3E). Compared to nontargeting controls,

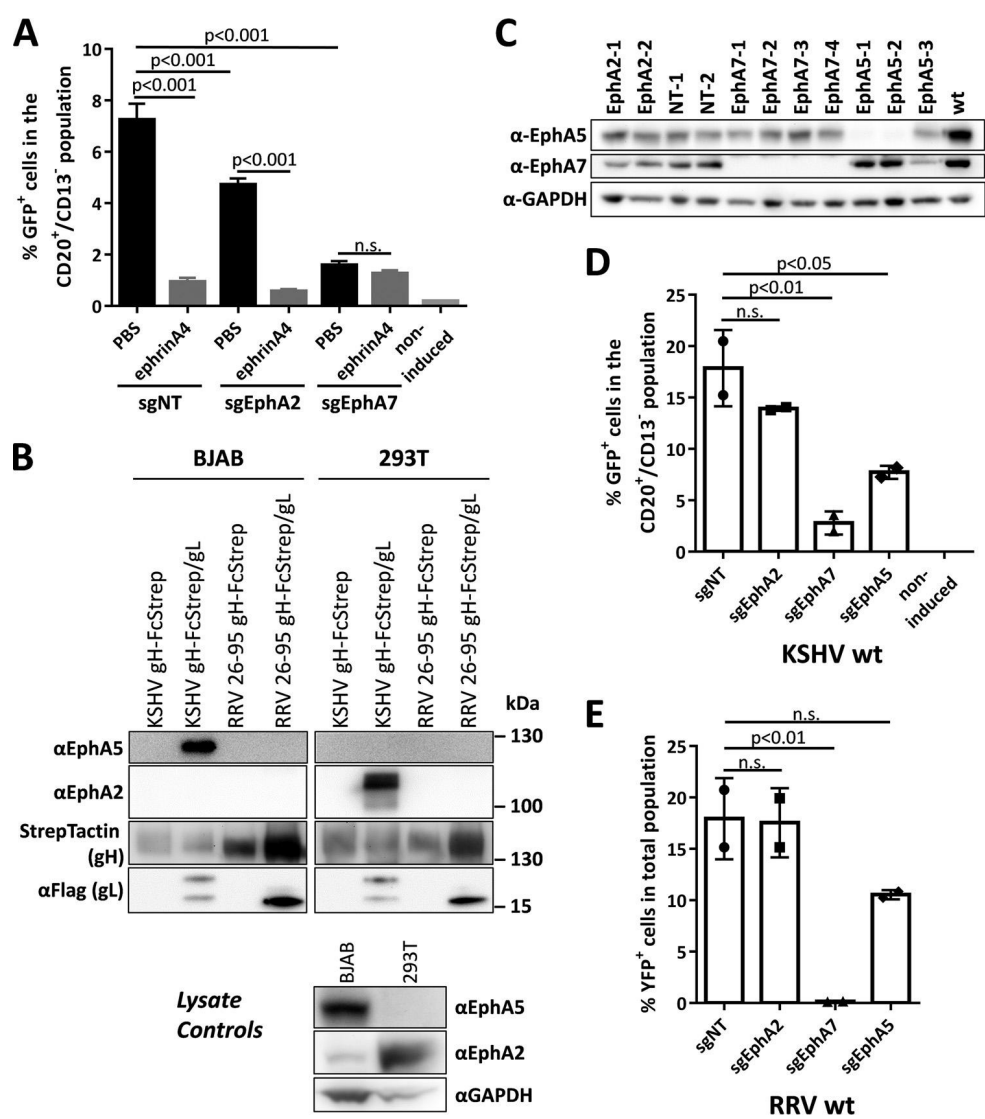


FIG 3 EphA7 is the predominant Eph receptor for infection of BJAB cells by KSHV. (A) BJAB knockout cell pools (sgNT-1, sgEPA2-1, and sgEPA7-1) were cocultured with iSLK cells harboring BAC16 KSHV wt. ephrinA4-Fc at a final concentration of 2 μ g/ml in PBS, or PBS alone as control, was added to the coculture. The indicated individual comparisons were made using one-way ANOVA with Bonferroni correction for multiple comparisons. (B) Pull-down from BJAB and 293T lysate using recombinant soluble KSHV or RRV 26-95 gH/gL complexes as bait. Input amounts were normalized to wet cell pellet. Precipitates were analyzed by Western blotting with the indicated antibodies. For KSHV gL, two bands, representing differentially glycosylated forms, were detected. (C) Knockout of EPHA7 and EPHA5 in BJAB cells. BJAB cells were transduced with the indicated lentiCRISPRv2-based constructs and briefly selected, and cell pools were analyzed by Western blotting. (D) BJAB cells transduced with the lentiCRISPRv2-based constructs targeting the indicated genes were cocultured with iSLK cells harboring BAC16 KSHV wt. GFP reporter gene expression in the CD13⁻ CD20⁺ population, as an indicator of BJAB cell infection, was analyzed by flow cytometry. The means across groups of sgRNAs ($n = 3$ infections per sgRNA) targeting EPHA2 (two sgRNAs), EPHA7 (two sgRNAs, sgEPA7-3 and sgEPA7-4), and EPHA5 (two sgRNAs, sgEPA5-1 and sgEPA5-2), or nontargeting sgRNAs (sgNT; two sgRNAs), are indicated by columns. The standard deviations from the means are indicated by the error bars. The means from the individual triplicate infections for each sgRNA BJAB population within a group are given as symbols within the respective columns. Statistical significance was determined by pairwise comparison to the sgNT control group using one-way ANOVA with Bonferroni correction for multiple comparisons. (E) The same BJAB cell pools as those use for panel D were infected with cell-free RRV-YFP wt. YFP reporter gene expression, as an indicator of infection, was analyzed by flow cytometry. Statistical analysis was performed as described for panel D.

treatment of BJAB cells with sgRNAs directed against EPHA2, EPHA7, and EPHA5 resulted in reduction of KSHV transmission into BJAB cells of approximately 23%, 84%, and 57%, respectively. In contrast, treatment with sgRNAs directed against EPHA2 had no effect on cell-free RRV infection of BJAB cells, while knockout of EPHA7 and EPHA5 reduced infection with RRV by approximately 99% and 40%, respectively.

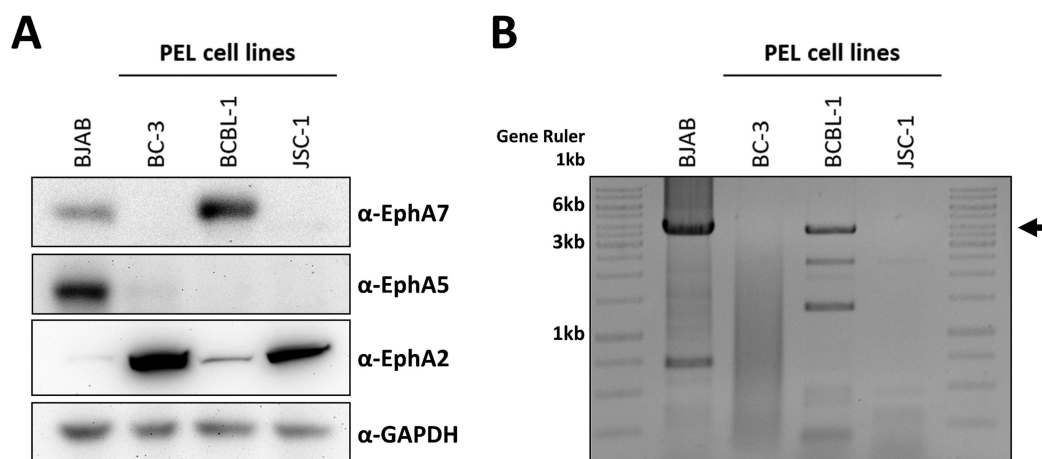


FIG 4 Expression of select Ephs in PEL cells. (A) Lysates prepared from BJAB cells and three PEL cell lines were analyzed by Western blotting with the indicated antibodies. (B) Nonquantitative RT-PCR of EphA7 cDNA using primers in the 5' and 3' UTRs common to transcript variant 1 ([NM_004440](#)), transcript variant 2 ([NM_001288629](#)), predicted transcript variant X1 ([XM_005248669](#)), predicted transcript variant X2 ([XM_017010365](#)), and predicted transcript variant X4 ([XR_001743218.2](#)) with an expected product size of approximately 5.2 kb for predicted transcript variant X4 and 3.9 kb for all other transcript variants (black arrow).

EphA7 expression in PEL cell lines. To address a possible role of EphA7 in KSHV-associated B cell malignancies, we tested three PEL cell lines, BC-3, BCBL-1, and JSC-1, for expression of different Ephs by Western blotting (Fig. 4A). All three PEL cell lines were positive for EphA2, the high-affinity KSHV receptor, and none was positive for EphA5. BCBL-1, which expressed only small amounts of EphA2, were highly positive for EphA7. Sequences of the 3.9-kb fragment obtained after reverse transcription-PCR (RT-PCR) (Fig. 4B, black arrow) were compatible with expression of EphA7 transcript variant 1 (GenBank accession no. [NM_004440](#)) and transcript variant 2 ([NM_001288629](#)) in BJAB cells and EphA7 transcript variant 1 and the predicted transcript variant X1 ([XM_005248669](#)) in BCBL-1 cells, respectively. Sequences obtained from fragments of lower molecular weight did not match deposited EphA7 sequences.

DISCUSSION

The use of EphA7 as a cellular receptor for the infection of BJAB cells by KSHV and RRV is consistent with previous studies that the gH/gL complexes of both viruses can interact with various members of the Eph family of receptor tyrosine kinases. While KSHV gH/gL binds EphA2 with highest affinity, we previously identified trace amounts of peptides of additional Ephs after pulldown with KSHV gH/gL in 293T lysate and demonstrated interaction of these Ephs, as well as EphA7, with KSHV gH/gL in overexpression experiments (6). Similarly, RRV interacts with both A-type and B-type Ephs with various levels of affinity, and the gH/gL complexes of both RRV subtypes precipitated EphA7 from 293T lysate in a previous study (6). While we readily precipitated endogenous EphA7 from BJAB lysate using the gH/gL complexes of either KSHV or RRV 26-95, we were not able to precipitate endogenous EphA7 from 293T lysate under similar conditions in this study. The reason for this lack of detectable EphA7-gH/gL interaction in 293T cells could lie in differences in relative expression levels of different Ephs (Fig. 1), an ability of EphA2 to outcompete for binding to the KSHV gH/gL complex, or the limits of antibody-based detection of EphA7 by Western blotting compared to mass spectrometry-based detection in past studies.

Recent publications suggest that other Ephs, such as EphA4 and EphA5, can substitute for EphA2 as receptors for KSHV in overexpression experiments (2, 24). However, as single knockout was not analyzed in one study (24) or even led to an increase rather than a reduction in KSHV infection in SLK cells both in the presence and absence of EphA2 in the case of EphA4 in a second study (2), a definitive conclusion

regarding the significance of endogenously expressed Eph receptors besides EphA2 for KSHV infection is hard to draw. So far, reduced KSHV infection upon single-gene knockout or knockdown has only been conclusively shown for EPHA2 in several publications (2–5). We now show that knockout of EPHA7 in BJAB cells resulted in a significant reduction in cell-to-cell transmission of KSHV and cell-free infection by RRV. Likewise, endogenously expressed EphA5 interacted with recombinant KSHV gH/gL (Fig. 1A and B and 3B), and knockdown of EphA5 resulted in similar but less pronounced reduction in KSHV transmission. However, we also observed a reduction of RRV infection by approximately 40% without detectable interaction of RRV gH/gL with EphA5 either by mass spectrometry or Western blot analysis. Furthermore, the slight reduction of KSHV transmission after transduction of sgRNAs directed against EPHA2, which reached significance in one set of infections, (Fig. 3A) hints at some residual function of EphA2 at expression levels below the limit of detection achievable in our Western blot analysis.

As the Eph receptor family forms a complex signaling network, in which interaction, (hetero-)oligomerization (25), and modulation between different members have been reported (26), the exact mechanism behind modulation of KSHV and RRV infection may be more complex than the sum of individual contributions by different members of the Eph family. In line with a mechanism that is more complex than a simple additive effect, we did not observe a statistically significant reduction of KSHV infection by treating the iSLK BAC16 KSHV wt/BJAB EPHA7^{KO} coculture with ephrinA4, a natural ligand which interacts with all A-type Ephs and therefore should be able to inhibit the gH/gL interaction with EphA5. Further, while residual KSHV wt infection of EPHA7^{KO} cells was not completely reduced to the levels achieved with the Eph-detargeted KSHV gH-ELAAN mutant on control cells, the difference was marginal (approximately 4% versus approximately 2% infection), and we found RRV infection was essentially abrogated after EphA7 knockout alone.

While EphA7 is reportedly not expressed in mature B cells (27), we found high EphA7 expression in one of three PEL cell lines that we tested. While BC-3 and JSC-1 were strongly positive for EphA2, BCBL-1 showed an expression pattern similar to that seen for BJAB cells with high EphA7 and low EphA2 levels. Thus, KSHV may utilize EphA2 and EphA7 for primary infection of cells that ultimately give rise to PEL. Alternatively, these receptors might be upregulated in infected cells. Of note, many PEL cell isolates harbor oligoclonal KSHV genomes, potentially as a result of superinfection, which was demonstrated to be possible by cell-to-cell transmission (12, 28) and could be promoted by EphA2 or EphA7.

KSHV transmission to BJAB cells and other lymphoblastoid cell lines as well as primary B cells is low even in cell-to-cell systems (12) compared to infection of adherent cells by free KSHV, which has been attributed to a heparan sulfate-dependent attachment defect of KSHV on BJAB (9). Additionally, a role for glycoprotein K8.1A, independent of its heparan sulfate binding activity, has been described for the infection of B cells by KSHV (29). Although infection of BJAB cells by cell-to-cell transmission was not analyzed in these studies, the role of glycoprotein K8.1A in the infection of B cells but not in the infection of other cell types (29, 30) and the described defect at the attachment step (9) hint at possible mechanistic differences specific for B cell infection.

An open question is whether the function of EphA7 in cell-to-cell transmission is somewhat different from the function of, e.g., EphA2 in the infection of epithelial or endothelial cells, and whether the specific nature of cell-to-cell transmission allows for more efficient use of receptors with comparatively lower affinity for gH/gL. This should be addressed in separate studies using loss-of-function methodology. The ability of KSHV to use different Ephs dependent on relative expression levels may parallel the interaction of ephrins with their receptors (31) and receptor usage by RRV (6). Whether there is a direct correlation between affinity and receptor function or whether the mechanism is more complicated will be a subject for future studies. Similarly, the question of whether Eph-associated signaling as described for cell-free KSHV infection

of adherent cells (reviewed in reference 32) also plays a role in KSHV cell-to-cell transmission warrants further analysis.

MATERIALS AND METHODS

Cells and viruses. BJAB cells were obtained from the Leibniz-Institute DSMZ (Deutsche Sammlung von Mikroorganismen und Zellkulturen GmbH). iSLK cells were a kind gift from Jinjong Myoung (33), 293T cells from Stefan Pöhlmann, the PEL cell line BC-3 (34) from Frank Neipel, PEL cell lines JSC-1 (35) and BCL-1 (36) from Armin Ensser, and primary rhesus monkey fibroblasts from Rüdiger Behr. BJAB and BCL-1 cells were propagated in RPMI 1640 medium (Thermo Fisher Scientific) containing L-glutamine supplemented with 10% fetal bovine serum (FBS) (Thermo Fisher Scientific) and 50 μ g/ml gentamicin (PAN Biotech). JSC-1 and BC-3 cells were maintained in RPMI 1640 containing L-glutamine supplemented with 20% FBS, 50 μ g/ml gentamicin, 1 mM sodium pyruvate (PAN Biotech), and 0.05 mM beta-mercaptoethanol (Carl Roth). 293T cells were cultured in Dulbecco's modified Eagle medium (DMEM) containing high glucose, GlutaMAX, 25 mM HEPES (Thermo Fisher Scientific) supplemented with 10% FBS and 50 μ g/ml gentamicin. iSLK cells were maintained in DMEM supplemented with 10% FBS, 50 μ g/ml gentamicin, 2.5 μ g/ml puromycin (InvivoGen), and 250 μ g/ml G418 (Carl Roth). RRV-YFP, RRV-YFP gH-ELAAN, and iSLK cells harboring BAC16 KSHV wt or BAC16 KSHV gH-ELAAN were produced as described previously (23).

Coculture and free virus infections. iSLK-BAC16 KSHV wt or iSLK-BAC16 KSHV gH-ELAAN cells were seeded in 48-well plates at 100,000 cells per well. After 5 h, lytic replication was induced with 1 μ g/ml doxycycline (Sigma) and 2.5 mM sodium butyrate (Carl Roth) overnight in DMEM containing high glucose, GlutaMAX, 25 mM HEPES, 50 μ g/ml gentamicin, and 10% FBS. After 1 day, the induction medium was discarded and the respective BJAB cell pools were added at 60,000 cells per well in 600 μ l fresh RPMI medium with 10% FBS and 50 μ g/ml gentamicin. After 4 days, cells were harvested for fluorescence-activated cell sorting (FACS) analysis as described below. For blocking experiments, recombinant ephrinA4-Fc protein (R&D Systems) was added at the start of the coculture to a final concentration of 2 μ g/ml. For cell-free RRV infection, BJAB cell pools were seeded at 60,000 cells per well in 48-well plates and infected on the same day with RRV preparations normalized to genome copy numbers as described before (23). One day after infection cells were harvested for FACS analysis.

Flow cytometry analysis. After 4 days of coculture, cells were harvested by pipetting, fixed with 2% formaldehyde (Carl Roth) in PBS for 15 min, and washed in PBS. After blocking in 5% FBS in PBS for 30 min, the cells were stained with anti-CD13 (clone WM15; phycoerythrin coupled; BioLegend) and anti-CD20 (clone 2H7; Alexa Fluor 647 coupled; BioLegend) antibodies at a 1:50 dilution in 5% FBS in PBS for 30 to 45 min. After 2 washes in PBS, the cells were resuspended in 2% formaldehyde in PBS. RRV-infected BJAB cell pools were harvested by pipetting, washed in PBS, and fixed in 2% formaldehyde in PBS. The samples were analyzed on an LSRII flow cytometer (BD Biosciences). Flow cytometry data were further analyzed using Flowing software (version 2.5); for details, see Fig. S1 in the supplemental material. KSHV cell-to-cell infection of BJAB cells was assayed by constitutive GFP reporter gene expression in the CD13⁺ CD20⁺ population. Cell-free RRV infection was measured by constitutive YFP reporter gene expression. Statistical analysis was carried out using GraphPad Prism, version 6, for Windows (GraphPad Software, La Jolla, California, USA).

Generation of knockout cell pools. Knockout cell pools were generated using the lentiCRISPRv2 system (37) as described previously (38), with the exception that transfection was carried out using polyethylenimine (PEI) MAX (Polysciences) (39). In short, BJAB cells were transduced with lentiviruses harboring the indicated sgRNAs. After 48 h, the selection antibiotic puromycin (InvivoGen) was added to a final concentration of 10 μ g/ml. After initial selection, the puromycin concentration was reduced to 1 μ g/ml. The following sgRNAs were inserted into plentiCRISPRv2 (a kind gift from Feng Zhang [Addgene plasmid number 52961]): 2 nontargeting controls, sgNT-1 (plasmid Ax127; ATCGTTCCGCTTAACGGCG) and sgNT-2 (Ax128; TTCGCACGATTGCACCTTGG); 4 sgRNAs directed against EPHA7, namely, sgEPA7-1 (Ax279; GGAGAATGGTTAGTGCCCAT), sgEPA7-2 (Ax280; GACATGTGTCAGCAGTGACG), sgEPA7-3 (Ax281; GGATTTCCTCTCCACCCAAT), and sgEPA7-4 (Ax282; GATTTCCTCTCCACCCAATG); 2 sgRNAs directed against EPHA2, namely, sgEPA2-1 (Ax122; CTACAATGTGCGCCGACCG) and sgEPA2-2 (Ax123; GGACTTTGCTGCAGCTGGAG); and 3 sgRNAs directed against EPHA5, namely, sgEPA5-1 (Ax299; GGATTCACGCACTGTCATGG), sgEPA5-2 (Ax300; GATTGCTTTTCCAAAAAATG), and sgEPA5-3 (Ax301; GGATTGCTTTTCCAAAAAAT). sgRNA sequences for all sgRNAs directed against EphA7, EphA5, and EPHA2-2 were determined using E-CRISP (40). The lentiCRISPRv2-sgEPA2-1 plasmid was purchased from GenScript. Nontargeting sgRNA sequences were taken from the GeCKO (version 2) library (37).

EphA7 reconstitution experiments. For the generation of monoclonal BJAB KO cells, cells were seeded at one cell per well in 96-well plates, expanded in RPMI 1640 containing L-glutamine, 10% FBS, 50 μ g/ml gentamicin, 1 μ g/ml puromycin, and tested for EphA7 knockout by Western blotting. Two monoclonal cell lines per target (nontargeting [sgNT-1] and EphA7 [sgEPA7-3 and sgEPA7-4]) were transduced with a lentivirus carrying an EphA7-Strep expression cassette (transcript variant 1 [NM_004440]) (pLenti-CMV-BLAST-EphA7-Strep) or an empty vector control. Lentiviral particles were generated as described previously (38), with the exception that transfection was carried out using PEI. Two days posttransduction the selection antibiotic blasticidin (InvivoGen) was added to a final concentration of 10 μ g/ml. After initial selection the blasticidin concentration was reduced to 1 μ g/ml. pLenti-CMV-BLAST-EphA7-Strep was based on pLenti CMV BLAST (Addgene plasmid number 17486; a gift from Eric Campeau and Paul Kaufman), which was previously modified to include the twin-Strep-tag (41) coding sequence following the XbaI recognition site (AGCGCTTGAGCCATCCACAGTTCGAAAAAGGGAGGTGGAAGCGGTGGAGGTAGTGGTGAAGTGATGGAGCCATCCTCAGTTTGAAAAAGTAAGTAGAGGG

CCCA). Mutation of the sgRNA binding sites in the EPHA7 coding sequence (described before [6]) and subcloning into the lentiviral vector were performed using a high-fidelity polymerase (Fusion S7; Biozym) with the following primers: sgRNA mutation_for (ACCGCCGAACGGTTGGGAAGAAATTAGTGGTTTG), sgRNA mutation_reverse (CTTCCCAACCGTTCCGGCGGTGAGGAAATCCACTC), EphA7_forward (AAAAAAGCAGGCTC CACCATGGTTTTTCAAACCTCGGTACC), EphA7_reverse (TGTGGATGGCTCCAAGCGCTCACTGAATGCCAGTTC CATG), vector_forward (TCTAGAAGCGCTTGGAGCCATCC), and vector_reverse (CATGGTGGAGCCTGCTTTT TTGATC). Three-fragment assembly was carried out using the Gibson Assembly master mix (New England Biolabs).

Pulldown experiments and Western blotting. Two-step pulldown with specific elution and reprecipitation using gH-FcStrep/gL complexes (3, 6, 19) for identification by mass spectrometry was performed as described previously (6). One ml of wet BJAB cell pellet was lysed with 5 ml of lysis buffer per sample for 30 min on ice as the starting material for the pulldowns (in total, 4 ml BJAB wet cell pellet was lysed with 20 ml lysis buffer, 1% NP-40, 150 mM NaCl, 2 mM EDTA, 50 mM HEPES, pH 7.2). The lysate was cleared by a 1-min spin at $20,000 \times g$ in 2-ml reaction tubes. The supernatant was then incubated for 30 min with agitation with Strep-Tactin Superflow beads (Qiagen). The beads were collected by a brief spin ($500 \times g$), and the supernatant was transferred to a fresh tube. The samples were then centrifuged at $20,000 \times g$ for 30 min. The supernatants were collected and pooled, and 5 ml was incubated overnight at 4°C with agitation with the respective Fc fusion proteins precoupled to Strep-Tactin beads (10 ml of transfected 293T cell supernatant was reacted with approximately 50 μ l Strep-Tactin beads overnight before the pulldown experiment) in a 15-ml tube. The beads were then collected by low-speed centrifugation for 5 min, the supernatant was discarded, and the beads were washed with 10 ml 0.75% NP-40 in PBS, which was repeated three times. Bound protein was then eluted for 5 min with 1 ml 2.5 mM desthiobiotin and 0.375% NP-40 in PBS by mixing with the beads, followed by resedimentation of the Strep-Tactin beads by low-speed centrifugation and careful collection of the supernatant. The eluate was incubated for 1 h with approximately 30 μ l of protein A agarose beads (GE Lifesciences) at 4°C with agitation. The protein A beads were then collected by centrifugation at $1,500 \times g$ for 1 min and were washed three times with 0.375% NP-40 in PBS. After removal of all washing buffer, 40 μ l of SDS sample buffer was added and the samples were heated to 95°C for 3 min. The samples then were analyzed by polyacrylamide gel electrophoresis using 8 to 16% gradient gels (Invitrogen), the gel was silver stained, and excised bands were destained using the SilverQuest staining kit (Life Technologies). Mass spectrometry analysis by liquid chromatography-tandem mass spectrometry of individual gel bands was carried out by the Taplin Mass Spectrometry Core Facility, Harvard Medical School. For pulldown followed by Western blot analysis, cells were lysed with 2 ml of lysis buffer (1% NP-40, 150 mM NaCl, 1 mM EDTA, 25 mM HEPES, pH 7.3, with addition of protease inhibitor cocktail [Amresco]) per ml of wet cell pellet. The lysate was clarified by centrifugation ($21,100 \times g$, 20 min) and reacted with gH-FcStrep/gL-Flag complexes that were precoupled to Strep-Tactin XT (IBA) beads. After three washes with lysis buffer, the precipitates were analyzed by polyacrylamide gel electrophoresis and Western blotting as described previously (23) using antibodies to EphA7 (clone E-7; sc-393973) and EphA2 (C-20; sc-924), both from Santa Cruz Biotechnology, 1:100 and 1:500, and EphA5 (clone number 86731; MAB541; R&D Systems), 1:500, in NETT gelatin (150 mM NaCl, 5 mM EDTA, 50 mM Tris, 0.05% Triton X-100, 0.25% gelatin, pH 7.5) and donkey anti-mouse horseradish peroxidase (HRP)-coupled (Dianova) or goat anti-rabbit HRP-coupled (Life Technologies) secondary antibody in 5% dry milk powder in PBS with 0.05% Tween 20. Membranes were imaged using Immobilon Forte substrate (Merck) on an INTAS ECL ChemoCam system. Similar lysis conditions were used for analysis of gene knockout cell pools by Western blotting.

RNA isolation, cDNA synthesis, and nonquantitative RT-PCR. For RNA isolation, cells were harvested in RNazol RT (Sigma) and RNA was isolated using the Direct-zol RNA MiniPrep plus kit (Zymo Research) according to the manufacturer's instructions. In short, 0.4 ml of RNase-free water per ml of RNazol RT, used for homogenization, was added, vortexed for 15 s, and incubated for 10 min at room temperature. After centrifugation (15 min, $12,000 \times g$, 4°C), the aqueous phase was mixed with an equal volume of 100% ethanol and column purified. In the column, DNase I (30 U) treatment was performed for 15 min at room temperature. RNA was eluted in RNase-free water. One μ g RNA was reverse transcribed using the SensiFast cDNA synthesis kit (Bioline) according to the manufacturer's instructions. PCR was performed using Fusion S7 with a primer pair (GGTCTGCAGTCGGAGACTTG and AGCTCTTGGC AACTGCATT) binding in the 5' and 3' untranslated regions (UTRs) of transcript variant 1 (GenBank accession no. [NM_004440](#)), transcript variant 2 ([NM_001288629](#)), predicted transcript variant X1 ([XM_005248669](#)), predicted transcript variant X2 ([XM_017010365](#)), and predicted transcript variant X4 ([XR_001743218.2](#)). PCR products were analyzed on 1% agarose gels, and bands at the expected sizes were excised and purified using the NucleoSpin gel and PCR clean-up kit (Macherey-Nagel). Sanger sequencing was carried out by Macrogen, Inc.

SUPPLEMENTAL MATERIAL

Supplemental material for this article may be found at <https://doi.org/10.1128/JVI.00064-19>.

SUPPLEMENTAL FILE 1, PDF file, 1.1 MB.

ACKNOWLEDGMENTS

This work was supported by grants to A.S.H. from the Deutsche Forschungsgemeinschaft (HA 6013/1, HA 6013/4-1), by grant RO1 AI072004 from the National Institutes of

Health (NIH) to R.C.D., and by base grant RR00168 from the NIH to the New England Primate Research Center.

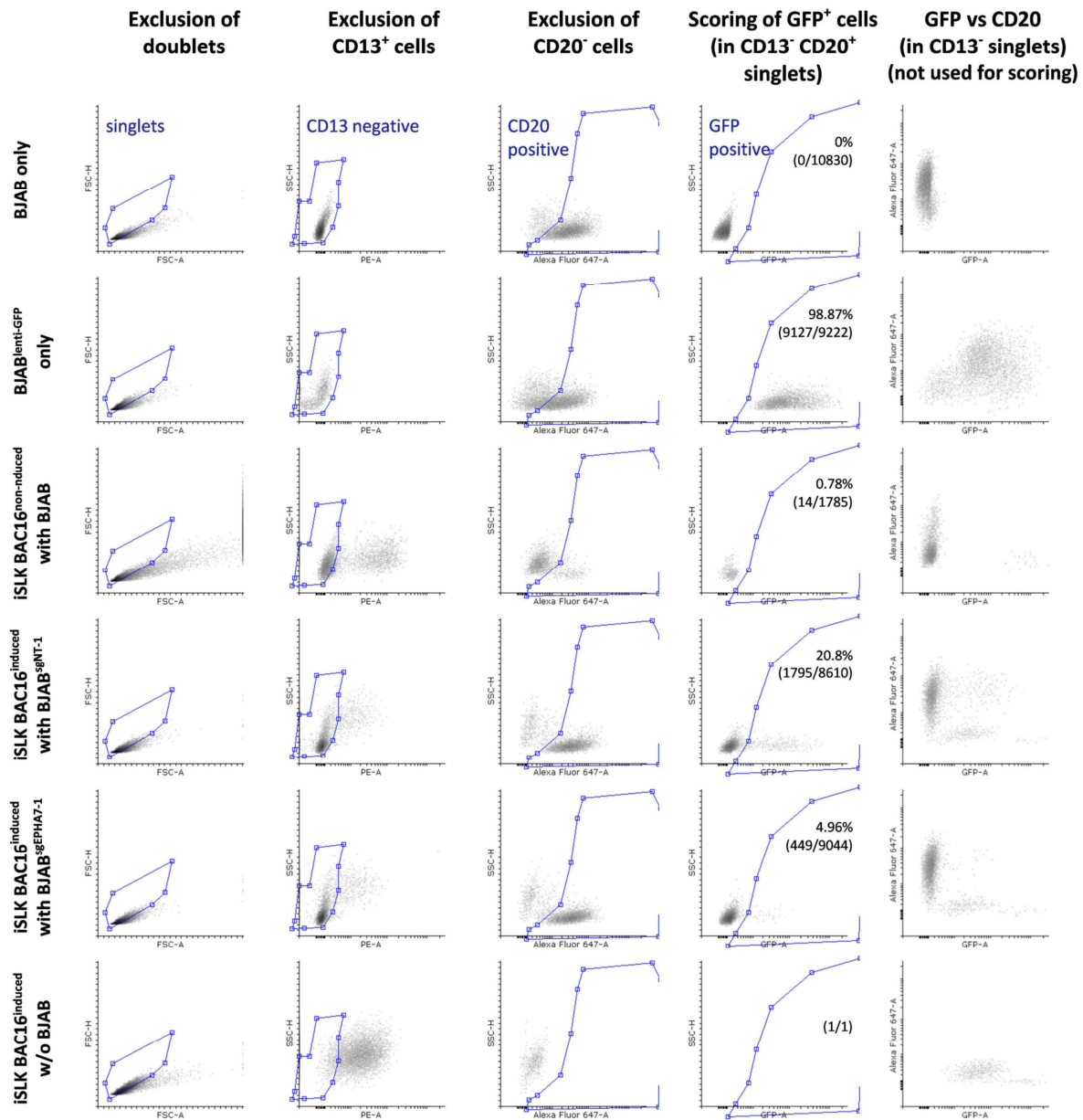
We thank Rüdiger Behr for primary rhesus monkey fibroblasts, Armin Ensser and Frank Neipel for PEL cell lines, and Stefan Pöhlmann and Jens Gruber for reagents.

REFERENCES

- Yarchoan R, Uldrick TS. 2018. HIV-associated cancers and related diseases. *N Engl J Med* 378:1029–1041. <https://doi.org/10.1056/NEJMra1615896>.
- TerBush AA, Hafkamp F, Lee HJ, Coscoy L. 2018. A Kaposi's sarcoma-associated herpesvirus infection mechanism is independent of integrins $\alpha 3\beta 1$, $\alpha V\beta 3$, and $\alpha V\beta 5$. *J Virol* 92:e00803-18. <https://doi.org/10.1128/JVI.00803-18>.
- Hahn AS, Kaufmann JK, Wies E, Naschberger E, Panteleev-Ivlev J, Schmidt K, Holzer A, Schmidt M, Chen J, König S, Ensser A, Myoung J, Brockmeyer NH, Stürzl M, Fleckenstein B, Neipel F. 2012. The ephrin receptor tyrosine kinase A2 is a cellular receptor for Kaposi's sarcoma-associated herpesvirus. *Nat Med* 18:961–966. <https://doi.org/10.1038/nm.2805>.
- Chakraborty S, Veettil MV, Bottero V, Chandran B. 2012. Kaposi's sarcoma-associated herpesvirus interacts with EphrinA2 receptor to amplify signaling essential for productive infection. *Proc Natl Acad Sci USA* 109:E1163–E1172. <https://doi.org/10.1073/pnas.1119592109>.
- Wang X, Zou Z, Deng Z, Liang D, Zhou X, Sun R, Lan K. 2017. Male hormones activate EphA2 to facilitate Kaposi's sarcoma-associated herpesvirus infection: implications for gender disparity in Kaposi's sarcoma. *PLoS Pathog* 13:e1006580. <https://doi.org/10.1371/journal.ppat.1006580>.
- Hahn AS, Desrosiers RC. 2013. Rhesus monkey rhadinovirus uses Eph family receptors for entry into B cells and endothelial cells but not fibroblasts. *PLoS Pathog* 9:e1003360. <https://doi.org/10.1371/journal.ppat.1003360>.
- Bechtel JT, Liang Y, Hvidding J, Ganem D. 2003. Host range of Kaposi's sarcoma-associated herpesvirus in cultured cells. *J Virol* 77:6474–6481. <https://doi.org/10.1128/JVI.77.11.6474-6481.2003>.
- Blackbourn DJ, Lennette E, Klencke B, Moses A, Chandran B, Weinstein M, Glogau RG, Witte MH, Way DL, Kutzkey T, Herndier B, Levy JA. 2000. The restricted cellular host range of human herpesvirus 8. *AIDS* 14: 1123–1133. <https://doi.org/10.1097/00002030-200006160-00009>.
- Jarousse N, Chandran B, Coscoy L. 2008. Lack of heparan sulfate expression in B-cell lines: implications for Kaposi's sarcoma-associated herpesvirus and murine gammaherpesvirus 68 infections. *J Virol* 82:12591–12597. <https://doi.org/10.1128/JVI.01167-08>.
- Renne R, Blackbourn D, Whitby D, Levy J, Ganem D. 1998. Limited transmission of Kaposi's sarcoma-associated herpesvirus in cultured cells. *J Virol* 72:5182–5188.
- Dollery SJ, Santiago-Crespo RJ, Kardava L, Moir S, Berger EA. 2014. Efficient infection of a human B cell line with cell-free Kaposi's sarcoma-associated herpesvirus. *J Virol* 88:1748–1757. <https://doi.org/10.1128/JVI.03063-13>.
- Myoung J, Ganem D. 2011. Infection of lymphoblastoid cell lines by Kaposi's sarcoma-associated herpesvirus: critical role of cell-associated virus. *J Virol* 85:9767–9777. <https://doi.org/10.1128/JVI.05136-11>.
- Menezes J, Leibold W, Klein G, Clements G. 1975. Establishment and characterization of an Epstein-Barr virus (EBV)-negative lymphoblastoid B cell line (BJA-B) from an exceptional, EBV-genome-negative African Burkitt's lymphoma. *Biomedicine* 22:276–284.
- Klein G, Lindahl T, Jondal M, Leibold W, Meneses J, Nilsson K, Sundström C. 1974. Continuous lymphoid cell lines with characteristics of B cells (bone-marrow-derived), lacking the Epstein-Barr virus genome and derived from three human lymphomas. *Proc Natl Acad Sci U S A* 71: 3283–3286. <https://doi.org/10.1073/pnas.71.8.3283>.
- Kati S, Tsao EH, Gunther T, Weidner-Glunde M, Rothamel T, Grundhoff A, Kellam P, Schulz TF. 2013. Activation of the B cell antigen receptor triggers reactivation of latent Kaposi's sarcoma-associated herpesvirus in B cells. *J Virol* 87:8004–8016. <https://doi.org/10.1128/JVI.00506-13>.
- Chen L, Lagunoff M. 2005. Establishment and maintenance of Kaposi's sarcoma-associated herpesvirus latency in B cells. *J Virol* 79: 14383–14391. <https://doi.org/10.1128/JVI.79.22.14383-14391.2005>.
- Desrosiers RC, Sasseville VG, Czajak SC, Zhang X, Mansfield KG, Kaur A, Johnson RP, Lackner AA, Jung JU. 1997. A herpesvirus of rhesus monkeys related to the human Kaposi's sarcoma-associated herpesvirus. *J Virol* 71:9764–9769.
- Großkopf AK, Schlagowski S, Hörnich BF, Fricke T, Desrosiers RC, Hahn AS. 2019. EphA7 functions as receptor on BJAB cells for cell-to-cell transmission of the Kaposi's sarcoma-associated herpesvirus and for cell-free infection by the related rhesus monkey rhadinovirus. *bioRxiv* <https://doi.org/10.1101/522243>.
- Hahn A, Birkmann A, Wies E, Dorer D, Mahr K, Stürzl M, Titgemeyer F, Neipel F. 2009. Kaposi's sarcoma-associated herpesvirus gH/gL: glycoprotein export and interaction with cellular receptors. *J Virol* 83:396–407. <https://doi.org/10.1128/JVI.01170-08>.
- Searles RP, Bergquam EP, Axthelm MK, Wong SW. 1999. Sequence and genomic analysis of a Rhesus macaque rhadinovirus with similarity to Kaposi's sarcoma-associated herpesvirus/human herpesvirus 8. *J Virol* 73:3040–3053.
- Shin YC, Jones LR, Manrique J, Lauer W, Carville A, Mansfield KG, Desrosiers RC. 2010. Glycoprotein gene sequence variation in rhesus monkey rhadinovirus. *Virology* 400:175–186. <https://doi.org/10.1016/j.virol.2010.01.030>.
- Thakker S, Strahan RC, Scurry AN, Uppal T, Verma SC. 2018. KSHV LANA upregulates the expression of epidermal growth factor like domain 7 to promote angiogenesis. *Oncotarget* 9:1210–1228. <https://doi.org/10.18632/oncotarget.23456>.
- Großkopf AK, Ensser A, Neipel F, Jungnickl D, Schlagowski S, Desrosiers RC, Hahn AS. 2018. A conserved Eph family receptor-binding motif on the gH/gL complex of Kaposi's sarcoma-associated herpesvirus and rhesus monkey rhadinovirus. *PLoS Pathog* 14:e1006912. <https://doi.org/10.1371/journal.ppat.1006912>.
- Chen J, Zhang X, Schaller S, Jardtetzky TS, Longnecker R. 2019. Ephrin receptor A4 is a new Kaposi's sarcoma-associated herpesvirus virus entry receptor. *mBio* 10:e02892-18. <https://doi.org/10.1128/mBio.02892-18>.
- Oricchio E, Nanjangud G, Wolfe AL, Schatz JH, Mavrakis KJ, Jiang M, Liu X, Bruno J, Heguy A, Olshen AB, Socci ND, Teruya-Feldstein J, Weis-Garcia F, Tam W, Shakhovich R, Melnick A, Himanen JP, Chaganti RSK, Wendel H-G. 2011. The Eph-receptor A7 is a soluble tumor suppressor for follicular lymphoma. *Cell* 147:554–564. <https://doi.org/10.1016/j.cell.2011.09.035>.
- Janes PW, Griesshaber B, Atapattu L, Nievergall E, Hii LL, Mensinga A, Chheang C, Day BW, Boyd AW, Bastiaens PI, Jørgensen C, Pawson T, Lackmann M. 2011. Eph receptor function is modulated by heterooligomerization of A and B type Eph receptors. *J Cell Biol* 195:1033–1045. <https://doi.org/10.1083/jcb.201104037>.
- Alonso-C LM, Trinidad EMA, de Garcillan B, Ballesteros M, Castellanos M, Coto I, Muñoz JJ, Zapata AG. 2009. Expression profile of Eph receptors and ephrin ligands in healthy human B lymphocytes and chronic lymphocytic leukemia B-cells. *Leuk Res* 33:395–406. <https://doi.org/10.1016/j.leukres.2008.08.010>.
- Boulanger E, Duprez R, Delabesse E, Gabarre J, Macintyre E, Gessain A. 2005. Mono/oligoclonal pattern of Kaposi sarcoma-associated herpesvirus (KSHV/HHV-8) episomes in primary effusion lymphoma cells. *Int J Cancer* 115:511–518. <https://doi.org/10.1002/ijc.20926>.
- Dollery SJ, Santiago-Crespo RJ, Chatterjee D, Berger EA. 2018. Glycoprotein K8.1A of Kaposi's sarcoma-associated herpesvirus is a critical B cell tropism determinant independent of its heparan sulfate binding activity. *J Virol* 93:e01876-18. <https://doi.org/10.1128/JVI.01876-18>.
- Luna RE, Zhou F, Baghian A, Chouljenko V, Forghani B, Gao S-J, Kousoulas KG. 2004. Kaposi's sarcoma-associated herpesvirus glycoprotein K8.1 is dispensable for virus entry. *J Virol* 78:6389–6398. <https://doi.org/10.1128/JVI.78.12.6389-6398.2004>.
- Gale NW, Holland SJ, Valenzuela DM, Flenniken A, Pan L, Ryan TE, Henkemeyer M, Strebhardt K, Hirai H, Wilkinson DG, Pawson T, Davis S, Yancopoulos GD. 1996. Eph receptors and ligands comprise two major specificity subclasses and are reciprocally compartmentalized during embryogenesis. *Neuron* 17:9–19. [https://doi.org/10.1016/S0896-6273\(00\)80276-7](https://doi.org/10.1016/S0896-6273(00)80276-7).
- Kumar B, Chandran B. 2016. KSHV entry and trafficking in target cells: hijacking of cell signal pathways, actin and membrane dynamics. *Viruses* 8:E305. <https://doi.org/10.3390/v8110305>.

33. Myoung J, Ganem D. 2011. Generation of a doxycycline-inducible KSHV producer cell line of endothelial origin: maintenance of tight latency with efficient reactivation upon induction. *J Virol Methods* 174:12–21. <https://doi.org/10.1016/j.jviromet.2011.03.012>.
34. Arvanitakis L, Mesri EA, Nador RG, Said JW, Asch AS, Knowles DM, Cesarman E. 1996. Establishment and characterization of a primary effusion (body cavity-based) lymphoma cell line (BC-3) harboring Kaposi's sarcoma-associated herpesvirus (KSHV/HHV-8) in the absence of Epstein-Barr virus. *Blood* 88:2648–2654.
35. Cannon JS, Ciuffo D, Hawkins AL, Griffin CA, Borowitz MJ, Hayward GS, Ambinder RF. 2000. A new primary effusion lymphoma-derived cell line yields a highly infectious Kaposi's sarcoma herpesvirus-containing supernatant. *J Virol* 74:10187–10193. <https://doi.org/10.1128/JVI.74.21.10187-10193.2000>.
36. Renne R, Zhong W, Herndier B, Mcgrath M, Abbey N, Kedes D, Ganem D. 1996. Lytic growth of Kaposi's sarcoma-associated herpesvirus (human herpesvirus 8) in culture. *Nat Med* 2:342–346. <https://doi.org/10.1038/nm0396-342>.
37. Sanjana NE, Shalem O, Zhang F. 2014. Improved vectors and genome-wide libraries for CRISPR screening. *Nat Methods* 11:783–784. <https://doi.org/10.1038/nmeth.3047>.
38. Hahn AS, Großkopf AK, Jungnickl D, Scholz B, Ensner A. 2016. Viral FGARAT homolog ORF75 of rhesus monkey rhadinovirus effects proteasomal degradation of the ND10 components SP100 and PML. *J Virol* 90:8013–8028. <https://doi.org/10.1128/JVI.01181-16>.
39. Longo PA, Kavran JM, Kim M-S, Leahy DJ. 2013. Transient mammalian cell transfection with polyethylenimine (PEI). *Methods Enzymol* 529: 227–240. <https://doi.org/10.1016/B978-0-12-418687-3.00018-5>.
40. Heigwer F, Kerr G, Boutros M. 2014. E-CRISP: fast CRISPR target site identification. *Nat Methods* 11:122–123. <https://doi.org/10.1038/nmeth.2812>.
41. Schmidt TGM, Batz L, Bonet L, Carl U, Holzapfel G, Kiem K, Matulewicz K, Niermeier D, Schuchardt I, Stanar K. 2013. Development of the twin-Strep-tag and its application for purification of recombinant proteins from cell culture supernatants. *Protein Expr Purif* 92:54–61. <https://doi.org/10.1016/j.pep.2013.08.021>.

Supplemental Data



Suppl. Figure S1. Gating strategy for scoring of KSHV infection in iSLK/BJAB cocultures. The percentage of GFP⁺ cells in the CD13⁻ CD20⁺ population is given for controls and one representative iSLK BAC16 KSHV wt/BJAB control or iSLK BAC16 KSHV wt/BJAB EPHA7^{KO} sample. Numbers in brackets represent event counts (CD13⁻ CD20⁺ GFP⁺ events/ CD13⁻ CD20⁺ events). It should be noted that the 'iSLK BAC16^{induced} w/o BJAB' control sample, which represents the assay background from e.g. spill-over, contained one CD13⁻ CD20⁺ GFP⁺ 'false positive' background event in 10 000 total events. The assay background amounts to no more than 1.54% (Figure 2B), 3.41% (Figure 2E, averaged over two independent experiments), 0% (Figure 3A) and 1.17% (Figure 3D) of the CD13⁻ CD20⁺ GFP⁺ population in any given sample in the respective experiments.

III.3 Publication 3: Plxdc family members are novel receptors for the rhesus monkey rhadinovirus (RRV)

BioRxiv (Preprint), Online: January 22, 2020

Author Contributions

Conceptualization: **Anna K. Großkopf**, Alexander S. Hahn
Formal analysis: **Anna K. Großkopf**, Alexander S. Hahn
*Data analysis of all Figures was performed by **Anna K. Großkopf** and reviewed by **Alexander S. Hahn**.*
Funding acquisition: Alexander S. Hahn
Investigation: **Anna K. Großkopf**, Sarah Schlagowski, Alexander S. Hahn
***Anna K. Großkopf:** designed and performed the experiments which led to the results in Fig 1B and C, Fig 2, Fig 3, Fig 4 and Fig 5; **Sarah Schlagowski:** prepared RRV stocks and cloned RRV gHΔ21-27-AELAAN and RRV gHΔ21-27^{rev9-4/10-3}; **Alexander S. Hahn:** designed and performed the experiments which led to the results in Fig 1A.*
Methodology: **Anna K. Großkopf**, Alexander S. Hahn
***Anna K. Großkopf:** designed experiments which led to the results in all Figures except Fig 1A; **Alexander S. Hahn:** designed experiments which led to the results in Fig 1A.*
Project administration: Alexander S. Hahn
Resources: Armin Ensser, Ronald C. Desrosiers
Supervision: Alexander S. Hahn
Visualization: **Anna K. Großkopf**
Writing - original draft: **Anna K. Großkopf**

The inability to completely abrogate KSHV and RRV infection by disruption of the interaction with described cellular host factors suggests the existence of additional, yet unidentified cellular receptors that play a role in rhadinoviral entry. Therefore, in this part of my thesis, I aimed to determine:

- 1) Whether we can identify additional receptors that interact with the rhadinoviral gH/gL complex or gH alone
- 2) If so, which domains or regions on gH mediate the interaction with identified receptors
- 3) Whether interactions with additional putative gH receptors are cell type-specific/ shape the rhadinoviral tropism

Using affinity enrichment followed by mass spectrometry, the family of Plexin domain containing proteins (Plxdc1/2) had been identified as novel interaction partners for the gH/gL complex of RRV, but not KSHV by Alexander Hahn in the laboratory of Ron Desrosiers. Using immunoprecipitation assays we characterized the binding specificities of the gH/gL complexes of isolates from the two defined RRV sequence groups²³⁵. While RRV isolate 17577 gH selectively binds to Plxdc1 in the

presence of gL, RRV 26-95 gH interacts with both Plxdc1 and Plxdc2, independently of gL. Blocking assays with soluble Plxdc2 decoy receptor demonstrated the functionality of the gH-Plxdc2 interaction on the virion. Ectopic overexpression of Plxdc1/2 further confirmed the importance of this interaction in the context of infection and verified Plxdc1/2 as a functional receptor for RRV 26-95. Furthermore, we could establish the independence of the Eph receptor and Plxdc receptor interaction by co-immunoprecipitation of gH/gL-Plxdc1/2-EphB3 complexes and blocking assays with soluble Plxdc2-Fc and EphB3-Fc.

We mapped the Plxdc-interaction motif to a seven/ six amino acid stretch on gH of RRV isolate 26-95/ isolate 17577 and characterized the amino acids which are crucial for the interaction in more detail. Deletion of this motif is sufficient to abrogate RRV 26-95 and RRV 17577 gH interaction with Plxdc1 and to de-target RRV 26-95 from Plxdc receptors in the context of infection.

We used RRV 26-95 recombinants, deleted in the seven amino Plxdc-interaction motif or mutated in the previously described Eph interaction motif (see Publication 1) to determine the contribution of the gH-Plxdc interaction to attachment and the cell line-specific infectivity of RRV 26-95. While RRV seems to be able to use both receptor families for the infection of adherent cell lines, we identified B cell lines which exhibit a preferential infection via interaction with either Plxdc receptors (namely MFB5487) or Eph receptors (Raji, MMB1845). Interestingly, even though Plxdc1 or Plxdc2 enhanced RRV 26-95 infection to similar levels upon ectopic overexpression, only Plxdc1 overexpression resulted in differences in the attachment efficiency of RRV 26-95 which could hint at differing functions of Plxdc1 and Plxdc2 in RRV infection and entry.

Plxdc family members are novel receptors for the rhesus monkey rhadinovirus (RRV)

Anna K. Großkopf¹, Sarah Schlagowski¹, Armin Ensser², Ronald C. Desrosiers³, Alexander S. Hahn¹

¹ German Primate Center - Leibniz Institute for Primate Research, Göttingen, Germany

² Universitätsklinikum Erlangen, Institute for Clinical and Molecular Virology, Erlangen, Germany

³ Miller School of Medicine, University of Miami, Miami, United States

ABSTRACT

The rhesus monkey rhadinovirus (RRV), a γ 2-herpesvirus of rhesus macaques, shares many biological features with the human pathogenic Kaposi's sarcoma-associated herpesvirus (KSHV). Both viruses, as well as the more distantly related Epstein-Barr virus, engage cellular receptors from the Eph family of receptor tyrosine kinases (Ephs). However, the importance of the Eph interaction for RRV entry varies between cell types suggesting the existence of Eph-independent entry pathways. We therefore aimed to identify additional cellular receptors for RRV by affinity enrichment and mass spectrometry. We identified an additional receptor family, the Plexin domain containing proteins 1 and 2 (Plxdc1/2) that bind the RRV gH/gL glycoprotein complex. *In vitro*, blocking assays with soluble Plxdc2 decoy receptor reduced RRV infection by approx. 60%, while overexpression of Plxdc1 and 2 dramatically enhanced RRV susceptibility in otherwise marginally permissive Raji cells. While the Plxdc2 interaction is conserved between two RRV strains, 26-95 and 17577, Plxdc1 specifically interacts with RRV 26-95 gH. The Plxdc interaction is mediated by a short motif at the N-terminus of RRV gH that is partially conserved between isolate 26-95 and isolate 17577, but absent in KSHV gH. Mutation of this motif abrogated the interaction with Plxdc1/2 in *in vitro* assays and reduced RRV infection in a cell-type specific manner. Taken together, our findings characterize Plxdc1/2 as novel interaction partners and entry receptors for RRV and support the concept of the N-terminal domain of the gammaherpesviral gH/gL complex as a multifunctional receptor-binding domain.

INTRODUCTION

The rhesus monkey rhadinovirus (RRV), a member of the genus γ 2-herpesvirus or rhadinovirus, is closely related to the only human pathogenic member of this genus, the Kaposi's sarcoma associated herpesvirus (KSHV) (1, 2). Due to the high similarity in both genome organization and biology RRV is considered as an animal model virus for KSHV (3) and has been used as such in various *in vitro* and *in*

vivo studies. Two major RRV sequence groups have been identified (4), which are represented by two cloned isolates, RRV 26-95 (5) and RRV 17577 (6). Analogous to KSHV infection, primary RRV infection is asymptomatic in healthy hosts and leads to life-long persistence, most likely in the B cell compartment (7). KSHV is associated with a solid tumor of endothelial origin, Kaposi's sarcoma (KS), and two B cell malignancies, primary effusion lymphoma (PEL) and the plasmablastic variant of multicentric Castleman's disease (MCD), most prominently in the context of human immunodeficiency virus (HIV) infection and in immunocompromised individuals. Similarly, simian immunodeficiency virus (SIV)-positive rhesus macaques developed B cell lymphomas upon experimental infection with RRV strain 17577 (8, 9) and several studies correlated RRV infection with lymphomagenesis in SIV/SHIV-infected animals (10, 11). While RRV is not consistently associated with solid malignancies, RRV has been identified in retroperitoneal fibromatosis tissue (9, 12), similar to retroperitoneal fibromatosis herpesvirus (RFHV)(11). Another shared characteristic of KSHV and RRV is the receptor usage on a range of cell types. Both viruses engage members of the Eph family of receptor tyrosine kinases (Ephs) through their glycoprotein (g)H/gL complex to facilitate entry into target cells. While KSHV preferentially interacts with A-type Ephs – specifically EphA2 as the high affinity receptor (13, 14) – RRV can utilize both A- and B-type Ephs (14) for entry. These interactions have been characterized on different adherent cells types (6–9) and we could recently show that both viruses can utilize EphA7 as receptor on BJAB cells (19), a model B lymphocyte line. While for KSHV, in addition to Eph family receptors, several membrane proteins have been proposed as cellular receptors for different viral glycoproteins mediating either attachment or entry on a range of target cells (reviewed in (20)) the receptor usage of RRV is comparatively less well characterized. Nevertheless, studies using receptor knock-down, receptor- and ligand-mediated blocking, and Eph de-targeted virus mutants (21) showed that both viruses can infect various cells independently of the Eph-interaction, which suggests that RRV engages at least one additional entry receptor that can functionally substitute for the Eph-interaction. This notion is also supported by a recent *in vivo* study that demonstrated that an RRV mutant deleted of gL and therefore unable to interact with Eph receptors still establishes persistent infection in RRV-naïve rhesus macaques upon intravenous inoculation (22). We therefore aimed to identify additional rhadinovirus receptors that bind the gH/gL complex or gH and identified Plexin domain containing protein 2 (Plxdc2) as novel interaction partner of the gH/gL complex of RRV, but not KSHV. The closest homolog to Plxdc2, Plxdc1 was initially identified as overexpressed in blood vessels of solid human tumors (23), resulting in the original terminology tumor endothelial marker 7 (TEM7, Plxdc1) and tumor endothelial marker 7 related (TEM7R, Plxdc2) (24). In general, the physiological functions of Plxdc1/2 are not well understood. Suggestive of a role in development, Plxdc2 has been described as mitogen for neural progenitor cells (25) and expression of both Plxdc1 and Plxdc2 in the developing nervous system has

been demonstrated (26, 27). Cortactin, nidogen and the pigment epithelium derived factor (PEDF) have been described as interactors for Plxdc1 and Plxdc2 (28–30). However, the physiological relevance of these interactions is not fully understood. In this study we characterize the interaction of Plxdc1/2 with the gH/gL glycoprotein complex of RRV and establish Plxdcs as novel cellular RRV entry receptors.

RESULTS

To identify potential cellular receptors for RRV glycoprotein H, we performed immunoprecipitation using soluble RRV 26-95 gH, consisting of the extracellular part fused to the Fc part of human IgG (RRV gH-FcStrep) as bait and 293T whole cell lysate as prey (Fig 1A). Bands present in the precipitation from 293T whole cell lysate, but not in control precipitation without 293T lysate were excised and analyzed by LC-MS/MS. The most abundant cell surface protein, identified in four of the five analyzed regions, was Plxdc2 or TEM7R, a cellular transmembrane protein. As described above, Plxdc1 or TEM7 is the only homolog of Plxdc2 in humans and rhesus macaques, and was therefore included in subsequent analyses. Human and rhesus Plxdc1 (ref |NM_020405.5|; ref |XM_028836436.1|) and Plxdc2 (ref |NM_032812.9|; ref |XM_028826043.1|) are 96.80% and 97.92% identical on the amino sequence level.

Co-immunoprecipitation of V5-tagged expression constructs of gH from KSHV and from the two RRV isolates 26-95 and 17577, in the presence or absence of the corresponding Flag-tagged gL proteins with myc-tagged human Plxdc1 or Plxdc2 (hPlxdc1-myc/ hPlxdc2-myc) from transfected 293T cells confirmed the interaction of both RRV gH/gL complexes with Plxdc2 (Fig 1B). Neither KSHV gH/gL nor RRV 17577 gH/gL interacted detectably with Plxdc1-myc, while RRV 26-95 prominently bound both Plxdc1 and Plxdc2 in the presence and absence of gL.

To evaluate the effect of Plxdc-binding to RRV gH on the interaction with EphB3, the high-affinity Eph family receptor for RRV gH/gL (14), we used soluble human Plxdc1 or Plxdc2, consisting of the extracellular part of Plxdc1 or Plxdc2 fused to the Fc part of human IgG followed by a TwinStrep tag (hPlxdc1-FcStrep/ hPlxdc2-FcStrep) in immunoprecipitation experiments. Co-immunoprecipitation of hPlxdc1-FcStrep/ hPlxdc2-FcStrep with the gH-V5/gL-Flag complexes of RRV isolates 26-95 and 17577 in the presence or absence of myc-tagged EphB3 from transfected 293T cells demonstrated the existence of a quaternary complex, indicating the ability of RRV gH/gL to interact with members of both receptor families simultaneously (Fig 1C).

While interaction in transfected cell lysates is strongly suggestive of a functional interaction, the biologically relevant interaction for the entry process would occur with virion gH/gL. To evaluate

the functionality of the gH/gL – Plxdc interaction on virus particles both for wildtype RRV and an Eph-binding-negative RRV mutant, we utilized RRV-YFP, an RRV 26-95 strain engineered for constitutive YFP expression upon infection, and RRV-YFP gH-AELAAN, an Eph-binding-negative RRV-YFP mutant that we had previously described (Fig 2A) (21). To analyze the impact of competition with soluble Plxdc decoy receptor, RRV-YFP and RRV-YFP gH-AELAAN preparations were incubated with a concentration series of soluble hPlxdc2-FcStrep or an FcStrep control prior to infection of HaCaT cells (Fig 2B). According to RNA-Seq data of 36 cell lines (Courtesy of Human Protein Atlas, www.proteinatlas.org, (31)), HaCaT cells exhibit the highest cell-line specific expression of Plxdc2 among the analyzed non-cancer cell lines and were therefore chosen for further analyses. Soluble Plxdc2-FcStrep inhibited RRV-YFP wt infection up to approx. 60% in a dose dependent manner when compared to FcStrep alone. Likewise, preincubation of RRV-YFP gH-AELAAN with hPlxdc2-FcStrep reduced infection by approx. 65%. RRV wt and RRV gH-AELAAN infection was normalized to approx. MOI 0.2. Inhibition of the gH/gL-Eph interaction, which served as control, lead to an approx. 50% reduction of RRV wt infection at a concentration of 10nM hEphB3-Fc while 100nM of soluble hPlxdc2-FcStrep exhibited a similar blocking efficiency. Preincubation with both hEphB3-Fc and hPlxdc2-FcStrep further reduced RRV wt infection on HaCaT cells, when compared to preincubation with either hEphB3-Fc or hPlxdc2-FcStrep alone (Fig 2C). While preincubation with EphB3-Fc did not reduce RRV gH-AELAAN infection, preincubation with either hPlxdc2-FcStrep or a combination of hPlxdc2-FcStrep and hEphB3-Fc reduced infection by approx. 50% as observed for RRV wt infection (Fig 2C). Infection of SLK cells and rhesus monkey fibroblasts was also slightly decreased by preincubation of the viral inoculum with hPlxdc2-FcStrep, infection of SLK by RRV-YFP wt to $63.5\% \pm 3.7\%$ and infection of RF by RRV-YFP wt to $73.9\% \pm 11.3\%$ relative to preincubation with FcStrep as control. However, this effect was less pronounced than on HaCaT and less pronounced than the effect of hPlxdc2-FcStrep on RRV gH-AELAAN infection of the same cell types (Fig 2D). Taken together, the immunoprecipitation and blocking experiments confirm the independence of the gH-Plxdc interaction of the previously described Eph-interaction motif (21) and EphB3-binding.

To establish receptor function, we performed gain-of-function experiments using ectopic Plxdc1/2 overexpression. Raji cells were transduced with lentiviruses encoding TwinStrep-tagged human Plxdc1/2 constructs (hPlxdc1-Strep/ hPlxdc2-Strep). The EBV-positive, human lymphoblast cell line only allows for low-level RRV 26-95 infection even with amounts of input virus corresponding to high MOI on adherent cells like SLK, HaCaT or RF. Therefore, changes in susceptibility to infection, mediated by Plxdc1/2 overexpression should be readily detectable and allow for a clear differentiation of the contribution of Plxdc1/2 to RRV infection over the very low intrinsic susceptibility to infection. Indeed, ectopic expression of hPlxdc1/2-Strep increased RRV-YFP wt and RRV-YFP gH-AELAAN infection 40 to 60-fold from approx. 0.5% basal infection dependent on the

expression plasmid and RRV strain (Fig 2E, G). However, we did not observe pronounced differences in effects mediated by hPlxdc1-Strep or hPlxdc2-Strep, indicating no clear Plxdc receptor preference of RRV 26-95.

In a next step we characterized the Plxdc binding motif on RRV gH. As the RRV 17577 gH-Plxdc2 interaction depends on gL whereas the RRV 26-95 gH-Plxdc2 interaction does not, we focused on the N-terminal domain I of gH which, in analogy to EBV gH/gL (32), most likely constitutes the gL-binding interface. The differences in the Plxdc interaction of RRV isolates 26-95 and 17577 as well as the lack of Plxdc – KSHV gH/gL interaction suggested a motif that is only partially conserved between the RRV isolates but missing in KSHV. Using sequence comparisons (Fig 3A) we identified a putative interaction motif spanning 7 or 6 amino acid motif in the N-terminal region of RRV 26-95 gH and RRV 17577 gH, respectively, that is not conserved in KSHV gH. The motif is located close to the Eph-interaction motif we described previously, facing in the opposite direction in a homology model of the RRV 26-95 gH/gL complex based on the EBV gH/gL crystal structure (3PHF) (Fig 3B). Deletion of this motif completely abrogated the gH/gL interaction with Plxdcs of both RRV 26-95 (Fig 3C) and RRV 17577 (Fig 3D). To further characterize the contribution of individual residues in the ‘Tyr(Y)-Glu(E)-Tyr(Y)-Asn(N)-Glu(E)-Glu(E)-Lys(K)’ (RRV 26-95) motif we performed single amino acid substitutions to alanine. The ability of mutant RRV 26-95 gH-V5 to bind myc-tagged Plxdc1/2 of human (hPlxdc1/2-myc) (Fig 3E) or rhesus macaque origin (mmPlxdc1/2-myc) (Fig 3F) was analyzed by immunoprecipitation of gH via the V5-tag and Western blot. While several single amino acid substitutions decreased the interaction of RRV gH with Plxdcs to some degree, residues Tyr23 and Glu25 that are conserved in isolates 26-95 and 17577 appear to be critical for the interaction of gH with human and rhesus macaque Plxdc1 and Plxdc2. Furthermore, substitution of glutamate with alanine at position 22, which is not conserved between isolates 26-95 and 17577, had a pronounced, albeit slightly weaker effect on the gH-Plxdc1/2 interaction (Fig 3E, F).

To further analyze the contribution of the gH/gL – Plxdc interaction in the context of infection we constructed virus mutants deleted in the seven amino acid interaction motif in the background of RRV-YFP 26-95 wildtype (RRV gH Δ 21-27), and in the background of an RRV-YFP 26-95 strain mutated in the Eph-interaction motif described previously by our group (RRV gH-AELAAN, RRV gH Δ 21-27-AELAAN) using a two-step, lambda red-mediated recombination system (33) (Fig 4A). Blocking experiments using soluble hPlxdc2-FcStrep decoy receptor on HaCaT cells confirmed that deletion of the seven amino acid motif was sufficient to abrogate the gH-Plxdc2 interaction on viral particles (Fig 4B). While infection of RRV wt and RRV gH-AELAAN was inhibited by approx. 60% to 70% respectively, infection of RRV gH Δ 21-27 and RRV gH Δ 21-27-AELAAN was not affected even by high concentrations of soluble hPlxdc2-FcStrep (Fig 4B). All infections were carried out at approx. MOI

0.05. Analogously, the Eph- or Plxdc-receptor-binding-negative RRV mutants were no longer inhibited by preincubation with the respective soluble receptor (hEphB3-Fc or hPlxdc2-FcStrep) in single or double inhibition experiments on HaCaT cells (Fig 4C). The receptor-specificity conveyed by the respective interaction motif was further analyzed in lentiviral vector-mediated Plxdc1/2-Strep overexpression experiments in Raji B lymphocytes. EphA7, which had previously been described by our group to be critical for RRV infection of BJAB B lymphocytes, was used as control for Eph-mediated infection. Expression of Plxdc1/2-Strep as well as EphA7-Strep dramatically enhanced susceptibility of Raji cells (Fig 4D, E). RRV-YFP wt infection increased from $0.14 \pm 0.04\%$ on empty vector transduced Raji cells to approx. 8.5% upon EphA7 overexpression and to approx. 17% upon Plxdc1/2 overexpression, without pronounced differences between the Plxdc family members. Mutation of the Eph-interaction motif in RRV-YFP gH-AELAAN completely abrogated the gain in susceptibility on EphA7 overexpressing cells while mutation of the Plxdc-interaction motif completely abrogated the gain in susceptibility on Plxdc1/2 overexpressing cells, confirming selective knockout of each individual receptor interaction in the respective mutant. Furthermore, deletion of the Eph-interaction motif in RRV-YFP gH-AELAAN did not impact the infection of Plxdc1/2 overexpressing cells in comparison to RRV-YFP wt infection. In contrast, we observed an approx. 2-fold higher infection of RRV-YFP gH Δ 21-27 on EphA7 overexpression cells, when compared to RRV-YFP wt. Together, the blocking and overexpression experiments indicate an independent rather than cooperative nature of Eph and Plxdc receptor function.

To quantitatively analyze the contribution of the Plxdc1/2-interaction to RRV infection of different cell types, RRV-YFP wt and RRV-YFP receptor binding mutant inocula were normalized to genome copies as determined by qPCR, and target cells were inoculated with the same number of encapsidated input virus genomes for wt and each mutant virus strain in an MOI range of 0.05 to 1 on adherent cells. Infection as determined by the percentage of YFP+ cells was normalized to RRV wt, which was set to 1. For suspension cell lines, experiments with RRV wt infection over 1% were included in the analysis. Four (three for RF, five for MFB5487) independent sets of RRV wt and mutant stocks were used to compensate for variability in stock preparation. None of the analyzed adherent cell lines showed a preferential use of Plxdc receptors over Eph receptors based on the reduction of specific infectivity of Eph-binding and Plxdc-interaction-deficient mutants (Fig 5A). On rhesus monkey fibroblasts (RF), compared to RRV-YFP, RRV-YFP gH Δ 21-27, RRV-YFP gH-AELAAN and RRV-YFP gH Δ 21-27-AELAAN exhibited a decrease in infection of approx. 30%, 50% and 70%, respectively. Similarly on HaCaT, infection with RRV-YFP gH-AELAAN and RRV-YFP gH Δ 21-27-AELAAN was reduced by approx. 60% and 75%, respectively, compared to RRV-YFP. While RRV-YFP gH Δ 21-27 exhibited a defect, comparable to RRV-YFP gH-AELAAN in three of the analyzed independent sets of RRV stocks, this reduction in infectivity did not reach significance due to one outlier. On SLK cells,

mutation of the Eph-interaction motif led to an approx. 65% decrease in infection, while RRV-YFP gHΔ21-27 infection was on average comparable to RRV-YFP infection. In contrast, we identified B lymphocyte lines of human and macaque origin that exhibit a preference in the receptor usage for either Eph or Plxdc family members (Fig 5B). When normalized to genome copies, RRV-YFP gHΔ21-27 infection on human Raji lymphoblasts was comparable to RRV wt infection while mutation of the Eph-interaction motif led to an approx. 90% decrease in infection, indicating preferential infection through Eph family receptors. Similarly, RRV-YFP gHΔ21-27 exhibited only a minor defect (approx. 20% reduced infection) on immortalized B lymphocytes of macaca mulatta origin (MMB1845) that did not reach significance, while infection with RRV-YFP gH-AELAAN and gHΔ21-27-AELAAN was reduced by approx. 90% in comparison to RRV-YFP, again indicating preferential infection through Eph family receptors. Conversely, deletion of the Plxdc-interaction motif decreased infection of a B lymphocyte cell line of macaca fascicularis origin (MFB5487) by approx. 75% whereas RRV-YFP gH-AELAAN exhibited an approx. 50% defect, indicating preferential use of the Plxdc interaction for infection of MFB5487 by RRV. Mutation of both the Eph- and Plxdc-interaction motif led to an even more pronounced defect of approx. 90%.

To evaluate the contribution of potential attachment effects on the observed differences in specific infectivity, we analyzed the capacity of virions to bind Plxdc1/2 overexpressing Raji cells in comparison to empty vector transduced Raji cells (Fig 5C, D). The ratio of cell-bound viral DNA to input genomes was used as a surrogate marker for virus attachment. Mutation of the Plxdc- and Eph-interaction motif had no detectable effect on attachment to control vector-transduced and Plxdc2-overexpressing Raji cells. In contrast, Raji cells overexpressing Plxdc1 showed increased attachment of RRV-YFP 26-95 and RRV-YFP 26-95 gH-AELAAN, while attachment of Plxdc-interaction negative RRV-YFP 26-95 mutants gHΔ21-27 and gHΔ21-27-AELAAN was not enhanced and remained comparable to empty vector control and Plxdc2-overexpressing cells.

To exclude effects of potential offsite genomic rearrangements in RRV-YFP 26-95 gHΔ21-27 we created two independent revertants (RRV 26-95 gHΔ21-27^{rev9-4} and RRV 26-95 gHΔ21-27^{rev10-3}). Restoration of the residues deleted in RRV-YFP 26-95 gHΔ21-27 restored infection on hPlxdc1/2-transduced Raji, MFB5487 and HaCaT cells to RRV wt levels, with no pronounced differences between RRV wt, RRV 26-95 gHΔ21-27^{rev9-4} and RRV 26-95 gHΔ21-27^{rev10-3} (Fig 5E). Similar to the approx. 11-fold increase of RRV wt infection upon hPlxdc1/2 overexpression, infection with RRV gHΔ21-27 revertants increased from $2.00 \pm 0.30\%$ ($2.54 \pm 0.29\%$) on empty vector transduced Raji cells to $35.25 \pm 1.21\%$ ($36.99 \pm 0.39\%$) and $37.27 \pm 0.68\%$ ($43.00 \pm 0.99\%$) upon hPlxdc1 and hPlxdc2 overexpression for RRV 26-95 gHΔ21-27^{rev9-4} (RRV 26-95 gHΔ21-27^{rev10-3}) respectively (Fig 5E).

DISCUSSION

In this study we identified the Plexin domain containing proteins 1 and 2 as a novel family of entry receptors for RRV. Plxdc1/2 interact with the gH/gL complex of RRV in a region close to the previously characterized binding motif for Eph receptors. While the Eph-interaction as well as the critical Eph binding motif in domain I of gH is conserved between RRV and the closely related human pathogenic KSHV (21), the interaction with Plxdc1/2 is exclusive to RRV and even exhibits differences between isolates 26-95 and 17577 as prototypic members of the described RRV sequence clades.

According to our results, differences between Plxdc1 and Plxdc2 may also exist in terms of function. While overexpression of both Plxdc1 and Plxdc2 in Raji cells, that were virtually “non-susceptible” under the conditions used, lead to robust RRV 26-95 infection (Fig 4D-E), only overexpression of Plxdc1 enhanced attachment of RRV wt and RRV gH-AELAAN in comparison to either non-transduced Raji cells or Plxdc-binding deficient RRV mutants (Fig 5D). Whether this is primarily due to differences in expression levels, consistently observed between Plxdc1 and Plxdc2 upon lentiviral overexpression or due to underlying functional differences in the gH interaction with these molecules remains to be determined.

Mutation of residues Tyr23 and Glu25 in gH domain I which are conserved between RRV isolate 26-95 and 17577 almost abolished the interaction with Plxdc2, which is bound by gH/gL of both isolates. Although the same residues are critical for the interaction of RRV gH 26-95 with Plxdc1, the partial conservation of the region appears to be insufficient to confer binding of 17577 gH to Plxdc1. Interestingly, the interaction of 17577 gH with Plxdc2 is dependent on the presence of gL in the gH/gL complex, whereas 26-95 gH is able to bind Plxdc1/2 independent of gL. These features of Plxdc1/2 binding specificities appear similar to the interaction of the gH/gL complex with Eph receptors, wherein mutation of the strictly conserved Eph interaction motif is sufficient to abrogate receptor binding, but differences in KSHV and RRV affinities for A- and B-type Eph RTKs indicate the existence of additional regions in gH or gL that contribute to or modulate the interaction. Whether these preferences for different members of conserved receptor families also influence e.g. cell or tissue tropism, viral spread or pathogenicity has not been determined. Sequence comparisons of over twenty RRV isolates identified dramatic differences in the extracellular domains of gH as well as in gL between isolates that fell in two discrete groupings either similar to 26-95 or 17577, while variation in other glycoproteins R1, gM, gN, orf68 was minimal between clades (4). However, if these clade-specific glycoprotein variations influence the observed differences in pathogenicity between RRV strains 26-95 and 17577 remains to be seen. Another interesting question would be if the receptor-binding function of the N-terminal region of gH is conserved between RRV and KSHV, and probably EBV, and whether KSHV and EBV can bind another receptor through this region. So far, we

273 did not to identify corresponding interactions for KSHV, but in principle the region of gH is present in
274 both viruses and it is tempting to assume some functional conservation.

275 Along those lines, the evolutionary factors that drive interaction with different receptor
276 families and the resulting multitude of herpesvirus–receptor interactions is highly interesting. For e.g.
277 EBV and HCMV, a clear correlation between receptor usage, dependent on viral interaction partners
278 of the gH/gL complex, and cell tropism has been demonstrated in various studies ((34), reviewed in
279 (35)). However, for rhadinoviruses, the picture is less clear. Even though we could show that RRV
280 infection of select cell lines exhibited a dependence on specific receptors, e.g. Raji infection was
281 dependent on the gH/gL – Eph interaction, MFB5487 infection was more dependent on the Plxdc-
282 interaction (Fig 5) and similarly mutation of the Eph-interaction motif did not impact infection on all
283 cell types equivalently (21), a definite correlation between exclusive receptor usage and infection of
284 specific cell types is still missing. While the notion of a role of different receptor interactions in KSHV
285 and RRV cell and tissue tropism is tempting, the possibility of a redundant function should not be
286 discarded. Redundancy could be driven by the need to escape antibodies e.g. to one receptor binding
287 site. For instance, *in vitro* infection of human keratinocytes or rhesus fibroblasts seemed to be
288 impacted to a similar degree by either deletion of the Eph- or of the Plxdc-interaction motif (Fig 5).
289 To ultimately address the correlation between receptor- and tissue-tropism, *in vivo* studies using
290 receptor-de-targeted mutants to analyze cell and tissue tropisms will be required. The importance of
291 *in vivo* studies is also supported by a recent report that showed that a gL-null RRV mutant still
292 established persistent infection in the B cell compartment upon intravenous inoculation, while
293 infection of B cells *in vitro* was drastically reduced (22), a finding that could be explained by the gL-
294 independent usage of Plxdc1/2 for B cell infection *in vivo*.

295 On a more speculative note, the apparent overlap between virus receptors and tumor-
296 associated membrane proteins may represent an interesting research subject. Eph receptors were
297 first identified in an attempt to characterize tyrosine kinases involved in cancer (36) and altered
298 expression in various cancer types has been demonstrated for several Eph family members (reviewed
299 in (37)). Similarly, Plxdc1 was first described in a screen for novel tumor endothelial members (23)
300 and expression of both Plxdc1 and Plxdc2 is elevated in the endothelium of solid tumors (23, 24, 38,
301 39). Plxdc1 expression has been described as prognostic marker and modulating factor for various
302 human cancers (38–42). Given the similarity in changes of e.g. metabolic, transcriptional, and
303 signaling networks in cancer cells and upon virus infection it is not unlikely that either elevated
304 expression or signaling of these molecules is favorable for both virus infection and cancer
305 progression.

FIGURES

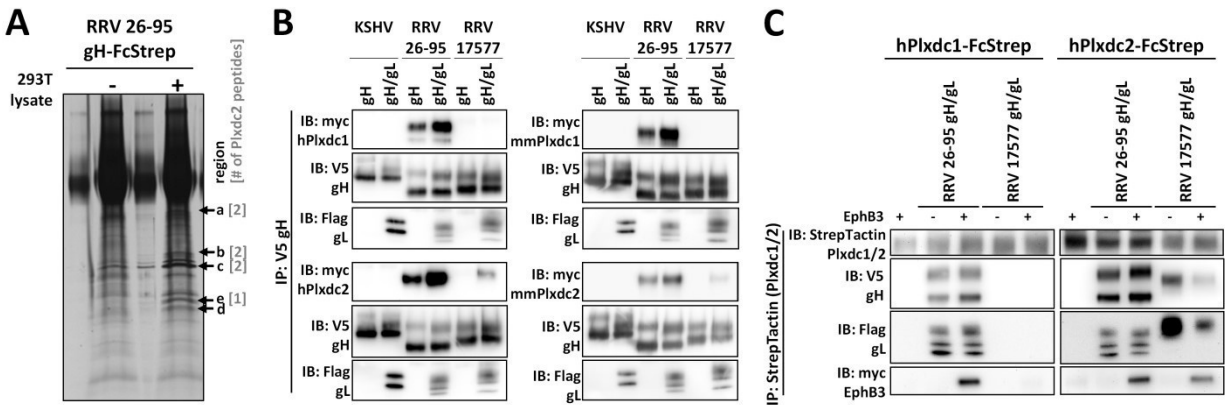


Figure 1 Plxdc family receptors are novel interaction partners for the RRV gH/gL. **A)** Immunoprecipitation of recombinant soluble RRV 26-95 gH-FcStrep in the presence or absence of 293T lysate. Precipitates were analyzed by PAGE, silver stained and bands at the indicated molecular weight (arrows, regions a-d) were excised and analyzed by mass spectrometry. Numbers in brackets indicate the number of Plxdc2 peptides identified by LC-MS/MS in each region. **B)** V5-tagged RRV 26-95 gH, RRV 17577 gH or KSHV gH alone or co-expressed with the respective Flag-tagged gL construct were immunoprecipitated in the presence of full-length Plxdc1 or Plxdc2 from human (h) or macaca mulatta (mm) origin using monoclonal antibody to the V5-tag. Precipitates were analyzed by Western blot with the indicated antibodies. **C)** Co-immunoprecipitation of soluble human Plxdc1-FcStrep or human Plxdc2-FcStrep with RRV 26-95 gH-V5/gL-Flag or RRV 17577 gH-V5/gL-Flag using StrepTactin Sepharose in the presence or absence of human full-length EphB3. Abbreviations: IP: immunoprecipitation, IB: immunoblotting, h: human, mm: macaca mulatta (rhesus macaque).

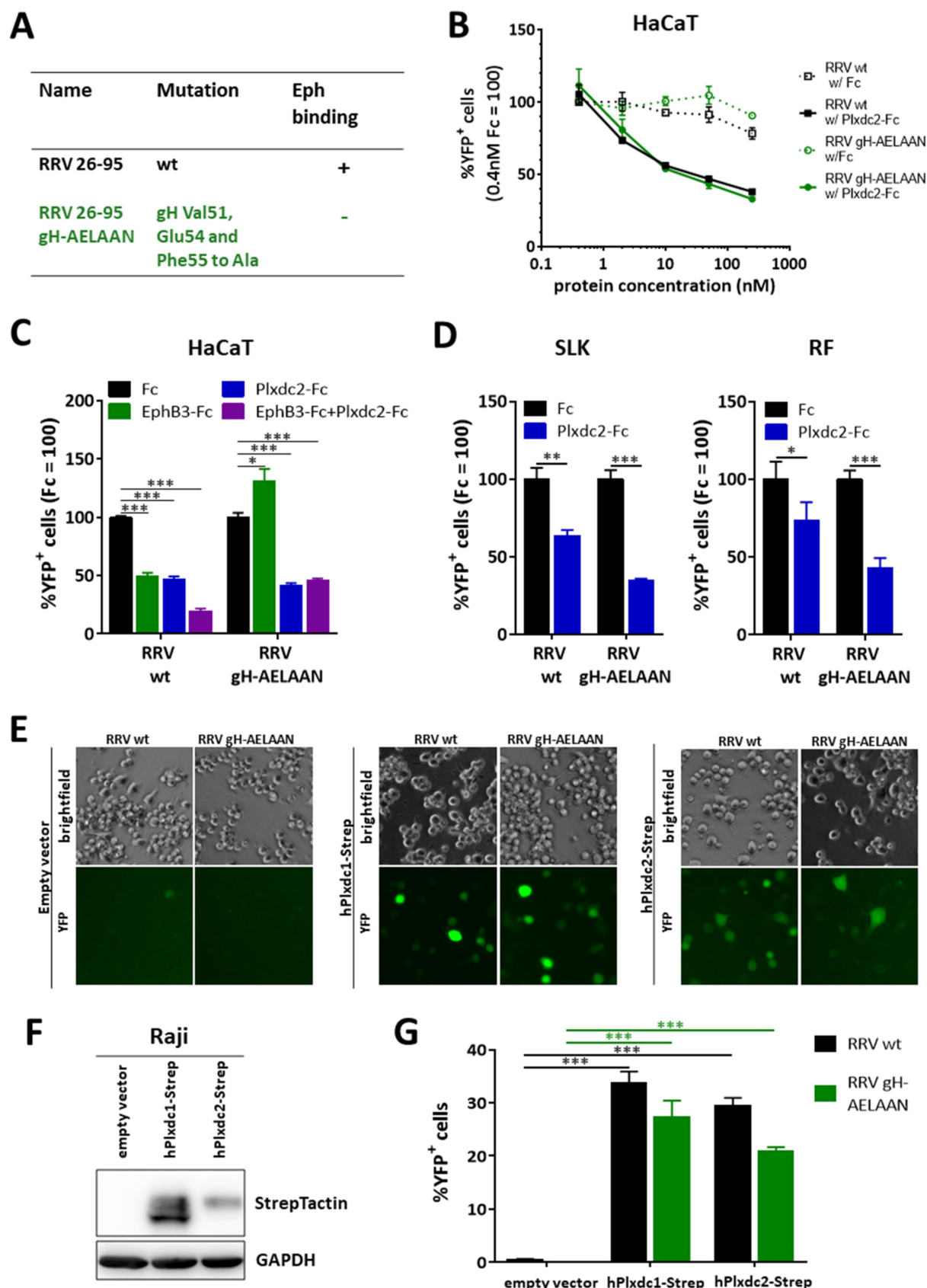


Figure 2 Plxdc1/2 function as entry receptors for RRV. **A)** List of BAC-derived recombinant viruses and introduced mutations used in this figure. **B)** Dose-dependent inhibition of RRV 26-95 infection by soluble human Plxdc2-FcStrep on HaCaT cells. RRV-YFP 26-95 wt and RRV-YFP 26-95 gH-AELAAN were pre-incubated with hPlxdc2-FcStrep for 30min at room temperature. FcStrep alone was used as

control. YFP expression as indicator of infection was measured by flow cytometry. Infection in the presence of 0.4nM FcStrep was set to 100% (MOI ~0.2, triplicates, error bars represent SD). **C)** Inhibition of RRV 26-95 infection by soluble Plxdc2-Fc and EphB3-Fc on HaCaT cells. RRV-YFP 26-95 wt and RRV-YFP 26-95 gH-AELAAN were pre-incubated with 100nM hPlxdc2-FcStrep, 10nM EphB3-Fc or a combination of 100nM hPlxdc2-FcStrep and 10nM EphB3-Fc for 30min at room temperature. FcStrep alone was used as control. YFP expression as indicator of infection was measured by flow cytometry. Infection with FcStrep was set to 100% (MOI ~0.2, triplicates, error bars represent SD). **D)** Inhibition of RRV 26-95 infection by soluble human Plxdc2-FcStrep on SLK cells and rhesus fibroblasts. RRV-YFP 26-95 wt and RRV-YFP 26-95 gH-AELAAN were pre-incubated with 250nM hPlxdc2-FcStrep for 30min at room temperature. FcStrep alone was used as control. YFP expression as indicator of infection was measured by flow cytometry. Infection with FcStrep was set to 100% (MOI ~0.05-0.1, triplicates, error bars represent SD). **E)** Raji cells were transduced with TwinStrep-tagged human Plxdc1 and Plxdc2 (hPlxdc1-Strep/ hPlxdc2-Strep) expression constructs or an empty vector control, briefly selected and infected with RRV-YFP 26-95 wt or RRV-YFP 26-95 gH-AELAAN normalized to genome copies as determined by qPCR. Micrographs show representative infection of the indicated cell pools. **F)** Lysates of transduced Raji cell pools were analyzed for Plxdc1/2-Strep expression by Western blot. **G)** Quantification of (E) by flow cytometric analyses of YFP reporter gene expression as indicator of infection.

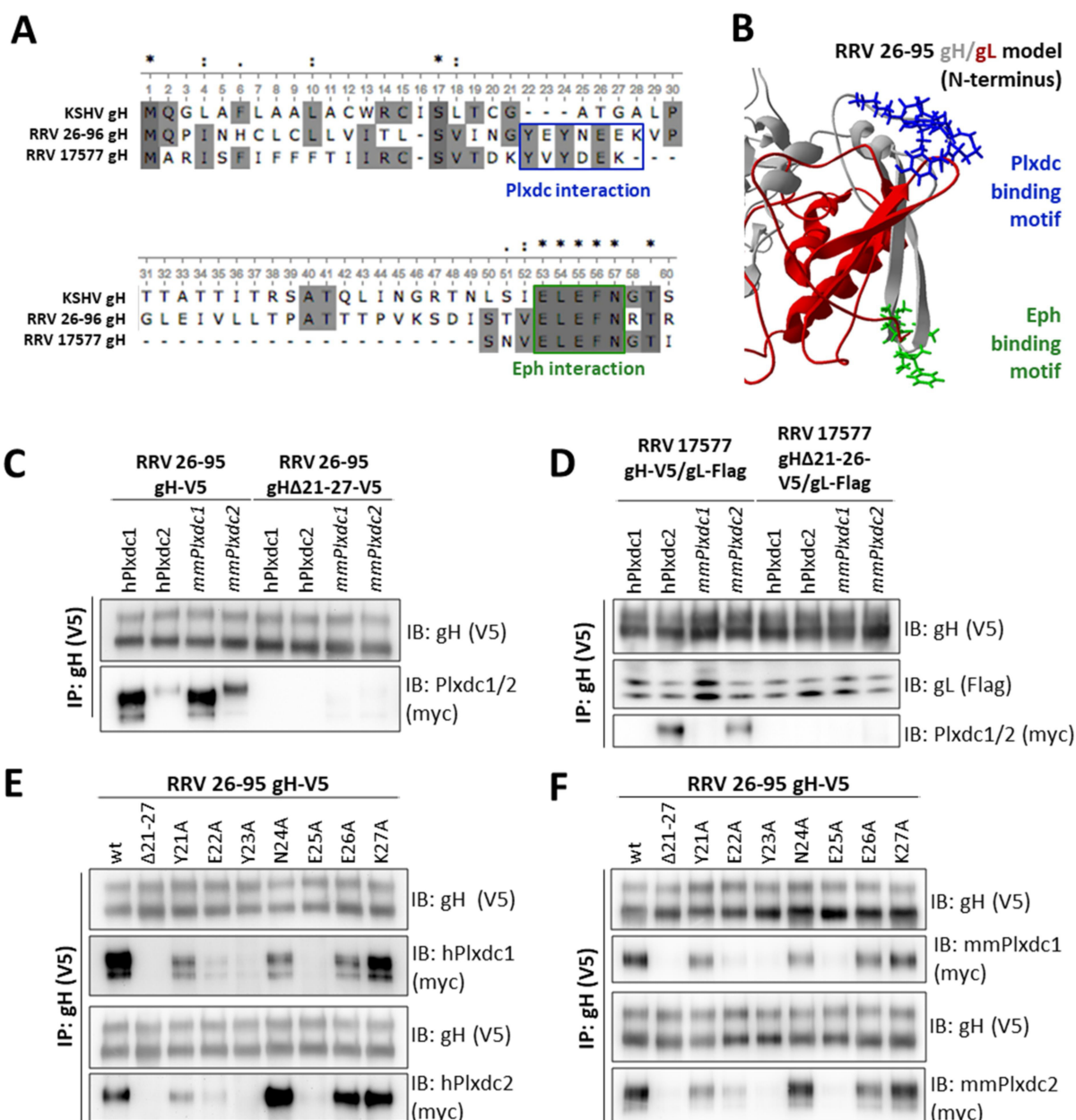


Figure 3 An amino acid sequence motif in the N-terminal region of RRV 26-95 and RRV 17577 gH is essential for the Plxdc-interaction. **A)** Multiple sequence alignment of the N-terminal region of gH of KSHV and the two RRV isolates 26-95 and 17577. Boxes indicate the binding motives for Eph receptors (green) and Plxdc receptors (blue). **B)** Homology-based structure prediction of the RRV 26-95 gH/gL complex based on the crystal structure of the EBV gH/gL complex (PDB number 3PHF) using the Iterative Threading ASSEMBLY Refinement (I-TASSER) server and the CO-THreader (COTH) algorithms for protein-protein complex structure and multi-chain protein threading. The Eph receptor interaction motif is shown in green, the Plxdc interaction motif is shown in blue, gL is shown in red, gH is shown in grey. **C)** Deletion of the Plxdc-interaction motif in RRV 26-95 gH (amino acid 21-27, "YEYNEEK") abrogates gH interaction with Plxdc1 and Plxdc2. V5-tagged gH wt or gHΔ21-27 were immunoprecipitated in the presence of full-length human or macaca mulatta Plxdc1-myc or Plxdc2-myc using monoclonal antibody to the V5-tag. Precipitates were analyzed by Western blot. **D)** Deletion of the Plxdc-interaction motif in RRV 17577 gH (amino acid 21-26, "YVYDEK") abrogates gH interaction with Plxdc2. V5-tagged gH wt or gHΔ21-26 was co-expressed with Flag-tagged RRV 17577 gL. gH-V5/gL-Flag complexes were immunoprecipitated in the presence of full-length human or macaca mulatta Plxdc1-myc or Plxdc2-myc using monoclonal antibody to the V5-tag. Precipitates were analyzed by Western blot. **E)** Mutational scan of Plxdc-interaction motif (amino acid 21-27,

“YEYNEEK”) of RRV 26-95 gH identifies human Plxdc1/2-interacting residues. V5-tagged gH mutants were immunoprecipitated in the presence of full-length human Plxdc1-myc or Plxdc2-myc using monoclonal antibody to the V5-tag. Precipitates were analyzed by Western blot. RRV gHΔ21-27 serves as negative control. **F)** Mutational scan of Plxdc-interaction motif (amino acid 21-27, “YEYNEEK”) of RRV 26-95 gH identifies rhesus macaque Plxdc1/2-interacting residues. V5-tagged gH mutants were immunoprecipitated in the presence of full-length human Plxdc1-myc or Plxdc2-myc using monoclonal antibody to the V5-tag. Precipitates were analyzed by Western blot. RRV gHΔ21-27 serves as negative control. Abbreviations: IP: immunoprecipitation, IB: immunoblotting, h: human, mm: macaca mulatta (rhesus macaque).

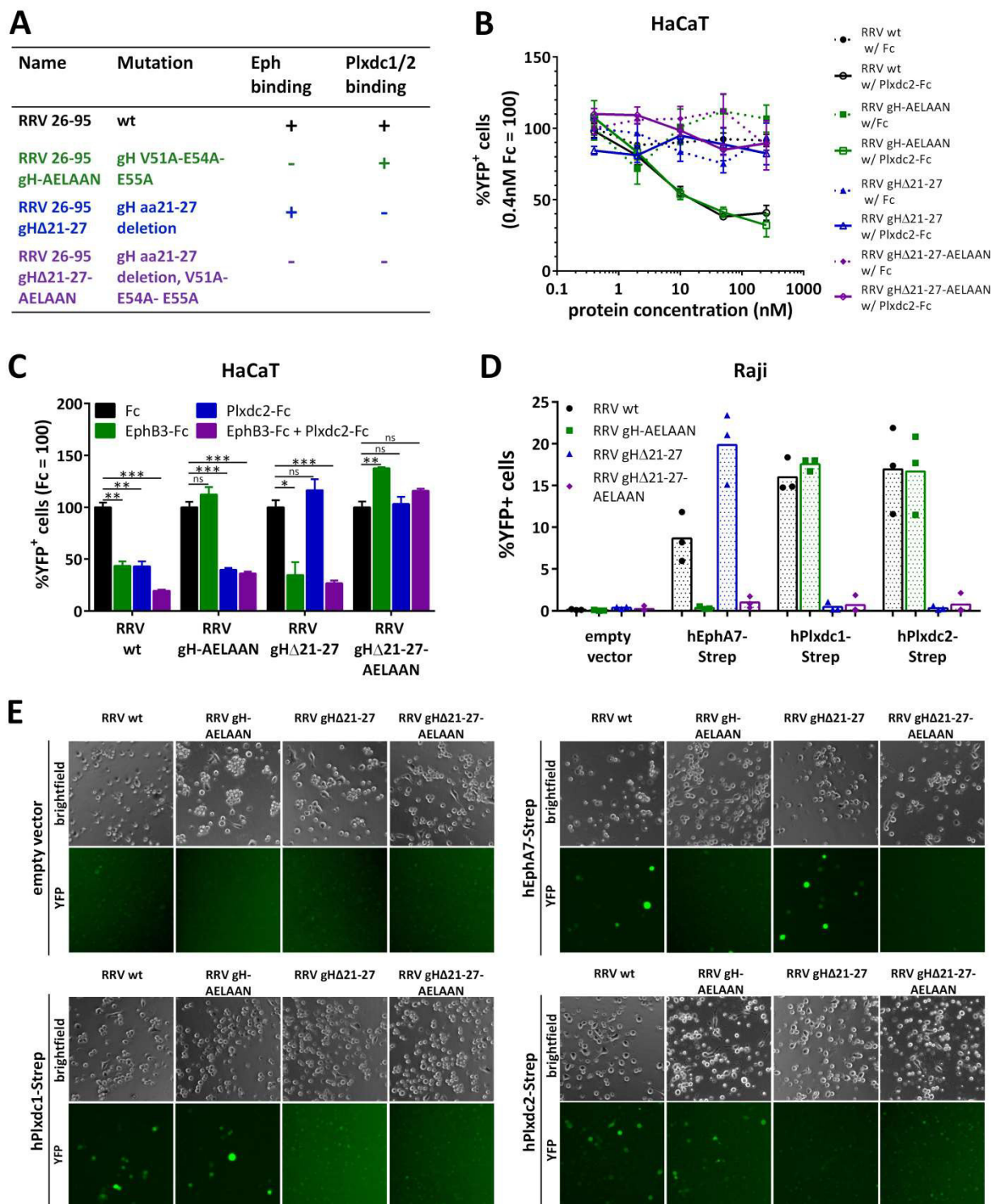


Figure 4 Deletion of the seven amino acid Plxdc-binding motif is sufficient to detarget RRV 26-95 from Plxdc receptors **A)** List of BAC-derived recombinant viruses and introduced mutations used in this figure. **B)** Dose-dependent inhibition of RRV-YFP 26-95 infection by soluble human Plxdc2-FcStrep on HaCaT cells. RRV-YFP 26-95 wt, RRV-YFP 26-95 gH-AELAAN, RRV-YFP 26-95 gHΔ21-27 and RRV-YFP 26-95 gHΔ21-27-AELAAN were pre-incubated with hPlxdc2-FcStrep for 30min at room temperature. FcStrep alone was used as control. YFP expression as indicator of infection was measured by flow cytometry. Infection in the presence of 0.4nM FcStrep was set to 100% (MOI ~0.05, triplicates, error bars represent SD). **C)** Inhibition of RRV 26-95 infection by soluble Plxdc2-Fc and EphB3-Fc on HaCaT cells. RRV-YFP 26-95 wt, RRV-YFP 26-95 gH-AELAAN, RRV-YFP 26-95 gHΔ21-27 and RRV-YFP 26-95 gHΔ21-27-AELAAN were pre-incubated with 100nM hPlxdc2-FcStrep, 10nM

392 EphB3-Fc or a combination of 100nM hPlxdc2-FcStrep and 10nM EphB3-Fc for 30min at room
393 temperature. FcStrep alone was used as control. YFP expression as indicator of infection was
394 measured by flow cytometry. Infection with FcStrep was set to 100% (MOI ~0.1-0.2, triplicates, error
395 bars represent SD). **D)** Raji cells were transduced with TwinStrep-tagged human EphA7, Plxdc1 or
396 Plxdc2 (hEphA7-Strep, hPlxdc1-Strep, hPlxdc2-Strep) expression constructs or an empty vector
397 control, briefly selected and infected with RRV-YFP 26-95 wt, RRV-YFP 26-95 gH-AELAAN, RRV-YFP
398 26-95 gHΔ21-27 or RRV-YFP 26-95 gHΔ21-27-AELAAN normalized to genome copies as determined by
399 qPCR. YFP expression as indicator of infection was measured by flow cytometry. The mean across
400 three independent sets of RRV stocks is indicated by columns. The means of individual triplicate
401 infections for each set of RRV stocks are given as symbols within the respective columns. **E)**
402 Micrographs show representative infection of one set of RRV stocks in (D).

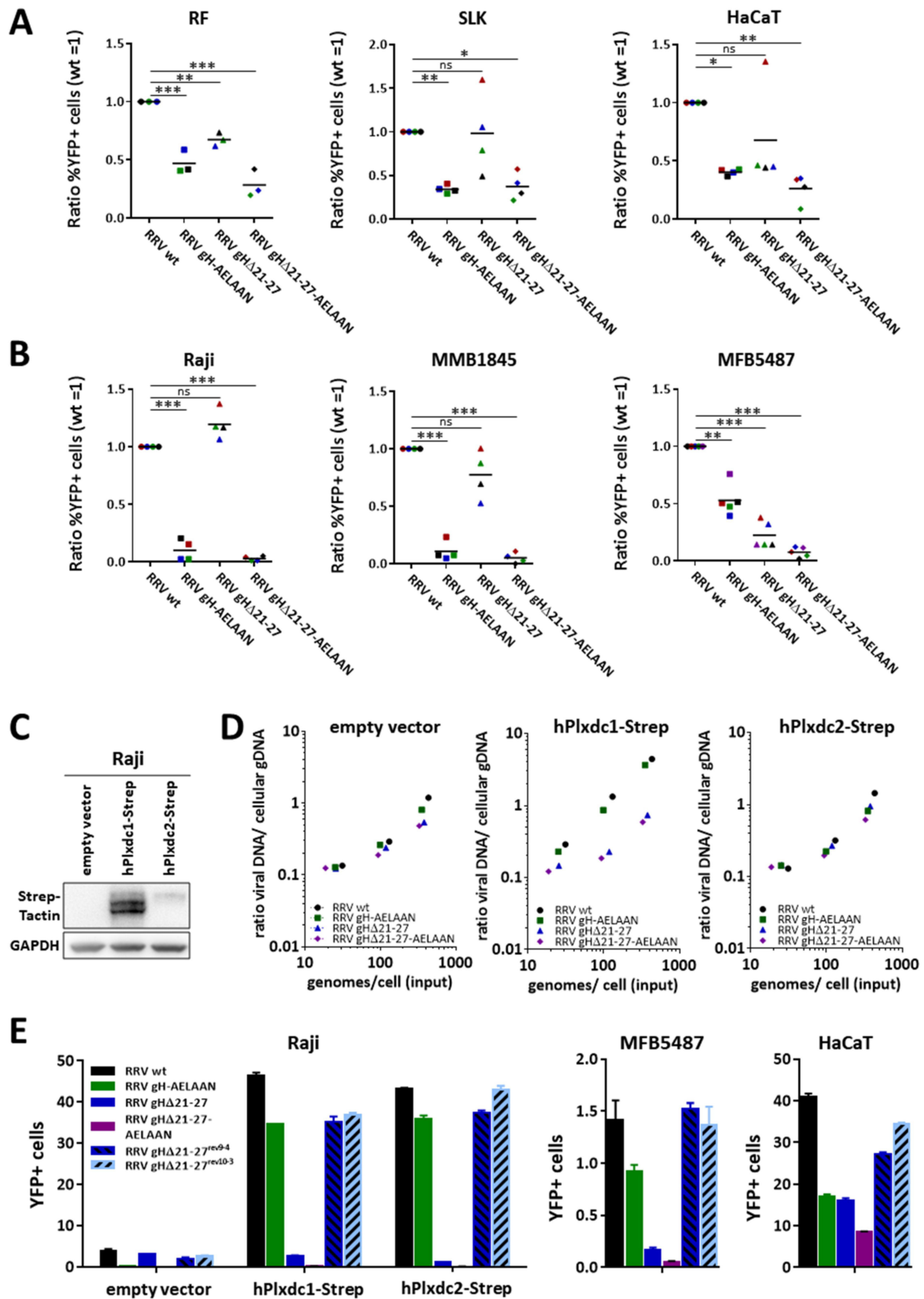


Figure 5 The contribution of the RRV 26-95 gH-Plxdc interaction to infection is cell type-specific and may in part be dependent on attachment effects. **A)** RRV 26-95 deleted in the Plxdc-interaction motif exhibits reduced specific infectivity on HaCaT and RF, but not SLK cells. Target cells were infected with RRV-YFP 26-95 wt, RRV-YFP 26-95 gH-AELAAN, RRV-YFP 26-95 gHΔ21-27 or RRV-YFP

408 26-95 gHΔ21-27-AELAAN normalized to genome copies as determined by qPCR. YFP expression as
 409 indicator of infection was measured by flow cytometry and normalized to RRV-YFP 26-95 wt
 410 infection. Means of individual normalized infections with three (RF) or four (HaCaT, SLK) independent
 411 sets of RRV stocks are given as symbols of different color. Sets with RRV-YFP 26-95 wt infection in an
 412 MOI range of 0.05 - 1 were used for analysis. The mean across the independent sets of RRV stocks is
 413 indicated by black lines. **B)** RRV 26-95 deleted in the Plxdc-interaction motif exhibits reduced specific
 414 infectivity on MFB5487, but not Raji and MMB1845 cells. Target cells were infected with RRV-YFP 26-
 415 95 wt, RRV-YFP 26-95 gH-AELAAN, RRV-YFP 26-95 gHΔ21-27 or RRV-YFP 26-95 gHΔ21-27-AELAAN
 416 normalized to genome copies as determined by qPCR. YFP expression as indicator of infection was
 417 measured by flow cytometry and normalized to RRV-YFP 26-95 wt infection. Means of individual
 418 normalized infections with four (Raji, MMB1845) or five (MFB5487) independent sets of RRV stocks
 419 are given as symbols of different color. Sets with RRV-YFP 26-95 wt infection exceeding 1% were used
 420 for analysis. The mean across the independent sets of RRV stocks is indicated by black lines. **C)**
 421 Western blot analysis of Raji cells transduced with TwinStrep-tagged human Plxdc1 and Plxdc2
 422 (hPlxdc1-Strep/ hPlxdc2-Strep) expression constructs or an empty vector control. **D)** Attachment of
 423 RRV 26-95 on transduced Raji cells is affected by hPlxdc1-Strep, but not hPlxdc2-Strep
 424 overexpression. Cells, analyzed in (C), were incubated with cold virus at the indicated concentrations
 425 at 4°C for 30min followed by genomic DNA isolation. The ratio of viral to cellular DNA as
 426 measurement for attached virus was calculated based on ΔCt values of a genomic (CCR5) and a viral
 427 locus (ORF73/ LANA) as determined by qPCR and plotted against input viral genome number. **E)** Re-
 428 introduction of the seven amino acid motif crucial for Plxdc-interaction rescues RRV-YFP 26-95
 429 gHΔ21-27 infection. Transduced Raji cells, analyzed in (C), were infected with RRV-YFP 26-95 wt, RRV-
 430 YFP 26-95 gH-AELAAN, RRV-YFP 26-95 gHΔ21-27, RRV-YFP 26-95 gHΔ21-27-AELAAN or two RRV-YFP
 431 26-95 gHΔ21-27 revertants (RRV-YFP 26-95 gHΔ21-27^{rev9-4}, RRV-YFP 26-95 gHΔ21-27^{rev10-3}) normalized
 432 to genome copies as determined by qPCR. YFP expression as indicator of infection was measured by
 433 flow cytometry (triplicates, error bars represent SD).

MATERIAL AND METHODS

Cells. Human embryonic kidney (HEK) 293T cells (RRID:CVCL_0063) (laboratory of Tobias Moser), SLK cells (RRID:CVCL_9569) (NIH AIDS Research and Reference Reagent program), rhesus monkey fibroblasts (RF) (laboratory of Prof. Rüdiger Behr) and HaCaT human keratinocytes (RRID:CVCL_0038) were cultured in Dulbecco's Modified Eagle Medium (DMEM), high glucose, GlutaMAX, 25mM HEPES (Thermo Fisher Scientific) supplemented with 10% fetal calf serum (FCS) (Thermo Fisher Scientific), and 50µg/ml gentamycin (PAN Biotech). iSLK cells (laboratory of Don Ganem, Novartis Institutes for BioMedical Research, Emeryville, CA, USA) were maintained in DMEM supplemented with 10% FCS, 50µg/ml gentamycin, 2.5µg/ml puromycin (InvivoGen) and 250µg/ml G418 (Carl Roth). Raji cells (RRID:CVCL_0511) (laboratory of Jens Gruber), MFB5487 (a clonal cell line established from macaca fascicularis PBMC, immortalized by infection with herpesvirus papio; a kind gift from Ulrike Sauermann) and MMB1845 cells (a clonal cell line established from macaca mulatta PBMC, immortalized by infection with herpesvirus papio; a kind gift from Ulrike Sauermann) were cultured in RPMI (Thermo Fisher Scientific) supplemented with 10% FCS and 50µg/ml gentamycin.

BAC mutagenesis and virus production. RRV recombinants (RRV gHΔ21-27, RRV gHΔ21-27-AELAAN) were generated based on BAC35-8 (43) and RRV gH-AELAAN (21) respectively, using a two-step, markerless λ-red-mediated BAC recombination strategy as described by Tischer et al. (33). In short, recombination cassettes were generated from the pEPKanS template by polymerase chain reaction (PCR) with Phusion High Fidelity DNA polymerase (Thermo Fisher Scientific) using long oligonucleotides (Ultramers; purchased from Integrated DNA Technologies (IDT)) (see S1 Table for a complete list of primers). Recombination cassettes were transformed into RRV-YFP-carrying GS1783 followed by kanamycin selection, and subsequent second recombination under 1% L(+)-arabinose (Sigma-Aldrich)-induced I-SceI expression. Colonies were verified by PCR of the mutated region followed by sequence analysis (Macrogen), pulsed-field gel electrophoresis and restriction fragment length polymorphism. For this purpose, bacmid DNA was isolated by standard alkaline lysis from 5ml liquid cultures. Subsequently, the integrity of bacmid DNA was analyzed by digestion with restriction enzyme *XhoI* and separation in 1% PFGE agarose (Bio-Rad) gels and 0.5×TBE buffer by pulsed-field gel electrophoresis at 6 V/cm, 120-degree field angle, switch time linearly ramped from 1s to 5s over 16 h (CHEF DR III, Bio-Rad). Infectious RRV-YFP recombinants were generated as described previously (21). In short, bacmid DNA (NucleoBond Xtra Midi) was transfected into 293T cells using GenJet Ver. II (Signagen) according to manufacturer's instructions. Transfected 293T cells were transferred onto a confluent rhesus monkey fibroblasts monolayer two days after transfection and co-cultivated until a visible cytopathic effect (CPE) was observed. For virus stocks preparations, confluent primary rhesus monkey fibroblasts were inoculated with infectious supernatant of 293T/rhesus monkey fibroblast co-cultures. After multiple rounds of replication virus-containing RF supernatant was clarified by centrifugation (4750g, 10 minutes), concentrated by overnight centrifugation (4200rpm, 4°C) and careful aspiration of approximately 95% of the supernatant. The pellet was resuspended overnight in the remaining liquid. Stocks of wt and recombinant viruses were aliquoted and stored at -80°C. Mutations were verified by PCR amplification of the respective region followed by sequence analysis (Macrogen).

Plasmids. The pcDNA4 vector containing full-length EphB3 (ref|BC052968|, pcDNA-EphB3-myc), pcDNA6aV5 vectors containing RRV/KSHV gH and gL coding sequences (ref|GQ994935.1|, pcDNA6aV5-KSHV-gH, pcDNA3.1-KSHV-gL-Flag (13); ref|AF210726.1|, pcDNA6aV5-RRV-26-95-gH, pcDNA3.1-RRV-26-95-gL-Flag (14, 44); ref|AF083501.3|, pcDNA6aV5-RRV-17577-gH, pcDNA3.1-RRV-17577-gL-Flag (14)) were described elsewhere. RRV 26-95/ RRV 17577 recombinant gH constructs were generated based on pcDNA6aV5-RRV-26-95-gH or pcDNA6aV5-RRV-17577-gH, respectively, using 'Round the Horn Site-directed mutagenesis. Expression plasmids pcDNA4-hPlxdc1-myc (Homo sapiens, full-length, ref |NM_020405.5|) and pcDNA4-hPlxdc2-myc (Homo sapiens, full-length, ref |NM_032812.9|) were generated by PCR based restriction cloning. The soluble ectodomain of human Plxdc2 (amino acids 31-453) without signal peptide was inserted behind a heterologous signal peptide of murine IgG-kappa into pAB61Strep by PCR based restriction cloning, resulting in a C-terminally fused IgG1 Fc-fusion protein with a C-terminal tandem Strep-Tag (pPlxdc2-FcStrep) as described previously (45). Expression plasmids pcDNA4-mmPlxdc1-myc (macaca mulatta, full-length, ref |XM_028836436.1|) and pcDNAmPlxdc2-myc (macaca mulatta, full-length, ref |XM_028826043.1|) were generated based on PCR-amplified gBlock gene fragments (purchased from IDT) of the regions varying from human Plxdc1 (nt1-1200) and Plxdc2 (nt1-1401), respectively, and ligated in the respective PCR-amplified backbone (pcDNA4hPlxdc1-myc, pcDNA4hPlxdc2-myc) by exonuclease-based Gibson-assembly (Gibson Assembly Mastermix, New England Biolabs). pLenti CMV Blast DEST (706-1) (a gift from Eric Campeau & Paul Kaufman (Addgene plasmid #17451)) constructs carrying a human Plxdc1-TwinStrep or Plxdc2-TwinStrep expression cassette (pLenti-CMV-Blast-Plxdc1-Strep/ pLenti-CMV-Blast-Plxdc2-Strep) were based on pcDNA4-hPlxdc1-myc/ pcDNA4-hPlxdc2-myc, which were PCR-amplified and ligated using exonuclease-based Gibson-assembly. pLenti-CMV-Blast-EphA7-Strep was described before (19). (See S1 Table for a complete list of primers and constructs).

Recombinant proteins. Recombinant, soluble FcStrep and Plxdc2-FcStrep-fusion proteins were purified under native conditions by Strep-Tactin chromatography from 293T cell culture supernatant. 293T cells were transfected using Polyethylenimine "Max" (PEI) (Polysciences) (46) as described before (19) with pAB61Strep or pPlxdc2-FcS. The protein-containing cell culture supernatant was filtered through 0.22µm PES membranes (Millipore) and passed over 0.5ml of a Strep-Tactin Superflow (IBA Lifesciences) matrix in a gravity flow Omniprep column (BioRad). Bound protein was washed with approximately 50ml phosphate buffered saline pH 7.4 (PBS) and eluted in 1ml fractions with 3mM desthiobiotin (Sigma-Aldrich) in PBS. Protein-containing fractions were pooled and buffer exchange to PBS via VivaSpin columns (Sartorius) was performed. Protein concentration was determined by absorbance at 280nm. Aliquots were frozen and stored at -80°C. Recombinant, human, soluble EphB3-Fc (5667-B3-050) was purchased from R&D Systems.

Lentivirus production and transduction. For production of lentiviral particles, 10cm cell culture grade petri dishes of approximately 80% confluent 293T cells were transfected with 1.4µg pMD2.G (VSV-G envelope expressing plasmid, a gift from Didier Trono (Addgene plasmid #12259), 3.6µg psPAX2 (Gag-Pol expression construct, a gift from Didier Trono (Addgene plasmid #12260), and 5µg of lentiviral expression constructs (pLenti CMV Blast DEST (706-1), pLenti-CMV-Blast-EphA7-Strep, pLenti-CMV-Blast-Plxdc1-Strep, pLenti-CMV-Blast-Plxdc2-Strep) using PEI as described before (19). The supernatant containing the pseudotyped lentiviral

particles was harvested 2 to 3 days after transfection and filtered through 0.45µm CA membranes (Millipore). For transduction, lentivirus stocks were used at a 1:5 dilution unless stated otherwise. After 48h, the selection antibiotic blasticidin (Invivogen) was added to a final concentration of 10µg/ml. After initial selection the blasticidin concentration was reduced to 5µg/ml.

Quantitative realtime-PCR-based viral genome copy number analysis and virus attachment assay.

Concentrated virus samples were treated with DNaseI (0.1 units/µl) to remove any non-encapsidated DNA (37°C, overnight). Subsequently, DNaseI was deactivated and viral capsids were disrupted by heating the samples to 95°C for 30 minutes. Realtime-PCR (qPCR) was performed on a StepOne Plus cycler (Thermo Fisher Scientific) in 20µl reactions using the SensiFAST Probe Hi-ROX Kit (Bioline) (cycling conditions: 3min initial denaturation at 95°C, 40 cycles 95°C for 10s and 60°C for 35s). All primer-probe sets were purchased from IDT as complete PrimeTime qPCR Assays (primer:probe ratio = 4:1). Samples were analyzed in technical triplicates. A series of five 10-fold dilutions of bacmid DNA was used as standard for absolute quantification of viral genome copies based on qPCR of ORF73 for RRV (see S1 Table for a complete list of primers). For virus attachment assays transduced Raji cells were incubated with ice-cold virus dilutions at the indicated concentrations, normalized to genomes per cell, at 4°C for 30min. After three washes with ice-cold PBS genomic DNA was isolated using the ISOLATE II Genomic DNA Kit (Bioline) according to manufacturer's instructions. Genome copies of used input virus preparations were determined after overnight DNaseI digest as described above. Relative values of bound viral genomes to cellular DNA were calculated on the basis of ΔC_t values for viral genomic loci (ORF73 for RRV) and a cellular genomic locus (CCR5) using the same conditions described above. For attachment assays all samples were analyzed in technical duplicates.

Infection assays, blocking experiments and flow cytometry. For infection assays cells were plated at 50 000 cells/cm² (SLK, HaCaT, Raji), 25 000 cells/cm² (RF) or 200 000 cells/ml (Raji, MFB5487, MMB1845) respectively. One day after plating (for adherent cells lines) or directly after plating (for suspension cell lines), cells were infected with the indicated amounts of virus. Adherent cells lines were harvested 24h post infection by brief trypsinization, followed by addition of 5% FCS in PBS to inhibit trypsin activity. Suspension cell lines were harvested 48h post infection (24h post infection for transduced Raji cells) by pipetting. Subsequently, cells were pelleted by centrifugation (1200rpm, 10min), washed once with PBS, re-pelleted and fixed in PBS supplemented with 4% formaldehyde (Carl Roth). Block of RRV infection with soluble decoy receptor was assayed by infection with virus inocula that were pre-incubated with the indicated concentrations of soluble EphB3-Fc, hPlxdc1-Fc, hPlxdc2-Fc or Fc alone at room temperature for 30min. Calculation of molarity was based on diametric proteins. Cell harvest and preparation for flow cytometry analyses was performed as described above. A minimum of 5 000 – 10 000 cells was analyzed per sample for YFP expression on a LSRII flow cytometer (BD Biosciences). Data was analyzed using Flowing Software (Version 2.5).

Immunoprecipitation and Western blot analysis. For interaction analysis of gH-V5/gL-Flag complexes with Plxdc1/2, 293T cells were transfected using PEI as described before. Lysates of 293T cells transfected with the respective expression constructs for recombination gH-V5/gL-Flag complexes were prepared in NP40 lysis buffer (1% Nonidet P40 Substitute (Sigma-Aldrich), 150mM NaCl (Sigma-Aldrich), 50mM HEPES (VWR), 1mM

EDTA (Amresco) with freshly added Protease Inhibitor Cocktail, General Use (Amresco)) and protein content was determined by Bradford assay using Roti-Quant (Roth) according to manufacturer's instructions. 20µg total protein was denatured in 1x SDS sample buffer (Morris formulation) at 95°C for 5min, separated by polyacrylamide gel electrophoresis (PAGE) using 8–16% Tris-Glycine polyacrylamide gradient gels (Thermo Fisher Scientific) with Tris-Glycine SDS running buffer (25mM Tris, 192mM glycine, 0.1% SDS) and transferred to 0.45µm (0.22µm for blots containing gL) Polyvinylidene difluoride (PVDF) membranes (200mA/Gel, max 30V, 1h in Towbin buffer (25mM Tris, 192mM glycine) with 20% methanol) in a wet tank system (Mini Blot Module, Thermo Fisher). The membranes were blocked in 5% dry milk powder in TBS-T (5mM Tris, 15mM NaCl, 0.05% Tween20) for 1h, at room temperature, washed once in TBS-T and incubated with the respective antibodies for 2h at room temperature or overnight at 4°C (see S1 Table for a complete list of antibodies). After three washes with TBS-T, the membranes were incubated with the respective HRP-conjugated secondary antibody in 5% dry milk powder in TBS-T for 1h at room temperature washed three times in TBS-T and imaged on an ECL ChemoCam 3.2 Imager (Intas) using Immobilon Forte Western HRP substrate (Merck Millipore). For pulldown of gH-V5 or gH-V5/ gL-Flag complexes, the amount of input lysate between wt and mutant gH constructs was normalized to gH expression as determined by Western blot and diluted to equal volume with cell lysate from non-transfected 293T cells prior to immunoprecipitation. Subsequently, lysates were incubated with 0.5µg V5-tag antibody (Bio-Rad) and ProteinG sepharose (GenScript) overnight at 4°C with agitation. After three washes in NP40 lysis buffer, ProteinG beads with pre-coupled complexes were incubated overnight at 4°C with agitation with lysate of full-length human or macaca mulatta Plxdc1-myc or Plxdc2-myc expression plasmid transfected 293T cells normalized to Plxdc expression. Volumes were adjusted with lysate from untransfected 293T cells. ProteinG beads were collected by brief centrifugation and washed 3 times in NP40 lysis buffer. Precipitates were heated in 2x SDS sample buffer (95°C, 5min) and analyzed by Western blot as described above. For co-immunoprecipitation of soluble Plxdc1/2-Strep constructs with gH-V5/gL-Flag and EphB3-myc, supernatant of Plxdc1/2-FcStrep transfected 293T cells was incubated with StrepTactinXT beads (IBA) overnight at 4°C with agitation. After three washes in NP40 lysis buffer, StrepTactinXT beads with pre-coupled Plxdc1/2-Strep were incubated overnight at 4°C with agitation with equal amounts of lysate of full-length human EphB3-myc, RRV 26-95 gH-V5/gL-Flag or 17577 gH-V5/gL-Flag expression plasmid transfected 293T cells or the indicated combinations. Volumes were adjusted with lysate of untransfected 293T cells.

Structure prediction and analysis. Homology based structure prediction was performed using the Iterative Threading ASSEMBLY Refinement (I-TASSER) server on standard settings for structure prediction of RRV 26-95 gH and gL based on the crystal structure of the EBV gH/gL complex (3PHF). Modeling of the RRV 26-95 gH/gL complex was additionally performed using both the SPRING and CO-THreader algorithms for protein-protein complex structure and multi-chain protein threading with no differences between determined structures. Resulting I-TASSER structures were aligned to the gH/gL CO-THreader model with the VMD 1.9.3 OpenGL RMSD Trajectory Tool based on amino acids 25 to 62 of gH (RMSD of 0.344Å) and amino acids 2 to 100 of gL (RMSD of 2.697Å) to generate the depicted model. All further analyses and visualizations were performed using VMD 1.9.3 OpenGL.

Mathematical and statistical analysis. Statistical difference between groups was determined by unpaired Student's t-tests followed by Bonferroni correction for multiple comparisons. All Statistical analyses were performed with GraphPad Prism version 6. For all statistics, *: p-value < 0.05, **: p-value < 0.01, ***: p-value < 0.001, ns: not significant.

ACKNOWLEDGMENTS

This work was supported by grants to A.S.H. from the Deutsche Forschungsgemeinschaft (HA 6013/1, HA 6013/4-1) and the Interdisciplinary Center for Clinical Research Erlangen (IZKF, grant J44), by the German Research foundation, grants CRC 796, TP B1 to A.E., by grant RO1 AI072004 from the National Institutes of Health (NIH) to R.C.D., and by base grant RR00168 from the NIH to the New England Primate Research Center.

LITERATURE

1. Desrosiers RC, Sasseville VG, Czajak SC, Zhang X, Mansfield KG, Kaur A, Johnson RP, Lackner AA, Jung JU. 1997. A herpesvirus of rhesus monkeys related to the human Kaposi's sarcoma-associated herpesvirus. *J Virol* 71:9764–9769.
2. Searles RP, Bergquam EP, Axthelm MK, Wong SW. 1999. Sequence and genomic analysis of a Rhesus macaque rhadinovirus with similarity to Kaposi's sarcoma-associated herpesvirus/human herpesvirus 8. *J Virol* 73:3040–3053.
3. O'Connor CM, Kedes DH. 2007. Rhesus Monkey Rhadinovirus: A Model for the Study of KSHV, p. 43–69. *In* Boshoff, C, Weiss, RA (eds.), *Kaposi Sarcoma Herpesvirus: New Perspectives*. Springer Berlin Heidelberg.
4. Shin YC, Jones LR, Manrique J, Lauer W, Carville A, Mansfield KG, Desrosiers RC. 2010. Glycoprotein gene sequence variation in rhesus monkey rhadinovirus. *Virology* 400:175–186.
5. Bilello JP, Morgan JS, Damania B, Lang SM, Desrosiers RC. 2006. A Genetic System for Rhesus Monkey Rhadinovirus: Use of Recombinant Virus To Quantitate Antibody-Mediated Neutralization. *J Virol* 80:1549–1562.
6. Estep RD, Powers MF, Yen BK, Li H, Wong SW. 2007. Construction of an Infectious Rhesus Rhadinovirus Bacterial Artificial Chromosome for the Analysis of Kaposi's Sarcoma-Associated Herpesvirus-Related Disease Development. *J Virol* 81:2957–2969.
7. Bilello JP, Lang SM, Wang F, Aster JC, Desrosiers RC. 2006. Infection and Persistence of Rhesus Monkey Rhadinovirus in Immortalized B-Cell Lines. *J Virol* 80:3644–3649.
8. Wong SW, Bergquam EP, Swanson RM, Lee FW, Shiigi SM, Avery NA, Fanton JW, Axthelm MK. 1999. Induction of B cell hyperplasia in simian immunodeficiency virus-infected rhesus macaques with the simian homologue of Kaposi's sarcoma-associated herpesvirus. *J Exp Med* 190:827–840.
9. Orzechowska BU, Powers MF, Sprague J, Li H, Yen B, Searles RP, Axthelm MK, Wong SW. 2008. Rhesus macaque rhadinovirus-associated non-Hodgkin lymphoma: animal model for KSHV-associated malignancies. *Blood* 112:4227–4234.

- 620 10. Bruce AG, Bielefeldt-Ohmann H, Barcy S, Bakke AM, Lewis P, Tsai C-C, Murnane RD, Rose TM.
621 2012. Macaque Homologs of EBV and KSHV Show Uniquely Different Associations with Simian
622 AIDS-related Lymphomas. *PLoS Pathog* 8:e1002962.
- 623 11. Marshall VA, Labo N, Hao X-P, Holdridge B, Thompson M, Miley W, Brands C, Coalter V, Kiser R,
624 Anver M, Golubeva Y, Warner A, Jaffe ES, Piatak M, Wong SW, Ohlen C, MacAllister R, Smedley
625 J, Deleage C, Del Prete GQ, Lifson JD, Estes JD, Whitby D. 2018. Gammaherpesvirus infection
626 and malignant disease in rhesus macaques experimentally infected with SIV or SHIV. *PLOS*
627 *Pathog* 14:e1007130.
- 628 12. Umbach JL, Strelow LI, Wong SW, Cullen BR. 2010. Analysis of rhesus rhadinovirus microRNAs
629 expressed in virus-induced tumors from infected rhesus macaques. *Virology* 405:592–599.
- 630 13. Hahn AS, Kaufmann JK, Wies E, Naschberger E, Panteleev-Ivlev J, Schmidt K, Holzer A, Schmidt
631 M, Chen J, König S, Ensser A, Myoung J, Brockmeyer NH, Stürzl M, Fleckenstein B, Neipel F.
632 2012. The ephrin receptor tyrosine kinase A2 is a cellular receptor for Kaposi's sarcoma–
633 associated herpesvirus. *Nat Med* 18:961–966.
- 634 14. Hahn AS, Desrosiers RC. 2013. Rhesus Monkey Rhadinovirus Uses Eph Family Receptors for
635 Entry into B Cells and Endothelial Cells but Not Fibroblasts. *PLoS Pathog* 9:e1003360.
- 636 15. TerBush AA, Hafkamp F, Lee HJ, Coscoy L. 2018. A Kaposi's Sarcoma-Associated Herpesvirus
637 Infection Mechanism Is Independent of Integrins $\alpha 3\beta 1$, $\alpha V\beta 3$, and $\alpha V\beta 5$. *J Virol* 92:e00803-18,
638 /jvi/92/17/e00803-18.atom.
- 639 16. Chen J, Zhang X, Schaller S, Jardetzky TS, Longnecker R. 2019. Ephrin Receptor A4 is a New
640 Kaposi's Sarcoma-Associated Herpesvirus Virus Entry Receptor. *mBio* 10:e02892-18,
641 /mbio/10/1/mBio.02892-18.atom.
- 642 17. Hahn AS, Desrosiers RC. 2014. Binding of the Kaposi's sarcoma-associated herpesvirus to the
643 ephrin binding surface of the EphA2 receptor and its inhibition by a small molecule. *J Virol*
644 88:8724–8734.
- 645 18. Kumar B, Chandran B. 2016. KSHV Entry and Trafficking in Target Cells-Hijacking of Cell Signal
646 Pathways, Actin and Membrane Dynamics. *Viruses* 8.
- 647 19. Großkopf AK, Schlagowski S, Hörnich BF, Fricke T, Desrosiers RC, Hahn AS. 2019. EphA7
648 Functions as Receptor on BJAB Cells for Cell-to-Cell Transmission of the Kaposi's Sarcoma-
649 Associated Herpesvirus and for Cell-Free Infection by the Related Rhesus Monkey Rhadinovirus.
650 *J Virol* 93:e00064-19, /jvi/93/15/JVI.00064-19.atom.
- 651 20. Möhl BS, Chen J, Longnecker R. 2019. Gammaherpesvirus entry and fusion: A tale how two
652 human pathogenic viruses enter their host cells, p. 313–343. *In* *Advances in Virus Research*.
653 Elsevier.
- 654 21. Großkopf AK, Ensser A, Neipel F, Jungnickl D, Schlagowski S, Desrosiers RC, Hahn AS. 2018. A
655 conserved Eph family receptor-binding motif on the gH/gL complex of Kaposi's sarcoma-
656 associated herpesvirus and rhesus monkey rhadinovirus. *PLOS Pathog* 14:e1006912.
- 657 22. Hahn AS, Bischof GF, Großkopf AK, Shin YC, Domingues A, Gonzalez-Nieto L, Rakasz EG, Watkins
658 DI, Ensser A, Martins MA, Desrosiers RC. 2019. A Recombinant Rhesus Monkey Rhadinovirus
659 Deleted of Glycoprotein L Establishes Persistent Infection of Rhesus Macaques and Elicits
660 Conventional T Cell Responses. *J Virol* JVI.01093-19, jvi;JVI.01093-19v1.

- 661 23. Croix BSt. 2000. Genes Expressed in Human Tumor Endothelium. *Science* 289:1197–1202.
- 662 24. Carson-Walter EB, Watkins DN, Nanda A, Vogelstein B, Kinzler KW, St Croix B. 2001. Cell surface
663 tumor endothelial markers are conserved in mice and humans. *Cancer Res* 61:6649–6655.
- 664 25. Miller-Delaney SFC, Lieberam I, Murphy P, Mitchell KJ. 2011. Plxdc2 is a mitogen for neural
665 progenitors. *PLoS One* 6:e14565.
- 666 26. Lee HK, Bae HR, Park HK, Seo IA, Lee EY, Suh DJ, Park HT. 2005. Cloning, characterization and
667 neuronal expression profiles of tumor endothelial marker 7 in the rat brain. *Brain Res Mol Brain*
668 *Res* 136:189–198.
- 669 27. Miller SFC, Summerhurst K, Rünker AE, Kerjan G, Friedel RH, Chédotal A, Murphy P, Mitchell KJ.
670 2007. Expression of Plxdc2/TEM7R in the developing nervous system of the mouse. *Gene Expr*
671 *Patterns* 7:635–644.
- 672 28. Nanda A, Buckhaults P, Seaman S, Agrawal N, Boutin P, Shankara S, Nacht M, Teicher B, Stampfl
673 J, Singh S, Vogelstein B, Kinzler KW, St. Croix B. 2004. Identification of a Binding Partner for the
674 Endothelial Cell Surface Proteins TEM7 and TEM7R. *Cancer Res* 64:8507–8511.
- 675 29. Cheng G, Zhong M, Kawaguchi R, Kassai M, Al-Ubaidi M, Deng J, Ter-Stepanian M, Sun H. 2014.
676 Identification of PLXDC1 and PLXDC2 as the transmembrane receptors for the multifunctional
677 factor PEDF. *eLife* 3:e05401.
- 678 30. Lee HK, Seo IA, Park HK, Park HT. 2006. Identification of the basement membrane protein
679 nidogen as a candidate ligand for tumor endothelial marker 7 in vitro and in vivo. *FEBS Lett*
680 580:2253–2257.
- 681 31. Uhlen M, Fagerberg L, Hallstrom BM, Lindskog C, Oksvold P, Mardinoglu A, Sivertsson A, Kampf
682 C, Sjostedt E, Asplund A, Olsson I, Edlund K, Lundberg E, Navani S, Szgyarto CA-K, Odeberg J,
683 Djureinovic D, Takanen JO, Hober S, Alm T, Edqvist P-H, Berling H, Tegel H, Mulder J, Rockberg J,
684 Nilsson P, Schwenk JM, Hamsten M, von Feilitzen K, Forsberg M, Persson L, Johansson F,
685 Zwahlen M, von Heijne G, Nielsen J, Ponten F. 2015. Tissue-based map of the human proteome.
686 *Science* 347:1260419–1260419.
- 687 32. Matsuura H, Kirschner AN, Longnecker R, Jardetzky TS. 2010. Crystal structure of the Epstein-
688 Barr virus (EBV) glycoprotein H/glycoprotein L (gH/gL) complex. *Proc Natl Acad Sci* 107:22641–
689 22646.
- 690 33. Tischer BK, Smith GA, Osterrieder N. 2010. En Passant Mutagenesis: A Two Step Markerless Red
691 Recombination System, p. 421–430. *In* Braman, J (ed.), *In Vitro Mutagenesis Protocols*. Humana
692 Press, Totowa, NJ.
- 693 34. Li Q, Turk SM, Hutt-Fletcher LM. 1995. The Epstein-Barr virus (EBV) BZLF2 gene product
694 associates with the gH and gL homologs of EBV and carries an epitope critical to infection of B
695 cells but not of epithelial cells. *J Virol* 69:3987–3994.
- 696 35. Nguyen C, Kamil J. 2018. Pathogen at the Gates: Human Cytomegalovirus Entry and Cell
697 Tropism. *Viruses* 10:704.
- 698 36. Hirai H, Maru Y, Hagiwara K, Nishida J, Takaku F. 1987. A novel putative tyrosine kinase
699 receptor encoded by the eph gene. *Science* 238:1717–1720.

- 700 37. Pasquale EB. 2010. Eph receptors and ephrins in cancer: bidirectional signalling and beyond.
701 Nat Rev Cancer 10:165–180.
- 702 38. Zhang Z-Z, Hua R, Zhang J-F, Zhao W-Y, Zhao E-H, Tu L, Wang C-J, Cao H, Zhang Z-G. 2015. TEM7
703 (PLXDC1), a key prognostic predictor for resectable gastric cancer, promotes cancer cell
704 migration and invasion. Am J Cancer Res 5:772–781.
- 705 39. Carpenter RL, Paw I, Zhu H, Sirkisoon S, Xing F, Watabe K, Debinski W, Lo H-W. 2015. The gain-
706 of-function GLI1 transcription factor TGLI1 enhances expression of VEGF-C and TEM7 to
707 promote glioblastoma angiogenesis. Oncotarget 6:22653–22665.
- 708 40. Czekierdowski A, Stachowicz N, Czekierdowska S, Łoziński T, Gurynowicz G, Kluz T. 2018.
709 Prognostic significance of TEM7 and nestin expression in women with advanced high grade
710 serous ovarian cancer. Ginekol Pol 89:135–141.
- 711 41. Kim GH, Won JE, Byeon Y, Kim MG, Wi TI, Lee JM, Park Y-Y, Lee J-W, Kang TH, Jung ID, Shin BC,
712 Ahn HJ, Lee YJ, Sood AK, Han HD, Park Y-M. 2018. Selective delivery of PLXDC1 small interfering
713 RNA to endothelial cells for anti-angiogenesis tumor therapy using CD44-targeted chitosan
714 nanoparticles for epithelial ovarian cancer. Drug Deliv 25:1394–1402.
- 715 42. Falchetti ML, D'Alessandris QG, Pacioni S, Buccarelli M, Morgante L, Giannetti S, Lulli V, Martini
716 M, Larocca LM, Vakana E, Stancato L, Ricci-Vitiani L, Pallini R. 2019. Glioblastoma endothelium
717 drives bevacizumab-induced infiltrative growth via modulation of PLXDC1. Int J Cancer
718 144:1331–1344.
- 719 43. Hahn AS, Großkopf AK, Jungnickl D, Scholz B, Ensser A. 2016. Viral FGARAT Homolog ORF75 of
720 Rhesus Monkey Rhadinovirus Effects Proteasomal Degradation of the ND10 Components SP100
721 and PML. J Virol 90:8013–8028.
- 722 44. Shin YC, Desrosiers RC. 2011. Rhesus Monkey Rhadinovirus ORF57 Induces gH and gL
723 Glycoprotein Expression through Posttranscriptional Accumulation of Target mRNAs. J Virol
724 85:7810–7817.
- 725 45. Hahn A, Birkmann A, Wies E, Dorer D, Mahr K, Sturzl M, Titgemeyer F, Neipel F. 2009. Kaposi's
726 Sarcoma-Associated Herpesvirus gH/gL: Glycoprotein Export and Interaction with Cellular
727 Receptors. J Virol 83:396–407.
- 728 46. Longo PA, Kavran JM, Kim M-S, Leahy DJ. 2013. Transient Mammalian Cell Transfection with
729 Polyethylenimine (PEI), p. 227–240. *In* Methods in Enzymology. Elsevier.

730

731

S1 Table List of primers, and antibodies used in this study.

| A) Oligos for BAC recombination, sequencing and qPCR | | | | | |
|---|---|---|--|--|---------------------------|
| | name | sequence | | | |
| BAC mutagenesis | RRV 26-95 gHΔ21-27 forward | 5'-CACTGTTTGTGTTTGTGTAATTACATTGTCTGTAATTAATGGAGTACCGGGACTTGAATAGTAGGATGACGACGATAAGTAGGG-3' | | | |
| | RRV 26-95 gHΔ21-27 reverse | 5'-TGTTGTTGTGGCAGGGGTAAGAAGAACTATTTCAAGTCCCGGTACTCCATTAAATACAGACAATGCAACCAATTAACCAATTCGTATTAG-3' | | | |
| | RRV 26-95 gHΔ21-27rev forward | 5'-CACTGTTTGTGTTTGTGTAATTACATTGTCTGTAATTAATGGATATGAATATAATGAAGAAAAGGTACCGGGACTTGAATAGTAGGATGACGACGATAAGTAGGG-3' | | | |
| | RRV 26-95 gHΔ21-27rev reverse | 5'-TGTTGTTGTGGCAGGGGTAAGAAGAACTATTTCAAGTCCCGGTACTCTTTCTCATTTATTCATATCCATTAAATACAGACAATGCAACCAATTAACCAATTCGTATTAG-3' | | | |
| Sequencing PCR | RRV 26-95 gHΔ21-27seq forward | 5'-TCCAAGATTGACTCATCGGTTTC-3' | | | |
| | RRV 26-95 gHΔ21-27seq reverse | 5'-TCCAATCGGCTGTCATAATACC-3' | | | |
| qPCR | RRV 26-95 ORF73 | primer1 | 5'-AAAGATGACTCCGTGACACC-3' | | |
| | | primer2 | 5'-GCGATACCCCATTTCCCATAC-3' | | |
| | | probe | 5'-/56-FAM/CCCGAAAA/ZEN/TACCGCCACAGAGAA/3IABkFQ/-3' | | |
| | genomic CCR5 (human/ rhesus) | primer1 | 5'-CCCACTGGGACTTTGGAAATA-3' | | |
| | | primer2 | 5'-CGATTGTCAGGAGGATGATGAA-3' | | |
| | | probe | 5'-/56-FAM/TGTGTCAAC/ZEN/TCTTGACAGGGCTCT/3IABkFQ/-3' | | |
| B) Primers for restricton mediated, Gibson Assembly and Around-the-horn cloning | | | | | |
| | | vector/ based on | Primer vector | Primer insert | |
| PCR based restriction cloning | pcDNA4MH-hPlxd1 | pcDNA4-MH | XbaI x KpnI digest | 5'-AA GGTACC ATGCGAGGCGAGCTCTGGC-3' | |
| | | | | 5'-AA TCTAGA GCACGTCTCAGCTCCATGAAG -3' | |
| | pcDNA4MH-hPlxd2 | pcDNA4-MH | XbaI x KpnI digest | 5'-AA GGTACC ATGCGCAGGTTCCCGAAGGC-3' | |
| | | | | 5'-AA TCTAGA GCACGTCTGTATACAATAAAGC-3' | |
| Gibson Assembly | pcDNA-hPlxd1-Strep | pAB61strep | GCGCGCCGTACGAAGCTTGGTACCTTGAGCCCCAGCCCGGAGCAGG | 5'-GGCGGCCGCTGTGACAAAACCTAC-3' | |
| | | | GTGAGTTTGTGCACAGCGGCCGCCAGGTGCACAGGAGTGCCCTTTGTC | 5'-GGTACCAAGCTTCGTACGGCGCGC-3' | |
| | pcDNA-hPlxd2-Strep | pAB61strep | KpnI x NotI digest | 5'-AAGGTACC AAACCCGAGAGCAAACTCTTG-3' | |
| | | | | 5'-TGCGGCCGCC GTGAGGGGTTCCCTCTTC-3' | |
| | pcDNA4MH-mmPlxd1 | pcDNA4MH-hPlxd1 | 5'-GGTACCAAGCTTAAGTACGCCAGC-3' | 5'-GCTGGCTAGTTAAGCTTGGTACCATCGGGGCGAGCTCTGGC-3' | |
| | | | 5'-AATCCCTATGCAGGAGGAGACGCG-3' | 5'-GCCGTCTCCTCTGCATAGGGATTTCGACTTGGTGTCACTCTCTGTG-3' | |
| | pcDNA4MH-mmPlxd2 | pcDNA4MH-hPlxd2 | 5'-GGTACCAAGCTTAAGTACGCAGC-3' | 5'-GCTGGCTAGTTAAGCTTGTGACCATGGCAGGTTCCCGAGGC-3' | |
| | | | 5'-GCCACAGCCATTCTTGTGACAGTC-3' | 5'-GACTGTCAAGAAGTGGCTGTGCTATAATGAGGACAGGATGAGG-3' | |
| | pLenti-CMV-Blast Plxd1-Strep | pLenti-CMV-Blast-EphA7-Strep | 5'-AAAAAAGCAGGCTCCACCATGCGAGGCGAGCTCTGGCTC-3' | 5'-TCTAGAAGCGCTTGGAGCCATCC-3' | |
| | | | 5'-TGTGGATGGCTCCAAGCGCTTCTAGAGCACTGCTCAGCCTCCATG-3' | 5'-CATGGTGGAGCGCTGCTTTTTGTAC-3' | |
| | pLenti-CMV-Blast Plxd2-Strep | pLenti-CMV-Blast-EphA7-Strep | 5'-AAAAGCAGGCTCCACCATGGCGAGGTTCCCGAAG-3' | 5'-TCTAGAAGCGCTTGGAGCCATCC-3' | |
| | | | 5'-TGTGGATGGCTCCAAGCGCTTCTAGAGCACTGCTGTATACAATAAG-3' | 5'-CATGGTGGAGCCTGCTTTTTGTAC-3' | |
| | pcDNA6V5-RRV 17577 gHΔ21-27 | pcDNA6V5-RRV 17577 gH | 5'-TCCAACGTGCTGGAATTC-3' | | |
| | | | 5'-TTTGTGCGTCACGCTGCACGG-3' | | |
| | pcDNA6V5-RRV 17577 gHY21A | pcDNA6V5-RRV 17577 gH | 5'-CGCTTTGTGCGTCACGCTGCACCG-3' | | |
| | | | 5'-GTGTACGACGAGAAGTCCAAC-3' | | |
| Around-the-horn | pcDNA6V5-RRV 17577 gH V22A | pcDNA6V5-RRV 17577 gH | 5'-TACGACGAGAAGTCCAACGTC-3' | | |
| | | | 5'-CGCGTATTGTGCGTCACGTGC-3' | | |
| | pcDNA6V5-RRV 17577 gH Y23A | pcDNA6V5-RRV 17577 gH | 5'-GACGAGAAGTCCAACGTCG-3' | | |
| | | | 5'-CGCCACGTATTGTGCGTCACGC-3' | | |
| | pcDNA6V5-RRV 17577 gH D24A | pcDNA6V5-RRV 17577 gH | 5'-GAGAAGTCCAACGTGAGC-3' | | |
| | | | 5'-CGGTACACGATTTGTGCGTAC-3' | | |
| | pcDNA6V5-RRV 17577 gH E25A | pcDNA6V5-RRV 17577 gH | 5'-AAGTCCAACGTGAGCTGG-3' | | |
| | | | 5'-CGCCCGACAAATACGTGTACGAC-3' | | |
| | pcDNA6V5-RRV 17577 gH K26A | pcDNA6V5-RRV 17577 gH | 5'-TCCAACGTGAGCTGGAATTC-3' | | |
| | | | 5'-CGCCTCGTGTACACGTATTGTCT-3' | | |
| | pcDNA6V5-RRV 26-95 gHΔ21-27 | pcDNA6V5-RRV 26-95 gH | 5'-Phos/GTGCCTGGCCTGGAGATTGTC-3' | | |
| | | | 5'-Phos/GCCGTTAATTACAGAAAGTGAATC-3' | | |
| | pcDNA6V5-RRV 26-95 gH Y21A | pcDNA6V5-RRV 26-95 gH | 5'-CGCGCCGTTAATTACAGAAAG-3' | | |
| | | | 5'-GAATATAATGAGGAGAAGGTG-3' | | |
| | pcDNA6V5-RRV 26-95 gH E22A | pcDNA6V5-RRV 26-95 gH | 5'-CGCGTAGCCGTTAATTACAG-3' | | |
| | | | 5'-TATAATGAGGAGAAGGTGCC-3' | | |
| pcDNA6V5-RRV 26-95 gH Y23A | pcDNA6V5-RRV 26-95 gH | 5'-CGCTTCGTAGCCGTTAATTAC-3' | | | |
| | | 5'-AATGAGGAGAAGGTGCTGG-3' | | | |
| pcDNA6V5-RRV 26-95 gH N24A | pcDNA6V5-RRV 26-95 gH | 5'-CGCATATTCGTAGCCGTTAATTC-3' | | | |
| | | 5'-GAGGAGAAGGTGCTGGCC-3' | | | |
| pcDNA6V5-RRV 26-95 gH E25A | pcDNA6V5-RRV 26-95 gH | 5'-GGCATTATATTCGTAGCCG-3' | | | |
| | | 5'-GAGAAGGTGCTTGGCTGG-3' | | | |
| pcDNA6V5-RRV 26-95 gH E26A | pcDNA6V5-RRV 26-95 gH | 5'-GGCCTCATTATATTCGTAGCC-3' | | | |
| | | 5'-AAGGTGCTTGGCCTGGAG-3' | | | |
| pcDNA6V5-RRV 26-95 gH K27A | pcDNA6V5-RRV 26-95 gH | 5'-GGCTCTCCTATTATTCGTAG-3' | | | |
| | | 5'-GTGCTGGCTGGAGATTG-3' | | | |
| C) Antibodies | | | | | |
| Western Blot | Target | Clone/ Catalogue Number | Species | concentration | Manufacturer |
| primary antibodies/ detection | V5 tag/ PK tag | SV5-Pk1 | mouse | 1:2000 | Bio-Rad |
| | c-myc | 9E10 | mouse | 1:1000 | Santa Cruz Bio |
| | c-myc | C3956 | rabbit | 1:4000 | Sigma-Aldrich |
| | DYKDDDDK tag (Flag) | D6W58 | rabbit | 1:5000 | Cell Signaling Technology |
| | GAPDH [Biotin] | A00915 | goat | 1:2000 | genscript |
| | StrepTactin-HRP conjugate (also secondary antibody for GAPDH-Biotin) | 2-1502-001 | | 1:5000 | IBA |
| secondary antibodies (HRP) | mouse | | donkey | 1:20 000 | Jackson ImmunoResearch |
| | rabbit | | donkey | 1:20 000 | Jackson ImmunoResearch |

IV DISCUSSION and OUTLOOK

IV.1 Key findings

The manuscripts that constitute the present thesis further define communalities and differences between KSHV and RRV receptor usage by 1) characterizing a conserved motif on the rhadinoviral gH essential for binding to members of the Eph family of receptor tyrosine kinases, 2) defining additional A-type Ephs on BJAB cells, a model B cell line, as cellular receptors for cell-to-cell transmission of KSHV and cell-free infection of RRV and 3) identifying Plexin domain containing proteins as a novel receptor family able to mediate RRV entry into various target cells (Figure 7).

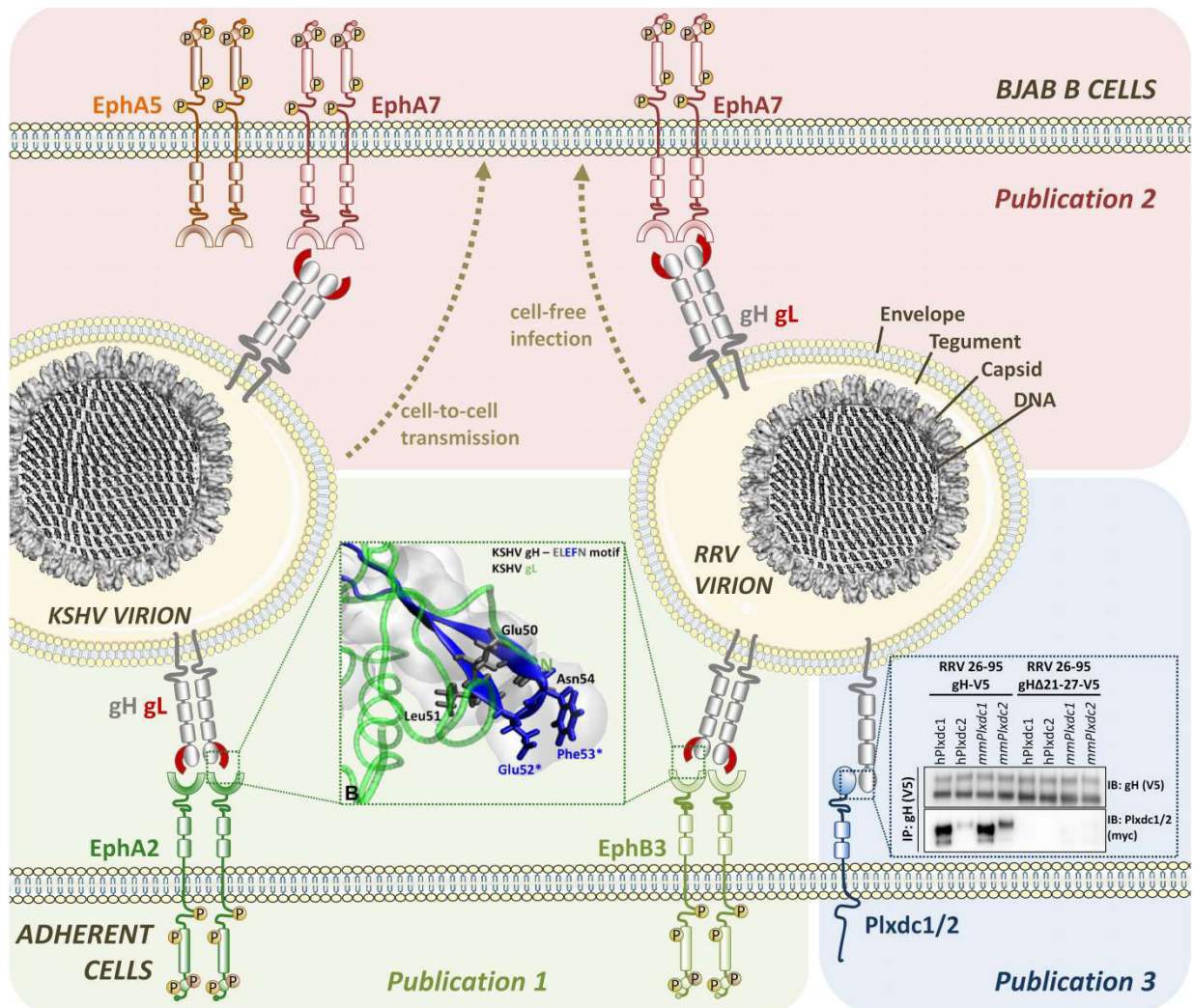


Figure 7 Graphic depiction of key findings that contribute to elucidation of rhadinoviral receptor usage and entry. Background colors indicate individual manuscripts.

IV.2 Determinants of affinity and receptor usage

The importance of the Eph receptor family for rhadinoviral infection of a range of adherent target cells as well as the region mediating this interaction on EphA2, as prototypic KSHV gH/gL interactor have been demonstrated^{86,143–150,247}. However, the crucial Eph-binding domain or motif on the viral gH/gL complex remained elusive. Due to the frequent co-expression of multiple Eph receptors on established cell lines the summed up contribution of Eph receptors to viral entry is hard to assess by knockdown or inhibition of single Eph family members. Another possible problem is the lack of adequate tools for the targeting and detection of proteins of interest (e.g. specific antibodies), which we encountered in case of Plxdc2^{249,250}. Disruption of the essential receptor-binding motif on the viral glycoprotein would allow circumventing these restrictions while excluding possible bystander effects of inhibitory molecules or decoy receptors. To facilitate this approach, we mapped independent, minimal amino acid motifs on KSHV and RRV gH that are crucial for the interaction with Eph family receptors and Plxdc receptors, respectively, providing the basis for future studies on the contribution of Eph and Plxdc receptor interactions to cell and tissue tropism as well as to virus-induced signaling.

While mutation or deletion of the described motifs abrogates the interaction with the corresponding receptor family, different affinities for distinct members of these families displayed by KSHV and RRV or even RRV isolates 26-95 and 17577²⁴⁷ indicate the existence of additional regions in gH or gL that shape the observed binding preferences.

Our study identified two key residues, RRV 26-95 gH Tyr23 and Glu25, which appear to be critical for the interaction of RRV isolate 26-95 with Plxdc1 and Plxdc2 (Publication 3). Even though these amino acids are conserved between RRV isolate 26-95 and isolate 17577, RRV 17577 selectively binds to Plxdc2 and not Plxdc1. Additionally, in contrast to RRV 26-95, this interaction is gL-dependent. Similarly, albeit mutation of two amino acids (KSHV gH Glu52 and Phe53, RRV gH Glu54 and Phe55) in the conserved rhadinoviral “ELEFN” motif is sufficient to completely disrupt the gH/gL interaction with both A-type and B-type Eph receptors, KSHV and RRV exhibit unique preferences for members of either receptor class. Furthermore, the recently described interaction of EBV gH/gL with EphA2 is clearly mediated by distinct binding sites, as the “ELEFN” motif is only partially conserved (“DIEGH”) in EBV gH^{226,227}. Which additional regions determine the preference of individual receptors and if they in turn impact virus biology, by influencing e.g. cell and tissue tropism, spread or pathogenicity has yet to be determined.

However, even if KSHV and RRV bind distinct high affinity Eph receptors, recent studies using adherent cell lines indicate that experimental overexpression of Eph receptors with comparable lower affinity for KSHV gH/gL (e.g. EphA4 and EphA5) can functionally substitute for EphA2 in KSHV

infection^{143,150}. Our study addressing the role of Eph receptors for rhadinoviral infection of B cells – the major reservoir of latent KSHV *in vivo* – now provides evidence that these additional, lower affinity gH/gL-Eph interactions, here shown for EphA7 and EphA5, can also mediate KSHV and RRV entry at endogenous protein levels (Publication 2). Naturally, besides differences in affinity, more basic factors such as the availability, e.g. expression levels of distinct Eph receptors, may influence the cell type-dependent receptor usage. However, the notion that any of the KSHV gH/gL-interacting Eph receptors could potentially substitute for EphA2 was rendered unlikely by a recent study demonstrating that knockout of endogenous EphA4 led to an increase in KSHV infection¹⁴³, which indicates differential properties of individual Ephs in rhadinoviral entry.

To integrate the whole complexity of Eph family receptors, additional studies – preferentially addressing endogenous Eph receptors with loss-of-function methodology – are needed to evaluate the role of specific Eph receptors in shaping rhadinovirus cell tropism, the selective Eph receptor-induced downstream signaling as discussed below as well as the possible impact of the interaction with different Ephs on disease establishment and progression.

IV.3 Determinants of rhadinovirus tropism

As the cellular origin of KSHV-associated pathologies is still under discussion, identifying determinants that shape the cell and tissue tropism of KSHV *in vitro* and *in vivo* could help elucidate initial target cells, and potential starting points for interventions and therapies.

A clear correlation between KSHV/ RRV receptor usage and cell tropism as seen for EBV^{251,252} and human cytomegalovirus (HCMV)^{253–256} has not become apparent yet. In EBV infection for instance, the gH/gL complex acts as determinant of tropism through either direct interaction with the epithelial cell receptor EphA2 or through viral gp42-dependent interaction with the B cell-specific HLA class II receptor²⁵⁷. Similarly, heteromeric glycoprotein complexes of gH/gL with different interaction partners govern the cellular tropism of HCMV. While the trimeric complex comprising gH/gL and the β -herpesvirus-specific gO is thought to primarily enable PDGFR α -dependent cell-free infection of fibroblasts and contribute to cell-free PDGFR α -independent infection of epithelial and endothelial cells, the pentameric gH/gL/UL128/UL130/UL131 complex is required for efficient infection of leukocytes, dendritic cells and enhances infection of endothelial and epithelial cells^{258–261}.

The recombinant virus strains described herein allow us to address the question whether individual receptor interactions shape rhadinoviral tropism to a similar degree or if different receptor families exert redundant functions. For instance, the presented studies provide evidence for a more prominent role of the Eph-gH/gL interaction in RRV infection of lymphatic endothelium than fibroblasts (Publication 1) and identify cell lines that are primarily dependent on Eph receptors (e.g.

Raji, MMB1845) or Plxdc receptors (MFB5487) for RRV infection (Publication 3). However, as Raji, MMB1845 and MFB5487 all express B cell markers, it remains to be determined how these results transfer to RRV cell type tropism *in vivo*. A definite clarification how specific receptors contribute to rhadinoviral cell and tissue tropism requires – besides detailed knowledge about virus-host interactions – a more adequate modelling of the *in vivo* situation than what is currently achieved by established cell culture systems. Prominent issues are the limited availability of or knowledge about potential cell subtypes and changes induced upon immortalization or transformation of cell lines, which could particularly influence expression of tumor-associated receptors such as Ephs and Plxdc. The problem is illustrated by our results on the usage of EphA7 as KSHV/ RRV receptor on BJAB cells. While BJAB cells are widely used as *in vitro* model for B cells, results obtained in this – or other cell lines – may not be easily transferable. For instance, while BJAB cells express both EphA7 and EphA5 to detectable levels (Publication 2), studies on the expression of Eph receptors on mature B cells suggest that only EphA4 is consistently expressed in freshly isolated or cultured B cells from peripheral blood and lymph nodes²⁶². While this further argues that *in vitro* experiments might not reliably predict tropism *in vivo*, data on receptor usage could give important hints regarding *in vivo* target cells. During B cell commitment and differentiation, EphA5 and EphA7 expression was only described in primitive CD34⁺ hematopoietic stem and progenitor cells (HSPC) and is lost after lineage-commitment²⁶³. Given the observed persistence of KSHV infection in CD34⁺ HSPCs after differentiation into CD19⁺ B cell and CD14⁺ monocyte lineages²⁶⁴ and the role of EphA5 and EphA7 in KSHV cell-to-cell transmission into BJAB cells described in this work, EphA5 and EphA7 expressing CD34⁺ HSPCs represent a candidate population for KSHV target cells *in vivo* which might be implicated in pathogenesis as well. Even though to date, KSHV-MCD and PEL are thought to originate at the stage of naïve B cells or possibly in a population of IgM memory B cells, further studies additionally addressing a potential reservoir formation at e.g. very early stages of hematopoietic cell development are necessary for a definite conclusion.

IV.4 Animal models in rhadinovirus research and vaccine vector development

To date, RRV infection of rhesus macaques is the most widely used animal model for KSHV pathogenesis and development of rhadinovirus vaccines and vaccine vectors. RRV infection reflects aspects of KSHV biology both on the scale of the whole host organism and the level of single molecule interactions which is exemplified in the conserved crucial Eph interaction motif (Publication 1) and the conserved EphA7 usage for infection of BJAB cells (Publication 2). However, the present manuscripts also underline divergences, e.g. the binding preferences of KSHV and RRV for distinct Eph receptors as well as the use of the Plxdc family for entry of RRV, but not KSHV.

Furthermore, the stark divergence in the susceptibility of BJAB cells for cell-free infection of RRV but not KSHV could hint to fundamental differences in either the natural target cells or the entry processes of both viruses. As KSHV and RRV belong to the RV1 and RV2 rhadinovirus lineage, respectively, the characterization of non-human primate viruses of the RV1 lineage, such as retroperitoneal fibromatosis viruses from different macaque species³⁹ or the colobine γ -herpesvirus 1⁴⁰ as potential alternative KSHV *in vitro* and *in vivo* models could prove informative for future studies.

The relevance of *in vivo* validation of cell culture experiments in general was strikingly emphasized by the pre-vaccination study our group performed in cooperation with the Desrosiers group. *In vitro*, RRV enters BJAB B cells in an Eph-dependent manner and infection can be inhibited by competition with soluble Eph receptors²⁴⁷ or by Eph receptor knockdown as we demonstrated for EphA7 (Publication 2). Similarly, an Eph-detargeted gL-deficient RRV mutant (RRV Δ gL), which was characterized in detail on adherent cells (Publication 1), did exhibit a drastically attenuated phenotype on B cells of human and rhesus macaque origin²⁴⁵. However, after high-dose intravenous inoculation, a RRV strain, similarly disrupted in gL expression and harboring the SIV-gag protein as vectored antigen readily established persistent infection, elicited robust anti-RRV antibody and gag-specific T cell responses and colonized the CD20⁺ B cell compartment with comparable efficiency as wild-type RRV virus in experimentally or naturally infected rhesus macaques²⁴⁵. Consequently, albeit technical advances in cell culture and organotypic systems allow for increasingly complex experimental approaches the unique features of animal models should not be disregarded.

An interesting example for the relevance of animal experiments not only in validating *in vitro* data but also in opening new directions for subsequent research projects is the use of attenuated rhesus CMV (RhCMV) as vaccination vector for HIV/SIV. Classical CD8⁺ T cell recognition is restricted by major histocompatibility complex (MHC) I and limited to few immunodominant antigen epitopes which do not facilitate protection against pathogens with efficient immune evasion such as HIV/SIV²⁶⁵. A series of studies demonstrated that a 68-1 RhCMV strain expressing SIV Gag, Rev/Nef/Tat, Pol, and Env elicits high-frequency effector-memory T cell responses with broad epitope-targeting and unconventional MHC restriction^{266–268}. Subsequently, the molecular basis for these distinct, unconventional T cell responses was pinpointed to a lack of UL128 and UL130²⁶⁵ which are necessary to form the pentameric complex – the major determinant of CMV tropism as described above – while the dominant presentation of non-canonical antigen epitopes depends on the expression of CMV US11²⁶⁵.

This example not only illustrates the importance of animal models for the development of antiviral strategies but also demonstrates that a detailed understanding of the molecular mechanisms of virus-host interactions during attachment and entry – the earliest steps in the viral

life cycle – is of critical importance for both, the design of intervention strategies (e.g. neutralizing antibodies or small molecule inhibitors) and the rational design of herpesvirus vaccines or their potential use as vaccine vectors. Rhadinoviruses *per se* represent a promising vector system as they can elicit strong T cell responses to vectored antigens – demonstrated in the aforementioned study in cooperation with the Desrosiers Group²⁴⁵ – and are non-pathogenic in healthy hosts. However, to increase the safety and exclude the development of KSHV-associated malignancies, rhadinovirus strains which are de-targeted from potential disease-contributing cell types should be used. The data on receptor usage on different cell types and receptor-binding motifs in the present manuscripts can therefore provide a basis for further studies concerning the potential development of rhadinoviruses as vaccine vectors.

IV.5 Rhadinovirus mutants as probes for receptor-induced signaling

A number of studies from a single lab addressed the induction of early signaling events upon KSHV binding and entry. Yet, several questions such as the distinct contribution of individual glycoprotein-receptor interactions to the temporal and spatial regulation of signaling cascades in different cell types remain unanswered. For instance, activation of the FAK/Src/PI3K pathway was initially attributed to the interaction of KSHV gB with integrin $\alpha_3\beta_1$ ¹⁶². Consequently, soluble KSHV gB was shown to be sufficient for the induction of Src and PI3K phosphorylation and recruitment of downstream effectors in human foreskin fibroblasts (HFF), while KSHV gB, mutated in the classical RGD motif failed to do so¹⁶². Subsequent studies of the same group showed a reduction of KSHV-induced phosphorylation of Src and PI3K upon knockdown of EphA2 (e.g. approx. 80% reduction of p-PI3K levels in shEphA2 transduced cells) in human dermal microvascular endothelial cells (HMVEC-d) and postulated the gB-dependent integrin signaling as upstream event of EphA2-dependent signal amplification¹⁴⁴. Interestingly, while crosstalk between EphA2 and integrins has been proposed in various systems, current literature indicates the activation of Eph receptors by ephrin ligands as upstream event of integrin-mediated signaling^{269–271}. For instance, a recent study linked ephrinA1-EphA2 mediated phosphorylation of Src with spatially divergent FAK activation and formation of integrin/Src/FAK/paxillin complexes in focal adhesions²¹⁹. While recruitment of a large number of signaling molecules into multimolecular complexes upon KSHV infection has been suggested^{141,144–146,164}, it is not clear which virus-receptor interaction initiates these complex signaling events, which interactions are crucial, which interactions only amplify virus entry and productive infection or if there are even any interactions that are strictly essential. As different studies used different cell types, which were proposed to vary in the route of KSHV infection (clathrin-mediated endocytosis was described in HFF⁸⁵ and Human umbilical vein endothelial cells (HUVEC)⁹²,

macropinocytosis was described in HMVEC-d^{91,272} and HUVEC²⁷²), the role of Eph receptor interaction should be addressed regarding different uptake pathways as well as additional cell types with roles in KSHV pathology. In this context, the question whether KSHV-interaction with additional Eph receptors, e.g. EphA5 and EphA7 on BJAB cells (Publication 2), induces signaling responses similar to EphA2-dependent events would also be of interest. Furthermore, it would be useful to compare Eph signaling upon KSHV infection with described canonical and non-canonical Eph pathways. While KSHV gH/gL was shown to interact with the ligand-binding domain of EphA2¹⁴⁹, which would be consistent with activation of the canonical signaling pathways similar to ephrin molecules, a recent study¹⁴⁸ stressed the importance of the non-canonical EphA2 Ser897 phosphorylation, induced upon KSHV infection, for virus entry (Figure 6). As the non-canonical Ser897 phosphorylation is thought to be pro-oncogenic, this could link Eph receptors to the development of KSHV-associated proliferative diseases. Thus far the correlation of described EphA2-signaling upon KSHV infection with specific phosphorylation events is hard to assess, as the initial studies did not provide detailed information on the analyzed phosphorylation sites¹⁴⁵. Unraveling the differential activation of EphA2 by KSHV and the impact of EphA2 sequence variants associated with KSHV infection and KS development²⁷³ could help guide future studies regarding the role of EphA2 in KSHV-associated tumorigenesis and provide a platform to extend these analyses to additional, EphA2-associated tumors.

A potential problem in the analysis of virus-induced signaling lies in the application of suitable controls. Lytic replication and production of virus stocks releases a multitude of signaling molecules and ligands which are hard to eliminate or control for and can potentially activate a multitude of cellular signaling pathways complicating the evaluation of signaling events induced by distinct virus-receptor interactions. The KSHV/ RRV strains mutated in the Eph receptor interaction motif as well as corresponding soluble glycoproteins, which do not interact with Eph receptors in comparison to wild-type versions, constitute a perfectly controlled system to specifically analyze the contribution of Eph receptor engagement to cellular signal transduction both in infection and pathophysiology.

A similar system could be used to shed light on potential signaling events upon binding of RRV gH to Plxdc receptors. Using glycoproteins from RRV isolate 26-95 and 17577, and corresponding constructs mutated in the Plxdc interaction motif, we can target either Plxdc2, or both Plxdc1 and Plxdc2 with perfectly matched controls. This system is of particular interest as most studies concerning the Plxdc family focus on their role as tumor marker, and mechanistic information on the physiological and pathophysiological role of Plxdc1/2 is still sparse.

Similar to the Eph receptor family, Plxdc1 or tumor endothelial marker 7 (TEM7) was first identified in gene expression profiles of endothelial cells from colorectal cancer tissue²⁷⁴. In the following, overexpression of either Plxdc1 or Plxdc2 was demonstrated in a variety of solid tumors^{275–278,278–280}. Plxdc1 was identified as negative prognostic marker in gastric cancer²⁸¹, osteogenic

sarcoma²⁸² and glioblastoma^{283,284} and down-regulation of Plxdc1 significantly reduced tumor cell migration and invasion²⁸¹ as well as tumor growth²⁸⁵, while Plxdc2 expression in different solid tumors was associated with radio- and chemo-resistance^{278,279} as well as poor prognosis²⁸⁰.

The analysis of specific cellular alterations upon Plxdc receptor activation is complicated by the limited information on physiological ligands together with their low specificity for Plxdc receptors. While nidogen²⁸⁶, cortactin²⁷⁷ and pigment epithelium derived factor (PEDF)²⁸⁷ have been suggested as interaction partners of Plxdc1/2, all three molecules interact with a variety of cellular proteins, which impedes the select analysis of Plxdc-dependent signaling. Furthermore, cortactin was characterized as an actin-associated, cytoplasmic protein²⁸⁸, making a role in the initiation of outside-in signaling unlikely. The use of Plxdc-interaction deficient RRV gH compared to wild-type RRV gH could help to identify Plxdc-specific signaling cascades and even decipher differences between Plxdc1 and Plxdc2 activation by using the Plxdc2-selectivity of RRV isolate 17577.

In general, the apparent preference of pathogens for receptors which are implicated in tumor development or maintenance, as shown here for Eph and Plxdc receptors, could provide interesting new research questions. Several tumor-associated phenotypical alterations, e.g. regarding metabolic, transcriptional, and signaling networks have also been demonstrated in KSHV-infected cells, suggesting common mechanisms for both pathologies. As KSHV-infection is associated with the development of three proliferative diseases, these similarities are not surprising in itself. However, the question whether elevated expression of tumor receptors in itself is already favorable for cancer development and infection or whether their role in KSHV pathogenesis relies on activation of signaling cascades upon virus binding remains to be determined in future studies.

REFERENCES

1. Chang, Y., Moore, P. S. & Weiss, R. A. Human oncogenic viruses: nature and discovery. *Philos. Trans. R. Soc. B Biol. Sci.* **372**, 20160264 (2017).
2. Kaposi. Idiopathisches multiples Pigmentsarkom der Haut. *Arch. Für Dermatol. Syph.* **4**, 265–273 (1872).
3. Cesarman, E. *et al.* Kaposi sarcoma. *Nat. Rev. Dis. Primer* **5**, 9 (2019).
4. Montpellier, J. & Mussini-Montpellier, J. *Le cancer en France d'outre-mer: Considérations pathogéniques*. (Librairie Ferraris, 1947).
5. D'oliveira, J. J. G. & Torres, F. O. Kaposi's sarcoma in the bantu of mozambique. *Cancer* **30**, 553–561 (1972).
6. Thijs, A. [Kaposi's angiosarcomatosis in the Belgian Congo & Ruanda-Urundi]. *Ann. Soc. Belge Med. Trop.* **1920** **37**, 295–308 (1957).
7. Ziegler, J. L. & Katongole-Mbidde, E. Kaposi's sarcoma in childhood: an analysis of 100 cases from Uganda and relationship to HIV infection. *Int. J. Cancer* **65**, 200–203 (1996).
8. Gj, G. *et al.* A preliminary communication on extensively disseminated Kaposi's sarcoma in young homosexual men. *Am. J. Dermatopathol.* **3**, 111–114 (1981).
9. Grulich, A. E. & Vajdic, C. M. The epidemiology of cancers in human immunodeficiency virus infection and after organ transplantation. *Semin. Oncol.* **42**, 247–257 (2015).
10. Unemori, P. *et al.* Immunosenescence is associated with presence of Kaposi's sarcoma in antiretroviral treated HIV infection. *AIDS Lond. Engl.* **27**, 1735–1742 (2013).
11. Thakker, S. & Verma, S. C. Co-infections and Pathogenesis of KSHV-Associated Malignancies. *Front. Microbiol.* **7**, (2016).
12. Beral, V., Peterman, T. A., Berkelman, R. L. & Jaffe, H. W. Kaposi's sarcoma among persons with AIDS: a sexually transmitted infection? *Lancet Lond. Engl.* **335**, 123–128 (1990).
13. Hermans, P. *et al.* Epidemiology of AIDS-related Kaposi's sarcoma in Europe over 10 years. (1996).
14. Elford, J., McDonald, A. & Kaldor, J. Kaposi's sarcoma as a sexually transmissible infection: an analysis of Australian AIDS surveillance data. The National HIV Surveillance Committee. *AIDS Lond. Engl.* **7**, 1667–1671 (1993).
15. International Collaboration on HIV and Cancer. Highly active antiretroviral therapy and incidence of cancer in human immunodeficiency virus-infected adults. *J. Natl. Cancer Inst.* **92**, 1823–1830 (2000).
16. Chang, Y. *et al.* Identification of herpesvirus-like DNA sequences in AIDS-associated Kaposi's sarcoma. *Science* **266**, 1865–1869 (1994).
17. Cesarman, E., Chang, Y., Moore, P. S., Said, J. W. & Knowles, D. M. Kaposi's sarcoma-associated herpesvirus-like DNA sequences in AIDS-related body-cavity-based lymphomas. *N. Engl. J. Med.* **332**, 1186–1191 (1995).
18. Soulier, J. *et al.* Kaposi's sarcoma-associated herpesvirus-like DNA sequences in multicentric Castleman's disease. *Blood* **86**, 1276–1280 (1995).
19. Oksenhendler, E. *et al.* Multicentric Castleman's disease in HIV infection: a clinical and pathological study of 20 patients. *AIDS Lond. Engl.* **10**, 61–67 (1996).
20. Dossier, A. *et al.* Human herpesvirus 8-related Castleman disease in the absence of HIV infection. *Clin. Infect. Dis. Off. Publ. Infect. Dis. Soc. Am.* **56**, 833–842 (2013).
21. Bower, M. *et al.* Clinical Features and Outcome in HIV-Associated Multicentric Castleman's Disease. *J. Clin. Oncol.* **29**, 2481–2486 (2011).
22. Swerdlow, S. H. *et al.* The 2016 revision of the World Health Organization classification of lymphoid neoplasms. *Blood* **127**, 2375–2390 (2016).
23. Nador, R. G. *et al.* Primary effusion lymphoma: a distinct clinicopathologic entity associated with the Kaposi's sarcoma-associated herpes virus. *Blood* **88**, 645–656 (1996).

REFERENCES

24. Chadburn, A. *et al.* KSHV-positive solid lymphomas represent an extra-cavitary variant of primary effusion lymphoma. *Am. J. Surg. Pathol.* **28**, 1401–1416 (2004).
25. Gaidano, G. *et al.* Molecular characterization of HHV-8 positive primary effusion lymphoma reveals pathogenetic and histogenetic features of the disease. *J. Clin. Virol.* **16**, 215–224 (2000).
26. Oksenhendler, E., Clauvel, J. P., Jouveshomme, S., Davi, F. & Mansour, G. Complete remission of a primary effusion lymphoma with antiretroviral therapy. *Am. J. Hematol.* **57**, 266 (1998).
27. Hocqueloux, L., Agbalika, F., Oksenhendler, E. & Molina, J. M. Long-term remission of an AIDS-related primary effusion lymphoma with antiviral therapy. *AIDS Lond. Engl.* **15**, 280–282 (2001).
28. Ripamonti, D., Marini, B., Rambaldi, A. & Suter, F. Treatment of primary effusion lymphoma with highly active antiviral therapy in the setting of HIV infection. *AIDS Lond. Engl.* **22**, 1236–1237 (2008).
29. Narkhede, M., Arora, S. & Ujjani, C. Primary effusion lymphoma: current perspectives. *OncoTargets Ther.* **11**, 3747–3754 (2018).
30. Uldrick, T. S. *et al.* An interleukin-6-related systemic inflammatory syndrome in patients co-infected with Kaposi sarcoma-associated herpesvirus and HIV but without Multicentric Castleman disease. *Clin. Infect. Dis. Off. Publ. Infect. Dis. Soc. Am.* **51**, 350–358 (2010).
31. Davison, A. J. *et al.* Virus Taxonomy: VIIIth Report of the International Committee on Taxonomy of Viruses. in *Virus Taxonomy: Classification and Nomenclature of Viruses, Eighth Report of the International Committee on the Taxonomy of Viruses* 193–212.
32. Pellett, P. E. & Roizman, B. Herpesviridae. in *Field's Virology* vol. 2 1802–1822 (Lippincott Williams & Wilkins, 2013).
33. Farley, C. A., Banfield, W. G., Kasnic, G. & Foster, W. S. Oyster herpes-type virus. *Science* **178**, 759–760 (1972).
34. Roizman, B. *et al.* Herpesviridae. Definition, provisional nomenclature, and taxonomy. The Herpesvirus Study Group, the International Committee on Taxonomy of Viruses. *Intervirology* **16**, 201–217 (1981).
35. McGeoch, D. J. & Cook, S. Molecular phylogeny of the alphaherpesvirinae subfamily and a proposed evolutionary timescale. *J. Mol. Biol.* **238**, 9–22 (1994).
36. McGeoch, D. J., Cook, S., Dolan, A., Jamieson, F. E. & Telford, E. A. Molecular phylogeny and evolutionary timescale for the family of mammalian herpesviruses. *J. Mol. Biol.* **247**, 443–458 (1995).
37. McGeoch, D. J., Gatherer, D. & Dolan, A. On phylogenetic relationships among major lineages of the Gammaherpesvirinae. *J. Gen. Virol.* **86**, 307–316 (2005).
38. McGeoch, D. J., Dolan, A. & Ralph, A. C. Toward a comprehensive phylogeny for mammalian and avian herpesviruses. *J. Virol.* **74**, 10401–10406 (2000).
39. Rose, T. M. *et al.* Identification of two homologs of the Kaposi's sarcoma-associated herpesvirus (human herpesvirus 8) in retroperitoneal fibromatosis of different macaque species. *J. Virol.* **71**, 4138–4144 (1997).
40. Dhingra, A. *et al.* Novel Virus Related to Kaposi's Sarcoma-Associated Herpesvirus from Colobus Monkey. *Emerg. Infect. Dis.* **25**, 1548–1551 (2019).
41. Greensill, J. *et al.* Two distinct gamma-2 herpesviruses in African green monkeys: a second gamma-2 herpesvirus lineage among old world primates? *J. Virol.* **74**, 1572–1577 (2000).
42. Desrosiers, R. C. *et al.* A herpesvirus of rhesus monkeys related to the human Kaposi's sarcoma-associated herpesvirus. *J. Virol.* **71**, 9764–9769 (1997).
43. Searles, R. P., Bergquam, E. P., Axthelm, M. K. & Wong, S. W. Sequence and genomic analysis of a Rhesus macaque rhadinovirus with similarity to Kaposi's sarcoma-associated herpesvirus/human herpesvirus 8. *J. Virol.* **73**, 3040–3053 (1999).
44. Estep, R. D., Hansen, S. G., Rogers, K. S., Axthelm, M. K. & Wong, S. W. Genomic characterization of Japanese macaque rhadinovirus, a novel herpesvirus isolated from a nonhuman primate with a spontaneous inflammatory demyelinating disease. *J. Virol.* **87**, 512–523 (2013).

REFERENCES

45. Auerbach, M. R., Czajak, S. C., Johnson, W. E., Desrosiers, R. C. & Alexander, L. Species specificity of macaque rhadinovirus glycoprotein B sequences. *J. Virol.* **74**, 584–590 (2000).
46. Strand, K. *et al.* Two distinct lineages of macaque gamma herpesviruses related to the Kaposi's sarcoma associated herpesvirus. *J. Clin. Virol. Off. Publ. Pan Am. Soc. Clin. Virol.* **16**, 253–269 (2000).
47. Kaleeba, J. A. R. & Berger, E. A. Broad target cell selectivity of Kaposi's sarcoma-associated herpesvirus glycoprotein-mediated cell fusion and virion entry. *Virology* **354**, 7–14 (2006).
48. Damania, B. & Cesarman, E. Kaposi's Sarcoma-Associated Herpesvirus. in *Field's Virology* vol. 2 2080–2128 (Lippincott Williams & Wilkins, 2013).
49. Mbulaiteye, S. *et al.* Molecular evidence for mother-to-child transmission of Kaposi sarcoma-associated herpesvirus in Uganda and K1 gene evolution within the host. *J. Infect. Dis.* **193**, 1250–1257 (2006).
50. He, J. *et al.* Seroprevalence of human herpesvirus 8 among Zambian women of childbearing age without Kaposi's sarcoma (KS) and mother-child pairs with KS. *J. Infect. Dis.* **178**, 1787–1790 (1998).
51. Pica, F. & Volpi, A. Transmission of human herpesvirus 8: an update. *Curr. Opin. Infect. Dis.* **20**, 152–156 (2007).
52. Pauk, J. *et al.* Mucosal shedding of human herpesvirus 8 in men. *N. Engl. J. Med.* **343**, 1369–1377 (2000).
53. Cannon, M. J. *et al.* Blood-borne and sexual transmission of human herpesvirus 8 in women with or at risk for human immunodeficiency virus infection. *N. Engl. J. Med.* **344**, 637–643 (2001).
54. Martin, J. N. *et al.* Sexual transmission and the natural history of human herpesvirus 8 infection. *N. Engl. J. Med.* **338**, 948–954 (1998).
55. Melbye, M. *et al.* Risk factors for Kaposi's-sarcoma-associated herpesvirus (KSHV/HHV-8) seropositivity in a cohort of homosexual men, 1981-1996. *Int. J. Cancer* **77**, 543–548 (1998).
56. Engels, E. A. *et al.* Risk factors for human herpesvirus 8 infection among adults in the United States and evidence for sexual transmission. *J. Infect. Dis.* **196**, 199–207 (2007).
57. Johnson, A. S., Maronian, N. & Vieira, J. Activation of Kaposi's sarcoma-associated herpesvirus lytic gene expression during epithelial differentiation. *J. Virol.* **79**, 13769–13777 (2005).
58. Myoung, J. & Ganem, D. Active lytic infection of human primary tonsillar B cells by KSHV and its noncytolytic control by activated CD4+ T cells. *J. Clin. Invest.* **121**, 1130–1140 (2011).
59. Blasig, C. *et al.* Monocytes in Kaposi's sarcoma lesions are productively infected by human herpesvirus 8. *J. Virol.* **71**, 7963–7968 (1997).
60. Duus, K. M., Lentchitsky, V., Wagenaar, T., Grose, C. & Webster-Cyriaque, J. Wild-type Kaposi's sarcoma-associated herpesvirus isolated from the oropharynx of immune-competent individuals has tropism for cultured oral epithelial cells. *J. Virol.* **78**, 4074–4084 (2004).
61. Seifi, A. *et al.* The lytic activation of KSHV during keratinocyte differentiation is dependent upon a suprabasal position, the loss of integrin engagement, and calcium, but not the interaction of cadherins. *Virology* **410**, 17–29 (2011).
62. Sirianni, M. C. *et al.* gamma-Interferon production in peripheral blood mononuclear cells and tumor infiltrating lymphocytes from Kaposi's sarcoma patients: correlation with the presence of human herpesvirus-8 in peripheral blood mononuclear cells and lesional macrophages. *Blood* **91**, 968–976 (1998).
63. Hassman, L. M., Ellison, T. J. & Kedes, D. H. KSHV infects a subset of human tonsillar B cells, driving proliferation and plasmablast differentiation. *J. Clin. Invest.* **121**, 752–768 (2011).
64. Myoung, J. & Ganem, D. Infection of Lymphoblastoid Cell Lines by Kaposi's Sarcoma-Associated Herpesvirus: Critical Role of Cell-Associated Virus γ . *J. Virol.* **85**, 9767–9777 (2011).
65. Reed, J. A. *et al.* Demonstration of Kaposi's sarcoma-associated herpes virus cyclin D homolog in cutaneous Kaposi's sarcoma by colorimetric in situ hybridization using a catalyzed signal amplification system. *Blood* **91**, 3825–3832 (1998).

REFERENCES

66. Foreman, K. E., Bacon, P. E., Hsi, E. D. & Nickoloff, B. J. In situ polymerase chain reaction-based localization studies support role of human herpesvirus-8 as the cause of two AIDS-related neoplasms: Kaposi's sarcoma and body cavity lymphoma. *J. Clin. Invest.* **99**, 2971–2978 (1997).
67. Chagas, C. A. *et al.* Detection of herpesvirus type 8 (HHV8) in children's tonsils and adenoids by immunohistochemistry and in situ hybridization. *Int. J. Pediatr. Otorhinolaryngol.* **70**, 65–72 (2006).
68. Webster-Cyriaque, J., Duus, K., Cooper, C. & Duncan, M. Oral EBV and KSHV infection in HIV. *Adv. Dent. Res.* **19**, 91–95 (2006).
69. Boshoff, C. *et al.* Kaposi's sarcoma-associated herpesvirus infects endothelial and spindle cells. *Nat. Med.* **1**, 1274–1278 (1995).
70. Ensoli, B., Stürzl, M. & Monini, P. Reactivation and role of HHV-8 in Kaposi's sarcoma initiation. *Adv. Cancer Res.* **81**, 161–200 (2001).
71. Roth, W. K., Brandstetter, H. & Stürzl, M. Cellular and molecular features of HIV-associated Kaposi's sarcoma. *AIDS Lond. Engl.* **6**, 895–913 (1992).
72. Jussila, L. *et al.* Lymphatic endothelium and Kaposi's sarcoma spindle cells detected by antibodies against the vascular endothelial growth factor receptor-3. *Cancer Res.* **58**, 1599–1604 (1998).
73. Sakakibara, S. & Tosato, G. Regulation of angiogenesis in malignancies associated with Epstein-Barr virus and Kaposi's sarcoma-associated herpes virus. *Future Microbiol.* **4**, 903–917 (2009).
74. Mesri, E. A., Cesarman, E. & Boshoff, C. Kaposi's sarcoma and its associated herpesvirus. *Nat. Rev. Cancer* **10**, 707–719 (2010).
75. Simonart, T. *et al.* Expression of the fibroblast/macrophage marker 1B10 by spindle cells in Kaposi's sarcoma lesions and by Kaposi's sarcoma-derived tumor cells. *J. Cutan. Pathol.* **29**, 72–78 (2002).
76. Uccini, S. *et al.* Kaposi's sarcoma cells express the macrophage-associated antigen mannose receptor and develop in peripheral blood cultures of Kaposi's sarcoma patients. *Am. J. Pathol.* **150**, 929–938 (1997).
77. Kaaya, E. E. *et al.* Heterogeneity of spindle cells in Kaposi's sarcoma: comparison of cells in lesions and in culture. *J. Acquir. Immune Defic. Syndr. Hum. Retrovirology Off. Publ. Int. Retrovirology Assoc.* **10**, 295–305 (1995).
78. Li, Y. *et al.* Evidence for Kaposi Sarcoma Originating from Mesenchymal Stem Cell through KSHV-induced Mesenchymal-to-Endothelial Transition. *Cancer Res.* **78**, 230–245 (2018).
79. Jarousse, N., Chandran, B. & Coscoy, L. Lack of heparan sulfate expression in B-cell lines: implications for Kaposi's sarcoma-associated herpesvirus and murine gammaherpesvirus 68 infections. *J. Virol.* **82**, 12591–12597 (2008).
80. Rappocciolo, G. *et al.* Human Herpesvirus 8 Infects and Replicates in Primary Cultures of Activated B Lymphocytes through DC-SIGN. *J. Virol.* **82**, 4793–4806 (2008).
81. Du, M. Q. *et al.* Kaposi sarcoma-associated herpesvirus infects monotypic (IgM lambda) but polyclonal naive B cells in Castleman disease and associated lymphoproliferative disorders. *Blood* **97**, 2130–2136 (2001).
82. Matolcsy, A., Nádor, R. G., Cesarman, E. & Knowles, D. M. Immunoglobulin VH gene mutational analysis suggests that primary effusion lymphomas derive from different stages of B cell maturation. *Am. J. Pathol.* **153**, 1609–1614 (1998).
83. Fan, W. *et al.* Distinct subsets of primary effusion lymphoma can be identified based on their cellular gene expression profile and viral association. *J. Virol.* **79**, 1244–1251 (2005).
84. Dollery, S. J., Santiago-Crespo, R. J., Kardava, L., Moir, S. & Berger, E. A. Efficient infection of a human B cell line with cell-free Kaposi's sarcoma-associated herpesvirus. *J. Virol.* **88**, 1748–1757 (2014).
85. Dollery, S. J. Towards Understanding KSHV Fusion and Entry. *Viruses* **11**, 1073 (2019).
86. Hahn, A. *et al.* The Ephrin Receptor Tyrosine Kinase A2 is a Cellular Receptor for Kaposi's Sarcoma-Associated Herpesvirus. *Nat. Med.* **18**, 961–966 (2012).

REFERENCES

87. Rappocciolo, G. *et al.* DC-SIGN is a receptor for human herpesvirus 8 on dendritic cells and macrophages. *J. Immunol. Baltim. Md 1950* **176**, 1741–1749 (2006).
88. Akula, S. M., Pramod, N. P., Wang, F. Z. & Chandran, B. Integrin $\alpha 3\beta 1$ (CD 49c/29) is a cellular receptor for Kaposi's sarcoma-associated herpesvirus (KSHV/HHV-8) entry into the target cells. *Cell* **108**, 407–419 (2002).
89. Dezube, B. J., Zambela, M., Sage, D. R., Wang, J.-F. & Fingerhuth, J. D. Characterization of Kaposi sarcoma-associated herpesvirus/human herpesvirus-8 infection of human vascular endothelial cells: early events. *Blood* **100**, 888–896 (2002).
90. Inoue, N., Winter, J., Lal, R. B., Offermann, M. K. & Koyano, S. Characterization of Entry Mechanisms of Human Herpesvirus 8 by Using an Rta-Dependent Reporter Cell Line. *J. Virol.* **77**, 8147–8152 (2003).
91. Akula, S. M. *et al.* Kaposi's Sarcoma-Associated Herpesvirus (Human Herpesvirus 8) Infection of Human Fibroblast Cells Occurs through Endocytosis. *J. Virol.* **77**, 7978–7990 (2003).
92. Greene, W. & Gao, S.-J. Actin dynamics regulate multiple endosomal steps during Kaposi's sarcoma-associated herpesvirus entry and trafficking in endothelial cells. *PLoS Pathog.* **5**, e1000512 (2009).
93. Naranatt, P. P., Krishnan, H. H., Smith, M. S. & Chandran, B. Kaposi's sarcoma-associated herpesvirus modulates microtubule dynamics via RhoA-GTP-diaphanous 2 signaling and utilizes the dynein motors to deliver its DNA to the nucleus. *J. Virol.* **79**, 1191–1206 (2005).
94. Ballestas, M. E., Chatis, P. A. & Kaye, K. M. Efficient persistence of extrachromosomal KSHV DNA mediated by latency-associated nuclear antigen. *Science* **284**, 641–644 (1999).
95. Samols, M. A., Hu, J., Skalsky, R. L. & Renne, R. Cloning and Identification of a MicroRNA Cluster within the Latency-Associated Region of Kaposi's Sarcoma-Associated Herpesvirus. *J. Virol.* **79**, 9301–9305 (2005).
96. Dittmer, D. *et al.* A cluster of latently expressed genes in Kaposi's sarcoma-associated herpesvirus. *J. Virol.* **72**, 8309–8315 (1998).
97. Cai, X. *et al.* Kaposi's sarcoma-associated herpesvirus expresses an array of viral microRNAs in latently infected cells. *Proc. Natl. Acad. Sci. U. S. A.* **102**, 5570–5575 (2005).
98. Lin, C. L. *et al.* Kaposi's sarcoma-associated herpesvirus lytic origin (ori-Lyt)-dependent DNA replication: identification of the ori-Lyt and association of K8 bZip protein with the origin. *J. Virol.* **77**, 5578–5588 (2003).
99. Deng, Z., Wang, Z. & Lieberman, P. M. Telomeres and viruses: common themes of genome maintenance. *Front. Oncol.* **2**, 201 (2012).
100. Davis, D. A. *et al.* Hypoxia induces lytic replication of Kaposi sarcoma-associated herpesvirus. *Blood* **97**, 3244–3250 (2001).
101. Ye, F. *et al.* Reactive oxygen species hydrogen peroxide mediates Kaposi's sarcoma-associated herpesvirus reactivation from latency. *PLoS Pathog.* **7**, e1002054 (2011).
102. Ye, F. & Gao, S.-J. A novel role of hydrogen peroxide in Kaposi sarcoma-associated herpesvirus reactivation. *Cell Cycle Georget. Tex* **10**, 3237–3238 (2011).
103. Zhu, F. X., Cusano, T. & Yuan, Y. Identification of the immediate-early transcripts of Kaposi's sarcoma-associated herpesvirus. *J. Virol.* **73**, 5556–5567 (1999).
104. Jenner, R. G., Albà, M. M., Boshoff, C. & Kellam, P. Kaposi's sarcoma-associated herpesvirus latent and lytic gene expression as revealed by DNA arrays. *J. Virol.* **75**, 891–902 (2001).
105. Saveliev, A., Zhu, F. & Yuan, Y. Transcription mapping and expression patterns of genes in the major immediate-early region of Kaposi's sarcoma-associated herpesvirus. *Virology* **299**, 301–314 (2002).
106. Carroll, K. D., Khadim, F., Spadavecchia, S., Palmeri, D. & Lukac, D. M. Direct interactions of Kaposi's sarcoma-associated herpesvirus/human herpesvirus 8 ORF50/Rta protein with the cellular protein octamer-1 and DNA are critical for specifying transactivation of a delayed-early promoter and stimulating viral reactivation. *J. Virol.* **81**, 8451–8467 (2007).

REFERENCES

107. Davis, Z. H., Hesser, C. R., Park, J. & Glaunsinger, B. A. Interaction between ORF24 and ORF34 in the Kaposi's Sarcoma-Associated Herpesvirus Late Gene Transcription Factor Complex Is Essential for Viral Late Gene Expression. *J. Virol.* **90**, 599–604 (2016).
108. Gradoville, L. *et al.* Kaposi's sarcoma-associated herpesvirus open reading frame 50/Rta protein activates the entire viral lytic cycle in the HH-B2 primary effusion lymphoma cell line. *J. Virol.* **74**, 6207–6212 (2000).
109. Damania, B. *et al.* Comparison of the Rta/Orf50 transactivator proteins of gamma-2-herpesviruses. *J. Virol.* **78**, 5491–5499 (2004).
110. Alconada, A., Bauer, U., Sodeik, B. & Hoflack, B. Intracellular traffic of herpes simplex virus glycoprotein gE: characterization of the sorting signals required for its trans-Golgi network localization. *J. Virol.* **73**, 377–387 (1999).
111. Granzow, H. *et al.* Egress of alphaherpesviruses: comparative ultrastructural study. *J. Virol.* **75**, 3675–3684 (2001).
112. Harley, C. A., Dasgupta, A. & Wilson, D. W. Characterization of herpes simplex virus-containing organelles by subcellular fractionation: role for organelle acidification in assembly of infectious particles. *J. Virol.* **75**, 1236–1251 (2001).
113. Close, W. L., Anderson, A. N. & Pellett, P. E. Betaherpesvirus Virion Assembly and Egress. *Adv. Exp. Med. Biol.* **1045**, 167–207 (2018).
114. Zhu, F. X., Chong, J. M., Wu, L. & Yuan, Y. Virion proteins of Kaposi's sarcoma-associated herpesvirus. *J. Virol.* **79**, 800–811 (2005).
115. Mark, L., Lee, W. H., Spiller, O. B., Villoutreix, B. O. & Blom, A. M. The Kaposi's sarcoma-associated herpesvirus complement control protein (KCP) binds to heparin and cell surfaces via positively charged amino acids in CCP1-2. *Mol. Immunol.* **43**, 1665–1675 (2006).
116. Mousavinezhad-Moghaddam, M., Amin, A. A., Rafatpanah, H. & Rezaee, S. A. R. A new insight into viral proteins as Immunomodulatory therapeutic agents: KSHV vOX2 a homolog of human CD200 as a potent anti-inflammatory protein. *Iran. J. Basic Med. Sci.* **19**, 2–13 (2016).
117. Connolly, S. A., Jackson, J. O., Jardetzky, T. S. & Longnecker, R. Fusing structure and function: a structural view of the herpesvirus entry machinery. *Nat. Rev. Microbiol.* **9**, 369–381 (2011).
118. Heldwein, E. E. gH/gL supercomplexes at early stages of herpesvirus entry. *Curr. Opin. Virol.* **18**, 1–8 (2016).
119. Möhl, B. S., Chen, J., Sathiyamoorthy, K., Jardetzky, T. S. & Longnecker, R. Structural and Mechanistic Insights into the Tropism of Epstein-Barr Virus. *Mol. Cells* **39**, 286–291 (2016).
120. Baghian, A. *et al.* Glycoprotein B of human herpesvirus 8 is a component of the virion in a cleaved form composed of amino- and carboxyl-terminal fragments. *Virology* **269**, 18–25 (2000).
121. Hahn, A. *et al.* Kaposi's sarcoma-associated herpesvirus gH/gL: glycoprotein export and interaction with cellular receptors. *J. Virol.* **83**, 396–407 (2009).
122. Cooper, R. S. & Heldwein, E. E. Herpesvirus gB: A Finely Tuned Fusion Machine. *Viruses* **7**, 6552–6569 (2015).
123. Chandran, B. & Hutt-Fletcher, L. Gammaherpesviruses entry and early events during infection. in *Human Herpesviruses: Biology, Therapy, and Immunoprophylaxis* (eds. Arvin, A. *et al.*) (Cambridge University Press, 2007).
124. Spiller, O. B. *et al.* Complement regulation by Kaposi's sarcoma-associated herpesvirus ORF4 protein. *J. Virol.* **77**, 592–599 (2003).
125. Spiller, O. B. *et al.* Dissecting the Regions of Virion-Associated Kaposi's Sarcoma-Associated Herpesvirus Complement Control Protein Required for Complement Regulation and Cell Binding. *J. Virol.* **80**, 4068–4078 (2006).
126. Koyano, S., Mar, E.-C., Stamey, F. R. & Inoue, N. Glycoproteins M and N of human herpesvirus 8 form a complex and inhibit cell fusion. *J. Gen. Virol.* **84**, 1485–1491 (2003).
127. Chandran, B. *et al.* Human herpesvirus-8 ORF K8.1 gene encodes immunogenic glycoproteins generated by spliced transcripts. *Virology* **249**, 140–149 (1998).

REFERENCES

128. Zhu, L., Puri, V. & Chandran, B. Characterization of human herpesvirus-8 K8.1A/B glycoproteins by monoclonal antibodies. *Virology* **262**, 237–249 (1999).
129. Wu, L., Renne, R., Ganem, D. & Forghani, B. Human herpesvirus 8 glycoprotein K8.1: expression, post-translational modification and localization analyzed by monoclonal antibody. *J. Clin. Virol. Off. Publ. Pan Am. Soc. Clin. Virol.* **17**, 127–136 (2000).
130. Raab, M. S. *et al.* The immunogenic glycoprotein gp35-37 of human herpesvirus 8 is encoded by open reading frame K8.1. *J. Virol.* **72**, 6725–6731 (1998).
131. Engels, E. A. *et al.* Latent class analysis of human herpesvirus 8 assay performance and infection prevalence in sub-saharan Africa and Malta. *Int. J. Cancer* **88**, 1003–1008 (2000).
132. Dollery, S. J., Santiago-Crespo, R. J., Chatterjee, D. & Berger, E. A. Glycoprotein K8.1A of Kaposi's Sarcoma-Associated Herpesvirus Is a Critical B Cell Tropism Determinant Independent of Its Heparan Sulfate Binding Activity. *J. Virol.* **93**, (2019).
133. Birkmann, A. *et al.* Cell Surface Heparan Sulfate Is a Receptor for Human Herpesvirus 8 and Interacts with Envelope Glycoprotein K8.1. *J. Virol.* **75**, 11583–11593 (2001).
134. Luna, R. E. *et al.* Kaposi's sarcoma-associated herpesvirus glycoprotein K8.1 is dispensable for virus entry. *J. Virol.* **78**, 6389–6398 (2004).
135. Gardner, M. R. & Glaunsinger, B. A. Kaposi's Sarcoma-Associated Herpesvirus ORF68 Is a DNA Binding Protein Required for Viral Genome Cleavage and Packaging. *J. Virol.* **92**, (2018).
136. Akula, S. M., Wang, F. Z., Vieira, J. & Chandran, B. Human herpesvirus 8 interaction with target cells involves heparan sulfate. *Virology* **282**, 245–255 (2001).
137. Maginnis, M. S. Virus-Receptor Interactions: The Key to Cellular Invasion. *J. Mol. Biol.* **430**, 2590–2611 (2018).
138. Wang, F.-Z., Akula, S. M., Sharma-Walia, N., Zeng, L. & Chandran, B. Human Herpesvirus 8 Envelope Glycoprotein B Mediates Cell Adhesion via Its RGD Sequence. *J. Virol.* **77**, 3131–3147 (2003).
139. Hynes, R. O. Integrins: bidirectional, allosteric signaling machines. *Cell* **110**, 673–687 (2002).
140. Garrigues, H. J., Rubinchikova, Y. E., DiPersio, C. M. & Rose, T. M. Integrin $\alpha V\beta 3$ Binds to the RGD Motif of Glycoprotein B of Kaposi's Sarcoma-Associated Herpesvirus and Functions as an RGD-Dependent Entry Receptor. *J. Virol.* **82**, 1570–1580 (2008).
141. Veettil, M. V. *et al.* Kaposi's Sarcoma-Associated Herpesvirus Forms a Multimolecular Complex of Integrins ($\alpha V\beta 5$, $\alpha V\beta 3$, and $\alpha 3\beta 1$) and CD98-xCT during Infection of Human Dermal Microvascular Endothelial Cells, and CD98-xCT Is Essential for the Postentry Stage of Infection. *J. Virol.* **82**, 12126–12144 (2008).
142. Veettil, M. V., Bandyopadhyay, C., Dutta, D. & Chandran, B. Interaction of KSHV with Host Cell Surface Receptors and Cell Entry. *Viruses* **6**, 4024–4046 (2014).
143. TerBush, A. A., Hafkamp, F., Lee, H. J. & Coscoy, L. A Kaposi's Sarcoma-Associated Herpesvirus Infection Mechanism Is Independent of Integrins $\alpha 3\beta 1$, $\alpha V\beta 3$, and $\alpha V\beta 5$. *J. Virol.* **92**, (2018).
144. Dutta, D. *et al.* EphrinA2 Regulates Clathrin Mediated KSHV Endocytosis in Fibroblast Cells by Coordinating Integrin-Associated Signaling and c-Cbl Directed Polyubiquitination. *PLoS Pathog.* **9**, (2013).
145. Chakraborty, S., Veettil, M. V., Bottero, V. & Chandran, B. Kaposi's sarcoma-associated herpesvirus interacts with EphrinA2 receptor to amplify signaling essential for productive infection. *Proc. Natl. Acad. Sci. U. S. A.* **109**, E1163–E1172 (2012).
146. Bandyopadhyay, C., Veettil, M. V., Dutta, S. & Chandran, B. p130Cas Scaffolds the Signalosome To Direct Adaptor-Effector Cross Talk during Kaposi's Sarcoma-Associated Herpesvirus Trafficking in Human Microvascular Dermal Endothelial Cells. *J. Virol.* **88**, 13858–13878 (2014).
147. Bandyopadhyay, C., Valiya-Veettil, M., Dutta, D., Chakraborty, S. & Chandran, B. CIB1 synergizes with EphrinA2 to regulate Kaposi's sarcoma-associated herpesvirus macropinocytic entry in human microvascular dermal endothelial cells. *PLoS Pathog.* **10**, e1003941 (2014).
148. Wang, X. *et al.* Male hormones activate EphA2 to facilitate Kaposi's sarcoma-associated herpesvirus infection: Implications for gender disparity in Kaposi's sarcoma. *PLoS Pathog.* **13**, e1006580 (2017).

REFERENCES

149. Hahn, A. S. & Desrosiers, R. C. Binding of the Kaposi's Sarcoma-Associated Herpesvirus to the Ephrin Binding Surface of the EphA2 Receptor and Its Inhibition by a Small Molecule. *J. Virol.* **88**, 8724–8734 (2014).
150. Chen, J., Zhang, X., Schaller, S., Jardetzky, T. S. & Longnecker, R. Ephrin Receptor A4 is a New Kaposi's Sarcoma-Associated Herpesvirus Virus Entry Receptor. *mBio* **10**, (2019).
151. Geijtenbeek, T. B. *et al.* DC-SIGN-ICAM-2 interaction mediates dendritic cell trafficking. *Nat. Immunol.* **1**, 353–357 (2000).
152. Mummidi, S. *et al.* Extensive repertoire of membrane-bound and soluble dendritic cell-specific ICAM-3-grabbing nonintegrin 1 (DC-SIGN1) and DC-SIGN2 isoforms. Inter-individual variation in expression of DC-SIGN transcripts. *J. Biol. Chem.* **276**, 33196–33212 (2001).
153. Lozach, P.-Y., Burleigh, L., Staropoli, I. & Amara, A. The C Type Lectins DC-SIGN and L-SIGN. in *Glycoviropology Protocols* (ed. Sugrue, R. J.) 51–68 (Humana Press, 2007). doi:10.1007/978-1-59745-393-6_4.
154. Hensler, H. R., Tomaszewski, M. J., Rappocciolo, G., Rinaldo, C. R. & Jenkins, F. J. Human herpesvirus 8 glycoprotein B binds the entry receptor DC-SIGN. *Virus Res.* **190**, 97–103 (2014).
155. Geijtenbeek, T. B. H., den Dunnen, J. & Gringhuis, S. I. Pathogen recognition by DC-SIGN shapes adaptive immunity. *Future Microbiol.* **4**, 879–890 (2009).
156. Mitchell, D. A., Fadden, A. J. & Drickamer, K. A Novel Mechanism of Carbohydrate Recognition by the C-type Lectins DC-SIGN and DC-SIGNR SUBUNIT ORGANIZATION AND BINDING TO MULTIVALENT LIGANDS. *J. Biol. Chem.* **276**, 28939–28945 (2001).
157. Tassaneetrithep, B. *et al.* DC-SIGN (CD209) mediates dengue virus infection of human dendritic cells. *J. Exp. Med.* **197**, 823–829 (2003).
158. Davis, C. W. *et al.* West Nile virus discriminates between DC-SIGN and DC-SIGNR for cellular attachment and infection. *J. Virol.* **80**, 1290–1301 (2006).
159. Shimojima, M., Takenouchi, A., Shimoda, H., Kimura, N. & Maeda, K. Distinct usage of three C-type lectins by Japanese encephalitis virus: DC-SIGN, DC-SIGNR, and LSECtin. *Arch. Virol.* **159**, 2023–2031 (2014).
160. Lin, C. L. *et al.* Macrophage-tropic HIV induces and exploits dendritic cell chemotaxis. *J. Exp. Med.* **192**, 587–594 (2000).
161. Geijtenbeek, T. B. *et al.* DC-SIGN, a dendritic cell-specific HIV-1-binding protein that enhances trans-infection of T cells. *Cell* **100**, 587–597 (2000).
162. Sharma-Walia, N., Naranatt, P. P., Krishnan, H. H., Zeng, L. & Chandran, B. Kaposi's Sarcoma-Associated Herpesvirus/Human Herpesvirus 8 Envelope Glycoprotein gB Induces the Integrin-Dependent Focal Adhesion Kinase-Src-Phosphatidylinositol 3-Kinase-Rho GTPase Signal Pathways and Cytoskeletal Rearrangements. *J. Virol.* **78**, 4207–4223 (2004).
163. Naranatt, P. P., Akula, S. M., Zien, C. A., Krishnan, H. H. & Chandran, B. Kaposi's Sarcoma-Associated Herpesvirus Induces the Phosphatidylinositol 3-Kinase-PKC- ζ -MEK-ERK Signaling Pathway in Target Cells Early during Infection: Implications for Infectivity. *J. Virol.* **77**, 1524–1539 (2003).
164. Chakraborty, S., ValiyaVeettil, M., Sadagopan, S., Paudel, N. & Chandran, B. c-Cbl-Mediated Selective Virus-Receptor Translocations into Lipid Rafts Regulate Productive Kaposi's Sarcoma-Associated Herpesvirus Infection in Endothelial Cells. *J. Virol.* **85**, 12410–12430 (2011).
165. Veettil, M. V., Sadagopan, S., Kerur, N., Chakraborty, S. & Chandran, B. Interaction of c-Cbl with Myosin IIA Regulates Bleb Associated Macropinocytosis of Kaposi's Sarcoma-Associated Herpesvirus. *PLOS Pathog.* **6**, e1001238 (2010).
166. Garrigues, H. J., DeMaster, L. K., Rubinchikova, Y. E. & Rose, T. M. KSHV attachment and entry are dependent on $\alpha\beta 3$ integrin localized to specific cell surface microdomains and do not correlate with the presence of heparan sulfate. *Virology* **464–465**, 118–133 (2014).
167. Garrigues, H. J., DeMaster, L. K., Rubinchikova, Y. E. & Rose, T. M. Corrigendum to: "KSHV attachment and entry are dependent on $\alpha\beta 3$ integrin localized to specific cell surface microdomains and do not correlate with the presence of heparan sulfate" [Virology 464-465 (2014) 118-133]. *Virology* **515**, 264–265 (2018).

REFERENCES

168. Kaleeba, J. A. R. & Berger, E. A. Kaposi's Sarcoma-Associated Herpesvirus Fusion-Entry Receptor: Cystine Transporter xCT. *Science* **311**, 1921–1924 (2006).
169. Fenczik, C. A. *et al.* Distinct domains of CD98hc regulate integrins and amino acid transport. *J. Biol. Chem.* **276**, 8746–8752 (2001).
170. Féral, C. C. *et al.* CD98hc (SLC3A2) participates in fibronectin matrix assembly by mediating integrin signaling. *J. Cell Biol.* **178**, 701–711 (2007).
171. Prager, G. W., Féral, C. C., Kim, C., Han, J. & Ginsberg, M. H. CD98hc (SLC3A2) interaction with the integrin beta subunit cytoplasmic domain mediates adhesive signaling. *J. Biol. Chem.* **282**, 24477–24484 (2007).
172. Kabir-Salmani, M. *et al.* The membrane-spanning domain of CD98 heavy chain promotes alpha(v)beta3 integrin signals in human extravillous trophoblasts. *Mol. Endocrinol. Baltim. Md* **22**, 707–715 (2008).
173. Chakraborty, S., ValiyaVeettil, M., Sadagopan, S., Paudel, N. & Chandran, B. c-Cbl-mediated selective virus-receptor translocations into lipid rafts regulate productive Kaposi's sarcoma-associated herpesvirus infection in endothelial cells. *J. Virol.* **85**, 12410–12430 (2011).
174. Committee, E. N. Unified Nomenclature for Eph Family Receptors and Their Ligands, the Ephrins. *Cell* **90**, 403–404 (1997).
175. Pitulescu, M. E. & Adams, R. H. Eph/ephrin molecules—a hub for signaling and endocytosis. *Genes Dev.* **24**, 2480–2492 (2010).
176. Kalo, M. S. & Pasquale, E. B. Multiple in Vivo Tyrosine Phosphorylation Sites in EphB Receptors. *Biochemistry* **38**, 14396–14408 (1999).
177. Pasquale, E. B. Eph-ephrin bidirectional signaling in physiology and disease. *Cell* **133**, 38–52 (2008).
178. Daar, I. O. “non-SH2/PDZ reverse signaling by ephrins”. *Semin. Cell Dev. Biol.* **23**, 65–74 (2012).
179. Pasquale, E. B. Eph receptor signalling casts a wide net on cell behaviour. *Nat. Rev. Mol. Cell Biol.* **6**, 462–475 (2005).
180. Davy, A. & Soriano, P. Ephrin signaling in vivo: Look both ways. *Dev. Dyn.* **232**, 1–10 (2005).
181. Egea, J. & Klein, R. Bidirectional Eph–ephrin signaling during axon guidance. *Trends Cell Biol.* **17**, 230–238 (2007).
182. Rohani, N., Canty, L., Luu, O., Fagotto, F. & Winklbauer, R. EphrinB/EphB Signaling Controls Embryonic Germ Layer Separation by Contact-Induced Cell Detachment. *PLoS Biol.* **9**, (2011).
183. Hirai, H., Maru, Y., Hagiwara, K., Nishida, J. & Takaku, F. A novel putative tyrosine kinase receptor encoded by the eph gene. *Science* **238**, 1717–1720 (1987).
184. Lindberg, R. A. & Hunter, T. cDNA cloning and characterization of eck, an epithelial cell receptor protein-tyrosine kinase in the eph/elk family of protein kinases. *Mol. Cell. Biol.* **10**, 6316–6324 (1990).
185. Brantley-Sieders, D. M. Clinical relevance of Ephs and ephrins in cancer: Lessons from breast, colorectal, and lung cancer profiling. *Semin. Cell Dev. Biol.* **23**, 102–108 (2012).
186. Pasquale, E. B. Eph receptors and ephrins in cancer: bidirectional signalling and beyond. *Nat. Rev. Cancer* **10**, 165–180 (2010).
187. Boyd, A. W., Bartlett, P. F. & Lackmann, M. Therapeutic targeting of EPH receptors and their ligands. *Nat. Rev. Drug Discov.* **13**, 39–62 (2014).
188. Wykosky, J. & Debinski, W. The EphA2 Receptor and EphrinA1 Ligand in Solid Tumors: Function and Therapeutic Targeting. *Mol. Cancer Res.* **6**, 1795–1806 (2008).
189. Chen, R. C. I. and J. EphA2 Receptor Tyrosine Kinase as a Promising Target for Cancer Therapeutics. *Current Cancer Drug Targets* <http://www.eurekaselect.com/60595/article> (2005).
190. Tandon, M., Vemula, S. V. & Mittal, S. K. Emerging strategies for EphA2 receptor targeting for cancer therapeutics. *Expert Opin. Ther. Targets* **15**, 31–51 (2011).
191. Rivera, R. S. *et al.* Involvement of EphA2 in head and neck squamous cell carcinoma: mRNA expression, loss of heterozygosity and immunohistochemical studies. *Oncol. Rep.* **19**, 1079–1084 (2008).

REFERENCES

192. Miyazaki, T., Kato, H., Fukuchi, M., Nakajima, M. & Kuwano, H. EphA2 overexpression correlates with poor prognosis in esophageal squamous cell carcinoma. *Int. J. Cancer* **103**, 657–663 (2003).
193. Kinch, M. S., Moore, M.-B. & Harpole, D. H. Predictive value of the EphA2 receptor tyrosine kinase in lung cancer recurrence and survival. *Clin. Cancer Res. Off. J. Am. Assoc. Cancer Res.* **9**, 613–618 (2003).
194. Wang, L.-F. *et al.* Increased expression of EphA2 correlates with adverse outcome in primary and recurrent glioblastoma multiforme patients. *Oncol. Rep.* **19**, 151–156 (2008).
195. Kamat, A. A. *et al.* EphA2 overexpression is associated with lack of hormone receptor expression and poor outcome in endometrial cancer. *Cancer* **115**, 2684–2692 (2009).
196. Brannan, J. M. *et al.* Expression of the receptor tyrosine kinase EphA2 is increased in smokers and predicts poor survival in non-small cell lung cancer. *Clin. Cancer Res. Off. J. Am. Assoc. Cancer Res.* **15**, 4423–4430 (2009).
197. Saito, T. *et al.* Expression of EphA2 and E-cadherin in colorectal cancer: correlation with cancer metastasis. *Oncol. Rep.* **11**, 605–611 (2004).
198. Duxbury, M. S., Ito, H., Zinner, M. J., Ashley, S. W. & Whang, E. E. EphA2: a determinant of malignant cellular behavior and a potential therapeutic target in pancreatic adenocarcinoma. *Oncogene* **23**, 1448–1456 (2004).
199. Fang, W. B., Brantley-Sieders, D. M., Parker, M. A., Reith, A. D. & Chen, J. A kinase-dependent role for EphA2 receptor in promoting tumor growth and metastasis. *Oncogene* **24**, 7859–7868 (2005).
200. Walker-Daniels, J. *et al.* Overexpression of the EphA2 tyrosine kinase in prostate cancer. *The Prostate* **41**, 275–280 (1999).
201. Lin, Y. G. *et al.* EphA2 overexpression is associated with angiogenesis in ovarian cancer. *Cancer* **109**, 332–340 (2007).
202. Cheng, N. *et al.* Blockade of EphA receptor tyrosine kinase activation inhibits vascular endothelial cell growth factor-induced angiogenesis. *Mol. Cancer Res. MCR* **1**, 2–11 (2002).
203. Zhuang, G. *et al.* Elevation of receptor tyrosine kinase EphA2 mediates resistance to trastuzumab therapy. *Cancer Res.* **70**, 299–308 (2010).
204. Amato, K. R. *et al.* EPHA2 Blockade Overcomes Acquired Resistance to EGFR Kinase Inhibitors in Lung Cancer. *Cancer Res.* **76**, 305–318 (2016).
205. Miao, H. *et al.* EphA2 Mediates Ligand-Dependent Inhibition and Ligand-Independent Promotion of Cell Migration and Invasion via a Reciprocal Regulatory Loop with Akt. *Cancer Cell* **16**, 9–20 (2009).
206. Macrae, M. *et al.* A conditional feedback loop regulates Ras activity through EphA2. *Cancer Cell* **8**, 111–118 (2005).
207. Brantley-Sieders, D. M. *et al.* The receptor tyrosine kinase EphA2 promotes mammary adenocarcinoma tumorigenesis and metastatic progression in mice by amplifying ErbB2 signaling. *J. Clin. Invest.* **118**, 64–78 (2008).
208. Larsen, A. B. *et al.* Activation of the EGFR gene target EphA2 inhibits epidermal growth factor-induced cancer cell motility. *Mol. Cancer Res. MCR* **5**, 283–293 (2007).
209. Zelinski, D. P., Zantek, N. D., Stewart, J. C., Irizarry, A. R. & Kinch, M. S. EphA2 overexpression causes tumorigenesis of mammary epithelial cells. *Cancer Res.* **61**, 2301–2306 (2001).
210. Yang, N.-Y. *et al.* Crosstalk of the EphA2 receptor with a serine/threonine phosphatase suppresses the Akt-mTORC1 pathway in cancer cells. *Cell. Signal.* **23**, 201–212 (2011).
211. Menges, C. W. & McCance, D. J. Constitutive activation of the Raf–MAPK pathway causes negative feedback inhibition of Ras–PI3K–AKT and cellular arrest through the EphA 2 receptor. *Oncogene* **27**, 2934–2940 (2008).
212. Duxbury, M. S., Ito, H., Zinner, M. J., Ashley, S. W. & Whang, E. E. Ligation of EphA2 by Ephrin A1-Fc inhibits pancreatic adenocarcinoma cellular invasiveness. *Biochem. Biophys. Res. Commun.* **320**, 1096–1102 (2004).
213. Liu, D.-P., Wang, Y., Koeffler, H. P. & Xie, D. Ephrin-A1 is a negative regulator in glioma through down-regulation of EphA2 and FAK. *Int. J. Oncol.* **30**, 865–871 (2007).

REFERENCES

214. Miao, H., Burnett, E., Kinch, M., Simon, E. & Wang, B. Activation of EphA2 kinase suppresses integrin function and causes focal-adhesion-kinase dephosphorylation. *Nat. Cell Biol.* **2**, 62–69 (2000).
215. Miura, K., Nam, J.-M., Kojima, C., Mochizuki, N. & Sabe, H. EphA2 engages Git1 to suppress Arf6 activity modulating epithelial cell-cell contacts. *Mol. Biol. Cell* **20**, 1949–1959 (2009).
216. Miao, H. *et al.* Activation of EphA receptor tyrosine kinase inhibits the Ras/MAPK pathway. *Nat. Cell Biol.* **3**, 527–530 (2001).
217. Pratt, R. L. & Kinch, M. S. Activation of the EphA2 tyrosine kinase stimulates the MAP/ERK kinase signaling cascade. *Oncogene* **21**, 7690–7699 (2002).
218. Salaita, K. *et al.* Restriction of receptor movement alters cellular response: physical force sensing by EphA2. *Science* **327**, 1380–1385 (2010).
219. Chen, Z. *et al.* Spatially modulated ephrinA1:EphA2 signaling increases local contractility and global focal adhesion dynamics to promote cell motility. *Proc. Natl. Acad. Sci.* **115**, E5696–E5705 (2018).
220. Wiedemann, E. *et al.* Regulation of endothelial migration and proliferation by ephrin-A1. *Cell. Signal.* **29**, 84–95 (2017).
221. Wykosky, J., Gibo, D. M., Stanton, C. & Debinski, W. EphA2 as a novel molecular marker and target in glioblastoma multiforme. *Mol. Cancer Res. MCR* **3**, 541–551 (2005).
222. Dodelet, V. C. & Pasquale, E. B. Eph receptors and ephrin ligands: embryogenesis to tumorigenesis. *Oncogene* **19**, 5614–5619 (2000).
223. Hafner, C. *et al.* Differential gene expression of Eph receptors and ephrins in benign human tissues and cancers. *Clin. Chem.* **50**, 490–499 (2004).
224. Cui, X.-D. *et al.* EFNA1 ligand and its receptor EphA2: potential biomarkers for hepatocellular carcinoma. *Int. J. Cancer* **126**, 940–949 (2010).
225. Li, X. *et al.* Up-regulation of EphA2 and down-regulation of EphrinA1 are associated with the aggressive phenotype and poor prognosis of malignant glioma. *Tumour Biol. J. Int. Soc. Oncodevelopmental Biol. Med.* **31**, 477–488 (2010).
226. Chen, J. *et al.* Ephrin receptor A2 is a functional entry receptor for Epstein-Barr virus. *Nat. Microbiol.* **3**, 172–180 (2018).
227. Zhang, H. *et al.* Ephrin receptor A2 is an epithelial cell receptor for Epstein-Barr virus entry. *Nat. Microbiol.* **3**, 1–8 (2018).
228. Lupberger, J. *et al.* EGFR and EphA2 are host factors for hepatitis C virus entry and possible targets for antiviral therapy. *Nat. Med.* **17**, 589–595 (2011).
229. Subbarayal, P. *et al.* EphrinA2 Receptor (EphA2) Is an Invasion and Intracellular Signaling Receptor for Chlamydia trachomatis. *PLoS Pathog.* **11**, (2015).
230. Aaron, P. A., Jamklang, M., Uhrig, J. P. & Gelli, A. The Human Blood-Brain Barrier Internalizes *Cryptococcus neoformans* via the EphA2-Tyrosine Kinase Receptor. *Cell. Microbiol.* **20**, (2018).
231. Kaushansky, A. *et al.* Malaria parasites target the hepatocyte receptor EphA2 for successful host infection. *Science* **350**, 1089–1092 (2015).
232. Chang, H. *et al.* Non-human primate model of Kaposi's sarcoma-associated herpesvirus infection. *PLoS Pathog.* **5**, e1000606 (2009).
233. Bilello, J. P., Morgan, J. S., Damania, B., Lang, S. M. & Desrosiers, R. C. A genetic system for rhesus monkey rhadinovirus: use of recombinant virus to quantitate antibody-mediated neutralization. *J. Virol.* **80**, 1549–1562 (2006).
234. Estep, R. D., Powers, M. F., Yen, B. K., Li, H. & Wong, S. W. Construction of an Infectious Rhesus Rhadinovirus Bacterial Artificial Chromosome for the Analysis of Kaposi's Sarcoma-Associated Herpesvirus-Related Disease Development. *J. Virol.* **81**, 2957–2969 (2007).
235. Shin, Y. C. *et al.* Glycoprotein gene sequence variation in rhesus monkey rhadinovirus. *Virology* **400**, 175–186 (2010).
236. Bruce, A. G. *et al.* Macaque homologs of EBV and KSHV show uniquely different associations with simian AIDS-related lymphomas. *PLoS Pathog.* **8**, e1002962 (2012).

REFERENCES

237. Marshall, V. A. *et al.* Gammaherpesvirus infection and malignant disease in rhesus macaques experimentally infected with SIV or SHIV. *PLoS Pathog.* **14**, e1007130 (2018).
238. Wong, S. *et al.* Induction of B cell hyperplasia in simian immunodeficiency virus- infected rhesus macaques with the simian homologue of Kaposi's sarcoma- associated herpesvirus. *J. Exp. Med.* **190**, 827–840 (1999).
239. Orzechowska, B. U. *et al.* Rhesus macaque rhadinovirus-associated non-Hodgkin lymphoma: animal model for KSHV-associated malignancies. *Blood* **112**, 4227–4234 (2008).
240. Umbach, J. L., Strelow, L. I., Wong, S. W. & Cullen, B. R. Analysis of rhesus rhadinovirus microRNAs expressed in virus-induced tumors from infected rhesus macaques. *Virology* **405**, 592–599 (2010).
241. Mansfield, K. G. *et al.* Experimental infection of rhesus and pig-tailed macaques with macaque rhadinoviruses. *J. Virol.* **73**, 10320–10328 (1999).
242. Bilello, J. P. *et al.* Vaccine protection against simian immunodeficiency virus in monkeys using recombinant gamma-2 herpesvirus. *J. Virol.* **85**, 12708–12720 (2011).
243. Shin, Y. C. *et al.* A recombinant herpesviral vector containing a near-full-length SIVmac239 genome produces SIV particles and elicits immune responses to all nine SIV gene products. *PLoS Pathog.* **14**, e1007143 (2018).
244. Gonzalez-Nieto, L. *et al.* Vaccine protection against rectal acquisition of SIVmac239 in rhesus macaques. *PLoS Pathog.* **15**, e1008015 (2019).
245. Hahn, A. S. *et al.* A Recombinant Rhesus Monkey Rhadinovirus Deleted of Glycoprotein L Establishes Persistent Infection of Rhesus Macaques and Elicits Conventional T Cell Responses. *J. Virol.* (2019) doi:10.1128/JVI.01093-19.
246. Bischof, G. F. *et al.* Use of a gamma-2 herpesvirus as a vector to deliver antibodies to rhesus monkeys. *Gene Ther.* **24**, 487–492 (2017).
247. Hahn, A. S. & Desrosiers, R. C. Rhesus Monkey Rhadinovirus Uses Eph Family Receptors for Entry into B Cells and Endothelial Cells but Not Fibroblasts. *PLoS Pathog.* **9**, (2013).
248. Muniraju, M. *et al.* Kaposi Sarcoma-Associated Herpesvirus Glycoprotein H Is Indispensable for Infection of Epithelial, Endothelial, and Fibroblast Cell Types. *J. Virol.* **93**, (2019).
249. Shimizu, H. *et al.* Improving the quality of a recombinant rabbit monoclonal antibody against PLXDC2 by optimizing transient expression conditions and purification method. *Protein Expr. Purif.* **146**, 27–33 (2018).
250. Dislich, B. *et al.* Label-free Quantitative Proteomics of Mouse Cerebrospinal Fluid Detects β -Site APP Cleaving Enzyme (BACE1) Protease Substrates In Vivo. *Mol. Cell. Proteomics* **14**, 2550–2563 (2015).
251. Li, Q., Turk, S. M. & Hutt-Fletcher, L. M. The Epstein-Barr virus (EBV) BZLF2 gene product associates with the gH and gL homologs of EBV and carries an epitope critical to infection of B cells but not of epithelial cells. *J. Virol.* **69**, 3987–3994 (1995).
252. Miller, N. & Hutt-Fletcher, L. M. Epstein-Barr virus enters B cells and epithelial cells by different routes. *J. Virol.* **66**, 3409–3414 (1992).
253. Martinez-Martin, N. *et al.* An Unbiased Screen for Human Cytomegalovirus Identifies Neuropilin-2 as a Central Viral Receptor. *Cell* **174**, 1158–1171.e19 (2018).
254. Stegmann, C. *et al.* A derivative of platelet-derived growth factor receptor alpha binds to the trimer of human cytomegalovirus and inhibits entry into fibroblasts and endothelial cells. *PLOS Pathog.* **13**, e1006273 (2017).
255. Wu, Y. *et al.* Human cytomegalovirus glycoprotein complex gH/gL/gO uses PDGFR- α as a key for entry. *PLOS Pathog.* **13**, e1006281 (2017).
256. Kabanova, A. *et al.* Platelet-derived growth factor- α receptor is the cellular receptor for human cytomegalovirus gHgLgO trimer. *Nat. Microbiol.* **1**, 1–8 (2016).
257. Wang, X., Kenyon, W. J., Li, Q., Müllberg, J. & Hutt-Fletcher, L. M. Epstein-Barr Virus Uses Different Complexes of Glycoproteins gH and gL To Infect B Lymphocytes and Epithelial Cells. *J. Virol.* **72**, 5552–5558 (1998).

REFERENCES

258. Hahn, G. *et al.* Human cytomegalovirus UL131-128 genes are indispensable for virus growth in endothelial cells and virus transfer to leukocytes. *J. Virol.* **78**, 10023–10033 (2004).
259. Patrone, M. *et al.* Human cytomegalovirus UL130 protein promotes endothelial cell infection through a producer cell modification of the virion. *J. Virol.* **79**, 8361–8373 (2005).
260. Gerna, G. *et al.* Dendritic-cell infection by human cytomegalovirus is restricted to strains carrying functional UL131-128 genes and mediates efficient viral antigen presentation to CD8+ T cells. *J. Gen. Virol.* **86**, 275–284 (2005).
261. Adler, B. *et al.* Role of human cytomegalovirus UL131A in cell type-specific virus entry and release. *J. Gen. Virol.* **87**, 2451–2460 (2006).
262. Alonso-C, L. M. *et al.* Expression profile of Eph receptors and ephrin ligands in healthy human B lymphocytes and chronic lymphocytic leukemia B-cells. *Leuk. Res.* **33**, 395–406 (2009).
263. Nguyen, T. M., Arthur, A., Zannettino, A. C. W. & Gronthos, S. EphA5 and EphA7 forward signaling enhances human hematopoietic stem and progenitor cell maintenance, migration, and adhesion via Rac1 activation. *Exp. Hematol.* **48**, 72–78 (2017).
264. Wu, W. *et al.* KSHV/HHV-8 infection of human hematopoietic progenitor (CD34+) cells: persistence of infection during hematopoiesis in vitro and in vivo. *Blood* **108**, 141–151 (2006).
265. Hansen, S. G. *et al.* Cytomegalovirus vectors violate CD8+ T cell epitope recognition paradigms. *Science* **340**, 1237874 (2013).
266. Hansen, S. G. *et al.* Effector-memory T cell responses are associated with protection of rhesus monkeys from mucosal SIV challenge. *Nat. Med.* **15**, 293–299 (2009).
267. Hansen, S. G. *et al.* Profound early control of highly pathogenic SIV by an effector-memory T cell vaccine. *Nature* **473**, 523–527 (2011).
268. Hansen, S. G. *et al.* Immune clearance of highly pathogenic SIV infection. *Nature* **502**, 100–104 (2013).
269. Prévost, N. *et al.* Eph kinases and ephrins support thrombus growth and stability by regulating integrin outside-in signaling in platelets. *Proc. Natl. Acad. Sci. U. S. A.* **102**, 9820–9825 (2005).
270. de Saint-Vis, B. *et al.* Human dendritic cells express neuronal Eph receptor tyrosine kinases: role of EphA2 in regulating adhesion to fibronectin. *Blood* **102**, 4431–4440 (2003).
271. Saeki, N., Nishino, S., Shimizu, T. & Ogawa, K. EphA2 promotes cell adhesion and spreading of monocyte and monocyte/macrophage cell lines on integrin ligand-coated surfaces. *Cell Adhes. Migr.* **9**, 469–482 (2015).
272. Raghu, H., Sharma-Walia, N., Veettil, M. V., Sadagopan, S. & Chandran, B. Kaposi's sarcoma-associated herpesvirus utilizes an actin polymerization-dependent macropinocytic pathway to enter human dermal microvascular endothelial and human umbilical vein endothelial cells. *J. Virol.* **83**, 4895–4911 (2009).
273. Blumenthal, M. J. *et al.* EPHA2 sequence variants are associated with susceptibility to Kaposi's sarcoma-associated herpesvirus infection and Kaposi's sarcoma prevalence in HIV-infected patients. *Cancer Epidemiol.* **56**, 133–139 (2018).
274. Croix, B. S. *et al.* Genes Expressed in Human Tumor Endothelium. *Science* **289**, 1197–1202 (2000).
275. Bagley, R. G. *et al.* Tumor endothelial marker 7 (TEM-7): A novel target for antiangiogenic therapy. *Microvasc. Res.* **82**, 253–262 (2011).
276. Beaty, R. M. *et al.* PLXDC1 (TEM7) is identified in a genome-wide expression screen of glioblastoma endothelium. *J. Neurooncol.* **81**, 241–248 (2007).
277. Nanda, A. *et al.* Identification of a Binding Partner for the Endothelial Cell Surface Proteins TEM7 and TEM7R. *Cancer Res.* **64**, 8507–8511 (2004).
278. Kim, J.-S. *et al.* Radioresistance in a human laryngeal squamous cell carcinoma cell line is associated with DNA methylation changes and topoisomerase II α . *Cancer Biol. Ther.* **16**, 558–566 (2015).
279. Wang, Y. & Li, H. Identification of proteins associated with paclitaxel resistance of epithelial ovarian cancer using iTRAQ-based proteomics. *Oncol. Lett.* **15**, 9793–9801 (2018).

REFERENCES

280. Lavorato-Rocha, A. M. *et al.* An Integrative Approach Uncovers Biomarkers that Associate with Clinically Relevant Disease Outcomes in Vulvar Carcinoma. *Mol. Cancer Res. MCR* **14**, 720–729 (2016).
281. Zhang, Z.-Z. *et al.* TEM7 (PLXDC1), a key prognostic predictor for resectable gastric cancer, promotes cancer cell migration and invasion. *Am. J. Cancer Res.* **5**, 772–781 (2015).
282. Fuchs, B. *et al.* High expression of tumor endothelial marker 7 is associated with metastasis and poor survival of patients with osteogenic sarcoma. *Gene* **399**, 137–143 (2007).
283. Carpenter, R. L. *et al.* The gain-of-function GLI1 transcription factor TGLI1 enhances expression of VEGF-C and TEM7 to promote glioblastoma angiogenesis. *Oncotarget* **6**, 22653–22665 (2015).
284. Falchetti, M. L. *et al.* Glioblastoma endothelium drives bevacizumab-induced infiltrative growth via modulation of PLXDC1. *Int. J. Cancer* **144**, 1331–1344 (2019).
285. Kim, G. H. *et al.* Selective delivery of PLXDC1 small interfering RNA to endothelial cells for anti-angiogenesis tumor therapy using CD44-targeted chitosan nanoparticles for epithelial ovarian cancer. *Drug Deliv.* **25**, 1394–1402 (2018).
286. Lee, H. K., Seo, I. A., Park, H. K. & Park, H. T. Identification of the basement membrane protein nidogen as a candidate ligand for tumor endothelial marker 7 in vitro and in vivo. *FEBS Lett.* **580**, 2253–2257 (2006).
287. Cheng, G. *et al.* Identification of PLXDC1 and PLXDC2 as the transmembrane receptors for the multifunctional factor PEDF. *eLife* **3**, e05401 (2014).
288. Wu, H. & Parsons, J. T. Cortactin, an 80/85-kilodalton pp60src substrate, is a filamentous actin-binding protein enriched in the cell cortex. *J. Cell Biol.* **120**, 1417–1426 (1993).

APPENDIX

A1 Abbreviations

| | | | |
|--------|---|----------|---|
| A | Alanine | crk | Adapter molecule crk |
| AHV1 | Alcelaphine herpesvirus 1 | D | Aspartic acid |
| AIDS | Acquired Immune Deficiency Syndrome | DNA | Deoxyribonucleic acid |
| Akt | Akt kinase | DC-SIGN | Dendritic Cell-Specific Intercellular adhesion molecule-3-Grabbing Non-integrin |
| AP-2 | Adaptor protein complex 2 | ds | Double-stranded |
| Arf6 | Adenosine diphosphate (ADP)-ribosylation factor 6 | E | Glutamic acid |
| Ala | Alanine | e.g. | Exempli gratia |
| Arg | Arginine | EBV | Epstein-Barr-Virus |
| Asn | Asparagine | EGF | Epidermal growth factor |
| Asp | Aspartic acid | ELAAN | Glu-Leu-Ala-Ala-Asn |
| bFGF | Basic fibroblast growth factor | ELEFN | Glu-Leu-Glu-Phe-Asn |
| c | Cellular | env | Envelope gene (HIV/ SIV) |
| caa | Chlorocebus aethiops aethiops | Eph | Erythropoietin-producing human |
| cap | Chlorocebus aethiops pygerythrus | receptor | hepatocellular receptor |
| cART | Combination antiretroviral therapy | Eps-15 | Epidermal growth factor receptor substrate-15 |
| cas | Chlorocebus aethiops sabaeus | ErbB2 | Receptor tyrosine-protein kinase ErbB2 |
| Cas | CRISPR associated | et al. | et alii |
| CbGHV1 | Colobine gammaherpesvirus 1 | F | Phenylalanine |
| c-cbl | Casitas B-lineage Lymphoma | FAK | Focal adhesion kinase |
| CD | Cluster of differentiation | FLIP | FADD-like interleukin-1- β -converting enzyme (FLICE)-inhibitory protein |
| cDNA | Complementary DNA | g | Glycoprotein |
| CHO | Chinese hamster ovary | gag | Group-specific antigen (HIV/ SIV) |
| CHV3 | Callitrichine herpesvirus 3 | GC | Germinal center |
| CIB1 | Calcium and integrin-binding protein 1 | GF | Growth factor |
| CMV | Cytomegalovirus | GFR | Growth factor receptor |
| CRD | Carbohydrate recognition domain | | |
| CRISPR | Clustered Regularly Interspaced Short Palindromic Repeats | | |

| | | | |
|---------|--|----------------|---|
| Git1 | G protein-coupled receptor kinase-interacting protein | KSHV | Kaposi's sarcoma-associated herpesvirus |
| Glu | Glutamic acid | L | Leucine |
| Gly | Glycine | LANA | Latency associated nuclear antigen |
| GPI | Glycosylphosphatidylinositol | LBD | Ligand-binding domain |
| h | Human | m | Mouse |
| HBV | Hepatitis B virus | M. | Macaca |
| HCV | Hepatitis C virus | MAPK | Mitogen-activated protein kinase |
| HFF | Human Foreskin Fibroblast | MCD | Multicentric Castleman disease |
| HGF/SF | Hepatocyte growth factor/scatter factor | McPyV | Merkel cell polyomavirus |
| HHV-8 | Human γ -herpesvirus 8 | mfa | Macaca fascicularis |
| HIV | Human immunodeficiency virus | MHC | Major histocompatibility complex |
| HLA | Human Leukocyte Antigen | mmu | Macaca mulatta |
| HMVEC-d | Human dermal microvascular endothelial cell | mne | Macaca nemestrina |
| HPV | Human papillomavirus infection | MneRV2 | Macaca nemestrina rhadinovirus |
| Hrs | Hepatocyte growth factor-regulated tyrosine kinase substrate | N | Asparagine |
| HSPC | Hematopoietic stem and progenitor cell | nck1 | Non-catalytic region of tyrosine kinase adaptor protein 1 |
| HSPG | Heparan sulfate proteoglycan | nef | Negative regulatory factor (HIV/ SIV) |
| HTLV | Human T-lymphotropic virus | nestin | Neuroectodermal stem cell marker |
| HVA | Herpesvirus ateles | ORF | Open reading frame |
| HVS | Herpesvirus saimiri | p | Phosphorylation |
| i.e. | id est | p130Cas | Crk-associated Substrate P130Cas |
| ICAM | Intracellular adhesion molecule | PDGF | Platelet-derived growth factor |
| Ig | Immunoglobulin | PDGFR α | Platelet-derived growth factor receptor alpha |
| JMRV | Japanese macaque rhadinovirus | PDZ | Post synaptic density protein, drosophila disc large tumor suppressor, zonula occludens-1 protein |
| K | Lysine | PEL | Primary effusion lymphoma |
| kb | Kilobases | Phe | Phenylalanine |
| KCP | KSHV complement control protein | PI3K | Phosphoinositide-3-kinase |
| kDa | Kilodalton | PLHV1 | Porcine lymphotropic herpesvirus |
| KICS | KSHV inflammatory syndrome | Plxdc | Plexin domain containing |
| KS | Kaposi's sarcoma | | |

APPENDIX – A1 Abbreviations

| | | | |
|-------|---|-----|--|
| pol | DNA polymerase (HIV/ SIV) | vav | Proto-oncogene vav |
| Rac1 | Ras-related C3 botulinum toxin substrate 1 | wt | Wild-type |
| Ras | Rat sarcoma | xCT | Glutamate/cysteine exchange transporter |
| rev | Regulator of expression of virion proteins (HIV/ SIV) | Y | Tyrosine |
| RFVH | Retroperitoneal fibromatosis- associated herpesvirus | | |
| RGD | Arg-Gly-Asp | | |
| rh | Rhesus | | |
| RLV | Rhesus lymphocryptovirus | | |
| RRV | Rhesus monkey rhadinovirus | | |
| RSK1 | p90 ribosomal S6 kinase1 | | |
| RTA | Replication and transcription transactivator | | |
| RV | Rhadinovirus | | |
| S | Serine | | |
| SAM | Sterile alpha motif | | |
| Ser | Serine | | |
| SHIV | Simian/human immunodeficiency virus | | |
| SHP2 | Src homology region 2 domain- containing phosphatase 2 | | |
| SIV | Simian immunodeficiency virus | | |
| Src | Sarcoma (Proto-oncogene tyrosine- protein kinase Src) | | |
| tat | Trans-activator of transcription (HIV/ SIV) | | |
| TEM7 | Tumor endothelial marker 7 | | |
| TEM7R | Tumor endothelial marker 7 related | | |
| Tyr | Tyrosine | | |
| UL | Unique long | | |
| US | Unique short | | |
| v | Viral | | |
| V | Valine | | |

A2 Publications

Grosskopf, A. K., Schlagowski, S. C., Ensser, A., Desrosiers, R. C. & Hahn, A. S. *Plxdc family members are novel receptors for the rhesus monkey rhadinovirus (RRV)*. bioRxiv 2020.01.20.912246 (2020) doi:10.1101/2020.01.20.912246.

Hahn, A. S., Bischof, G. F., **Großkopf, A. K.**, Shin, Y. C., Domingues, A., Gonzalez-Nieto, L., ... Desrosiers, R. C. (2019). *A Recombinant Rhesus Monkey Rhadinovirus Deleted of Glycoprotein L Establishes Persistent Infection of Rhesus Macaques and Elicits Conventional T Cell Responses*. Journal of Virology. doi:10.1128/jvi.01093-19

Großkopf AK, Schlagowski S, Hörnich BF, Fricke T, Desrosiers RC, Hahn AS. *EphA7 Functions as Receptor on BJAB Cells for Cell-to-Cell Transmission of the Kaposi's Sarcoma-Associated Herpesvirus and for Cell-Free Infection by the Related Rhesus Monkey Rhadinovirus*. J Virol. 2019 Jul 17; 93(15). pii: e00064-19. doi: 10.1128/JVI.00064-19. Print 2019 Aug 1.

Ensser, A.*, **Großkopf, A. K.***, Mätz-Rensing, K., Roos, C., & Hahn, A. S. (2018). *Isolation and sequence analysis of a novel rhesus macaque foamy virus isolate with a serotype-1-like env*. Archives of Virology, 163(9), 2507–2512. doi:10.1007/s00705-018-3892-9 *these authors contributed equally

Großkopf AK, Ensser A, Neipel F, Jungnickl D, Schlagowski S, Desrosiers RC, Hahn AS.; *A conserved Eph family receptor-binding motif on the gH/gL complex of Kaposi's sarcoma-associated herpesvirus and rhesus monkey rhadinovirus*. PLoS Pathog. 2018 Feb 12;14(2):e1006912. doi: 10.1371/journal.ppat.1006912.

Full, F., Hahn, A., **Großkopf, A.**, & Ensser, A. (2017). *Gammaherpesviral Tegument Proteins, PML-Nuclear Bodies and the Ubiquitin-Proteasome System*. Viruses, 9(10), 308. doi:10.3390/v9100308
Review

Hahn, A. S., **Großkopf, A. K.**, Jungnickl, D., Scholz, B., & Ensser, A. (2016). *Viral FGARAT Homolog ORF75 of Rhesus Monkey Rhadinovirus Effects Proteasomal Degradation of the ND10 Components SP100 and PML*. Journal of Virology, 90(17), 8013–8028. doi:10.1128/jvi.01181-16

A3 Awards and Travel Grants

- 2019 **Abstract Award** of the 44th International Herpesvirus Workshop in Knoxville (USA)
Trainee Award of the 22nd International Workshop on Kaposi's sarcoma Herpesvirus (KSHV) and Related Agents in New York (USA)
- 2017 **Abstract Award** of the 42nd International Herpesvirus Workshop in Ghent (Belgium)
Travel grant for the 42nd International Herpesvirus Workshop in Ghent (Belgium), German Academic Exchange Service (DAAD)
Travel grant for the 20th International Workshop on Kaposi's Sarcoma Herpesvirus (KSHV) and Related Agents in Berlin (Germany), Göttingen Graduate Center for Neurosciences, Biophysics, and Molecular Biosciences (GGNB)
Travel grant for the 27th Annual Meeting of the Society for Virology in Marburg (Germany), Gesellschaft für Virologie e.V.

A4 Conference contributions - Oral presentations

2019 **44th International Herpesvirus Workshop**

Anna K. Großkopf, Sarah Schlagowski, Bojan F. Hörnich, Thomas Fricke, Ronald C. Desrosiers, Alexander S. Hahn

“EphA7 Functions as a Receptor on BJAB Cells for cell-to-cell Transmission of KSHV and cell-free Infection by the Related Rhesus Monkey Rhadinovirus (RRV)”

22nd International Workshop on Kaposi’s Sarcoma Herpesvirus (KSHV) and Related Agents

Anna K. Großkopf, Sarah Schlagowski, Bojan F. Hörnich, Thomas Fricke, Ronald C. Desrosiers, Alexander S. Hahn

“EphA7 Functions as a Receptor on BJAB Cells for cell-to-cell Transmission of KSHV and cell-free Infection by the Related Rhesus Monkey Rhadinovirus (RRV)”

2018 **43rd International Herpesvirus Workshop**

Anna K. Großkopf, Armin Ensser, Sarah Schlagowski, Ronald C. Desrosiers, Alexander S. Hahn

“The rhesus monkey rhadinovirus interacts through gH with Plxdc2, a novel cellular receptor”

28th Annual Meeting of the Society for Virology

Anna K. Großkopf, Armin Ensser, Sarah Schlagowski, Ronald C. Desrosiers, Alexander S. Hahn

“The rhesus monkey rhadinovirus interacts through gH with Plxdc2, a novel cellular receptor”

2017 **42nd International Herpesvirus Workshop**

Anna K. Großkopf, Armin Ensser, Frank Neipel, Doris Jungnickl, Sarah Schlagowski, Ronald C. Desrosiers, Alexander S. Hahn

„A conserved Eph family receptor-binding motif and novel receptor interactions of the gH/gL complexes of KSHV and RRV – determinants of infectivity and tropism“

20th International Workshop on Kaposi’s Sarcoma Herpesvirus (KSHV) and Related Agents

Anna K. Großkopf, Armin Ensser, Frank Neipel, Doris Jungnickl, Sarah Schlagowski, Ronald C. Desrosiers, Alexander S. Hahn

„A conserved Eph family receptor-binding motif and novel receptor interactions of the gH/gL complexes of KSHV and RRV – determinants of infectivity and tropism“

27th Annual Meeting of the Society for Virology

Anna K. Großkopf, Armin Ensser, Frank Neipel, Doris Jungnickl, Sarah Schlagowski, Ronald C. Desrosiers, Alexander S. Hahn

„A conserved Eph family receptor-binding motif and novel receptor interactions of the gH/gL complexes of KSHV and RRV – determinants of infectivity and tropism“

A5 Acknowledgements

I want to express my sincere gratitude to Dr. Alexander Hahn for giving me the opportunity to work on this project, for his guidance and continuous encouragement throughout my doctoral thesis. Thank you for providing such an open and productive environment, for always making time and for motivating me to develop and follow own ideas as well as expanding my scientific knowledge through thought-provoking discussions and the opportunity to attend a multitude of fascinating conferences.

I would like to show my gratitude for Prof. Lutz Walter and Prof. Friedemann Weber for agreeing to supervise my thesis as members of my thesis advisory committee, for their valuable suggestions and for their time and effort. Furthermore, I would like to thank Prof. Uwe Groß for reviewing my thesis as well as all further members of the Examination Board.

I would like to express my appreciation for the administration of the Göttingen Graduate Center for Neurosciences (GGNB) and the Leibniz Graduate School for Emerging Infectious Diseases (EIDIS), especially for Stefan Pöhlmann as Head of the graduate school. Additionally, I would like to thank the “Pöhlmann Lab”, in particular Michael Winkler for the exchange of ideas and resources.

I am grateful to all the past and present members of the “Hahn Lab” for their valued scientific input and for contributing to a great atmosphere. Special thanks go to Sarah Schlagowski for her continued help on all things experimental, for always keeping a positive attitude and coping with oftentimes spontaneous changes in plan.

I would also like to thank all the co-authors of our studies for their contribution to successful publications.

I would like show my gratitude to Armin Ensser for allowing me to gather my first experiences in the fascinating field of virology and for the encouragement to always explore new topics and methods during my Bachelor’s and Master’s Thesis. Furthermore, I would like thank the members of the “Ensser Lab”, especially Doris Jungnickl and Brigitte Scholz for “showing me the ropes” around the lab. Thank you all for the good times and the ongoing support and collaborations.

Moreover, I would like to thank my fellow “MolMed” students for many great experiences and discussions both scientifically and about life, the universe and everything.

I would like to thank my family, my mother Heidi, my father Rudi and my sister Eva for their invaluable support and endorsement of all my endeavors and Robert for his continuous encouragement, reassurance, patience and love. Thank you all for always listening, putting all emerging troubles in perspective, reminding me to enjoy life to the full and always being there for me.

A6 Curriculum vitae

Anna Katharina Großkopf

Personal Information

Place of birth: Fürth

E-Mail: agrosskopf@dpz.eu

Nationality: german

Education and Academic Career

| | |
|---------------------|--|
| 06/2016 – present | Doctoral student in the Leibniz Graduiertenschule Emerging Infectious Diseases (EIDIS) (Göttingen Graduate Center for Neurosciences, Biophysics, and Molecular Biosciences (GGNB)) <i>Deutsches Primatenzentrum, Göttingen</i> PhD thesis: “Cell and Receptor Tropism of γ 2-Herpesviruses” Supervisor: Dr. Alexander Hahn |
| 06/01/15 – 12/31/15 | Research Associate, <i>Institute for clinical and molecular Virology, Erlangen</i> |
| 12/01/14 – 05/31/15 | Research Intern, <i>Massachusetts General Hospital, Boston, USA</i> Establishing a system of tracking oHSV infection and effects in Glioblastoma multiforme therapy |
| 10/2012 – 11/2014 | M.Sc. in Molecular Medicine, <i>Friedrich Alexander University, Erlangen</i> Final mark: 1.3 Master’s thesis: “Analysis of the interactions of Kaposi’s sarcoma-associated herpesvirus tegument protein ORF75 with newly identified cellular targets” <i>Institute for clinical and molecular virology</i> |
| 10/2009 – 09/2012 | B.Sc. in Molecular Medicine, <i>Friedrich Alexander University, Erlangen</i> Final mark: 1.8 Bachelor’s thesis: “Sequence diversity of HVS strains from three subgroups” <i>Institute for clinical and molecular virology</i> |
| 05/2009 | Abitur at the secondary school Herzogenaurach, Herzogenaurach Abitur (equivalent to A-level), final mark: 1.4 Focus subjects: English, Mathematics Further examination subjects: History, Geography |

Additional Experience and Qualifications

| | |
|-------------------|---|
| 06/2017 – 01/2020 | Student representative for the Leibniz Graduate School for Emerging Infectious Diseases (EIDIS) |
| 04/2019 | Fortbildungsveranstaltung zu Sicherheitsmaßnahmen und Arbeitsschutz nach §15 Abs. 2 Satz 1 Nr. 3 GenTSV |
| 2013/ 2014 | Member of the planning committee and treasurer for the 9th biomedical students' symposium 2014 in Erlangen |
| 10/2012 – 12/2012 | Training course: FELASA-B This course complies with category B-FELASA and meets the requirements according to the Protection of Animals Act, paragraph 9, for people involved in animal experimentation. |
| 03/2012 | Training course: Radiation protection Acquirement of the requisite qualification of category S4.1 |